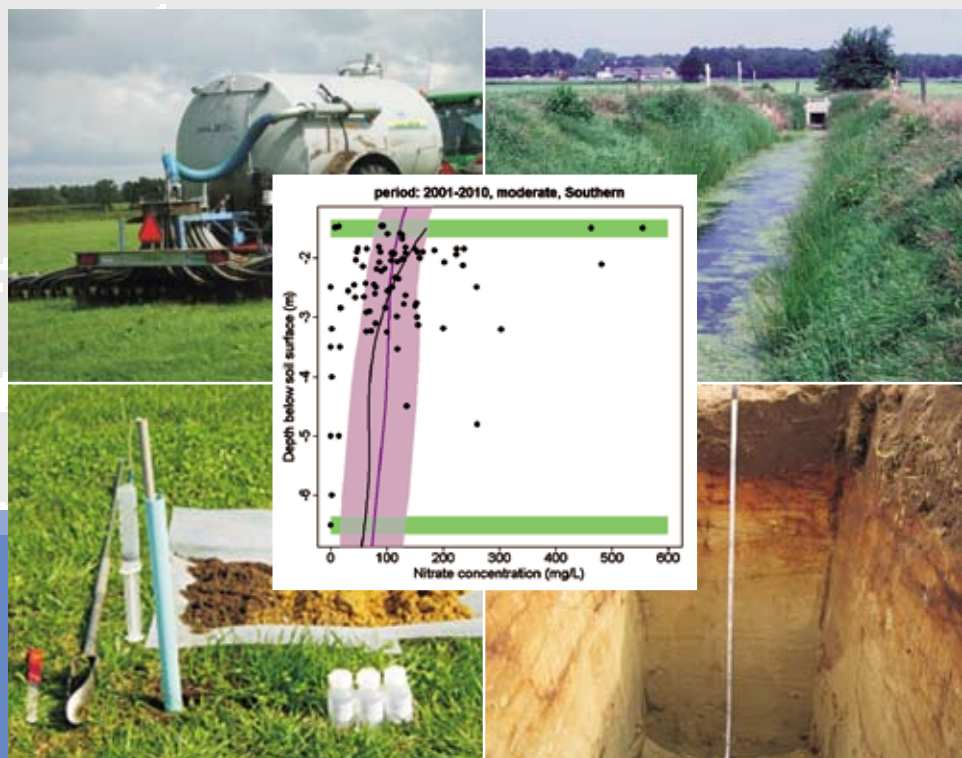




# A new compliance checking level for nitrate in groundwater

Modelling nitrate leaching and the fate of nitrogen in the upper 5 meter of the groundwater system

P. Groenendijk  
L.V. Renaud  
J. Roelsma  
G.M.C.M. Janssen  
S. Jansen  
R. Heerdink  
J. Griffioen  
B. van der Grift



A new compliance checking level for nitrate in groundwater. Modelling nitrate leaching and the fate of nitrogen in the upper 5 meter of the groundwater system.

Commissioned by National Institute for Public Health and the Environment, in the framework of  
“Research on the compliance checking level of nitrate in groundwater”

Project code [5235198-01]

# A new compliance checking level for nitrate in groundwater

Modelling nitrate leaching and the fate of nitrogen in the upper 5 meter of the groundwater system

P. Groenendijk  
L.V. Renaud  
J. Roelsma  
G.M.C.M. Janssen  
S. Jansen  
R. Heerdink  
J. Griffioen  
B. van der Grift



Alterra-report 1820.doc

Alterra, Wageningen, 2008

## ABSTRACT

Groenendijk, P, L.V. Renaud, J. Roelsma, G.M.C.M. Janssen, S. Jansen, R. Heerdink, J. Griffioen & B. van der Grift, 2008. *A new compliance checking level for nitrate in groundwater. Modelling nitrate leaching and the fate of nitrogen in the upper 5 meter of the groundwater system.* Wageningen, Alterra, Alterra report 1820; 215 pages; 26 figs.; 10 tables; 14 append.; 89 refs.

Research was conducted on the implications of a possible lowering of the sampling depth for the nitrate compliance checking level in the Netherlands. The STONE model was used to simulate nitrate concentrations and nitrogen balances for the three main sand districts (North, Central, South) and for three groundwater classes (dry, moderate, wet). Results of sediment samplings were evaluated to refine the model input and to obtain information for model validation. Water quality data of regular monitoring networks were processed for an assessment of the model performance. In the dry sand districts the current nitrate concentration does not decrease with depth but the future concentrations are expected to decrease with depth due to denitrification. The current pattern is confirmed by field observations and is explained by the combination of the decreasing trend of the historical nitrate loading of the groundwater and denitrification. Despite the reduction of future nitrate concentrations, the drinking water standard of 50 mg l<sup>-1</sup> will still be exceeded at 5 meter below the groundwater level in the dry sandy soils. The dry sandy soils show a nitrate load on surface waters which should be taken into account for the evaluation of Water Framework Directive related targets and progress.

Keywords: Groundwater, Nitrate, Denitrification, Compliance checking level, Leaching model

ISSN 1566-7197

The pdf file is free of charge and can be downloaded via the website [www.alterra.wur.nl](http://www.alterra.wur.nl) (go to Alterra reports). Alterra does not deliver printed versions of the Alterra reports. Printed versions can be ordered via the external distributor. For ordering have a look at [www.boomblad.nl/rapportenservice](http://www.boomblad.nl/rapportenservice).

© 2008 Alterra

P.O. Box 47; 6700 AA Wageningen; The Netherlands

Phone: + 31 317 480700; fax: +31 317 419000; e-mail: [info.alterra@wur.nl](mailto:info.alterra@wur.nl)

No part of this publication may be reproduced or published in any form or by any means, or stored in a database or retrieval system without the written permission of Alterra.

Alterra assumes no liability for any losses resulting from the use of the research results or recommendations in this report.

[Alterra-report 1820.doc/October/2008]

## Contents

Preface .....	7
Summary.....	8
1 Introduction	15
1.1 Background	15
1.2 Aim of the project	17
1.3 Setup of the study	18
1.4 Reading guide	19
2 Models used, input data and analysis approach	21
2.1 Concise model description of STONE	21
2.2 Concise model description of PHREEQC	22
2.3 Organic matter input data for the subsoil	22
2.4 Investigation of the denitrification rates in the subsoil	23
2.5 Investigation of groundwater quality observations for model validation	23
2.6 Assumptions and definitions	24
3 STONE model calibration and validation	29
3.1 Model calibration on observed potential denitrification rates and previously simulated nitrate concentrations	29
3.2 Model validation at regional scale on nitrate profiles with depth	31
4 Results of the STONE model application	33
4.1 Nitrate concentrations in groundwater	33
4.2 Nitrate- and total N-transport to surface waters	36
4.3 Actual and potential denitrification in groundwater	38
4.4 Nitrate and total-N balances in groundwater	41
5 Discussion on uncertainties and band widths	45
5.1 Applicability at field and farm scale	45
5.1.1 Setup of the field scale modelling study	45
5.1.2 Field scale validation results	46
5.1.3 Influence of reactivity of solid organic matter	49
5.2 Influence of thin peat layers in the subsoil	53
5.3 Influence of drought classification	55
5.4 Effects of temporal and spatial aggregation	57
5.5 Fluctuating versus constant depth	59
5.6 Influence of land use	60
6 Risks of undesirable side effects and sustainability	62
6.1 Introduction	62
6.2 The act of side effects	62
6.3 The occurrence of side effects	63
6.4 Sustainability of denitrification	65

7	Conclusions	67
7.1	Investigation of organic matter and pyrite contents in the subsoil	67
7.2	Denitrification rates in sandy aquifers	67
7.3	Investigation of groundwater quality investigations	67
7.4	Conclusions based on model results	68
7.5	Answers to research questions	70
	References .....	75
	Appendix 1 Model description.....	82
	Appendix 2 Literature survey of the denitrification rates in the subsoil.....	92
	Appendix 3 Sediment analysis of aquifer samples to support refinement of regional model input .....	101
	Appendix 4 Investigation and analysis of groundwater quality monitoring results to support model validation.....	132
	Appendix 5 Comparison of flux weighted concentrations at MLG level with concentrations in the first meter below a fluctuating groundwater level .....	146
	Appendix 6 Calibration of SWAP and ANIMO on observed groundwater levels and nitrate concentrations at four dairy farms.....	148
	Appendix 7 Flux averaged nitrate concentrations in groundwater.....	172
	Appendix 8 Time patterns of flux averaged concentrations .....	174
	Appendix 9 Total-N and nitrate -transport to surface waters per sand district.....	176
	Appendix 10 Actual and potential denitrification in groundwater .....	178
	Appendix 11 Schematic representation of total N and nitrate balances per region and/or per groundwater class.....	180
	Appendix 12 Nitrate balances of the upper 5m groundwater zone .....	195
	Appendix 13 Tentative sensitivity analysis at farm level of subsoil organic matter attribution to pools.....	196
	Appendix 14 Modelling side effects of denitrification in groundwater .....	200

## Preface

At the end of 2007, the ministries of Ministry of Agriculture, Nature and Food Quality and the Ministry of Housing, Spatial Planning and the Environment addressed a request to RIVM, Deltares and Alterra to conduct a follow-up research on the nitrate compliance checking level depth. This topic is mentioned in the letter of Minister Verburg to the House of Parliament (DL 2007/3529; 13 December 2007). The research approach includes the application of a nationwide nutrient leaching model, as has been described in the RIVM-tender of the over-all project.

This underlying report describes the setup, the results and the conclusions of 1) the modeling study on a regional assessment of nitrate concentrations as function of depth and the consequences on the leaching to surface waters; 2) the possible undesirable side effects of denitrification in groundwater; 3) the investigation of groundwater quality at the regional scale and; 4) the analysis of the organic matter and the pyrite contents in sediment samples in regional investigations.

Intermediate results have been presented and discussed at a workshop on the occasion of an international scientific review of previous reports on the depth, on 12 June 2008. A draft version of this report has been reviewed by the same committee in October 2008. The committee was chaired by Prof. dr. ir. Oswald Van Cleemput (Ghent University), accompanied by dr. Jean-Claude Germon, (INRA Dijon), prof. dr. Steve Jarvis (University of Exeter), dr. Jens Stockmarr (GEUS, Denmark), prof. dr. Kristine Walraevens (Ghent University) and dr. Frank Wendland (Forschungszentrum Juelich).

During the achievement of this research the setup and results have been discussed frequently with drs. A. de Klijne, ir. B. Fraters, drs. M. van Vliet (RIVM) and dr. G. Velthof (Alterra). Ir. E.M.P.M. van Boekel and ing. H.P. Oosterom (Alterra) contributed to this study by processing some of model inputs or model outputs. The authors wish to express their gratitude for their valuable comments and contributions.

Wageningen, February 2009.

Piet Groenendijk.

## Summary

### *Background*

The Dutch Fertiliser Act became effective on the 1<sup>st</sup> January 2006. The adapted Fertiliser Act includes a system of application standards that should lead to the compliance with aims of the Nitrate Directive as well as with objectives of the Water Framework Directive.

The Nitrate Directive and the Water Framework Directive show a strong relationship. Both directives oblige the EU member states to ensure a groundwater and surface water quality suitable for the preparation of drinking water. Eutrophication of surface water should be combated. A threshold value of 50 mg l<sup>-1</sup> for the nitrate concentration in groundwater has been laid down. None the Nitrate Directive and the Water Framework Directive indicate a position for the compliance checking level.

The compliance with the threshold value of 50 mg l<sup>-1</sup> nitrate in groundwater has been a basic principle for the Dutch Government in their negotiation with the European Commission on the system of application standards and on the derogation for a certain class of soils. The European draft guideline on monitoring for the Nitrate Directive leaves some space for an alternative depth for sampling groundwater.

The Dutch government wants to examine the defensibility of a threshold level higher than 50 mg l<sup>-1</sup> nitrate in the upper meter of the groundwater body. This mainly depends on the underpinning scientific basis that such higher threshold level would not lead to a shift of problems to surface waters; and that the threshold level of 50 mg l<sup>-1</sup> nitrate can still be achieved within the upper 5 meter of the groundwater. Insight in the governing processes (transport and denitrification) is needed. These processes have been insufficiently quantified until now.

The processes in the upper groundwater have been examined by means of investigations of monitoring data and by model simulation. Recent information which was made available in a research parallel to the modelling effort has been used to refine and validate the models. The models have been used to respond to the main research questions from the Ministry of Agriculture, Nature and Food Quality and the Ministry of Housing, Spatial Planning and the Environment.

The study aimed at the quantification at the regional scale of the possible changes of the nitrate concentrations in the upper 5 meter of the groundwater in sandy areas and an assessment of causal relations.

### ***Data exploration and field study***

An investigation of organic matter and pyrite contents in the subsoil showed clear differences between the various sand districts, with pyrite and organic matter contents being highest in North Netherlands, lower in South Netherlands, and lowest in Central Netherlands. The dependency of the denitrification capacity and the denitrification rate on the distribution of organic matter and pyrite is not straightforward. A literature survey turned out that there is a clear relation between the decay rate and the age of the organic material, but within an age group there is a wide variety of decay rates. The reported denitrification rates for aquifers range from 10 to 1000 meq l<sup>-1</sup> yr<sup>-1</sup>.

Groundwater quality data from national and provincial monitoring networks, as well as LMM monitoring network (National Program for Monitoring the Effectiveness of the Minerals Policy) were investigated. It appeared that denitrification in agricultural areas with wet sandy soils is generally completed within the first 5 meters of the groundwater zone and some denitrification occurs within the first 5 meters of the groundwater body in areas with dry sandy soils. These conclusions agree in large with the findings of a previous study by Fraters *et al.* (2006).

A validation study for four dairy farms on sandy soils was conducted to gain insight in the model performance at field level. The annual predicted nitrate concentrations in the upper meter of the groundwater were compared with the measured concentrations extracted from monitoring results. The average of the predicted concentration time series for Maarheeze fits reasonably with the averaged value of the observations. The predicted values lie within the range of observed concentrations, but for the other farms the model overestimated the measured values. The weak validation results for the nitrate concentrations in the upper meter at field scale do not restrain the model application at regional scale, because the agreement of simulated concentrations with observations in the national and provincial monitoring networks is sufficient. The results of a regional model application are only applicable at the model scale itself.

### ***Setup and assumptions of the modeling study***

The nation-wide STONE-model has been used to investigate the evolution of the nitrate concentration as a function of depth and to quantify the governing processes in the upper groundwater zone. Results of the STONE model have been aggregated for the period 2001–2010 as being representative for the current situation. The nitrate concentrations and denitrification and transport rates that can be expected in the future are indicated by the aggregated results of the period 2031–2040. The assumed fertilization rates slightly decrease until 2015 and are constant after 2015. So, in the current situation, represented by the average of the 2001–2010 period, the fertilization rates are not constant. Future fertilization rates have been adopted from the preparatory study in the framework of the Evaluation of the Fertiliser Act 2007. The “2015AT–20” scenario was used in this current study. This scenario assumes a reduction of the nitrogen application standard of 20%

compared to the rates in 2006 for arable crops and horticultural crops. This scenario should be seen only as a possible situation. The real fertilization rates in the future will depend on the issuing of rules and by bringing them into practice. No decision has been made yet on the application standards.

The results refer to the sandy areas in the main sand districts. The sandy soils in the coastal areas have been excluded. The results are presented for three groundwater classes (dry, moderate and wet) and for the three main sand districts (North, Central, South).

The PHREEQC model was used for an exploratory study on side effects of denitrification, such as sulphate formation and heavy metal release associated to pyrite oxidation. The geochemical data on organic matter contents and pyrite contents available in data bases and groundwater quality data (redox conditions, nitrate concentrations) have been investigated for the shallow subsoil between 1 and 15 meter below soil surface. Additional data (organic matter content, pyrite, potential denitrification rate) have been assembled from a field campaign, parallel to this study.

### ***Results and conclusions***

*At a constant fertilization rate in future, but at a lower rate than the current one, the nitrate concentration will decrease with depth in the upper 5 meter of the groundwater body. The decrease is calculated for all groundwater classes and for all sand regions. But also nitrate leaching to surface water systems by the conveyance of water through the upper 5 meter of the groundwater body is expected for all groundwater classes and for all sand regions.*

Model simulations resulted to a decrease of the nitrate concentration with depth at a constant fertilization with depth in the future. This holds also for the dry sandy soils. The decrease is smallest for the dry soils, followed by the moderate soils and largest for the wet soils. The reduction of the nitrate concentration at 5 meter below the Mean Lowest Groundwater level (MLG), compared to the concentration at MLG ranges from 10 to 39% and amounts to 24% on average. The reduction ranges from 39 to 87% for the moderate soils and with an average value of 61%. The reduction is largest for the wet soils (78 – 98%) and is 88% on average for these soils.

The phenomenon of a decrease of the nitrate concentration with depth holds also when the model results are aggregated to average values for the sand districts. However, the differences between the districts are less pronounced than the differences between the groundwater classes. The variation of the reduction of the concentration at greater depth, compared to the concentration at MLG, is large due to the variation of sandy soil types and groundwater classes within a district. The differences between the reduction percentages of the districts are smaller than the band widths. The differences between the groundwater classes are more important than the differences between the sand districts to gain insight in the nitrate governing processes in the upper groundwater.

The current situation (2001 – 2010) is characterized by decreasing fertilization rates with time. The nitrate concentration as a function of depth is influenced by this trend. No decrease of nitrate concentrations with depth in the upper 5 meter of the groundwater body is calculated for the dry sandy soils in the current situation. This complies with field observations. The phenomenon is explained by the combination of the nitrate delivery from the historically accumulated stock in groundwater and the nitrate reduction by denitrification. For the moderate and wet sandy soils the model results indicate a nitrate decrease with depth. This also complies with field observations<sup>1</sup>.

Denitrification occurs in all sandy soils, but the denitrification rate is smallest for the dry sandy soils, followed by the moderate sandy soils and is largest for the wet sandy soils. The main part of the total denitrification (55 – 95%) occurs in the topsoil between the soil surface and the Mean Lowest Groundwater level. The denitrification in the topsoil leads to the reduction of the nitrate influx in the groundwater and has already been accounted for in the current compliance checking level. The denitrification in the upper 5 meter of the groundwater body is much smaller than the denitrification rate in the topsoil (5 – 25% of the total denitrification).

The denitrification capacity in the subsoil decreases by the denitrification. The store of minerals and organic compounds in the subsoil that contribute to the total denitrification capacity is large enough to continue the nitrate reduction for tens to hundreds of years. The denitrification rates increase with higher nitrate leaching rates. The total store of denitrifying compounds in the subsoil is largest in the Northern and smallest in the Central sand district. The Southern sand district takes an intermediate position. The potential denitrification rate is expected to be constant within the coming decades. The role of dissolved organic matter, originating from manure inputs, in the denitrification process at this depth is still unresolved.

Negative side effects of denitrification in groundwater are related to the occurrence of pyrite oxidation and not to organic matter oxidation. When nitrate in the upper groundwater is partly denitrified by pyrite oxidation, it is expected that the side effects will increase with higher nitrate leaching rates. The potential negative side effects hold in particular for arsenic, copper and nickel, due to relatively high contents of these trace impurities in pyrite. When groundwater is not exposed nitrate concentrations exceeding 50 mg l<sup>-1</sup> NO<sub>3</sub>, the negative side effects for sulphate and hardness are small to negligible. Zinc and cadmium show an intermediate behaviour. The prediction of the extent of side effects is unreliable primarily due to missing information on the trace metal contents in pyrite in Dutch aquifer sediments. Based on the sediment analyses for pyrite and sedimentary

---

<sup>1</sup> Fraters *et al.*, (2006). A new compliance checking level for nitrate in groundwater? Feasibility study on monitoring the upper five metres of groundwater. RIVM report 680100005/2006.

organic matter, the potential of negative side effects is expected to be highest for the Southern Netherlands, followed by the Northern Netherlands and lowest for the Central Netherlands.

An unambiguous explanation of the decrease of the nitrate concentration with depth cannot be given for a certain district or groundwater class, due to the large variation of land use types, sandy soil types and groundwater sub-classes within. The nitrate transport fluxes, the water fluxes and the denitrification rates have been quantified by the STONE model. The band widths of the denitrification rate and the transport fluxes in the upper 5 meter of the groundwater are larger than the mutual differences between these sink terms of the nitrate balance. The variation of the mutual division between the sink terms show a great variation. The large variability complies with previous research results.

The downward leaching to groundwater layers at greater depth is the largest sink term of the nitrate balance for the zone between the Mean Lowest Groundwater level and 5 meter below this level. For the moderate sandy soil, the denitrification, the downward leaching and the lateral transport to surface waters are more or less equal sink terms of the nitrate balance for this layer. The lateral transport to surface waters is the largest sink term of the nitrate balance of the upper groundwater zone for the wet sandy soils.

In the dry sandy soils, 69% of each kg nitrate that enters the top 5 meter layer of the groundwater body is transported to deeper layers, 21% is denitrified within this top layer and 10% is transported to surface waters. For the moderate soils, the percentages amount to 31% for transport to deeper layers, 38% for denitrification and 31% for transport to surface water. In the wet sandy soils 2% is transported to deeper layers, 38% is denitrified and 60% is transported to surface waters.

Some dilution of the upper groundwater may occur in moderate and wet sandy soils by the supply of groundwater from deeper layers. The extent of the dilution effect depends on the upward seepage flux and the nitrate concentration in this upward seeping water. In the dry sandy soils, no dilution is expected at this depth.

Nitrogen and nitrate transport to surface waters is expected to occur in all types of sandy soil, also in the sandy soil classified as “dry”. The transport to surface waters should be taken into account when one considers an adjustment of the compliance checking level for nitrate in groundwater. The nitrogen transport to surface waters in dry soils was not considered in previous studies because of another definition of dry soils. In our study, the groundwater class dry soils include all the sandy with a Mean Highest Groundwater level deeper than 80 cm below soil surface. Also artificially drained soils are included. The nitrogen load on surface water is the smallest for the dry sandy soils

The present *nitrogen* load on surface waters amounts to 25 kg ha<sup>-1</sup> yr<sup>-1</sup> for the dry soils and ca. 38 kg ha<sup>-1</sup> yr<sup>-1</sup> for the moderate and wet soils. In the dry and moderate soils, the main compound in the nitrogen transport is nitrate. Transport of ammonium and organic bounded nitrogen places also a role in the wet soils. The largest part of the nitrogen load on surface water is conveyed through the topsoil between soil surface and 5 meter below the Mean Lowest Groundwater level. Irrespective the groundwater class, half of this load stems from the zone between the soil surface and MLG, the other half is conveyed through the zone below MLG. A higher *nitrate* concentration in the upper groundwater will inevitably lead to a higher *nitrogen* load on surface waters for all sandy soils.

Examining the differences between the sand districts, the present *nitrogen* load on surface waters is largest in the Southern sand district (38 kg ha<sup>-1</sup> yr<sup>-1</sup>) and smallest in the Northern sand district (28 kg ha<sup>-1</sup> yr<sup>-1</sup>). The present *nitrogen* load is calculated at 34 kg ha<sup>-1</sup> yr<sup>-1</sup> for Central sand district.

The flux averaged total N-concentration<sup>2</sup> in the water discharged to surface waters is largest in the dry sandy soils (21 mg l<sup>-1</sup>), followed by the moderate sandy soils (15 mg l<sup>-1</sup>) and is at smallest for the wet sandy soils (7 mg l<sup>-1</sup>)<sup>3</sup>. This flux averaged concentration in drainage water can differ from the actual concentration in the surface water itself, due to other sources, supply of surface water with deviating concentrations from adjacent upstream areas and retention processes.

The denitrification as a result of pyrite oxidation was ignored in the analysis of the fate of nitrate due to a insufficient data availability. Because the occurrence of thin peat layers was difficult to include in the model, this was addressed by a sensitivity analysis. A maximum accounting for the reactivity of thin peat layers resulted in a decrease of the nitrate concentration less than 8 mg l<sup>-1</sup>. A possible accounting for the influence of pyrite, the regional patterns of pyrite occurrences in the subsoil and the influence of thin peat layers would imply the recalibration of the model on potential denitrification rates and nitrate concentrations.

In this study, progress was made with the processing of regional specific input data of subsoil organic matter contents. Also insights in the regional patterns of denitrification capacity were made accessible. In this study the possibility to exploit this new information was limited. The discretization of the STONE model into plots, the spatial variability of model attributes within mapping classes and the sampling strategy of the LMM monitoring network in the past limit the possibilities for a regional differentiated calibration of the current STONE model. The new geo-chemical characterisation of the subsoil is an important contribution to future improvements of the leaching model.

---

<sup>2</sup> Load divided by water flow

<sup>3</sup> If the nitrogen in the discharge water exists for 100% of nitrate, the concentrations are equivalent to 93, 66 and 31 mg l<sup>-1</sup> NO<sub>3</sub> in drainage water of dry, moderate and wet sandy soils



# 1 Introduction

## 1.1 Background

In the past two decades, Dutch agriculture has been subject to increasingly stringent policies regarding fertilizer use (methods, amounts and period of application). The Dutch Fertiliser Act became effective on the 1<sup>st</sup> January 2006. The adapted Fertiliser Act includes a system of application standards that should lead to the compliance with aims of the Nitrate Directive as well as with objectives of the Water Framework Directive. The Nitrate Directive and the Water Framework Directive show a strong relationship. Both directives oblige the EU member states to ensure a groundwater and surface water quality suitable for the preparation of drinking water. Eutrophication of surface water should be combated. A threshold value of 50 mg l<sup>-1</sup> for the nitrate concentration in groundwater was determined. None the Nitrate Directive or the Water Framework Directive indicates a position for the compliance checking level.

The new system of application standards was the basis for the negotiations of the Dutch government with the European Commission on the derogation for a certain group of farms (Schröder *et al*, 2004). The compliance of the target level for not exceeding the 50 mg l<sup>-1</sup> nitrate concentration in the upper meter of the groundwater zone (Fraters *et al*, 2006) was always a starting point in these discussions.

An evaluation of the Fertiliser Act was conducted in 2007. (MNP, 2007). It was concluded that the objectives of the Nitrate Directive are not realized everywhere. On average, the nitrate concentration in clay and peat regions is lower than the European standard value, but in the sand and loess regions, the standard is exceeded (Klijne *et al*, 2007; Zwart *et al*, 2008). Even when additional measures are taken, it is expected that the standard value will still be exceeded in some areas. These conclusions confirm the finding of previous evaluations (MNP, 2002; MNP, 2004).

In the evaluation of the Fertiliser Act in 2002 it was suggested to choose a lower sampling depth in so-called infiltration areas to monitor the nitrate compliance with the objectives. The draft monitoring guideline for groundwater composed by the European Commission (EU, 2003) leaves room for such a decision, although the guideline has not been approved officially. The guideline states:

*“Both shallow and deep groundwater should be included in the monitoring network [...] For example, both the upper and lower parts of the aquifer that are connected to the soil should be sampled, as the upper parts (the first five meters of the saturated zone) will tend to respond quickest to changes in agricultural practice, ...”.*

In 2004, the Evaluation of the Fertiliser Act (MNP, 2004) concluded that, on the basis of a study by Broers *et al.*, (2004) insufficient information is available to decide on a lower compliance checking level. The discussions in the Dutch Parliament on this Evaluation, and the preparation of the new Fertiliser Act in 2006, resulted in a promise to conduct an additional study which should provide information for taking a go-nogo decision for choosing a lower sampling depth.

Fraters *et al.* (2006) presents and summarizes different aspects of monitoring methods, monitoring results and detailed geo-chemical investigations related to the occurrence and fate of nitrate in the upper groundwater zone. His study concluded that the nitrate concentration does not decrease with depth in the upper 5 meter of the groundwater zone in vulnerable nitrate leaching areas (dry sandy soils<sup>4</sup>). The nitrate concentration decreases with depth in moderate<sup>5</sup> and wet sandy areas. Denitrification<sup>6</sup> is expected to play a role, but these type of soils contribute to the surface water loading by nitrogen (eutrophication). Therefore, the objectives for the surface water quality should be considered (Fraters *et al.*, 2006).

The discussions on these findings in the Dutch Parliament resulted in a repeated commitment to investigate the possibilities for lowering the compliance checking level for nitrate from the current 1 meter to 5 meter below groundwater level in the sandy regions. This commitment was confirmed by Minister for Agriculture, Nature and Food Quality, also on behalf of the Minister of Housing, Spatial Planning and the Environment in a letter (dated on 13 December 2007; 28 385, nr. 104) to the Dutch Parliament.

The Dutch government wants to examine the defensibility of a threshold level higher than 50 mg l<sup>-1</sup> nitrate in the upper meter of the groundwater body. This mainly depends on the underpinning scientific basis that such higher threshold level would not lead to a shift of problems to surface waters; and that the threshold level of 50 mg l<sup>-1</sup> nitrate can still be achieved within the upper 5 meter of the groundwater. Insight in the governing processes (transport and denitrification) is needed. These processes have been insufficiently quantified until now.

---

<sup>4</sup> The study of Fraters *et al.*, (2006) presumes infiltrating sandy soils, not connected to visible surface water elements, as typical dry sandy soils.

<sup>5</sup> Soils with a moderate groundwater table are defined by the mean highest groundwater level less between 40 and 80 cm below soil surface and the mean lowest groundwater level deeper than 120 cm below soil surface.

<sup>6</sup> Denitrification is the microbial process whereby nitrate and nitrite (NO<sub>2</sub><sup>-</sup>) in the soil are converted into the gaseous nitrogen compounds N<sub>2</sub>, N<sub>2</sub>O and NO<sub>x</sub>. Denitrification only takes place in oxygen-free conditions. The main energy source for denitrifying bacteria is readily degradable organic matter. In addition to organic matter, some bacteria can also use inorganic compounds as an energy source, e.g. the iron sulphide (FeS<sub>2</sub>) present in pyrite

## 1.2 Aim of the project

The project aimed at the quantification of the possible changes of the nitrate concentrations in the upper 5 meter of the groundwater in sandy areas and assessment of the causes of these changes. The sink terms for N (i.e. processes leading to lower N concentration and leaching, such as denitrification, transport to surface waters, and dilution) that contribute to the expected reduction will be quantified at regional level for the Northern, Central and Southern sand district.

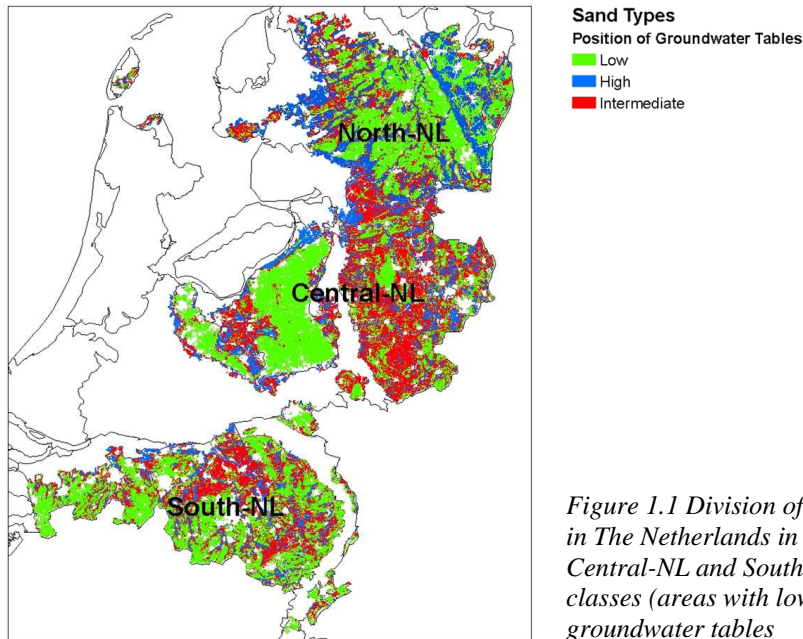


*Figure 1.1 Division of the Pleistocene sandy areas in The Netherlands in sand districts (North-NL, Central-NL and South-NL) and groundwater classes (areas with low, high and intermediate groundwater tables)*

The evolution in time of the factors that causes the reduction will be depicted. The results will be analyzed and reported in a joint scientific background report. The report comprises also the results of and the synthesis with the results of Deltares obtained within the framework of this research.

The project aims also at a contribution to the international review of results and reports of research conducted in 2005 and 2006. Results of the modelling efforts will be presented and discussed with the international review committee.

The research responds (partially) to questions directed to the over-all project. The research questions read:

1. What is the average regional change of the nitrate concentration in groundwater between groundwater surface and five metres below groundwater surface for agriculture areas with a constant level of fertilization?
2. Regional's are specified as North, Central and South sand areas distinguished by different water table classes (dry sand, medium dry sand and wet sand). Please indicate: (1) which part of the change is due to denitrification; (2) which part of the change is

due to hydrological phenomena (seepage, dilution); (3) the average decrease and the uncertainty in the decrease

3. What is the expected regional development of denitrification capacity in time? (Indicate at least increase, steady state or decrease and the time frame?)
4. Specify the present nitrogen load to surface waters caused by agriculture activities on regional scale? What percentage originates from nitrate in groundwater (beneath agricultural areas) at a depth between the groundwater table and five metres below groundwater table?
5. What is the present total N-concentration in groundwater beneath agricultural areas leaching directly to surface waters? What percentage originates from nitrate in groundwater at a depth between groundwater table and five metres below groundwater table on agricultural lands?
6. On the scale of areas, what are the expected side-effects of denitrification? Indicate the expected change in concentration for heavy metals, sulphate and increase of hardness of water. Furthermore specify the uncertainty in the change.

### **1.3 Setup of the study**

The main objective of the study is the estimation of any reduction of nitrate concentrations 5m below the current monitoring level and the attribution to the possible decrease by different processes as denitrification, transport to surface waters and dilution. An additional objective is the assessment of undesirable side effects such as the formation of sulphate and release of heavy metals as a result of denitrification. It was decided to use the STONE model for the quantification of nitrate concentrations in the upper groundwater zone and the main sink terms affecting nitrate concentrations and the PHREEQC model for an exploratory study on sulphate formation and heavy metal release. Also the band width of possible nitrate reduction and associated sink terms has to be assessed. For this purpose the STONE model needed to be refined with state-of-the-art information on organic matter contents in the subsoil and recalibrated on observed potential denitrification rates and nitrate concentrations in the upper groundwater. A number of working blocks were defined to organize the efforts. The subtasks and sub-results are described in the paragraphs indicated in the sub-tasks boxes of Fig. 1.2.

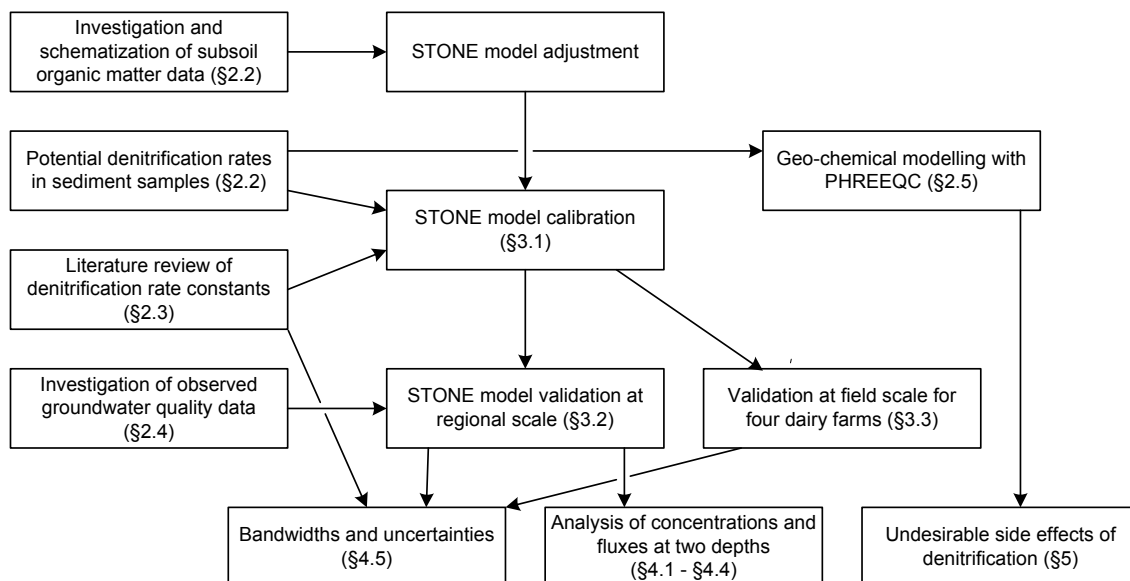


Fig. 1.2 Relationship between different sub-tasks of the study

## 1.4 Reading guide

The main text puts emphasis on the results and the conclusions referring to the questions mentioned in Par. 1.2. The materials and methods used are summarized in chapter 2. An unofficial release of the STONE model was used for the analysis. The confidence in the model application is supported by the model validation. The calibration and validation results are part of the materials and methods applied, but are described briefly in chapter 3. The main results of nitrate concentrations at two depths, the nitrogen and nitrate transport to surface waters and the nitrate removal by denitrification are given in chapter 4. The main results are given for two periods to get an impression of the evolution in time and. A discussion is included with respect to the influences of drought classification, assumed land use, the occurrence of thin peat layers in sandy subsoil's and the reactivity of organic matter. Chapter 5 presents the main conclusions.

Investigation methods, model approaches and results of the sub-tasks which contributed to the answering to the main questions in a direct or an indirect way are presented in a number of appendices. Table 1.1 gives the reference of the appendices to paragraphs of the main text.

*Table 1.1 Reference of appendices to paragraphs of the main text*

Paragraph	Appendix
2.1	A1
Concise model description	Model description
2.2	A3
Organic matter input data for the subsoil	Appendix 3 Sediment analysis of aquifer samples to support refinement of regional model input
2.3	A2
Investigation of the denitrification rates in the subsoil	Literature survey of the denitrification rates in the subsoil
2.4	A4
Investigation of groundwater quality observations for model validation	Investigation and analysis of groundwater quality monitoring results to support model validation
3.1	A5
Model calibration on observed potential denitrification rates and previously simulated nitrate concentrations	Comparison of flux weighted concentrations at MLG level with concentrations in the first meter below a fluctuating groundwater level
3.3	A6
Model validation at field scale	Calibration of SWAP and ANIMO on observed groundwater levels and nitrate concentrations at four dairy farms
4.1	A7
Nitrate concentrations in groundwater	Flux averaged nitrate concentrations in groundwater per sand district
4.4	A8
Nitrate and total-N balances in groundwater	Time patterns of flux averaged concentrations
4.2	A9
Nitrate- and total N-transport to surface waters	Total-N and Nitrate transport to surface waters per sand district
4.3	A10
Actual and potential denitrification in groundwater	Actual and potential denitrification in groundwater per sand district
4.4	A11
Nitrate and total-N balances in groundwater	Schematic representation of total N and nitrate balances per sand district
4.4	A12
Nitrate and total-N balances in groundwater	Nitrate balances of the upper 5m groundwater zone per sand district
4.5.4	A13
Influence of reactivity of solid organic matter	Tentative sensitivity analysis at farm level of subsoil organic matter attribution to pools and reaction rates
5	A14
Risks of undesirable side effects	Side effects of denitrification in groundwater

## 2 Models used, input data and analysis approach

### 2.1 Concise model description of STONE

STONE, a model system for calculating nutrient emissions (Wolf *et al.*, 2003), is the result of integration of knowledge, models and ongoing work from a large number of Dutch research institutes in the fields of plant production, land use, environment, surface waters and agricultural economics (Alterra, RIVM, RIZA, Plant Research International, LEI). The main reason for the development of STONE was the conflicting information on nutrient emissions being provided by different research groups. Dutch policy makers in need for consistent state-of-the-art information on N and P emissions to ground and surface waters at the national scale did not accept that situation. Consequently, the development of a consensus model was initiated in 1996 with the following objectives: (1) use of best models and data systems in all relevant research fields; (2) improved integration of knowledge from the various disciplines involved; (3) improved and consistent scientifically sound support for decision makers in identifying the most efficient and appropriate environmental policy measures. This resulted in a unique modelling approach which is shown by the typical aspects of STONE: (1) translation of environmental policy measures into model input data; (2) model application at national and regional scales; (3) spatially distributed input data on land characteristics; (4) chain of models with an optimization model for calculating the N and P input into soils from manure and inorganic fertilizer allocation, a metamodel for calculating the N deposition from air, and a process-based deterministic model for calculating the N and P cycling in the soil and the N and P nutrient emissions to ground and surface waters

The ANIMO model for simulation of nutrient leaching to groundwater and surface waters is used within the STONE model chain to assess the impact of agricultural policy measures at the national scale. A detailed description of the ANIMO model is given by Groenendijk *et al.* (2005).

QUAD-MOD (four QUADrant MODEL relating crop production to fertilizer application, fertilizer recovery fraction and soil nutrient supply) is an empirical model for calculating the nutrient uptake by crops and the yield, as based on fertilizer experiments. The model consists mainly of two relationships: (1) curvy-linear relationship between biomass yield and uptake of one nutrient (N or P); (2) linear relationship between nutrient application (N or P in inorganic and organic fertilizers) and nutrient uptake which relationship bends off near the maximum biomass yield level (Ten Berge, 2000).

The flows of nitrogen and phosphate in animal manure at farm level are assessed by means of using the MAMBO model (Luesink and Kruseman, 2007; Vrolijk *et al.*, 2008). This is a

static model for support of policy evaluation. The objective of the model is to calculate emission from several sources, manure production and -allocation, the transport of animal manure and the costs of transport and the mineral input to the soil. The transport of surplus manure is optimized by minimizing costs of distribution, export and processing. The model distinguishes a number of items: manure production, potential manure allocation, manure surplus, manure transport and input to the soil. Results of the MAMBO model are transferred at an aggregated level and disaggregated to STONE-plots by a procedure developed by Beusen *et al.* (2004).

A more extensive description of the STONE model is given in Appendix 1.

## **2.2 Concise model description of PHREEQC**

PHREEQC is a computer program that is designed to perform a wide variety of aqueous geochemical calculations (Parkhurst & Appelo, 1999). PHREEQC is based on an ion-association aqueous model and has capabilities for (1) speciation and saturation-index calculations, (2) reaction-path and advective-transport calculations involving specified irreversible reactions, mixing of solutions, mineral and gas equilibria surface-complexation reactions and ion-exchange reactions and (3) inverse modelling, which finds sets of mineral and gas mole transfers that account for composition differences between waters, within specified compositional uncertainties. The model includes the capabilities to use redox couples to distribute redox elements among their valence states in speciation calculations; to model ion-exchange and surface-complexation reactions; to model reactions with a fixed-pressure, multicomponent gas phase (that is, a gas bubble); to calculate the mass of water in the aqueous phase during reaction and transport calculations; to keep track of the moles of minerals present in the solid phases and determine automatically the thermodynamically stable phase assemblage; to simulate advective transport in combination with PHREEQC's reaction-modelling capability; and to make inverse modelling calculations that allow for uncertainties in the analytical data.

## **2.3 Organic matter input data for the subsoil**

To support the modelling in STONE and to obtain information about differences in redox conditions, soil contents of pyrite and organic matter were collected for South, Central and North Netherlands. For South and North Netherlands, (old and recent) existing data was used, for Central Netherlands new data was collected. A more extensive description is given in Appendix 3. The organic matter data were schematized by Van Boekel (2008) to make them applicable in the STONE model. The newly deduced information resulted in much lower organic matter contents in some Holocene areas (Fig. 2.1). These areas are out of scope in this study. However, the subsoil organic matter contents in the sand districts in the STONE model had to be raised two – five times based on the new information.

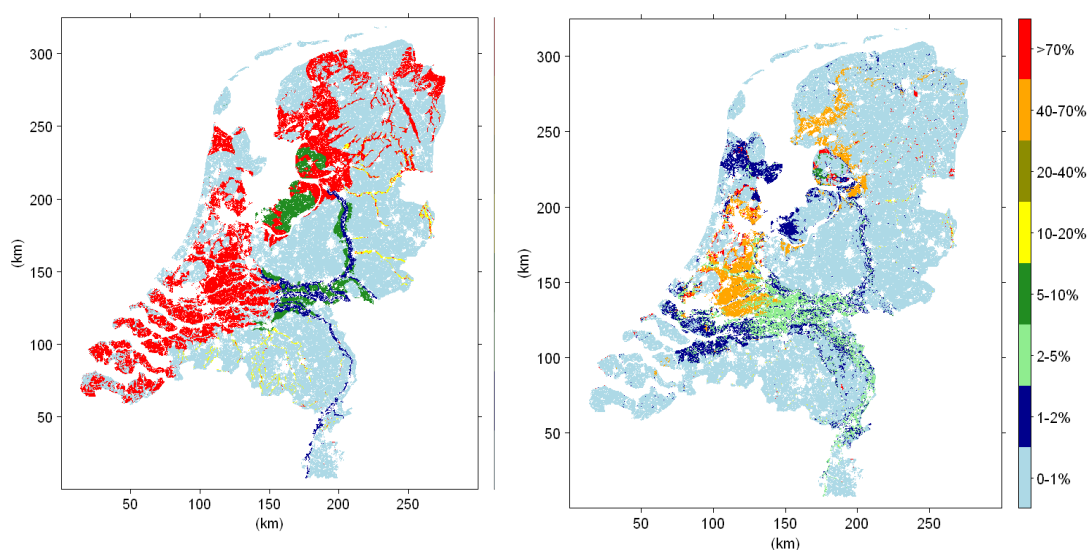


Fig. 2.1 Original (left) and new (right) organic matter contents (%) in the layer between 1 and 2 m below surface of subsoil (thin peat layers have been ignored).

## 2.4 Investigation of the denitrification rates in the subsoil

Denitrification is a much-studied phenomenon and one to which a wide range of decomposition constants applies. However, the vast majority of studies to date have been conducted in the unsaturated zone. For this project, the scientific literature was consulted specifically with regard to reported denitrification rates in aquifers. Since few papers have been reported on this subject, we also looked more broadly at the decomposition rates of organic matter with other electron acceptors. An attempt has been made to determine the band width of decomposition constants in relation with the age of the material. A more extensive description is given in Appendix 2.

## 2.5 Investigation of groundwater quality observations for model validation

An extensive analysis of available groundwater data was performed to serve a better parameterization of the used groundwater flow and transport model STONE, by providing a means to validate its results. Special attention was given to whether differences in the fate of nitrate can be found between the various “sand districts” (south, central and north Netherlands) and groundwater classes (low, intermediate and high groundwater levels).

For the data analysis, existing databases of national and provincial groundwater and soil quality networks were used. Six supplementary groundwater quality data sets were made available to the project team by the steering committee. These additional data sets could

only be utilized in the analysis if they meet a number of conditions regarding completeness of information:

- XY coordinates;
- sampling depths;
- complete chemical analyses, to allow for a quality check (electro neutrality);
- spatial representative;
- located in agricultural area;

The abovementioned distinction between different sand districts and different groundwater classes was applied to perform both a regional and a groundwater class based differentiation of:

- 1) depths of redox clines. Gaining insight in the depth at which redox conditions in the groundwater change is important for getting a feeling of the depth at which the nitrate concentration will start to decrease due to denitrification;
- 2) nitrate concentration profiles. Whereas redox clines can provide information on the reactive capacity of the subsurface and thus provide indirect information on the expected fate of nitrate, the most direct information on the extent to which nitrate is transported from the upper groundwater to greater depths is provided by evaluation of the changes in nitrate concentration itself with depth, i.e. nitrate profiles.

The variability and the resulting uncertainty surrounding the occurrence of redox clines and the fate of nitrate have been evaluated as well, by explicitly quantifying and visualizing the variability in the data sets of the relevant geochemical parameters. A more extensive description is given in Appendix 4.

## 2.6 Assumptions and definitions

The STONE model has been applied for the simulation of nitrate concentrations and the quantification of water-, total nitrogen and nitrate balances. The most recent official application of the STONE model refers to the study of Willems *et al.* (2008), conducted within the framework of the evaluation fertilizer legislation 2007. After refinement of organic matter contents in the subsoil, calibration on measured potential denitrification rates and previous results of simulated nitrate concentrations, and validation on observed nitrate concentrations the STONE model was applied for this study. The following assumptions were made:

- The assumed fertilization rates were based on the scenario “2015AT–20”, because this scenario was described and discussed the most extensively of a number a future scenario’s by Willems *et al.* (2008). In this scenario, the fertilization rates decrease until 2015 and after 2015 the rates are constant.
- The future prediction lasted until 2040 and two periods were chosen for further examination. The first period includes the ten year average between 2001 and 2010

and represents the current situation. In this period, the fertilization rates decrease as a result of legislation, but the simulated nitrate concentrations can be compared with observations. The second period (2031–2040) is a prediction for the future with assumed reduced but constant fertilization rates, whereas a comparison with measured concentrations is not useful. By comparing the results of both periods, one gets an impression of the future trends.

- Only the simulation units in the STONE model characterized by a sandy soil and with agricultural land use were selected for further analysis of results. The plots were assigned to one of the three main sand districts in the Netherlands: North, Central or South. The sand plots in the Western part of the Netherlands and the plots which appeared to be liable to schematization artefacts (80 plots; 2.5%) have been excluded.
- Three main groundwater classes were distinguished for the analysis of the model results (see Table 2.1). Simulation plots have been assigned to one of the groundwater classes on the basis of the simulated “groundwater table class” as resulted from the modelling effort of Van Bakel *et al.* (2008).

Table 2.1 Definition of groundwater classes. MHG = Mean Highest Groundwater Level

Class	Criterion	Groundwater table class
Wet	MHG < 40 cm below surface	Gt I – V*
Moderate	MHG 40–80 cm below surface and MLG > 120 cm below surface	Gt VI
Dry	MHG > 80 cm below surface	Gt VII and Gt VII*

It should be noted that the definition of a “dry” soil is based on the Mean Highest Groundwater Level. Contrary to the general idea of a dry soil as not having a relation with surface waters, a part of the “dry” plots within the STONE model show a considerable discharge to surface waters (Fig. 2.2)

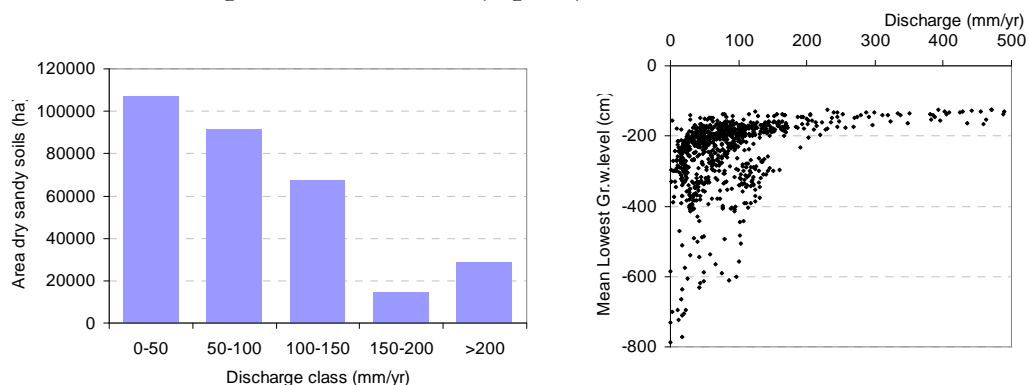


Fig. 2.2 Distribution of the area dry sandy soils with agriculture over discharge classes (left) and the relation between the long term averaged discharge of dry sandy soils used for agriculture and the mean lowest groundwater level (right), as simulated by Van Bakel *et al.*, (2008).

- The group of “dry” plots also include the fields in which the groundwater levels have been lowered due to the construction of field drains over the last fifty years and the

fields which discharge to streams at a certain distance by deeper flow paths. The relatively wet plots in the “dry” class can have a mean highest groundwater level of 80 cm below soil surface. During high precipitation events during winter time the water is discharged to adjacent field drains and to streams at a certain distance.

- Balances per simulation plot were calculated for a fixed soil depth. For each of the plots, the depth of the Mean Lowest Groundwater Level (MLG) was chosen as the top and the level of 5m below MLG was chosen as the bottom of the groundwater zone to be considered. The items of the balances can be aggregated to larger spatial units by multiplying with the area and summing them up for the aggregation unit considered. However, the MLG-depth can differ per simulation unit. The average MLG-depth for the aggregation unit is then surrounded by a distribution of depth values.
- Average concentrations in groundwater for a certain district or for a certain groundwater class can be calculated by at least four methods:
  - as an area weighted average of the observed or simulated concentration in groundwater

$$\frac{\sum_i a_i c_i}{\sum_i a_i}$$

- as an area weighted average of the volume weighted concentration in groundwater, derived from the simulated transport divided by the water flow;

$$\frac{\sum_i a_i \left( \frac{T_i}{Q_i} \right)}{\sum_i a_i}$$

- as a volume weighted average by multiplying the nitrogen or nitrate transport with the area and after summation dividing by the summed product of water flux and area. Transports and fluxes refer to net values over the time span considered.

$$\frac{\sum_i a_i T_i}{\sum_i a_i Q_i}$$

- By taking the seasonal variations of flow direction into account. The summed product of transport and area is then calculated as the sum of absolute upward transport times area and absolute downward transport times area and the summed product of water flux and area is then calculated as the sum of absolute upward flux times area and absolute downward flux times area.

$$\frac{\sum_i a_i (T_i^{\uparrow} + T_i^{\downarrow})}{\sum_i a_i (Q_i^{\uparrow} + Q_i^{\downarrow})}$$

Where  $c_i$  is the total nitrogen soluble nitrogen or nitrate concentration [ $M L^{-3}$ ],  $a_i$  is the area [ $L^2$ ],  $T_i$  is the transport [ $M L^{-2} T^{-1}$ ] and  $Q_i$  is the water flux [ $L T^{-1}$ ]. The arrows in method four refer to the direction of transport and water flow. Method 1, 2 and 4 are applied in this study.

- The aggregation method for assessing a regional average concentration (area weighted, flux weighted) influences the result to some extent. The area weighted concentration is used for evaluation of the nitrate concentration in groundwater, since the proportion of an area exceeding a certain concentration value is a research item. The flux weighted concentration is used for the evaluation of the nitrogen and nitrate concentration in drainage water. The evaluation of surface water quality occurs often at the outlet of a catchment, the total load and total water discharge of the entire catchment should then be taken into account.
- The band width or the range of a certain entity in this study is defined by the difference between the 82.5% and the 17.5% value of the variable distribution. The variable distribution is composed from the results of a certain district of groundwater class, taking account for the area of the plots.
- The following method is applied for the calculation of the decrease of the nitrate concentration over 5m groundwater depth, averaged for a certain area or groundwater class:
  - o The flux weighted annual nitrate concentration is calculated for the mean lowest groundwater level and 5m below this level for each plot;
  - o The 10 year averaged concentration is computed for both depths on the basis of the annual concentrations;
  - o The concentration decrease per plot is determined by one minus the ratio of these 10 year averaged concentrations;
  - o A “decrease” distribution is setup for the plots within the area of group of plots considered, taking account for the area of the plots;
  - o The average decrease value and the 17.5% and 82.5% decrease value are derived from this distribution.
- A nitrate concentration decrease with depth can be attributed to 1) a historical evolution of the land management; 2) a removal by denitrification; or 3) the dilution with other water types. In this study a possible dilution is only due to seasonal upward seepage flow, since the lateral groundwater inflow from higher adjacent areas is not accounted for in the STONE model. Also in a wet sandy soil cluster with predominantly upward seepage flow at the depth of 5m below MLG, the seepage water can be mixed with polluted infiltration water, because of the averaging of different hydrological conditions within the cluster. The relatively dry plots in the regional model within the wet cluster can have a predominantly downward flux at this depth and nevertheless belong to the “wet” groundwater class. The dilution factor is derived from the ratio between downward flow and the upward seepage flow at 5m below MLG level, according to:

$$\text{dilution factor} = \frac{\text{upward seepage flow}}{\text{upward seepage flow} + \text{downward flow}}$$

The decrease of the nitrate concentration by dilution with seepage water can be expressed as the complement:

$$\text{decrease by dilution factor} = \frac{\text{downward flow}}{\text{upward seepage flow} + \text{downward flow}}$$

The “decrease by dilution” is a maximum number based on the assumption that the upward seepage water has a zero concentration. The seasonal upward seepage at this depth can contain some nitrate leached in a previous infiltration period.

### 3 STONE model calibration and validation

#### 3.1 Model calibration on observed potential denitrification rates and previously simulated nitrate concentrations

For the evaluation of nitrogen and nitrate balances, a fixed level of the MLG-depth was chosen. The implications for the assessment of nitrate concentrations in groundwater were evaluated (see Appendix 5). It was concluded that the method of calculating flux weighted nitrate concentrations at MLG-level overestimates the concentrations in the first meter below a fluctuating groundwater level with 10%.

In the regular development cycle of the STONE model, the moisture response curve for denitrification in sandy soils is calibrated on observed nitrate concentrations in the 'LMM'-network (Willems *et al.*, 2008 Groenendijk *et al.*, 2008, in prep.). In the framework of this study two additional data sources became available for refinement of the model:

- organic matter schematization as briefly described in Par. 2.2 and described in more detail in Appendix 3
- potential denitrification rates of sediment samples as measured in the laboratory (Velthof *et al.*, 2008).

After introducing the refinement of the organic matter schematization the STONE model was calibrated on the potential denitrification data. For this purpose, the STONE model was adjusted to generate output with respect to potential denitrification rates at 20°C for the subsoil between mean lowest groundwater level (MLG) and 5 m below this level and the results of the individual samples were aggregated to potential rates per boring location (Fig. 3.1). An extensive description of the calibration procedure followed is given in Appendix 5.

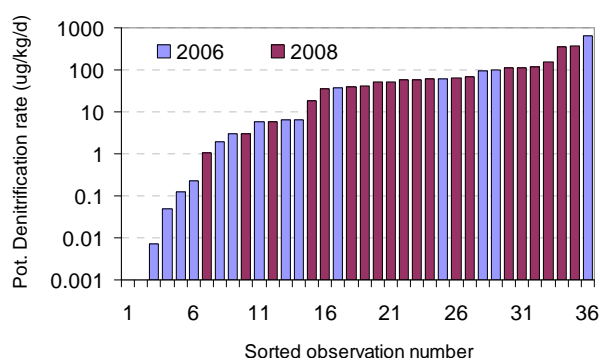


Fig. 3.1 Potential denitrification rates measured in sediment samples and aggregated per boring location

From these data it was concluded that the median value of the aggregated observations amounts to  $40 \mu\text{g kg}^{-1} \text{d}^{-1}$ . Initially the reference version of the STONE model (Willems *et al.*, 2008; Groenendijk *et al.*, 2008, in prep.) overestimated the potential denitrification rate 5–10 times. The parameter to be adjusted was chosen on the basis of a tentative sensitivity analysis. It appeared that the reaction rate constant of the dissolved organic matter pool influenced the potential denitrification rate the most. Different model runs with adjusted values for this parameter were conducted and it was concluded that a value of 11.7% times the original value yields a median potential denitrification rate results that fits the observations well. Fig.3.2 depicts a distributions curve of the number of STONE plots within a certain class of potential denitrification rate. It can be seen that after the adjustment, the potential denitrification rate amounts to 20–50  $\mu\text{g kg}^{-1} \text{d}^{-1}$  for most of the STONE plots.

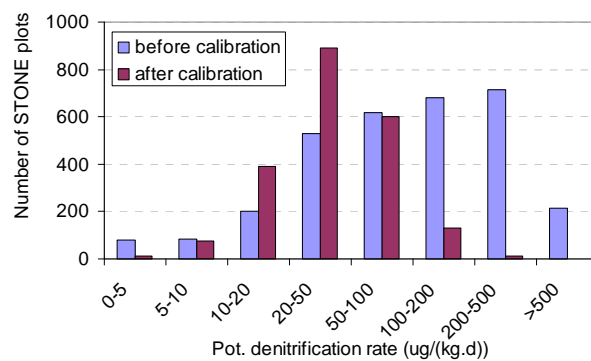


Fig. 3.2 Potential denitrification rate in the soil layer 5m below the groundwater level, before and after calibration on aggregated measured results

Since both the organic matter schematization and the parameterization of organic matter transformation were adjusted, there was a need to re-calibrate the moisture response curve for denitrification. This was done by running the model with variations of the most sensitive parameter of this curve and comparing the results to the results obtained by Willems *et al.*, (2008). It was concluded that the critical parameter of the curve should be set at a lower value, which indicates that denitrification starts at lower moisture saturation values than in the reference model. Aggregated final results of the calibration of the two parameters are given in Fig. 3.3. After calibration of the concentrations at MLG-level, the nitrate concentrations at 5m below this level (Fig. 3.3 right) are significantly higher for most of the sand district – groundwater class clusters.

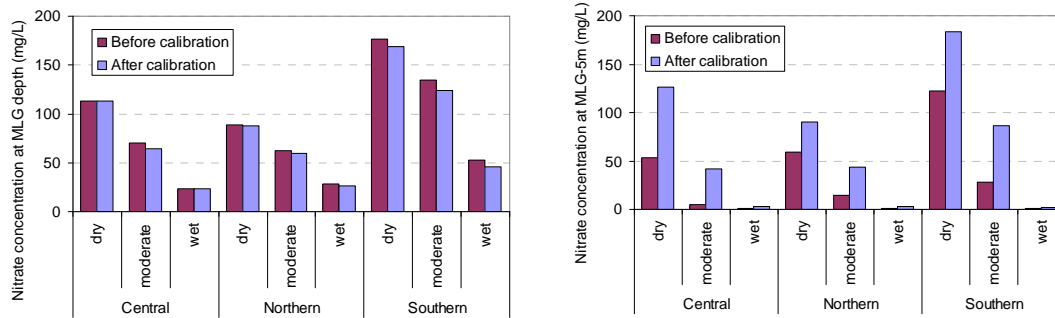


Fig. 3.3 Flux weighted nitrate concentration at MLG depth (left) and at 5m below MLG depth (right) before and after the calibration on potential denitrification rates and previously simulated nitrate concentrations in the study of Willems et al., 2008

### 3.2 Model validation at regional scale on nitrate profiles with depth

Simulated nitrate concentrations were validated by comparing with observed nitrate concentration in monitoring networks (see Par. 2.4 and Appendix 4). The number of simulations plots for each groundwater class – sand district cluster is large enough to allow a statistical analysis. The band width of the simulated nitrate concentration is indicated by the 17.5% – 82.5% interval of the result distribution (Fig. 3.4). The position of the MLG level and the position of 5m below MLG level are indicated by horizontal bars. The height of a bar shows the variation of the levels, calculated as the average level plus or minus the standard deviation.

The observed concentrations are median values of time series in different wells of a monitoring network. Each dot in Fig.3.4 represents an observation location. A LOWESS smoothing line of the observed concentrations has been added to the graph to get an impression of the trend. The span width of the LOWESS procedure amounted to 50% which means that for each point of the line 50% of total population of observations, nearest with depth, was taken into account. In some cases, the number of observations is too small and the distribution of observed values at greater depth is too asymmetric to allow for a sound statistical analysis.

The band width of the simulated results is smaller than the range of the observations. This is maybe due to the number of observations which is far less than the number of simulation results used to draw the result band. Another reason can be the differences of the spatial scale. The observations refer to the point scale and the model simulations are performed for homogeneous areas (STONE-plots) ranging from 500 – 5000 ha. The model consists of a number of simulation plots and each plot represents an area with averaged characteristics of a soil unit, a geological unit, a land use and land management unit and a surface water management unit. Possible variability within such an area has been averaged out already in the model input. The result band width refers to the variability of results of the STONE-plots.

It can be seen that for the dry soils, the nitrate concentrations increase slightly with depth. For the wet soil of the Central and Southern sand district, the model seems to underestimate the measurements, but for the dry soil of the Southern district the model overestimates the observations. For the moderate soils, the fit between simulated concentrations and observed values is good. We consider the results as sufficient to inspire confidence in the use of the model for further analysis.

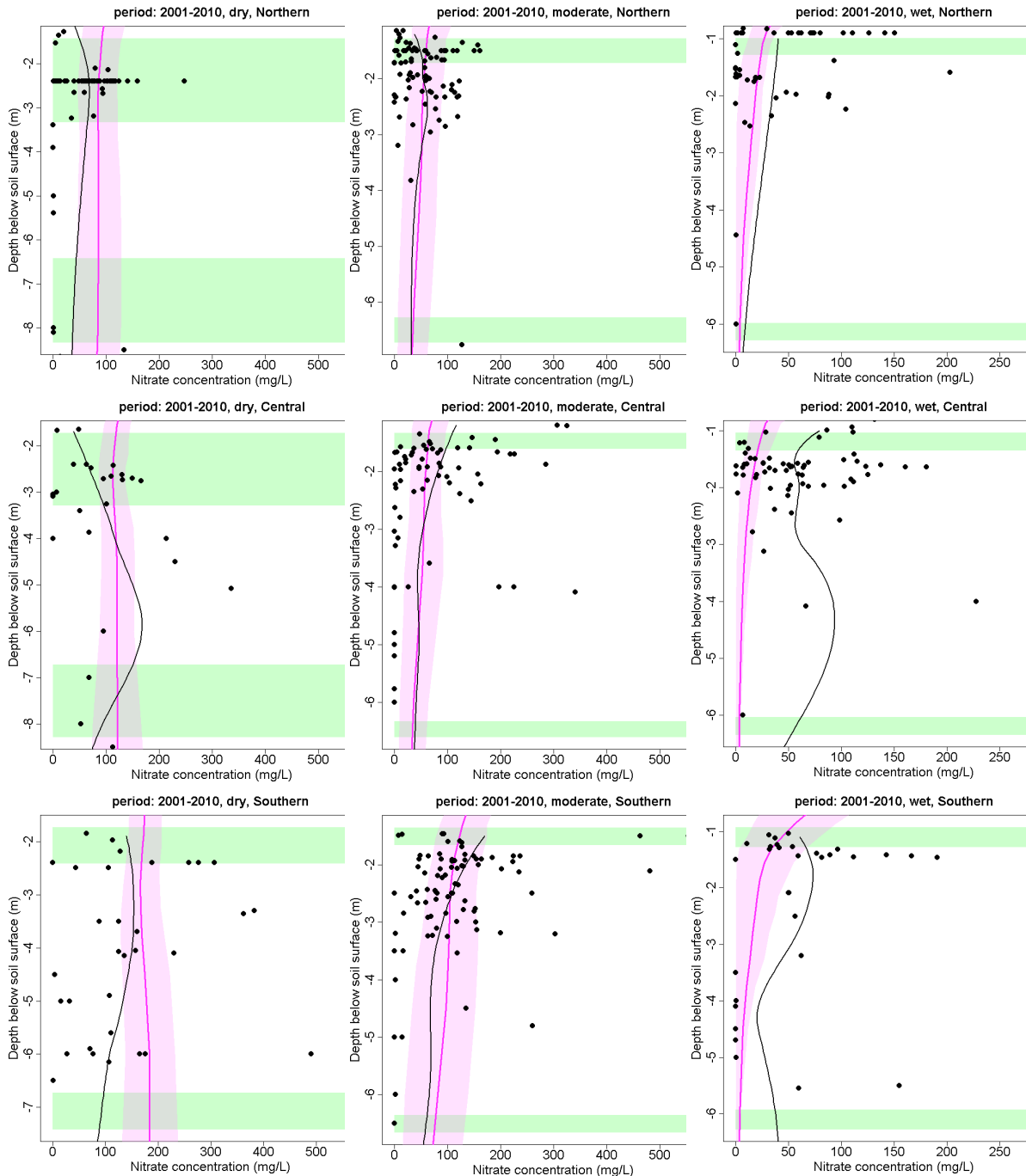


Fig. 3.4 Comparison of simulated areal averaged nitrate concentrations as a function of depth with observed concentrations (dots). Black lines are trend lines generated with a LOWESS smoothing algorithm; light green bars indicate the range of the MLG level and the level 5m below MLG (17.5%–82.5% interval); area average concentrations are indicated by pink lines which are surrounded by the 17.5%–82.5% interval of the concentration distribution.

## 4 Results of the STONE model application

### 4.1 Nitrate concentrations in groundwater

After adjusting and calibrating the STONE model on the basis of state of the art information of organic matter contents of the subsoil and potential denitrification rates, a simulation run was conducted for a future scenario. The assumed N-surpluses do not change after 2015. The time span of the prediction (15 years) is considered as long enough to reach equilibrium between the land use at the soil surface and the nitrate concentrations in groundwater at a certain depth. The resulting nitrate concentrations were averaged for a period of ten years to eliminate the influence of variability of rainfall patterns and were aggregated per groundwater class and sand district. Prediction results for the dry soils are shown in Fig. 4.1.

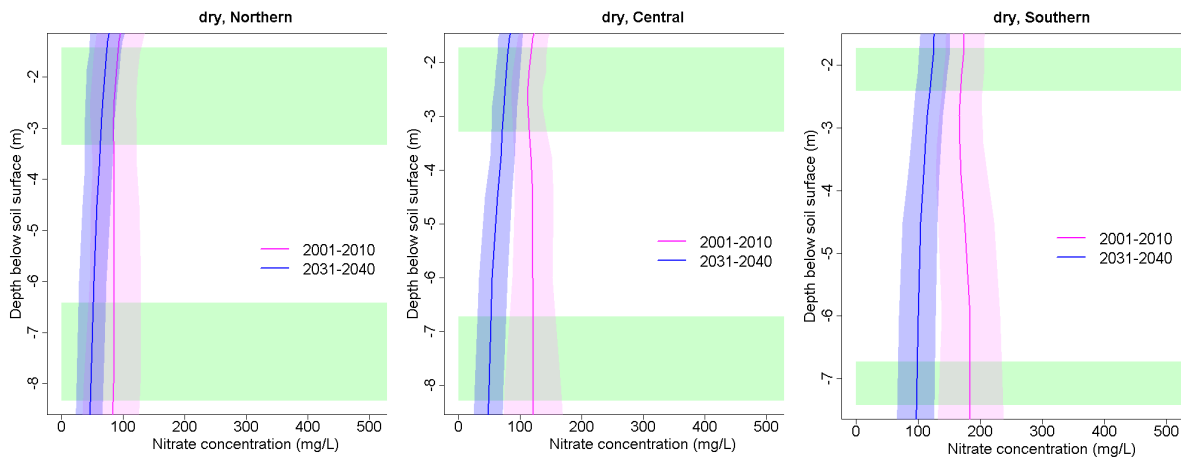


Fig. 4.1 Simulated nitrate concentrations in dry soils as a function of depth, averaged for 2001–2010 and for 2031–2040. Light green bars indicate the range of the MLG level and the level 5m below MLG (17.5%–82.5% interval); area average concentrations are indicated by lines which are surrounded by the 17.5%–82.5% interval of the concentration distribution.

The mean lowest groundwater level can differ for the plots within a certain group or groundwater class. The band width of the MLG values has been depicted by a light green bar. The range of MLG-values is largest for the Northern sand district and smallest for the Southern sand district.

In all sand districts the future nitrate concentrations (2031–2040) decrease slightly with depth. The Northern sand district shows the lowest area averaged nitrate concentrations ( $69 \text{ mg l}^{-1}$  at MLG depth and  $51 \text{ mg l}^{-1}$  at 5m below MLG). The Central sand district takes up an intermediate position by  $77 \text{ mg l}^{-1}$  at MLG depth and  $54 \text{ mg l}^{-1}$  at 5m below MLG and the Southern sand district exhibits the highest nitrate concentrations ( $124 \text{ mg l}^{-1}$  at MLG depth and  $100 \text{ mg l}^{-1}$  at 5m below MLG). Although a decrease of 18–24  $\text{mg l}^{-1}$  is

predicted at 5m below MLG relative to the values at MLG depth, the future concentrations still exceed the 50 mg l<sup>-1</sup> standard value.

The difference between the 82.5% and the 17.5% value of the result distribution for a certain cluster was used to indicate the band width (Fig. 4.2). The difference between the 82.5% value and the 17.5% value coincides more or less with a value two times the standard deviation. The main results per groundwater class are depicted in Fig. 4.2; band widths per groundwater class for the main sand districts are given in Appendix 7. Not only are the concentrations lower in the future (period 2031–2040) than for the first period, also the band widths are smaller. The “median” concentrations are slightly lower than the “average” concentrations.

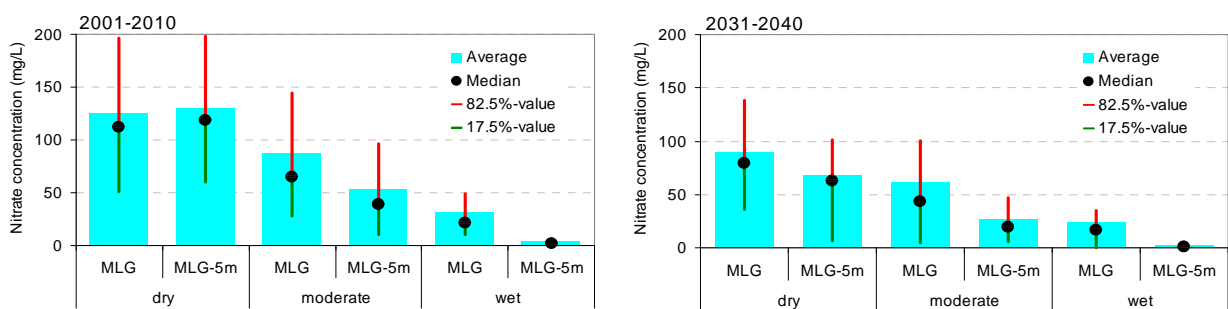


Fig. 4.2 Statistical properties of the area weighted nitrate concentrations at MLG depth and 5m below MLG for two periods and for three groundwater classes

For the dry soils in the Northern sand district the band width of future concentrations amounts to 52 mg l<sup>-1</sup> at MLG and 43 mg l<sup>-1</sup> at 5m below MLG. For the Central sand district band widths of 44 mg l<sup>-1</sup> and 45 mg l<sup>-1</sup> are calculated for the concentration at MLG and 5m below MLG and for the Southern sand district the band widths comes to 52 mg l<sup>-1</sup> and 59 mg l<sup>-1</sup>. The relative band widths at 5m below MLG are larger than the relative bandwidths at MLG depth due to the lower concentrations at MLG–5m.

The dependence of the nitrate concentration on the groundwater class can be clearly seen from Fig. 4.2. The moderate sandy soils show an average nitrate concentration at 5m below MLG which exceeds 50 mg l<sup>-1</sup> in the first period. For the period 2031–2040 an average concentration of 27 mg l<sup>-1</sup> is predicted for the 5m–MLG level. The 82.5%–value at 5m–MLG level is similar to the 50 mg l<sup>-1</sup> standard value. The wet soils show nitrate concentration below this standard value, also the 82.5%–value of the result distribution for 2001–2010 does not exceed this value.

Both the nitrate fluxes and the concentrations are relevant for the assessment of the decrease of nitrate with depth. The reduction of nitrate with depth is assessed by calculating the ratio between the nitrate fluxes at 5m below MLG level and the fluxes at MLG level (Table 4.1). The decrease of concentrations and the ranges of the decrease are

given in Table 4.2. The method for calculating the concentration decrease is explained in Par. 2.6.

*Table 4.1 Ratio between downward nitrate transport at MLG–5m and nitrate downward transport at MLG level*

		Groundwater class		
		Dry	Moderate	Wet
North	2001–2010	91%	47%	6%
	2031–2040	69%	34%	5%
Central	2001–2010	98%	39%	3%
	2031–2040	65%	25%	1%
South	2001–2010	99%	51%	2%
	2031–2040	76%	38%	2%
average	2001–2010	96%	46%	4%
	2031–2040	72%	33%	2%

The dry soils show the highest ratios for both periods. Although Fig. 4.1 shows an increase of the current concentrations with depth for the Central and the Southern district, the fluxes at greater depth are lower. The water fluxes also decrease with depth and compensate for the concentration increase with depth. For the dry areas an average ratio is assessed at 96%. In the current situation, hardly any reduction of the nitrate flux occurs. The future value is 72% on average with 69% for the Northern sand, 65% for the central sand district and 76% for the Southern sand district. The current values are influenced by both the land use history of the last decades and the nitrate removal by denitrification and the future values represent more or less the impact of solely denitrification. Although the relative reduction is higher in Northern sand district than in the Southern district, the absolute reduction is lower due to the lower concentration in this district. The ranking of districts with respect to the reduction of future nitrate fluxes also holds for the moderate and wet soils. The differences between the two periods are less pronounced for the moderate and wet soils.

An indication of the range of concentration decrease is given in Table. 4.2.

*Table 4.2 Averaged concentration decrease between MLG level and 5m below MLG level. Numbers between parentheses indicate the 17.5% and 82.5% value of the distribution*

		Groundwater class			
		Dry	Moderate	Wet	Average
North	2001-2010	1% (-29% ; 31%)	41% (2% ; 76%)	84% (75% ; 98%)	31% (-17% ; 84%)
	2031-2040	25% (9% ; 39%)	56% (28% ; 87%)	86% (73% ; 97%)	47% (15% ; 88%)
Central	2001-2010	-8% (-31% ; 16%)	44% (21% ; 80%)	84% (71% ; 98%)	47% (-3% ; 93%)
	2031-2040	29% (16% ; 43%)	68% (48% ; 90%)	88% (79% ; 97%)	66% (35% ; 94%)
South	2001-2010	-6% (-25% ; 14%)	40% (10% ; 72%)	89% (82% ; 99%)	35% (-9% ; 95%)
	2031-2040	20% (8% ; 33%)	56% (34% ; 80%)	89% (82% ; 99%)	51% (15% ; 95%)
average	2001-2010	-4% (-29% ; 23%)	42% (11% ; 78%)	85% (75% ; 98%)	38% (-10% ; 92%)
	2031-2040	24% (10% ; 39%)	61% (39% ; 87%)	88% (78% ; 98%)	56% (20% ; 93%)

On average the decrease of future nitrate concentrations between MLG and 5m below MLG amounts to 24% for the dry soils, with 25% for the dry soils of the Northern district, 29% for the Central district and 20% for the Southern district. The band width ranges from

10%–39% for the dry soils on average. Band widths of the dry soils in the different districts are of the same order of magnitude. For the current situation a slight increase of concentrations with depth is simulated. The band width for the current situation is larger than for the future situation. The future fertilization rates are less diverging than the rates of the last decade rates. In the fertilization scenario more or less uniform levels are assumed per crop type.

The decrease of future nitrate concentrations in the moderate soils is 61% on average, with 56% for the Northern district, 68% for the Central district and 56% for the Southern district. The band width ranges from 39% to 87% for the total group of moderate soils. For the wet soils the decrease of future nitrate concentrations ranges from 78% to 98% with 88% as an average value. The band widths for the total area with a certain district are very large. This indicates a large variability. The average decrease value per district is only a weak indication exposed to many uncertainties.

## 4.2 Nitrate- and total N-transport to surface waters

Total-N transport to surface waters can be a major threat for surface water by causing eutrophication. Total-N consists of multiple components: nitrate, ammonium and dissolved organic nitrogen. The simulated transport depends on the water flows and the concentrations. The water flows for the groundwater class – sand district clusters are presented in appendix 11. It should be kept in mind that dry soils are defined by the Mean Highest Groundwater Level deeper than 80 cm below soil surface. When field ditches are present, they have often bottom depths ranging from 1 – 1.5 m. For this reason, a large number of model plots in the “dry” class discharge their precipitation excess during winter time to adjacent surface waters. The net water flux passing at MLG depth amounts to 320 mm yr<sup>-1</sup> for dry soils. A small part of it (40 mm yr<sup>-1</sup>) is conveyed to surface water and the other part flows downward to deeper layers. Combined with high nitrate concentrations, the water flux amounting to 40 mm yr<sup>-1</sup> can yield high loads. The high concentrations in soil combined with discharge during winter periods results for the dry soils to a load of 25 kg ha<sup>-1</sup> yr<sup>-1</sup> in the first period and a load of 17 kg ha<sup>-1</sup> yr<sup>-1</sup> in the second period, respectively.

For the moderate soils the downward water flux at MLG level amounts to 245 mm yr<sup>-1</sup> where 125 mm yr<sup>-1</sup> leaves this layer sideways to surface waters and 150 mm yr<sup>-1</sup> flows downward to deeper layers. In some moderate soils, an upward seepage flux compensates the downward flux partially. For the total area, the net downward flux is 120 mm yr<sup>-1</sup> on average. In these soils with a moderate groundwater class, the total nitrogen transport equals 38 and 25 kg ha<sup>-1</sup> yr<sup>-1</sup> for the first and the second period.

In the wet soils, half of the precipitation surplus is conveyed to surface waters in the top soil above the Mean Lowest Groundwater level. The remaining part (165 mm yr<sup>-1</sup>) enters

the upper 5 m groundwater zone and is mixed with an upward seepage flux which has a density of the same order of magnitude. The water flow from this specific layer to the surface water amounts to 315 mm yr<sup>-1</sup>. The upward seepage flux at 5m below MLG of 195 mm yr<sup>-1</sup> is partly compensated by a seasonal downward flux at this depth of 45 mm yr<sup>-1</sup>. The total nitrogen load on surface waters from the wet soils was estimated at 39 and 31 kg ha<sup>-1</sup> yr<sup>-1</sup> for both periods. It can be seen from Fig. 4.3 that the nitrate contribution to the total N transport to surface waters decreases with higher groundwater levels. The contribution of nitrate transport from the upper 5m groundwater zone to the total N load to surface waters amounts to 43%; 47% and 26% for the dry; the moderate soils and the wet soils in the first period and 40%; 43% and 23% in the second period(Fig. 4.3).

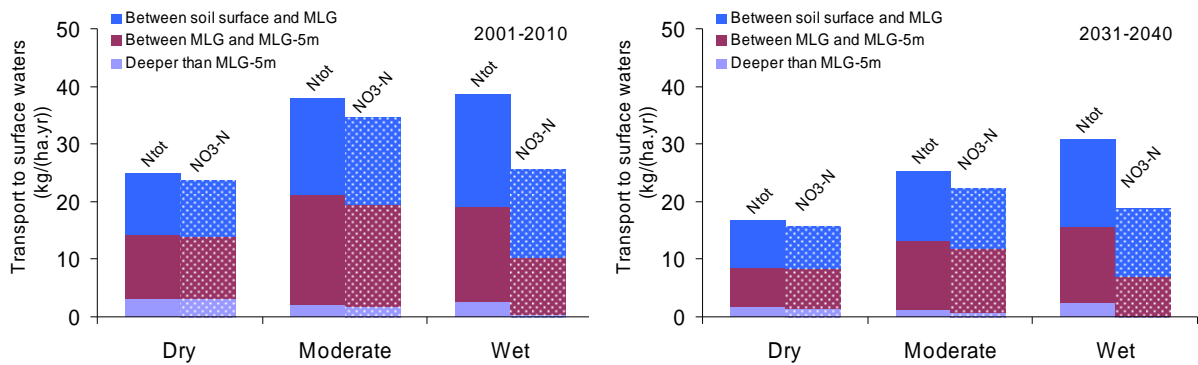


Fig. 4.3 Total-N and nitrate-N transport to surface water from three soil layers for three groundwater classes and for two periods

The nitrate from the layer deeper than 5m below MLG contributes 13% and 10% to the total load for the dry soil in the first and the second period. Transport through the deeper layers is attributed to water flow along deeper pathways to streams in sloping landscapes. The nitrate transport in the 5m deep upper groundwater zone is approximately the same for dry soils as for wet soils. The water flows through this layer is less for the dry soil, but the concentrations are higher. In the wet soil the nitrate concentrations are lower because the nitrification process is faced with less favourable conditions in the wet soils, whereas moisture conditions are more in favour of the removal of nitrate in the upper soil layers by denitrification.

The proportion of the nitrogen input in the layer between MLG and 5m below MLG transported surface waters is given in table 4.3. The input is composed from the influx at the top of this layer and the depletion of the storage already present in this layer.

Table 4.3 Nitrogen transport to surface waters from the layer between MLG and 5m below MLG expressed as percentages of the input into this layer.

		Groundwater class		
		Dry	Moderate	Wet
North	2001-2010	12%	29%	58%
	2031-2040	13%	32%	61%
Central	2001-2010	10%	30%	55%
	2031-2040	12%	34%	58%
South	2001-2010	7%	26%	66%
	2031-2040	7%	29%	69%
average	2001-2010	9%	28%	60%
	2031-2040	10%	31%	63%

The proportion in the dry soils is ca. 10% and 31% and 63% in the moderate and wet soils. There is only a little variation between the sand districts. Also the results for the two periods are more or less the same. Although the contribution of the storage depletion to the total input in this layer is different for both periods, no major changes in time of the proportion can be observed.

The highest total-N transports from the 5m groundwater zone are estimated in the first period for the moderate soils and in the second period for the wet soils (Fig. 4.4).

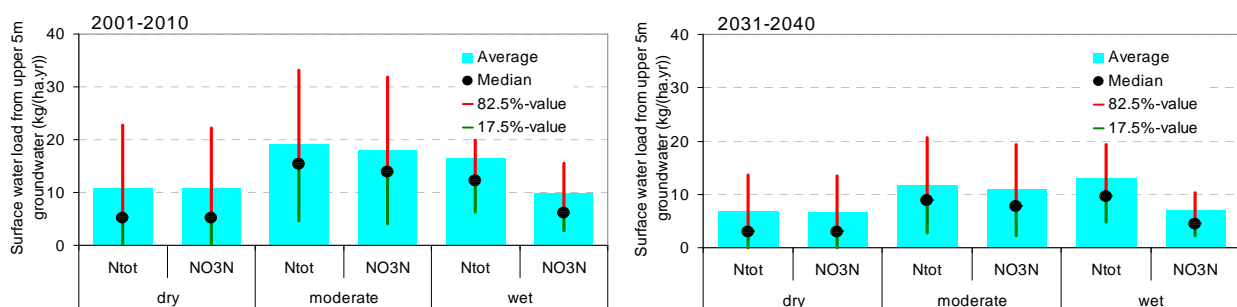


Fig. 4.4 Statistical properties of the total-N and nitrate-N transport to surface water for three groundwater classes and for two periods

The band width of total-N and nitrate transport has been defined by the difference between the 82.5% and the 17.5% value of the result distribution for a certain cluster. The relative band width (band width divided by the cluster average) is relatively high for the dry soils and lower for the moderate and wet soils. The relative band widths are lower in the second period after at least 15 years of constant land management than for the first period with decreasing fertilization rates. Results sub-divided for the main sand districts are given in Appendix 9.

### 4.3 Actual and potential denitrification in groundwater

The actual denitrification in soil and groundwater is in the STONE model calculated as a function of the potential denitrification rate, the presence of nitrate and the soil moisture

conditions. The potential denitrification rate is described as a function of microbial respiration processes. The largest part of the actual denitrification occurs in the top soil between land surface and MLG. For the topsoil, the model predicts the lowest actual denitrification rates in the dry soils and the highest in the wet soils. In the wet soils, the nitrate loss by denitrification in the topsoil and by lateral transport to surface waters result to low nitrate concentrations in the groundwater zone below MLG and as a consequence the actual denitrification rates are low in this zone. After 20 years of constant fertilization at a lower rate than the current one, the actual denitrification is estimated at 64, 81 and 91 kg ha<sup>-1</sup> yr<sup>-1</sup> for the dry, the moderate and the wet soils.

The removal of nitrate by denitrification in the current situation ranges from 111 kg ha<sup>-1</sup> yr<sup>-1</sup> for dry soils to 142 kg ha<sup>-1</sup> yr<sup>-1</sup> for moderate soils. The wet soils take an intermediate position with an average denitrification of 133 kg ha<sup>-1</sup> yr<sup>-1</sup>. The future prediction for the second period amounts to 60 kg ha<sup>-1</sup> yr<sup>-1</sup> for the dry soils, 81 kg ha<sup>-1</sup> yr<sup>-1</sup> for the moderate soils and 88 kg ha<sup>-1</sup> yr<sup>-1</sup> for the wet soils. The contribution of the different soil layers to the total denitrification is depicted in Fig. 4.5. The denitrification in the topsoil between soil surface and the MLG-level is largest and smallest in the subsoil below 5m-MLG. This is due to the combination of the nitrate concentration and the microbial respiration rate which are highest in the topsoil. Especially the denitrification in the wet soils occurs mainly in the top soil. The decreased nitrogen losses as caused by reduced fertilization rates result to lower denitrification rates in the second period relative to the rates in the first period.

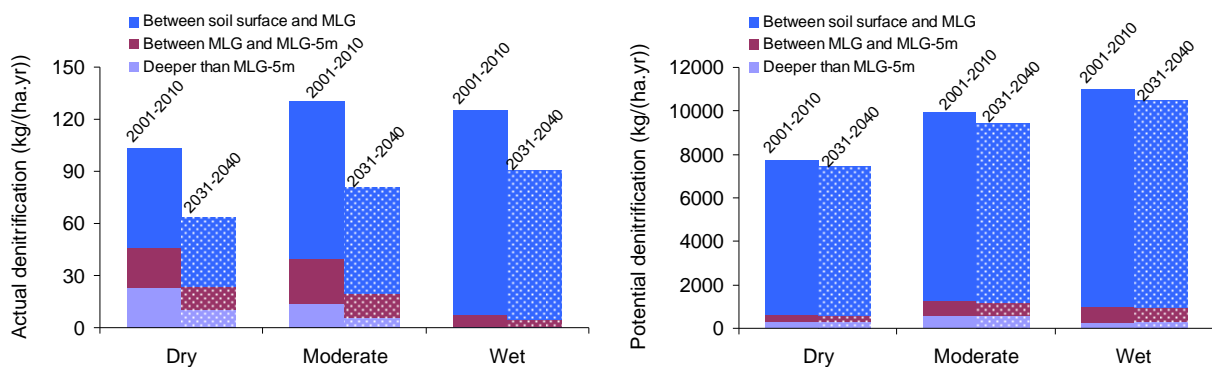


Fig. 4.5 Actual denitrification (left) and potential denitrification (right) in the distinguished soil layers for two periods and for three groundwater classes

The potential denitrification rate is calculated from the potential soil organic matter respiration rate. The availability of nitrate and the moisture saturation degree as such do not influence the potential rates. The model predicts much higher potential denitrification rates than actual denitrification rates, especially for the top soil. For this zone, the rate ranges from 87 – 92% of the total rate. The potential denitrification rate in the soil zone between MLG and 5m below MLG ranges from 4 – 7% of the total rate in the soil. In spite of the relatively thin top layer of the wet soils, the potential rate is highest for this groundwater class. The reduction of the potential denitrification after 30 years amounts to

3 – 5% and is mainly due to the reduction of inputs of organic compounds in animal manure.

The band widths of the actual denitrification in the upper 5m groundwater zone below MLG are depicted in Fig. 4.6.

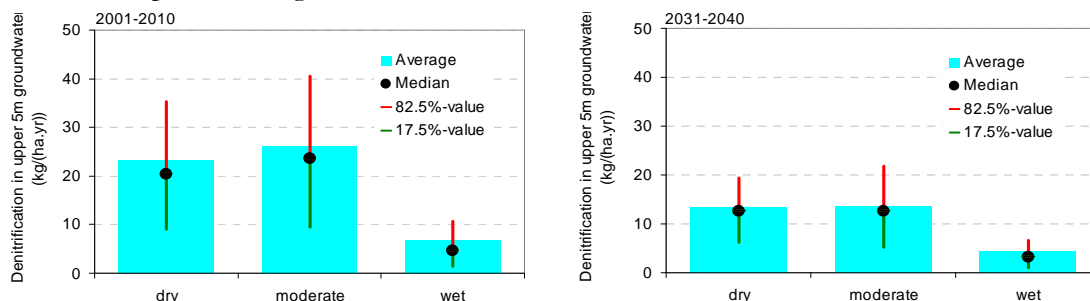


Fig. 4.6 Statistical properties of the denitrification in the upper 5m groundwater zone for three groundwater classes and for two periods

For the dry soils, the band width ranges from 26 kg ha<sup>-1</sup> yr<sup>-1</sup> in the first period to 13 kg ha<sup>-1</sup> yr<sup>-1</sup> in the second period. The 10 kg ha<sup>-1</sup> yr<sup>-1</sup> decrease of the average value is mainly due to the decrease of the dissolved organic matter input to this layer. The decrease of the average denitrification rate in this layer amounts to 13 and 2 kg ha<sup>-1</sup> yr<sup>-1</sup> for moderate and wet soils. The band width for moderate soils decreases from 31 kg ha<sup>-1</sup> yr<sup>-1</sup> for the first period to 17 kg ha<sup>-1</sup> yr<sup>-1</sup> for the second period and the for the wet soil the band width decreases from 9 kg ha<sup>-1</sup> yr<sup>-1</sup> to 5 kg ha<sup>-1</sup> yr<sup>-1</sup>. Specific results for the main sand districts are given in Appendix 10.

Similar to nitrogen transport to surface waters, the proportion of the nitrogen input in the layer between MLG and 5m below MLG denitrified in this layer is given in table 4.3.

Table 4.4 Denitrification in the layer between MLG and 5m below MLG expressed as percentages of the input into this layer.

		Groundwater class		
		Dry	Moderate	Wet
North	2001-2010	19%	37%	39%
	2031-2040	21%	38%	38%
Central	2001-2010	22%	45%	47%
	2031-2040	23%	42%	46%
South	2001-2010	19%	38%	36%
	2031-2040	19%	36%	34%
average	2001-2010	20%	41%	41%
	2031-2040	21%	39%	40%

From the total nitrogen input in the layer between MLG and 5m below MLG in dry sandy soils, ca. 20% is denitrified. This proportion amounts to ca. 40% in both moderate and wet soils. However, the absolute rate in wet soils is lower than in moderate soils. The differences between the districts and the differences between the periods are small (19% - 23%) for the dry soils and largest for the wet soils (34% - 47%). Within the cluster of dry soils, the highest proportions are predicted for the Central sand area.

#### 4.4 Nitrate and total-N balances in groundwater

The nitrate balance of the upper 5m groundwater zone below MLG consists of the following items: net input at the top (downward transport subtracted with upward transport at MLG level), upward transport from below at 5m below MLG level, downward transport to deeper layers at 5m below MLG level, denitrification within the specific layer and transport to surface waters from this specific zone (Fig. 4.7). Specific results of the nitrate balance for the main sand districts are given in Appendix 11.

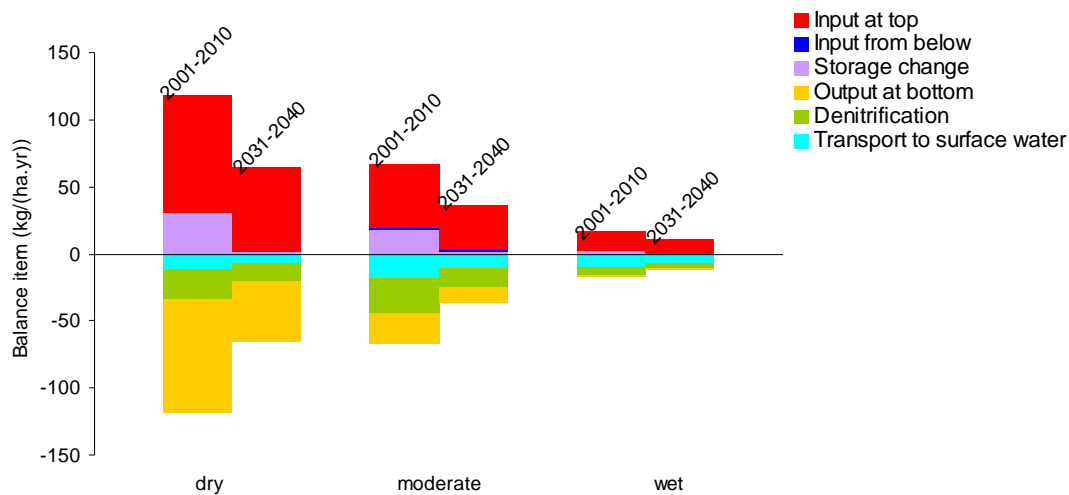


Fig. 4.7 Nitrate balance of the soil layer between MLG and 5m below MLG, averaged for all sandy soils for two periods and for three groundwater classes

For the dry soils the net input at the top of the upper groundwater zone comes close to the downward transport at this dept, but for the wet soils the downward transport is 16% - 23% higher than the net transport. The transport terms at the top and at the bottom of this layer are the main sources and sinks in the nitrate balance. It can be seen that the storage change in the first period has a considerable contribution (15 - 28%) to the sources, whereas in the second period the depletion of the nitrate storage approaches is only 3 - 5% of the total input. The input from deeper soil layers to the upper groundwater layer only plays a role for the wet soils (3% of the input). In the dry soils ca. 70% of the nitrate is transported downward to deeper soil layers. For the moderate soils this amounts to ca. 33% and for the wet soils the downward transport is estimated about 5%. The reversible trend can be seen for the transport to surface waters. In the dry soils ca. 10% is transported to the surface water. In de moderate and wet soils this amounts to 29% and 57%. Denitrification is the remaining part of the balance of this 5m groundwater zone and amounts to 20% of the output in the dry soils, 38% of the output in both the moderate soils and the wet soils. The ratio between the output items changes only little with time.

The complete nitrate balance for the entire soil profile is schematically presented in Fig.4.8. The left part of each figure shows the topsoil and the subsoil. The dashed lines refer to the Mean Groundwater Level and the depth 5m below Mean Groundwater Level. The right part of each figure depicts the surface water system at regional scale. Nitrate transport pathways are denoted by arrows. The formation of nitrate within a soil compartment by nitrification has been presented by a bowed arrow. It should be noted that the soil layer below 5m–MLG stretches to 13m below soil surface in the STONE model. This artificial boundary has not been depicted in the schemes. The vertical transport at this level is not presented in the figures, but could be calculated as a closing term from the balance of the deeper soil layer.

The connection between groundwater and surface waters is schematically presented by one field and only one adjacent field ditch or canal, but in reality it can exist of a number surface water systems (field ditches, tile drains, canals, streams), which can be partly connected to fields at greater distance by deep groundwater flow. It should be kept in mind that the area of a simulation unit ranges from 500 – 5000 ha and covers a large number of fields and surface water elements.

The input by nitrification of ammonium exceeds the direct input by fertilizer and atmospheric deposition to a large extent. Most of the nitrogen input comes with organic bounded nitrogen and ammonium in animal manure. In grassland, the turn-over of plant residues can also be a substantial part of the organic nitrogen cycle. Most of the supplied organic bounded nitrogen is mineralized to ammonium within the growing season and the nitrification rate in the topsoil is also very high, which results to high nitrification rates. The crop off take is calculated by subtracting the crop residues which arose during the growing and on the occasion of the harvest from the gross uptake of nitrogen by the plant roots. The net extraction by crops in Fig. 4.8 consists of a mixture of the values for grassland, silage maize and arable land. The crop off take is largest for the soils with the moderate groundwater class.

The source by depletion of the nitrate storage is greater than the loss by denitrification. The total nitrate transport to surface waters amounts to  $23.6 \text{ kg ha}^{-1} \text{ yr}^{-1}$  for the dry soils. Half of it ( $10.8 \text{ kg ha}^{-1} \text{ yr}^{-1}$ ) comes from the layer 5m below MLG.

The nitrification in the top layer between soil surface and MLG decreases with time due to the reduction of fertilization rates up to 2015. The storage change in the different soil layers approaches zero in the second period. The flux averaged nitrate concentrations in Fig. 4.8 are expressed as nitrate-N concentrations and should be multiplied by 4.57 to obtain nitrate concentrations. Although the nitrate transport in the first period for the dry soils at 5m below MLG is lower than the transport at MLG level, the flux averaged nitrate concentration is higher at the MLG–5m level. In the dry soils, the vertical water flow pattern decreases stronger with depth than the vertical nitrate transport pattern. In the

second period the reduction of the nitrate transport at 5m below MLG relative to the transport at MLG level amounts to 28% on average and the reduction of the vertical water flux equals 14% (see appendix 11). Both the volume weighted total N and nitrate concentrations reduce 20% over the first 5m of groundwater depth.

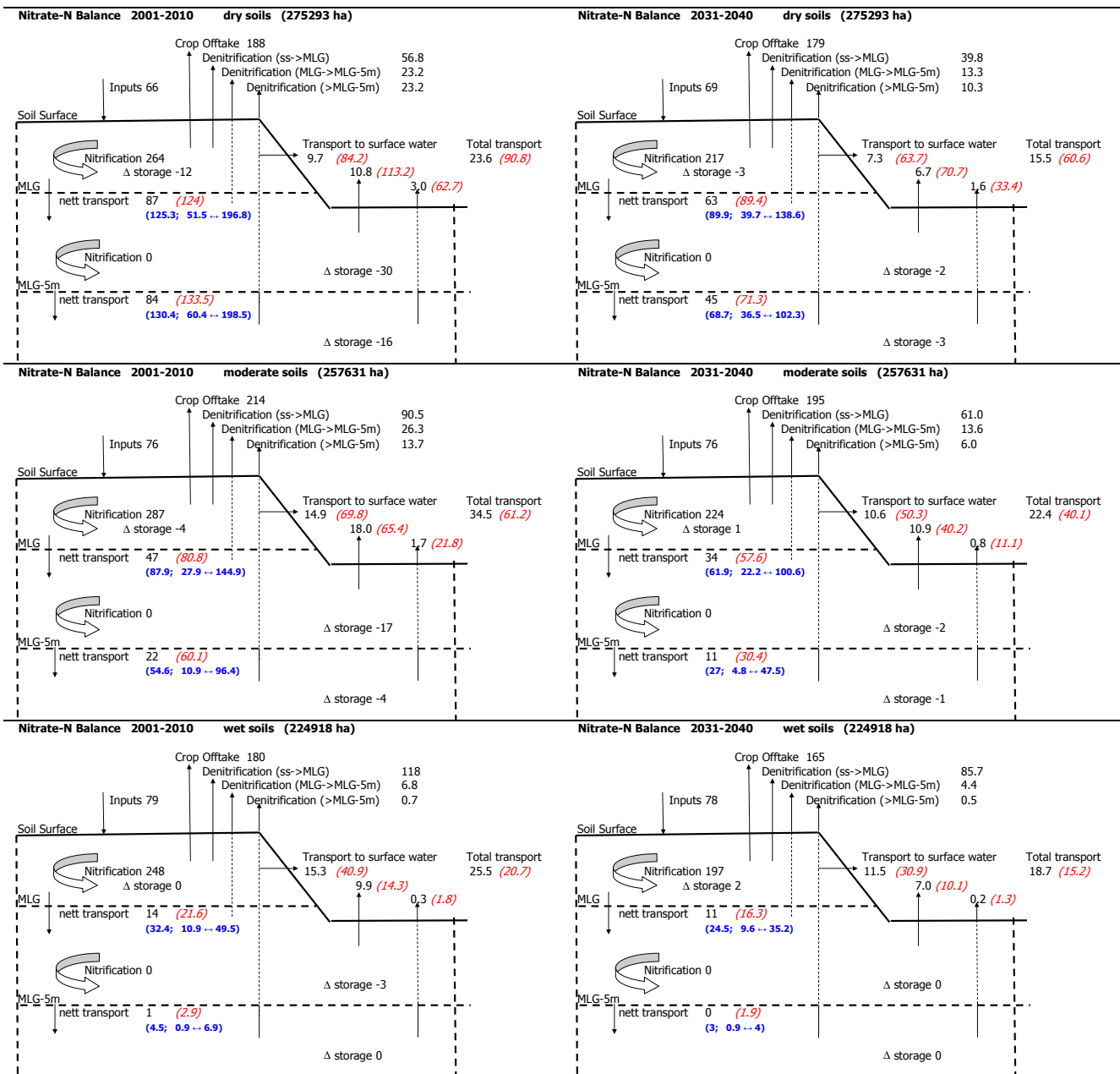


Fig. 4.8 Schematic representation of nitrate balances of three soil layers for two periods and for three groundwater classes.

Legend:  
 MLG Mean Lowest Groundwaterlevel (m-ss)  
 MLG-5m 5 m below the Mean Lowest Groundwaterlevel (m-ss)  
 19.5 Fluxes over system boundaries (kg/ha N)  
 (11.4) Flux weighted nitrate concentration (mg/l N)  
 (4.5; 0.9 ↔ 6.9) Area averaged nitrate concentration (mg/l); p17.5%-value ↔ p82.5%-value

In the moderate soils, the downward nitrate transport at MLG level amounts to 47 and 34 kg ha<sup>-1</sup> yr<sup>-1</sup> for the first and the second period. The decrease of vertical nitrate transport between MLG level and 5m below MLG level equals 25 and 23 kg ha<sup>-1</sup> yr<sup>-1</sup> for the first and the second period which means a reduction of 53% and 68% relative to the input in the upper groundwater zone at MLG-level. The vertical water flux decreases with 50% over this depth and the resulting nitrate concentration reduces by 48%.

The wet soils show much lower vertical transport rates at MLG level, while the nitrification rate is lower and the denitrification rate is higher than in moderate or dry soils. At the level of MLG the downward water rate equals 165 mm yr<sup>-1</sup>, but at 5m below this level, a net upward seepage occurs at a rate of 145 mm yr<sup>-1</sup>. The upper 5m groundwater zone contributes with 315 mm yr<sup>-1</sup> to the total water discharge of 562 mm yr<sup>-1</sup>. The vertical nitrate transport reduces with 98% over the upper 5m groundwater zone.

The effects of calculating flux averaged concentrations on the basis of accumulated nitrate transport and water flow over a certain time span are analyzed in appendix 8.

Additional results for Northern, Central and Southern sand region are given in appendix A11. Appendix 12 gives the results the nitrate balances of the upper 5m groundwater zone per sand district. For the dry soils it can be seen that the flux weighted nitrate concentration in discharge to surface water is lower than the nitrate concentrations at MLG or at MLG-5m. This is due to the method of calculating the concentration on the basis of accumulated transports and flows over longer time spans. An analysis of the influence of the time span on the averaged concentration is given in Appendix 8.

## 5 Discussion on uncertainties and band widths

### 5.1 Applicability at field and farm scale

#### 5.1.1 Setup of the field scale modelling study

A validation study for four dairy farms on sandy soils was conducted to gain insight in the model performance at field level. The study focused on the core simulation models within the STONE model chain: SWAP for water flow (Van Dam *et al*, 2008) and ANIMO for nutrient dynamics and leaching (Groenendijk *et al*, 2005). The study was sub-divided into a number of actions:

1. *Attribution of default input data on the basis of STONE.* Although a number of model inputs are available from field investigations, most of model input had to be assigned from other data sources. To fill this data gap, the model input of STONE plots was used. The selection of STONE-plots is conducted on the basis of similarity with respect to land use, soil mapping unit, geo-chemical characteristics of the sub-soil, groundwater class and distance to the farm. The distribution between grassland and maize was not exactly known at each of the observation points and the land use can change every year. For each location a grassland and a maize plot was selected from the STONE database;
2. The hydrological model SWAP was calibrated on groundwater time series in the nearest wells of the groundwater monitoring network. The SWAP model was attuned by:
  - Imposing the rainfall figures of the most nearby rainfall station instead of the regionally up scaled rainfall figures of the STONE model
  - Examination of the drainage levels and drainage resistances on the basis of a description of the local geo-hydrological system (Janssen, pers. comm.)
  - Calibration by adjusting the boundary bottom flux (upward / downward seepage)
3. Refinement of the ANIMO input data by using farm specific data with respect to fertilization rates and nitrogen excesses;
4. Refinement of the ANIMO input by imposing the organic matter contents in the borings as observed in the study of Fraters *et al.*, (2006);
5. Evaluation of the model results;
6. Tentative sensitivity analysis of the ANIMO model with respect to the assignment of organic matter to pools and to the decay rate constants of organic matter pools;

Background data and calibration results are presented in appendix 6.

## 5.1.2 Field scale validation results

In the field scale validation study, the hydrological model was adjusted only for rainfall data. A tentative calibration was conducted on the basis of scarce groundwater level observations in the fields and groundwater time series of nearby monitoring wells. The fertilization rates were tuned on the basis of farm scale information and the organic matter contents in the subsoil below the Mean Lowest Groundwater level were adjusted on the basis of measurement results of a sampling campaign (Fraters *et al.*, 2006; Griffioen and Velthof, 2008).

The annual predicted nitrate concentrations in the upper meter of the groundwater were compared with the measured concentrations extracted from monitoring results. The measured concentrations are only given as aggregated values at farm scale and information on the land use history per observation location is not available. It should be noticed that the comparison concerns predicted values at field scale and observations at farm scale. The predicted values given for the four locations are liable to different hydrologic regimes (groundwater level) and different subsoil organic matter contents. Results for both grassland and silage maize are presented (Fig. 5.1). Information on crop rotation was not available. A constant land use for the “grassland” and the “maize” variant was assumed.

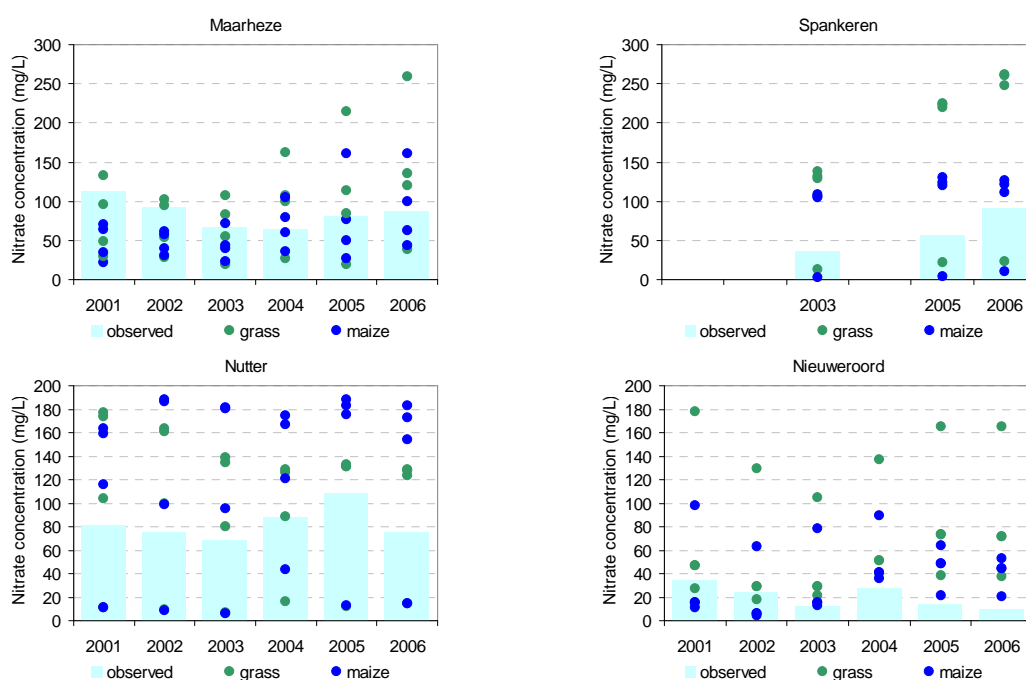


Fig. 5.1 Farm averaged observed and simulated nitrate concentrations in the first meter groundwater at the four validation farms.

The range of predicted nitrate concentrations in the first meter below a dynamically fluctuating groundwater level is largely due to differences in soil, land use and groundwater

level. The concentrations in the upper groundwater concern observations taken once or only a few times per year, but the model predictions concern averages of a complete year. Both the observations and the model predictions (appendix 6) show strong variations within a year. A mismatch between the predicted results and observed concentrations may be due to differences of observation timing and prediction time scale.

The average of the predicted concentration time series for Maarheeze fits reasonably with the averaged value of the observations. The observed value lies within the range of predicted values, but for the other farms the model overestimated the measured values. For the Spankeren and the Nutter farm the overestimation is partly due to the groundwater levels which were calibrated on only very sparse information on groundwater levels, with possibly limited representativity. For both farms the predicted groundwater levels in the majority of the fields are low (appendix 6). The fertilization level at the Nutter farm has evolved in time. Fertilization rates at the grassland fields decreased, whereas the rates at the maize fields increased. The rates were derived from the average fertilization rates at farm level.

The Nieuweroord farm is characterized by large deviations of the phreatic level within short distances and a complex organic matter stratification of the subsoil (Fraters *et al* 2006). The groundwater level in some fields had unexpected low values and another field had very wet conditions. Although the subsoil schematization was adjusted for the organic matter content, the organic matter contents between one and three meter below surface are still low because only the subsoil organic matter contents deeper than the Mean Lowest Groundwater level were adjusted (Fig. 5.2). The measured nitrate in the first meter of the groundwater stems from this zone and it is expected that thin layers of organic matter rich sediment are present and have influenced the nitrate concentrations. A more accurate organic matter sampling at this depth can improve the model results for this farm. The relatively high gradients of the phreatic level point to horizontal water flow in the upper ground water. The nitrate observations in the monitoring wells can be influenced by a number of unaccounted factors.

Results are presented of the original model version (STONE2.3) before calibration of groundwater levels in Fig. 5.2 as well as the results of the refinement of fertilization rates and subsoil organic matter contents and the final model version for the fields. For each of the farms one field is presented for which a tentative sensitivity analysis was conducted with respect to organic matter reaction rates. The results of the other locations are presented in Appendix 6. The result of each location consists of two figures: the left one presents the organic matter schematization of the subsoil of the original model and the model refined on the basis of field specific fertilization rates and organic matter contents of the subsoil. The results for the subsoil organic matter schematization of the corresponding plots in the adjusted model STONE have also been given for organic matter contents, but not for nitrate concentrations.

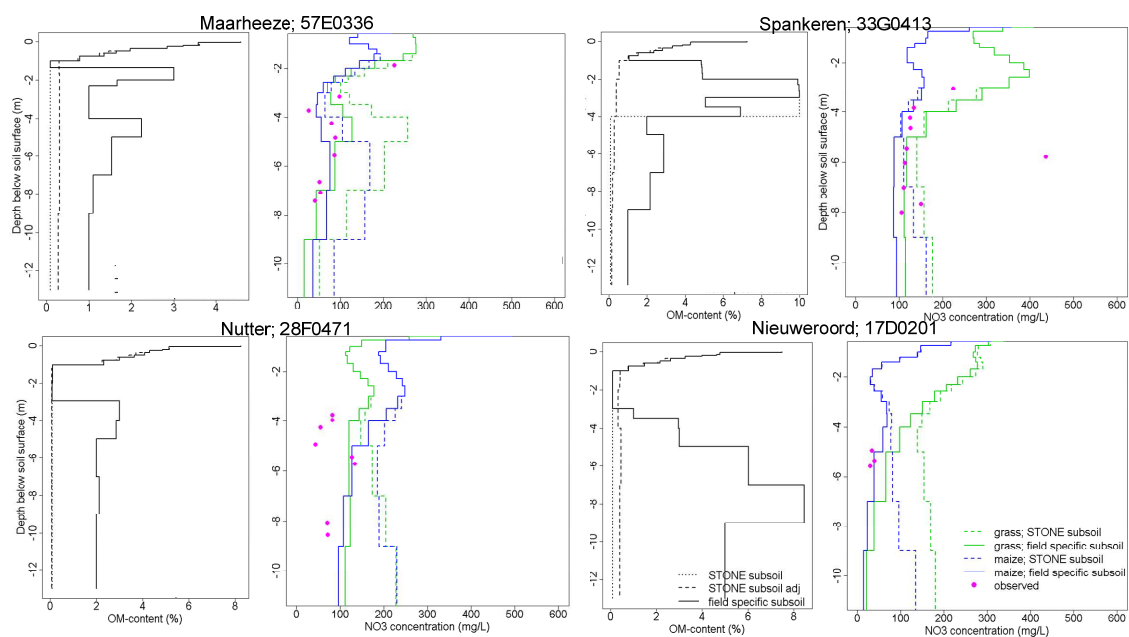


Fig. 5.2 Solid organic matter contents in the STONE schematization and in the field study (left part of the figures) and observed and simulated nitrate concentrations for grassland and silage maize as a function of depth for fields of the four validation farms. Results for the STONE schematization are indicated by interrupted lines and results for the schematization on the basis of observed OM-contents are given by solid lines.

The nitrate concentrations are given for both grassland and silage maize because information on the accurate land use history at the measuring location is not available and it is expected that both land use types have influenced the nitrate concentrations. The field specific organic matter data of the subsoil indicate much higher values than is assumed in the STONE schematization. This applies to both the original STONE2.3 schematization and the adjusted version used in the regional analysis. The field specific organic matter contents are higher than the values assumed in the STONE schematization, only in one case the values are lower (Maarheeze; 57E0337). This is by coincidence, since the STONE schematization is based on a large number of sediment samples.

The higher organic matter contents in the subsoil and the refinement of fertilization information for the farms yield lower predicted nitrate values than was calculated with the original STONE model. The decrease of the nitrate concentration at 5m below soil surface due to the new subsoil schematization is largest for Maarheeze and smallest for Spankeren.

For three of the four presented locations, the agreement between model predictions and observed data is good. The concentrations are only overestimated for the Nutter location. Examining the complete set of observations in 2005 and simulated nitrate concentrations at greater depth (Appendix 6), it is shown that the model overestimates the observed data for four of the 10 locations with sufficient data to make a comparison. For 6 of the 10 locations the agreement between predictions and observed data is satisfactory.

Although the agreement between simulated and observed concentrations is better for the model with field specific data than for the original STONE model, the results give rise to the following remarks:

- The results presented in Fig. 5.2 refer to only one period. The comparison of simulated annual nitrate concentrations in the first meter below a fluctuating groundwater level with observations in the LMM monitoring network shows a weak result (Appendix 6). The hydrological model simulates a groundwater level decrease in 2004–2006 as a result of relatively dry years which is not reflected in the observed groundwater time series. The simulated increase of nitrate concentrations is also not reflected by the farm averaged nitrate concentrations in the LMM monitoring network.
- The comparison of annual averaged prediction results with occasional observations may lead to a mismatch. Field observations with a higher time resolution can support a better understanding of similarities and differences between predictions and observations.
- The quality of field specific data was too weak to allow for a statistical validation. Better calibration and validation results will be obtained if accurate groundwater level series of the nitrate monitoring locations and information on the historical land use at field scale become available.
- Prudence is called for the application of the model with a regional schematization of land use, soil and hydrology at field scale or at farm scale. The results of a regional model application are only applicable at the model scale itself.
- The variability of the predicted concentrations at field scale is large. For the interpretation of farm scale averaged concentrations for model validation studies, accurate information on the land management practice and history, the soils and the hydrological regimes of each of the fields is required.
- The weak validation results for the nitrate concentrations in the upper meter at field scale do not restrain the model application at regional scale, due to a large number of uncertainties involved in this study. This conclusion is supported by the predicted nitrate concentrations at greater depth (Fig. 5.2).

### **5.1.3 Influence of reactivity of solid organic matter**

The potential denitrification rate in the STONE model depends on:

- the solid organic matter content
- the assignment of the organic matter to pools with different reactions rates
- the dissolved reactive organic matter (DOM) concentration

Only potential denitrification rates under laboratory conditions in subsoil samples were observed. The interpretation of these data to field conditions relies on model assumptions. The conclusions of this study would be better underpinned if experimental data on actual denitrification rates were available, but this type of in-situ observations in groundwater were not available.

Although the amount of DOM as calculated to be present in the subsoil is small relative to the solid organic matter content, the reaction rate of the DOM-pool is assumed to be a thousand times larger than the solid organic matter transformation rate. An indicative sensitivity analysis showed that the DOM pool determines the potential denitrification rate at the most. The influence of DOM on the denitrification has been probably overestimated and the impact of pyrite has been underestimated. The degree to which DOM is formed and is leached from top soils and its reactivity is described in the STON model as strongly related to the land use and the land management. The reactivity of the DOM pool in the subsoil was calibrated on the basis of laboratory observations of potential denitrification rates in sediment samples. The comparison of model results with laboratory observations is hampered by:

- The observations were done in soil cores of only some decimetres thickness. To make them comparable to the model parameters assigned to the subsoil, the results were up scaled by calculating a weighted average value per drilling location. The non-linear features of the nitrate removal process are ignored by assuming the denitrification capacity and rate to be distributed homogeneously with depth.
- The number of drilling locations is limited to 36, whereas the number of STONE plots amounts to some thousands. The observations show a wide range between 0.001 and 1000  $\mu\text{g kg}^{-1} \text{d}^{-1}$  and only the median value of 40  $\mu\text{g kg}^{-1} \text{d}^{-1}$  was chosen to calibrate the model.

The model calibration conducted in this study should be seen as a first attempt and further methods and data to refine the model input should be searched for. The regional patterns with respect to the distribution of organic matter and other reducing components should be taken into account.

The influence of pyrite oxidation is not described in the STONE model, but can be imitated by defining a distinguished pool with a rate constant applicable to pyrite and a assimilation/dissimilation ratio set to zero. This means that none of the pyrite oxidation products is incorporated into a stable organic matter pool. The denitrification as a result of pyrite oxidation can have impact at the local scale, but the influence on water quality at regional and national scale is unclear. The investigation in Appendix 3 showed that pyrite is present in only a (small) part of the samples and attributing a pyrite fraction to all layers and plots in the model would certainly lead to an overestimation of its effect. However, if the influence of pyrite occurrence on regional denitrification patterns should be accounted for, this can be accomplished by defining a highly reactive pool in the model.

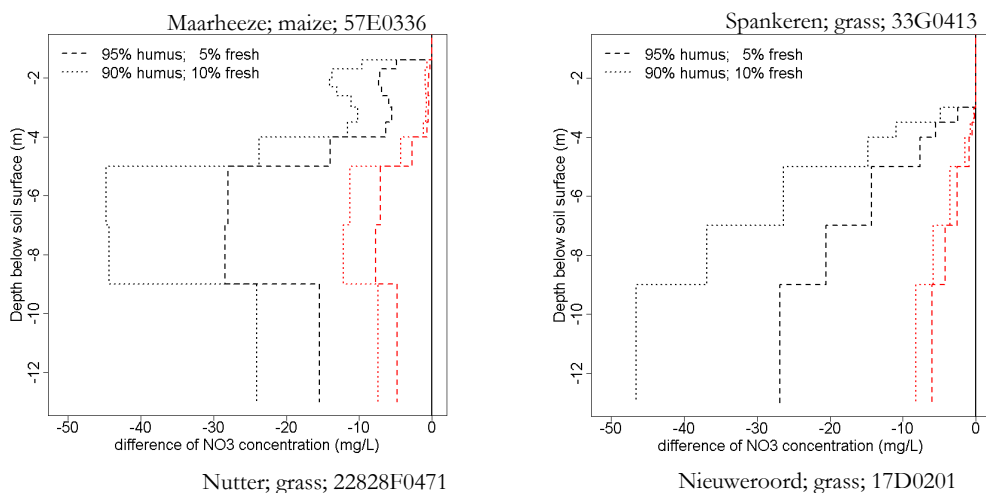
It is expected that accounting for the regional pattern of pyrite contents in the subsoil would lead to slightly other results for the main sand districts. The highest pyrite contents are found in the Northern sand district and the lowest values are found in the Central district. If these data are incorporated in the model, the Northern sand district would show a higher denitrification rate. Incorporation of this process requires a new model calibration on observed potential denitrification rates and on observed nitrate concentration in LMM

monitoring network. It is unclear whether the nitrate concentrations in the Central and the Southern district would be affected by such model modifications.

The reactivity of the organic matter pools was studied for the field scale simulations by defining alternative options for the attribution to the pools. An additional pool was defined which can be considered as either a highly reactive organic matter pool or a pyrite pool. In the reference model 100% of the solid organic matter in the subsoil is attributed to a stable pool with a low reaction rate. Simulations with alternative options for the organic matter attribution and with reduced rate constants have been conducted:

1. 5% of the material is attributed to a relatively highly reactive pool and 95% to the stable organic matter pool;
2. 10% of the material is attributed to a relatively highly reactive pool and 90% to the stable organic matter pool;
3. as option 1, but with rate constants set at 10% of the original value;
4. as option 2, but with rate constants set at 10% of the original value.

The rate constant at the annual averaged temperature of the stable organic matter pool is set at  $0.01 \text{ yr}^{-1}$  in the reference model and the rate constant of the relatively highly reactive pool at the annual averaged temperature takes a value of  $0.22 \text{ yr}^{-1}$  under optimal conditions. The ratio 1:22 is more or less reflected by the proportion attributed to the relatively fast pool in option 1 and 3. The resulting nitrate concentrations as a function of depth have been presented as a difference relative to the results of the model run with the subsoil organic matter 100% attributed to the stable pool (Fig. 5.3). The black lines refer to option 1 and 2, whereas the red lines refer to option 3 and 4.



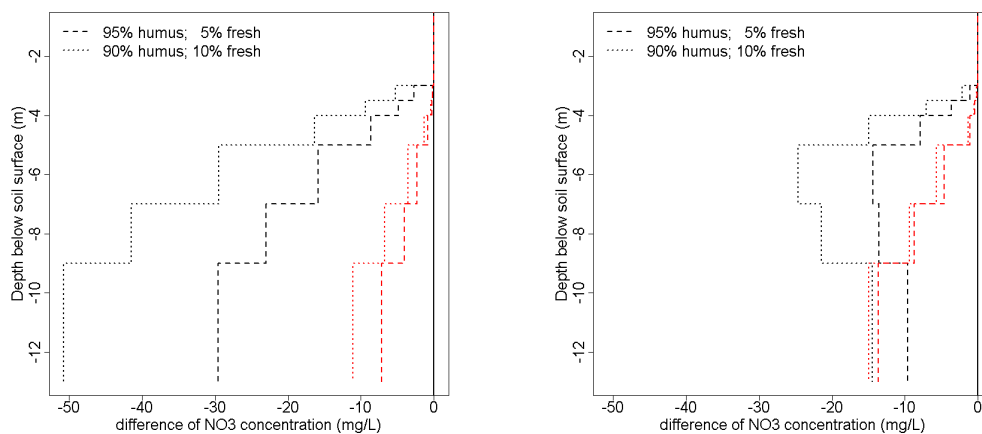


Fig. 5.3 Difference of nitrate concentrations relative to the concentrations predicted by the model with the subsoil organic matter 100% attributed to the stable pool. The black lines refer to the options with 5 or 10% of subsoil organic matter attributed to a relatively highly reactive, the red lines refer to the same options with reduced reaction rate constants

The alternative sub-division over different pools, where 10% is assigned to a relatively highly reactive pool, results to a reduction of  $50 \text{ mg l}^{-1}$  nitrate at greater depth for the Maarheeze, Spankeren and Nutter farm, but ca.  $10 \text{ mg l}^{-1}$  for the Nieuweroord farm. In the reference model the organic matter contents in the subsoil amount up to 2% for the three first farms and 5 – 8% for the Nieuweroord farm. The nitrate concentrations appear less sensitive for the attribution to the pools for the higher organic matter contents.

The reduction of the rate constants by 90% results in much lower concentration differences at greater depth relative to the reference values. For the Maarheeze farm the adjusted process parameters yield an increase of more than  $40 \text{ mg l}^{-1}$  nitrate at a depth of 8 m below soil surface. The reduction is largest between 5 and 9 m-s.s. for the Maarheeze and the Nieuweroord farm, while the reduction increases with depth for the other farms. The shape of the reduction pattern complies to a large extent with the concentration course with depth (Fig. 5.2).

It should be noted that a recalibration of the reaction rate constant of dissolved reactive organic matter and the critical moisture content as trigger for denitrification in the STONE model was not conducted. If an alternative option for organic matter attribution to pools or the incorporation of a pyrite pool is considered for predictions of future nitrate concentrations, a recalibration of the model is required. The presented nitrate concentrations in Fig. A13.1 – A13.4 only show the sensitivity of nitrate concentrations for the model parameterization and should not be valued highly.

The important role of dissolved reactive organic matter pool as a driving force for denitrification is not confirmed by the study of Velthof (2006). However, Velthof focuses on Soluble Organic Carbon which is not identical to the dissolved reactive organic matter pool in the model. We think nevertheless that the presence of DOM as the main source for denitrification is an overestimation of its role. The results of the tentative sensitivity

analysis show that an alternative attribution of solid organic matter to pools in the subsoil affects the nitrate concentration quite heavily. The model has the potential ability to describe the denitrification process as a function of solid organic matter and pyrite contents. A model refinement with respect to the role of pyrite and the reactivity of DOM should be accompanied by a critical analysis of the reactivity of the subsoil organic matter. The total organic matter is considered as potential degradable and this is questionable for subsoil organic matter compounds. A part of the subsoil organic matter occurs as stable “black carbon”. Information on the proportion is lacking and the total pool of organic matter is assumed to be reactive and the decay rate is described by one lumped rate constant.

If the model would have been extended with pyrite as a reductant to simulate denitrification, it would have required a recalibration on observed nitrate concentrations. The STONE model has been calibrated on a nationwide dataset derived from results of the LMM monitoring network. A possible accounting for regional patterns of pyrite contents (§2.3, Appendix 3), a reconsidering of the reaction rate of DOM and the distinguishing of a stable “black carbon” part of subsoil organic matter implies the recalibration on observed potential denitrification rates and nitrate concentrations. At present, the dataset of the LMM monitoring network does not allow for such a regionally differentiated calibration.

More results of the tentative sensitivity analysis of the subsoil organic matter quality is given in appendix 13.

## **5.2 Influence of thin peat layers in the subsoil**

One of the supporting activities within the project was the incorporation in the STONE model of the state-of-the-art information with respect to organic matter contents in the subsoil. The STONE model has been adjusted based on new information obtained by Deltares/TNO from the analysis of additional subsoil samples (§2.3, appendix 3). The new information is partly reported by Griffioen *et al* (2006). The implementation of the new information in the STONE model is reported by Van Boekel (2008). It is still a discussion whether relatively thin peat layers as they appear in many field campaigns should be accounted for in the assessment of average organic matter contents. Possibly the thin peat layers contain some stable “black carbon”.

Van Boekel combined the newly derived geochemical information with information from the National Sampling of Soil Units (LSK) database (Finke *et al*, 2001) and concluded that in the sand regions the thin peat layers could better be ignored for two reasons:

- to reach a better fit with the LSK soil data for the subsoil between 1 en 2 m below soil surface (Fig. 2.1).
- The organic matter in the thin organic rich layers in sandy sub-soils is partly inert and should not be assigned to the reactive organic matter pools of the STONE model.

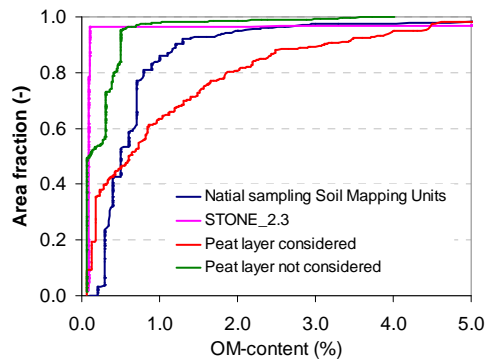


Fig. 5.4 Comparison of the areal exceedance fraction of the organic matter content in the subsoil of sandy soils for LSK-data, the STONE2.3 which served as a reference for this study, and two option for dealing with thin peat layers

The existence of the thin peat layers is an uncertainty one has to deal with and the occurrence of stable “black carbon” is another uncertainty generating issue with respect to the content of reactive organic matter and its reactivity. To gain some insight in the possible consequences of these uncertainties, a simulation run was conducted based on a subsoil schematization where the thin peat layers were supposed to be 100% reactive. The results of the prediction for the second period are given in Fig. 4.13a; 4.13b and 4.13c.

Denitrification depends heavily on the presence of reactive organic matter and an increase of the contents in the subsoil by mixing the thin layers of the model compartments causes an increase of the actual denitrification in the upper 5m groundwater zone.

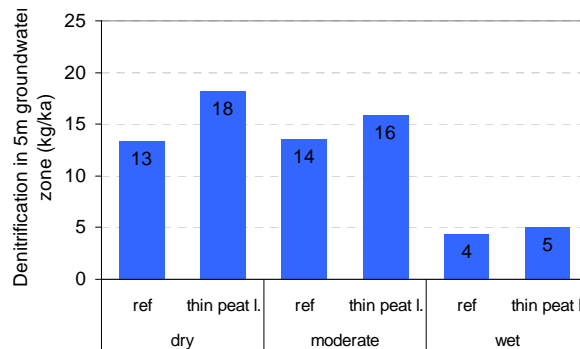


Fig. 5.5a Denitrification in the upper 5m groundwater zone in 2031–2040 simulated by the reference model and simulated by the model adjusted for a maximum influence of thin peat layers

The increase is largest for the dry soils (18 instead 13 kg ha<sup>-1</sup> yr<sup>-1</sup>) and smallest for the wet soils, because the nitrate input rates in this zone are highest for the dry soils.

Taking account for the thin peat layers results in a concentration reduction of 1 mg l<sup>-1</sup> at MLG level and 8 mg l<sup>-1</sup> at 5m below MLG level for the dry soils. The reduction is less for the moderate and wet soils.

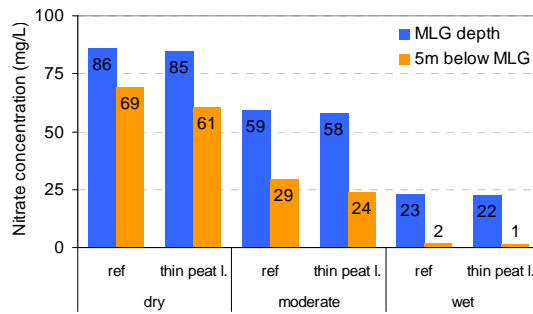


Fig. 5.5b Nitrate concentrations in 2031–2040 simulated by the reference model and simulated by the model adjusted for a maximum influence of thin peat layers

The presence of the thin peat layers can also affect the transport to surface waters due to the increase of the potential denitrification rate. The impact on the transport from the zone between MLG and 5m below MLG has been depicted in Fig. 4.13b. For the dry soils only a minor change of the surface water load from this specific zone is predicted. The difference is largest for the moderate soils, but do not exceed 11% of the predicted value based on not taking account for these layers.

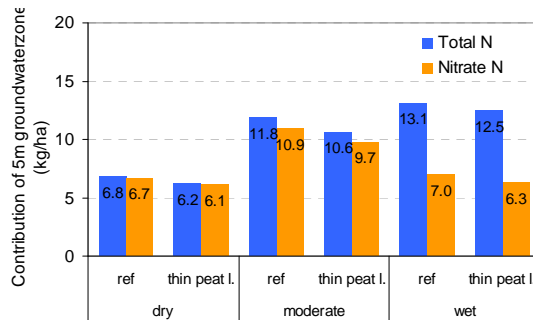


Fig. 5.5c Total N and nitrate-N load on surface waters in 2031–2040 simulated by the reference model and simulated by the model adjusted for a maximum influence of thin peat layers

### 5.3 Influence of drought classification

In the earlier study of Fraters *et al.* (2006) on the implications of lowering the monitoring depth, it is pre-supposed that the precipitation excess in “dry” soils is conveyed vertically to deep groundwater layers. In this study, it appears that “dry” soils contribute to the nitrogen loading of surface waters. The definition of a “dry” soil implies a Mean Groundwater Level deeper than 80 cm below soil surface. During winter time the groundwater level can reach this level, or can rise temporarily to some higher levels. The precipitation excess in such periods is conveyed for an important part to field drains and canals. Also the fields having tile drains at 1 m depth can have a groundwater dynamics that corresponds to the definition of a “dry” soil.

The class of “dry” soils in the STONE model represents a wide range of different hydrological conditions. For the dry soils more than 66% of the area shows a discharge

greater than 50 mm yr<sup>-1</sup> and in more than 36% of the area the discharge exceeds 100 mm yr<sup>-1</sup>. An additional groundwater class was defined to investigate the effects of the drought class definition on the nitrate concentrations in groundwater. The Mean Highest Groundwater Level in this class is greater than 120 cm and the annual discharge in this class does not exceed 100 mm yr<sup>-1</sup>. This criterion applies to 50% of the dry soils area. Volume average nitrate concentrations have been depicted in Fig. 5.6 for two periods for both the “extra dry” soils and the “dry” soils”.

The nitrate concentrations in the “extra dry” soils at MLG level for the first period are 14 mg l<sup>-1</sup> higher than the average concentrations for the “dry” soils. For the second period the difference equals 12 mg l<sup>-1</sup>. At the depth of 5m below MLG level the difference is greater: 26 mg l<sup>-1</sup> for the current situation and 15 mg l<sup>-1</sup> for the second period. Balances for “extra dry” soils and for “dry” soils are depicted schematically in Fig. 5.7.

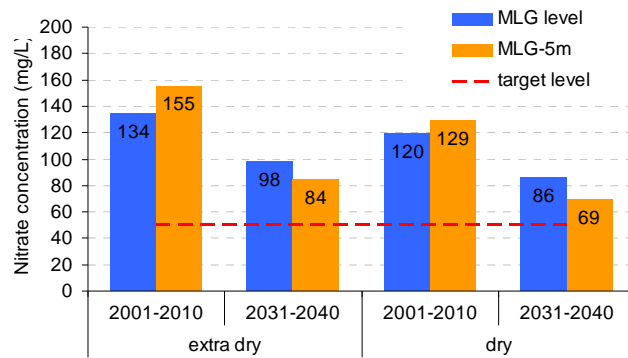


Fig. 5.6 Comparison of volume averaged nitrate concentrations in “extra dry” soils with concentrations in “dry” soils

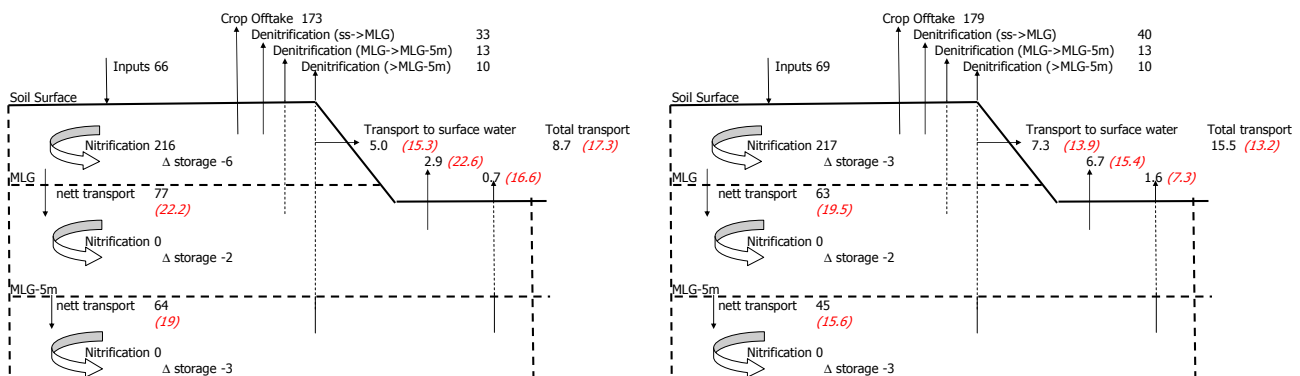


Fig. 5.7 Comparison of nitrate balances of different soils layers in “extra dry” soils (left) with balances in “dry” soils (right).

Denitrification losses in the topsoil of “extra dry” soils and crop off take rates are lower than for the “dry” soils, which leads to higher inputs to the 5m upper groundwater zone. Within this zone, the denitrification rates and the lateral transport to surface waters are lower, which results in 19 kg ha<sup>-1</sup> yr<sup>-1</sup> higher transport rates to deep groundwater. The

reduction of the nitrate transport rates over the first 5m groundwater amounts to 17% for the “extra dry” soils and 28% for the “dry” soils.

#### 5.4 Effects of temporal and spatial aggregation

In this study the evolution of concentrations and fluxes are evaluated by comparing the results of two periods. Averaged values are presented over a range of 10 years. The variation within such a range can be significant, even larger than the differences between the sand districts. For the evaluation of 10 year averaged values, it should be noted that the history still influences the concentrations and fluxes. The age of pore water increases more than proportionally with depth. The age of infiltrated water in dry soils at a depth of 5m below MLG ranges from 5 – 10 years. The first evaluation period (2001–2010) is clearly influenced by the higher fertilisation levels in the years nineties. Fig. 5.8 shows that also the influence of a particularly dry or wet year is noticeable in the concentrations for a number of years.

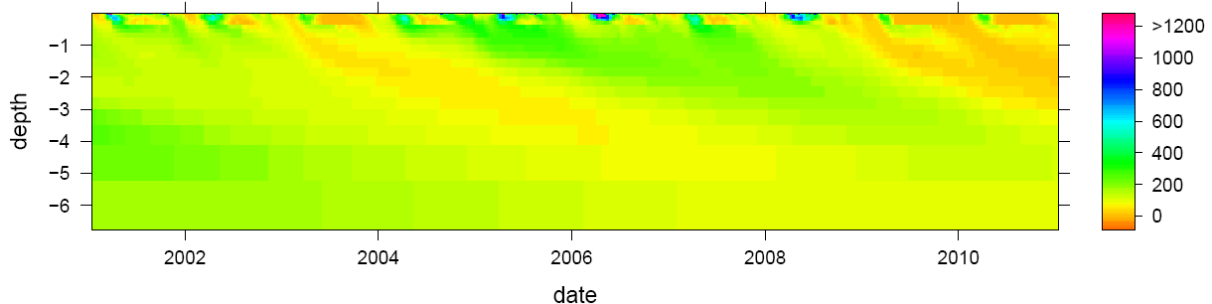


Fig. 5.8 Simulated nitrate concentrations as a function of time and depth for grassland on dry soils in the Central sand district

Fig. 5.8 it was constructed from the results of dry soils covered with grass in the Central sand district. Strong variations were already averaged by the aggregation. But still the plume of relatively clean water that originates from spring of 2003 is visible in the spring of 2006 at 4–5m depth.

The time aggregation also has consequences for the flux-weighted concentration. This concentration is calculated as a quotient of the time integral of the mass flux and the time integral of the water flux. The mass flux and water flux can both have different dynamics, because the course of the actual nitrate concentration at a certain depth can differ from the water flux pattern (Fig. 5.9).

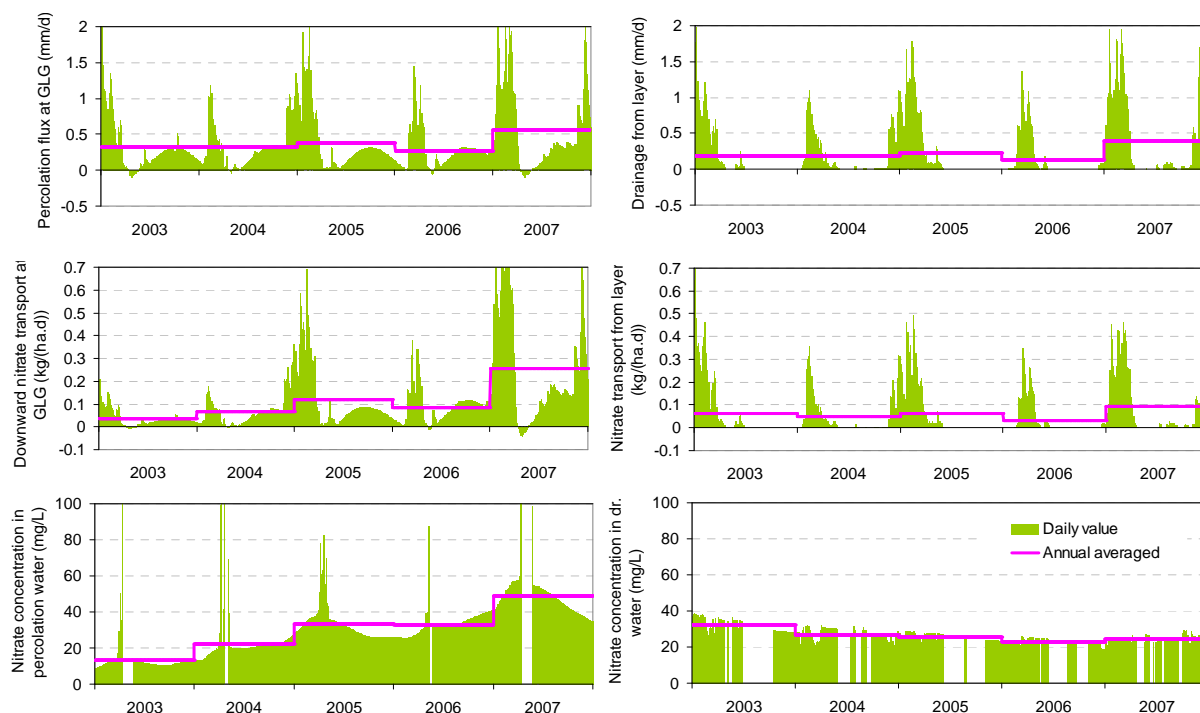


Fig. 5.9 Water flow (top), nitrate transport (middle) and nitrate concentration (bottom) at MLG depth (left) and at the interface between the 5m groundwater zone and surface waters (right) on a daily and an annual scale.

The daily water flux pattern shows peaks which are wiped out in the annual flux pattern. At the MLG-level interface of the 5m thick subsystem the nitrate input has another pattern at the interface between the subsystem and the surface water. The concentration at the MLG-level shows an upward trend, whereas the concentration at the output side (surface water) shows a decreasing course. If one averages all the data over the entire period, as was done in the evaluation procedure of this study, these trends are not visible anymore. In spite of the fact that for the subsystem "5m groundwater zone" both a closing water balance and a closing nitrate balance was calculated, a flux weighted concentration in drainage water can occur which deviates from the average of the top and the bottom concentration of the 5m zone.

The three dimensional solute transport in the upper groundwater is approached by a conceptual 1-D model. In this one dimensional model the water flows vertically to deeper layers and the discharge to surface waters is described by a lateral sink term. The size of a spatial unit ranges from 500 – 5000 ha and the unit covers a large number of fields and surface water elements.

The horizontal flow which may occur is completely attributed to the drainage flow within the calculation unit and the horizontal transport from high infiltration areas to the stream valleys is neglected. The only source of dilution is a possible upward seepage flow in the relatively wet areas. If an upward seepage flow occurs in the wet areas, the concentration in this can be affected by a seasonal downward flow with higher concentrations. Therefore, a

dilution factor derived on the basis of long term averaged downward and upward flows should be considered as a maximum value.

In the conceptual model, the connection between groundwater is schematically described by a lateral sink term in the vertical 1D approach. A possible influence of a highly reactive sediment layer at the ditch bottom of the ditch wall is neglected. Although the residence time in such a layer is small, the passage of this layer can have impact on the nitrate concentrations. The nitrate loads on surface waters presented in this study should be considered as gross estimates without taking account of retention in the surrounding reactive ditch envelope.

The model concepts and the model parameters have been derived for the regional scale. The results apply to this scale and not to the typical field scale as was pre-supposed in the classification of “dry” soils by Fraters *et al.* (2006). In their analysis the “dry” soils have been typified as being vulnerable for nitrate leaching to deeper groundwater bodies and the possible transport to surface waters have been ignored. The main reason is that many “dry” fields are not surrounded by field ditches. In our regional model concept the connection between groundwater and surface waters applies to a number surface water systems (field ditches, tile drains, canals, streams), which can be partly connected to fields at greater distance by deep groundwater flow. Although not directly surrounded by field ditches, a part of the precipitation excess of “dry” soil can be conveyed to surface waters. As a consequence of this drainage concept, the results obtained at the regional scale can not be applied at the field scale. The local circumstances differ often from the regional averaged characteristics of calculation unit.

## **5.5 Fluctuating versus constant depth**

A constant depth in the analysis of the fate of nitrate on the basis of balances, but in the monitoring of the nitrate compliance, a fluctuating depth is used. Flux averaged nitrate concentrations were calculated at the constant depth of the Mean Lowest Groundwater Level by dividing the annual averaged nitrate load by the annual averaged water flux. In the National Program for Monitoring the Effectiveness of the Minerals Policy (LMM), samples are taken from a bore hole equipped with a filter between 25 and 75 cm below the actual groundwater level.

In Appendix 5 a comparison was made of the simulated nitrate concentrations between 0 and 100 cm below the actual groundwater level and the flux averaged nitrate concentrations at the constant MLG-depth. Ten year averaged concentrations were calculated, because it was found that the meteorological variation affects the nitrate concentrations calculated by the two methods in a different way. The ratio between the concentrations calculated by both methods equals 1.11 and 1.09 for the first period and the second period. The flux weighted nitrate concentrations at the constant MLG-depth are on

average 11% and 9% higher than the concentrations calculated by a method which resembles the sampling procedure of the sampling in the LMM.

Appendix 9 shows the time courses of nitrate concentrations in the fluctuating upper meter of the groundwater zone and the flux averaged concentrations at the constant MLG-depth. These figures confirm the results of Appendix 5. The figures in Appendix 9 also show clearly that the difference between both methods is not constant in time. Both quantities react different to climatic variation. Averaged values for the current situation and the future situation with constant, but lower fertilization rates than the current ones, are presented in Table 5.1

*Table 5.1 Comparison of ten year averaged nitrate concentrations in groundwater ( $mg\ l^{-1}$ ) calculated by two methods and the flux averaged nitrate concentration at 5 meter below the Mean Lowest Groundwater Level*

Period	Groundwater class	Fluctuating upper 1 m groundwater	Constant depth at MLG	Dept at 5m below MLG
2001-2010	Dry	114	125	130
	Moderate	80	87	54
	Wet	27	32	4
2031-2040	Dry	82	89	68
	Moderate	55	61	27
	Wet	20	24	3

The concentrations at the constant depth of the Mean Lowest Groundwater level are higher for all groundwater classes. If one want to consider the assessment of fertilizer application standards by using a balance approach for relating the load on surface water to the leaching to the groundwater zone, it should be realized that the balance approach yields higher groundwater concentrations. A correction of 10% seems plausible, but it should be kept into in mind that the nitrate concentrations in groundwater for nearly all combinations exceeds the maximum admissible risk values for total nitrogen in surface waters.

## 5.6 Influence of land use

The N-surplus is the main driving force of the presence of nitrate in groundwater bodies. In the model simulations the N-surpluses decrease with time until 2015 and are constant thereafter. The removal of nitrate in the upper 5m groundwater zone, expressed as the reduction of nitrate concentration between MLG level and 5m below MLG, as a function of the N-surplus was deduced from the model results to examine the relation between nitrate reduction and land use. The results for the second period were clustered per land use type, per groundwater class and per sand district. The results of the dry and moderate groundwater class are shown in Fig. 5.10. A general trend between the reduction of nitrate concentration and the N-surplus is visible. Higher reductions are simulated for higher N-surpluses. Also the groundwater class exerts influence on the reduction. The simulated

reductions are higher for the moderate groundwater class than for the dry groundwater class.

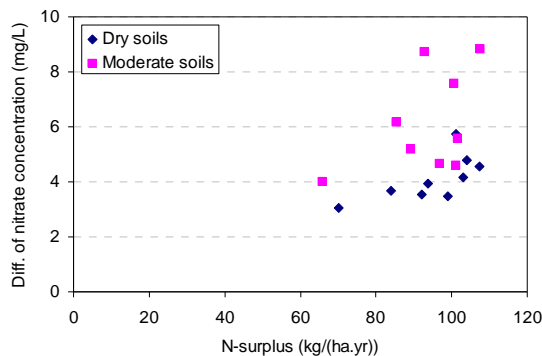


Fig. 5.10 Decrease of nitrate concentration between MLG and 5m below MLG, as a function of N-surplus (fertilization+deposition – crop off take), aggregated for crop-sand district clusters for dry and moderate soils.

Higher nitrate input rates into the upper groundwater system favour the nitrate removal rate because of the higher concentrations, but it can be argued that the model predictions over estimated the effect for two reasons:

- the simulated potential denitrification rate in the upper groundwater depends on the leaching of dissolved reactive organic compounds, to a large extent introduced by the application of animal manure. It is expected that the relation between potential denitrification rate and dissolved reactive organic matter is less clear than presumed.
- The hydraulic and geochemical stratification of the upper aquifer in the model schematization is more spread out than reality because of the regional spatial aggregation procedures applied. The existence of thin low conductive layers or thin highly reactive layers has not been taken into account in the regional model. If they are present, they disturb the water flow pattern and concentration profile with depth and result to less clear relations between concentrations at greater depth and the land use.

## 6 Risks of undesirable side effects and sustainability

### 6.1 Introduction

The questions are raised what the side effects are of denitrification within the first 5 meters below groundwater level and whether denitrification is sustainable or not (see section 1.2). The side effects refer to release of contaminating species in pore water associated with denitrification. Sustainability directs to the time period during which denitrification may be an on-going buffering process.

The side effects of denitrification are investigated by combining generic model results on reactive transport modelling (see Appendix 14) with regional data on the sediment and groundwater chemistry (see Appendices 3 and 4). In this way, the importance of side effects becomes apparent for the various regions. The regions are combinations of sand area (North, Central, South), GEOTOP region (see Fig. A3.8 in Appendix 3) and sand type (dry, moderate, wet).

### 6.2 The act of side effects

As explained in Appendix 14 the side effects for pyrite oxidation are different to that of sedimentary organic matter oxidation. For oxidation of organic matter, the side effects are negligible when we deal with nitrate concentration of  $50 \text{ mg l}^{-1}$ . This holds for both the trace metals and the major compounds hardness and sulphate. When pyrite oxidation in association with denitrification happens, two kinds of side effects happen: first, direct release of trace metals with sulphate from pyrite and, second, sorption/desorption of trace metals by deprotonation/protonation of the exchange complex. For the latter, humic and fulvic acids are primarily held responsible. The results presented in Appendix 14 point out that the worst side effects are found for arsenic and copper, and nickel (as well as manganese) may deserve attention as well. For zinc, it holds that leaching from the unsaturated zone is a more dominant phenomenon than release from pyrite. The Cd-content in pyrite is usually that low that no major side effects can happen for Cd. The side effect for sulphate release by pyrite oxidation can be straightforwardly calculated from mass balance and reaction stoichiometry. Under incomplete pyrite oxidation, i.e., sulphide is oxidised and Fe(II) is not,  $55.3 \text{ mg l}^{-1} \text{ SO}_4$  is released when  $50 \text{ mg l}^{-1} \text{ NO}_3$  becomes completely reduced (Table 6.1). Such a concentration change is smaller than the target value for sulphate in groundwater, which is  $150 \text{ mg l}^{-1}$ .

To further explore side effects by oxidation of pyrite containing trace impurities on a generic basis, it is worth calculating the release of trace metals as happens when pyrite

becomes oxidised by 50 mg l<sup>-1</sup> NO<sub>3</sub>. Little data on trace metals contents of pyrite are present for Dutch sediments and Appendix 14 reviews existing literature. Two types of pyrite are defined for the modelling investigation: one having relatively low trace metals contents and one having relatively high contents (where a factor 4 was set between these two). A third reference situation is obtained from Huerta-Diaz *et al.* (1992), who studied pyrite compositions in various sedimentary deposits: the maximum average content in pyrite for an individual sedimentary deposit studied.

Table 6.1 compares the resulting trace metal concentration for the three scenarios with the Dutch target values for shallow groundwater. It is obvious that for the low content pyrite, only As gives a concentration above target value. For the high content pyrite, Ni and Cu do in addition to As. For the high average content scenario, all 5 trace metals considered have a substantially higher concentration than the target value. This straightforward mass balance calculation confirms the more advanced model exercises presented in Appendix 14, where no buffering mechanisms by sorption are taken into account in this simple approach.

Table 6.1. Stoichiometric release of elements from pyrite containing impurities with trace elements, when 50 mg l<sup>-1</sup> NO<sub>3</sub> oxidizes pyrite compared to target value for shallow groundwater.

Element	Target values for shallow groundwater	Model low content (appendix 14)	Model high content (appendix 14)	High average content (Huerta-Diaz <i>et al.</i> , 1992, table 2)
Ni (µg l <sup>-1</sup> )	15	4.2	16.8	213
Zn (µg l <sup>-1</sup> )	65	8.47	33.9	382
Cd (µg l <sup>-1</sup> )	0.4	0	0	0.94
Cu (µg l <sup>-1</sup> )	15	0	29.3	733
As (µg l <sup>-1</sup> )	10	31.3	135.2	70.8
SO <sub>4</sub> (mg l <sup>-1</sup> )	150	55.3	55.3	55.3
Ni (µg l <sup>-1</sup> )	15	4.2	16.8	213

### 6.3 The occurrence of side effects

A next step is the identification of areas where pyrite oxidation happens versus those where organic matter oxidation happens, a combination happens or no denitrification at all happens. Table 6.2 summarises the SOM and pyrite contents for the various sand areas and possibly GEOTOP regions based on the data presented in Appendix 3. The median and average values are presented as prime characteristics. A considerable difference between these two (larger than factor 2) indicates that the frequency distribution is concave instead of linear. A consequence is that the denitrification capacity is heterogeneous at the regional scale. In some parts the capacity may be relatively high and inflowing nitrate is buffered and in other parts the buffering is relatively low and fast nitrate breakthrough is likely.

The general pattern is that in the Central Netherlands both SOM and pyrite are low and reduction capacity is thus small. In North Netherlands, SOM contents are high and average pyrite contents are relatively high, but median values are not. In South Netherlands, SOM

contents are low and pyrite contents are low but substantial. Various individual denitrification studies in the Netherlands confirm these observations: denitrification is negligible in Eastern Netherlands, dominated by organic matter oxidation in North Netherlands and dominated by pyrite oxidation in South Netherlands (e.g. Van der Aa, 2003).

This regional differentiation can be combined with insight in the extent of denitrification within 5 meters below phreatic surface, as obtained from groundwater data (See Appendix 4). Table 6.3 presents in the second column an overview of the nitrate removal for the various combinations of sand area and sand type. It will be clear that no side effects can happen when no denitrification happens. This holds for the low groundwater level parts of the Central Netherlands. For the other combinations, denitrification is ongoing or complete within the first 5 meters of groundwater. In general, complete denitrification may give rise to larger side effects than ongoing denitrification, when the biogeochemical conditions are further identical.

*Table 6.2. Geochemical characteristics of shallow geological formations in the three sand areas of the Netherlands.*

Sand area and GEOTOP region	Geological formation	Median and average content of sedimentary org. matter (weight %)	Median and average content of pyrite (weight %)	Saturation Index for calcite (p17.5 to p82.5)
North				
all	Boxtel	0.5/1.3	<0.09/0.12	-3.6 to -0.9/-0.2
5a1	Drenthe	0.45/0.55	<0.09/<0.09	-3.6 to -0.2
5c1	Drenthe	0.45/0.55	<0.09/0.57	-3.6 to -0.3
5c1	Drachten	0.36/2.14	<0.09/0.14	-3.6 to -0.3
5c3	Urk-Tynje	0.5	<0.09/0.28	-3.7 to -0.9
Central				
all - 3b	Boxtel	0.07/0.09	<0.09/0.10	-2.7 to 0.3
3b	Boxtel	0.07/0.09	<0.09/0.10	-0.4 to 0.3
all	Drenthe	0.07	<0.09	-2.5 to 0.2
2b+3a	Kreftenheije	0.1/0.12	<0.09/<0.09	-0.5 to 0.2
South				
all	Boxtel	0.30/0.7		
4a1	Boxtel		0.13/0.36	-4.6 to -2.0
4b	Boxtel		0.06/0.09	-2.8 to -0.3
4a1	Beegden	0.1/0.2	0.02/0.15	-4.6 to -2.0
4b	Beegden	0.1/0.2	0.02/0.15	-2.8 to -0.3
4c	Sterksel	0.1/0.1	0.06/0.1	-4.7 to -1.0
4c	Stramproy	0.2/0.4	0.05/0.06	-4.7 to -1.0
4d1	Stramproy	0.2/0.4	0.03/0.08	-4.8 to -1.3

When we combine the sediment information on active reductant with the groundwater information on extent of denitrification, we can deduce the risk of side effects. This is presented in the 5th column of Table 6.3. Here, range in groundwater pH is also taken into

account: trace metals as Cu and Ni are more mobile under acid condition than under neutral conditions, except arsenic. Mobility of arsenite (the most likely product after release by pyrite oxidation in anaerobic groundwater) is pH independent in the pH range from 4 to 8. A second step in the risk evaluation of side effects is the interaction with surface water: do the trace metals mobilised leach to the surface water system. generally, this risk is highest in the wet areas and smaller in the intermediate areas. A counteracting effect is, however, that for the wet areas more denitrification happens in the unsaturated zone and nitrate leached to groundwater is lower for these areas under similar N-application (see Chapter 4). The last column in Table 6.3 takes all these effects into account and qualitatively summarises the risk of side effects.

Table 6.3. Overview of the act of denitrification in shallow groundwater and the associated risk of side effects for the combinations of sand area and sand type.

Sand area/ Sand types	Nitrate removal at 5 m - MLG	pH range in upper 5m groundwater	Reductant	Side effect	Interaction with surface water and substantial denitrification	Risk of side effects ?
N, Low	Ongoing	4.5-6	SOM +pyrite	Some trace metals	Little	+ -
C, Low	Not occurring	5-7.5	no	No	„	--
S, Low	Ongoing	4-6	Pyrite +SOM	Favourable for trace metals	„	+
N, Interm.	Ongoing	4.5-6.5	SOM +pyrite	Some trace metals	High	-+
C, Interm.	Complete	5-8	SOM	Little or no	„	-
S, Interm.	Ongoing	4.2-6.5	Pyrite +SOM	Favourable for trace metals	„	++
N, High	Complete	5-7	SOM +pyrite	Slightly favourable for trace metals	Intermediate	-+
C, High	Ongoing	5-7	SOM	Little or no	„	-
S, High	Complete	5-7	Pyrite +SOM	Intermediately favourable for trace metals	„	++

## 6.4 Sustainability of denitrification

The sustainability of denitrification depends on the buffering capacity of the subsurface versus the nitrate leaching. A mass balance approach provides good, first insight. This will first be investigated by answering the question how fast the reductants are depleted by inflowing nitrate and what is the downward velocity of the redox cline between nitrate-bearing, suboxic groundwater and nitrate-free, anaerobic groundwater. Here, we will assume a sharp interface between these two.

When we consider  $50 \text{ mg l}^{-1} \text{ NO}_3$  and a precipitation excess of  $360 \text{ mm yr}^{-1}$ ,  $180 \text{ kg ha}^{-1} \text{ NO}_3$  is leached to groundwater. When we have 0.5 SOM weight content, a sediment layer of 10 cm contains  $8745 \text{ kg ha}^{-1} \text{ SOM}$ . For 0.1 weight % pyrite, this corresponds to 1750

kg ha<sup>-1</sup> pyrite. Note that these contents are typical for the sediments studied (Table 6.2). Taking into account the reaction stoichiometry between nitrate and SOM or nitrate and pyrite, 87.1 kg SOM or 114 kg pyrite can be oxidized with 180 kg NO<sub>3</sub>. This implies that it takes, for the SOM situation, about 100 years to oxidise a layer of 10 cm under steady nitrate leaching of 50 mg l<sup>-1</sup>. For the pyrite situation, it would take 15 years.

The buffering capacity of 5 meters of shallow groundwater thus becomes exhausted during tens to hundreds of years. We need to remind that we assume all SOM is active as reductant which is certainly not true. About 50% of SOM is recalcitrant, black carbon type of SOM. The buffering capacity is thus likely at least a factor of two smaller for SOM. Briefly, the buffering capacity of sandy areas cannot be indicated to be infinite. The sustainability lies in the range of tens of years to a few hundreds of years, when nitrate gets leached to groundwater at the drinking water concentration of 50 mg l<sup>-1</sup>. Any higher concentration gives rise to a proportionally smaller buffering time. Based on the reductant contents in shallow sediments, the sustainability of denitrification is smallest or absent in the Central Netherlands and highest in the Northern Netherlands. For the Southern Netherlands, it is substantial but critical, as the buffering capacity is provided by low contents of pyrite.

## **7 Conclusions**

### **7.1 Investigation of organic matter and pyrite contents in the subsoil**

The data show clear differences between the various sand districts, with pyrite and organic matter contents being highest in North Netherlands, lower in South Netherlands, and lowest in Central Netherlands. Overall, the organic matter and pyrite data indicate that the subsurface of North Netherlands is most reduced, followed by South Netherlands and finally Central Netherlands. These findings correspond well to the patterns found for nitrate and iron in groundwater. Under more reduced conditions, denitrification is more likely to occur and based on these investigations higher potential denitrification rates are expected in the Northern sand district and lower rates in the central sand district.

The link between the distribution of organic matter and pyrite and denitrification is not straightforward. Especially the nature of the organic matter deserves further attention: it is expected that the reactivity of the organic matter, which can vary, will have a big influence on the denitrification.

### **7.2 Denitrification rates in sandy aquifers**

The main conclusions of the scientific literature survey are:

- there is a clear relation between the decay rate and the age of the organic material;
- within any given age group there is a wide variety of decay rates by a factor of at least two;
- the denitrification rates in aquifers with residence times exceeding one million years are higher than the decomposition rates under full anaerobic conditions; the reported denitrification rates observed under field conditions do not differ significantly from the denitrification rates measured in the laboratory;
- the reported denitrification rates for aquifers range from 10 to 1000  $\text{meq l}^{-1} \text{yr}^{-1}$ .

### **7.3 Investigation of groundwater quality investigations**

From the analysis of the available groundwater quality data the following major conclusions are deduced:

- denitrification in agricultural areas with high groundwater tables is generally completed within the first 5 meters below ground water level;
- some denitrification within the first 5 meters below groundwater level is observed in areas with low groundwater levels ;

- a clear difference in redox capacity of the shallow subsurface was found between the three distinguished sand areas of the Netherlands.

The first two conclusions confirm in large the findings of the study conducted by Fraters *et al.* (2006).

#### 7.4 Conclusions based on model results

The first model runs with the STONE model yielded an overestimation of the potential denitrification rate in the upper groundwater of sandy soils relative to the up scaled observations in samples obtained in a drilling campaign. The reaction rate of dissolved reactive organic matter appeared to be the most sensitive parameter in the model for calibration of the potential denitrification. An adjustment of this parameter yielded satisfying results with respect to the potential denitrification rate. The sensibility of denitrification for dissolved organic matter in sandy subsoils is not confirmed by field research, but many aspects of this process are unclear. The calibration of this parameter followed by the recalibration of a threshold value of the water filled pore space where the denitrification starts action on previously simulated nitrate concentrations yielded a model suitable for the analysis of the fate of nitrate in the upper groundwater.

The model has been compared to field observations at regional, farm and field scale. The performance was satisfying for specific field circumstances with sufficient input data, but for most of the farms with a poor data availability on groundwater time series and the historical land management the results were poor. Although the model overestimated the available nitrate concentration at regional scale in the Southern sand district and underestimates the concentrations in the wet areas, the agreement with field observations in the other districts of for other groundwater classes reasonable. The results are considered as sufficient to inspire confidence in the use of the model for the analysis of the fate of nitrate in the upper groundwater zone.

Contrary to the current situation, the model results indicate a future nitrate concentration decrease with depth in all sandy soils. At presents the concentrations in the dry soils show more or less a uniform depth pattern, due to the combination of the historical loading and the denitrification. The shallow water at lower age has been polluted less heavily than water which infiltrated earlier, but was less exposed to the denitrification process. At a constant future lower fertilization rate, lower nitrate concentration can be expected in groundwater and the concentrations will decrease with depth. The decrease of the nitrate concentration with depth is lowest for the dry soils.

The predicted future nitrate concentrations in dry soils are the lowest for the Northern sand district and the highest for the Southern sand district. The concentrations at 5m below MLG will decrease to a concentration level slightly above the drinking water standard. The highest decrease percentages are expected for the Central sand district. This is due to the highest input of dissolved reactive organic matter, as will be supplied by slurry

applications or will be formed from readily decomposable organic compounds in animal manure. The application rate of animal manure is related to the land use type. The Central sand district has the highest proportion of grassland and maize and the Northern district is relatively more covered by arable land.

The flux weighted nitrate concentrations as calculated by the STONE model at the constant depth of the Mean Lowest Groundwater overestimate the nitrate concentrations calculated for the fluctuating depth of 1 meter below the groundwater level with ca. 10%. For specific years and for specific plots the deviation between the two methods can be larger, but can also lead to an underestimation. The adjusted STONE was used to simulate nitrate concentrations in the upper meter of the groundwater body. The resulting nitrate concentrations were not calibrated against field observations. Although these concentrations can deviate slightly from the non-adjusted STONE model application, and could therefore only be used with great care, the relative nitrate courses with depth are useful for gaining insight in the fate of nitrate in the upper groundwater.

The total-N and nitrate transport to surface waters is determined by the water flow and the occurring concentrations in the soil. The drain discharge is lowest in the dry soils and largest in the wet soils, but the soil concentrations show a reversed order. The loads show a decrease with time due to the historical and foreseen future fertilization reductions. After 20 years of constant fertilization at a lower rate than the current one, the total-N load on surface waters is estimated at 17, 25 and 31 kg ha<sup>-1</sup> yr<sup>-1</sup> for the dry, the moderate and the wet soils. The contribution of the specific soil layer between MLG and 5m below MLG to this load is quantified at 41%, 47% and 43% for the three groundwater classes. The contribution of the nitrate transport to surface waters to the total-N load on surface waters is estimated at 93%, 89% and 61% for the dry, moderate and wet soils. The calculated loads show a wide range due to the large variability of hydrological and soil characteristics within a groundwater class. The ranges will decrease with time due to lower and levelled out inputs to the soil.

The dry soils are defined by the Mean Highest Groundwater Level (MHG) deeper than 80 cm below soil surface. A part of the dry soils shows drainage rates exceeding 200 mm yr<sup>-1</sup>. A closer inspection of these dry soils was conducted by defining a class “extra dry” with MHG deeper than 120 cm and a drainage rate less than 100 mm yr<sup>-1</sup>. In these “extra dry” soils, the nitrate concentrations at 5m below MLG in 2031–2040 are 15 mg l<sup>-1</sup> higher than for the dry soils on average. Due to lower drainage rates, the nitrate load on surface waters from these soils is 44% lower than the load from dry soils.

The actual denitrification in the soil is described by the STONE model as a function of the potential denitrification rate, the presence of nitrate and the soil moisture conditions. The largest part of the actual denitrification occurs in the top soil between land surface and MLG. In principle, the STONE model is able to describe the denitrification as a result of

pyrite oxidation. This process was addressed by a tentative sensitivity analysis for some fields. A possible accounting for the influence of pyrite, the regional patterns of pyrite occurrences in the subsoil and the influence of thin peat layers would imply the recalibration of the model on potential denitrification rates and nitrate concentrations. This was outside the scope of this study, but is advised for a future refinement of the STONE model.

The spatial and temporal aggregation methods in this study relate to the regional scale and to the research questions. The results of the regional model application are only applicable at the model scale itself. Prudence is called for the application of the model with a regional schematization of land use, soil and hydrology at field scale or at farm scale.

## 7.5 Answers to research questions

*What is the average regional change of the nitrate concentration in groundwater between groundwater surface and five metres below groundwater surface for agriculture areas with a constant level of fertilization?*

*Regional's are specified as North, Central and South sand areas distinguished by different water table classes (dry sand, medium dry sand and wet sand). Please indicate: (1) which part of the change is due to denitrification; (2) which part of the change is due to hydrological phenomena (seepage, dilution); (3) the average decrease and the uncertainty in the decrease*

When fertilization levels are maintained at a constant level in the future<sup>7</sup>, a reduction of the nitrate concentration at 5m below the mean lowest groundwater level (MLG–5m) relative to the concentration at the mean lowest groundwater (MLG) is expected for the three sand regions (North, Central, South). The decrease is expected for all groundwater classes. The decrease of the nitrate concentration with depth is smallest for the dry soils. The average decrease for these soils amounts to 24% and ranges<sup>8</sup> from 10% to 39%. In the decrease ranking, the moderate soils take an intermediate position by 61% on average and 39%–87% as range. The decrease with depth is largest for the wet soils with 88% as an average decrease for these soils and 78%–98% as range. In the current situation (2001–2010) no decrease of nitrate concentrations with depth in the upper 5 m of the groundwater body is calculated for the dry sandy soils.

The model results indicate a reduction in the Northern sand area of 47% (range: 15%–88%), followed by the Southern sand district with 51% (range: 15%–95%). The decrease is largest for the Central sand district by 66% on average with 35%–94% as range. The

---

<sup>7</sup> Use has been made of the scenario “2015AT-20” in the Evaluation of the Dutch fertiliser and manure policy in 2007, which supposes constant fertilization rates after 2015 and a 20% reduction of the nitrogen application standard of for arable and horticultural crops relative to the levels of 2006.

<sup>8</sup> In this study, the range is defined by the 82.5 percentile and the 17.5 percentile value of the area weighted result distribution

distinction between the sand areas with respect to the decrease of the nitrate concentration with depth is to the distinction between the groundwater classes. The order of the nitrate concentration reductions differs from the ranking of the sand districts regarding the subsoil reduction capacity on the basis of the sediment analyses, but the capacity is not necessarily proportional to the actual reduction rate.

Denitrification in soils and groundwater is expected to occur in all sandy soils, but the total denitrification in the topsoil and the subsoil is smallest for the dry soils. The denitrification rates in “moderate” and “wet” sandy soils are higher. The majority of the denitrification occurs in the active top soils above the mean lowest groundwater level (55–95%). The model simulations are liable to the simulated input of dissolved reactive organic matter in the upper groundwater zone.

The nitrate transport fluxes, the water fluxes and the denitrification can be quantified, but an unambiguous explanation of the nitrate concentration decrease can not be given. An indication of the mutual relation between the nitrate sink terms of the layer between MLG and 5m below MLG can be given by the fate of each kg nitrate that either is transported into this layer or is released by the depletion of the nitrate stored at the beginning of the time period considered. In the dry sandy soils, 69% of each kg nitrate is transported to deeper layers, 21% is denitrified and 10% is transported to surface waters. For the moderate soils, the percentages amount to 31% for transport to deeper layers, 38% for denitrification and 31% for transport to surface water. In the wet sandy soils 2% is transported to deeper layers, 38% is denitrified and 60% is transported to surface waters. These percentages apply more or less also for the current situation.

The fate of a kg nitrate in the layer between MLG and 5m below MLG in the Northern sand district is expressed as 55% transport to deeper layers, 25% denitrification and 20% transport to surface water. For the Central sand district the percentages amount to 40% for the transport to deeper layers, 33% for the removal by denitrification and 26%<sup>9</sup> for the transport to surface water. In the Southern sand district the transport to deeper layers is estimated at 56% of the input+storage depletion, 26% is removed by denitrification and 19% is transported to surface waters.

Dilution of water at 5m below MLG is likely to occur in the moderate and the wet soils, but not in the dry soils. Based on the ratio between seasonal upward flow and seasonal downward flow at this depth, the water from the topsoil which reaches this depth will be diluted for 17% by seepage water in the moderate soils at the large scale. The maximum decrease of the nitrate concentration by dilution at this depth is then 17%. For the wet soils at the large scale, the mixture of water at 5 m below MLG consists of 81% water by upward seepage and 19% water by downward flow.

---

<sup>9</sup> Percentages are rounded off to integers and therefore the sum is not always equal to 100%.

*What is the expected regional development of denitrification capacity in time? (Indicate at least increase, steady state or decrease and the time frame?)*

The denitrification capacity should not be confused with the denitrification rate. The capacity is not necessarily proportional to the actual denitrification rate. Both items were evaluated. If sustainability is expressed in terms of depletion of the total denitrification capacity, it ranges from decades to hundreds of years. The total storage of potential denitrifying subsoil compounds is largest in the Northern sand district and smallest for the Central sand district. The Southern sand district takes an intermediate position.

The calculated actual denitrification rate depends on the nitrate concentration and the potential denitrification rate. The potential rate is determined by the content and the reactivity of the organic matter and reduced minerals (e.g. pyrite). The model was calibrated on some experimental data concerning the potential denitrification rate, but experimental data of the actual denitrification were not available for calibration. The potential rate is expected to be stable within the coming decades, because the actual denitrification lead to only small annual decreases of the total amounts of denitrifying compounds. Small differences of the model results are secondary to the uncertainties of the driving forces of the denitrification process. The role of dissolved organic matter, originating from manure inputs, in the denitrification process at this depth is still unresolved. Higher nitrate fluxes to groundwater in general lead to higher actual denitrification rates and to higher decreases of the denitrification capacity.

*Specify the present nitrogen load to surface waters caused by agriculture activities on regional scale? What percentage originates from nitrate in groundwater (beneath agricultural areas) at a depth between the groundwater table and five metres below groundwater table?*

Nitrogen and nitrate transport to surface waters is expected to occur in all types of sandy soil, also in the sandy soil classified as “dry”. Higher nitrate concentrations in the upper groundwater zone yield higher nitrate transports to surface water systems in all sandy soils.

The present nitrogen load on surface waters amounts to 25 kg ha<sup>-1</sup> yr<sup>-1</sup> for the dry soils and ca. 38 kg ha<sup>-1</sup> yr<sup>-1</sup> for the moderate and wet soils. The bulk (ca. 90%) of the nitrogen transport to surface water takes place between the soil surface and 5m below soil surface. Irrespective the groundwater class, half of this load stems from the zone between soil surface and MLG, the other half is conveyed through the zone below MLG. In the dry and moderate soils, most of the nitrogen load on surface is in the form of nitrate (85–90%). In the wet soils, the transport of ammonium and dissolved organic matter contributes to the N loading of surface waters.

The current nitrogen load on surface waters is the highest in the Southern sand district (38 kg ha<sup>-1</sup> yr<sup>-1</sup>). The load in the Central sand district equals 34 kg ha<sup>-1</sup> yr<sup>-1</sup>. The regional averaged load on surface water is the smallest in the Northern sand district (28 kg ha<sup>-1</sup> yr<sup>-1</sup>).

At present, the proportion of the total nitrogen load on surface water by the nitrate transport from the layer between MLG and 5m below MLG in dry soils is estimated at 43%. For the moderate and the wet soils the proportion is estimated at 47% and 26%. For the sand districts the proportions are on average 38% for the Northern sand district, 34% for the Central sand district and 45% for the Southern sand district.

For the future the proportions of the total nitrogen load on surface water by the nitrate transport from the specific soil layer are estimated at 23%, 43% and 40% for the wet, the moderate and the dry soils.

*What is the present total N-concentration in groundwater beneath agricultural areas leaching directly to surface waters? What percentage originates from nitrate in groundwater at a depth between groundwater table and five metres below groundwater table on agricultural lands?*

The flux averaged total N-concentration (load divided by water flow) in the water discharged to surface waters is largest for the dry soils (21 mg l<sup>-1</sup>), followed by the moderate soils (15 mg l<sup>-1</sup>). The flux averaged total N-concentration in the drainage water is the smallest in wet soils (7 mg l<sup>-1</sup>). This flux averaged concentration in drainage water can differ from the actual concentration in the surface water itself, due to other sources and removal processes which affect the nitrogen levels in surface waters.

The flux averaged total N-concentration in drainage water on regional scale is largest in the Southern sand district (14 mg l<sup>-1</sup>). The concentration in the Central and Northern sand district is estimated at 10 mg l<sup>-1</sup>.

The origin of total-N and nitrate entering a surface water body can only be evaluated by considering the different pathways of water, nitrogen and nitrate. The part of nitrate transported from the layer between MLG and 5m below MLG in the total nitrogen load is already presented in the answer to the previous research question.

*On the scale of areas, what are the expected side-effects of denitrification? Indicate the expected change in concentration for heavy metals, sulphate and increase of hardness of water. Furthermore specify the uncertainty in the change.*

Negative side effects of denitrification in groundwater are related to the occurrence of pyrite oxidation and not of organic matter oxidation. Side effects increase with increasing nitrate leaching under the assumption of pyrite oxidation. The potential negative side effects hold in particular for arsene, copper and nickel, due to relatively high contents of

these trace impurities in pyrite. When groundwater is not exposed to nitrate concentrations exceeding  $50 \text{ mg l}^{-1} \text{ NO}_3$ , the negative side effects for sulphate and hardness are small to negligible. Zinc and cadmium show an intermediate behaviour. The extent of side effects cannot be reliably indicated, which is primarily due to unknown composition of pyrite in Dutch aquifer sediments. Trace metal contents in pyrite may vary a factor of 50 according to literature and side effects will vary accordingly. Based on the sediment analyses for pyrite and sedimentary organic matter, the potential of negative side effects is assessed the highest for the Southern Netherlands, followed by the Northern Netherlands and the lowest for the Central Netherlands. The occurrence of buffering sorption reactions, the pH dependency of release processes and the history of manure application complicate the further regional investigation.

## References

- Alvarez-Iglesias, P. & B. Rubio 2008. The degree of trace metal pyritization in subtidal sediments of a mariculture area: Application to the assessment of toxic risk. *Marine Pollution Bulletin* **56** 973–983.
- Appelo, C.A.J. & D. Postma, 2005. *Geochemistry, Groundwater and Pollution*. Taylor & Francis Ltd Netherlands. ISBN 9780415364287.
- Bakker, I., P., Kiden, J., Schokker, J. & Griffioen, 2007. *De geotop van de ondergrond: Een reactievat. Deelrapport 2. Eerste statistische karakterisatie van de geochemische reactiecapaciteit van het topsysteem in Noord-Brabant en het noorden van Limburg*. TNO Bouw en Ondergrond, Utrecht. rapport 2007-U-R0324/A.
- Beusen, A.H.W., C.C.G. Schotten, J. Roelsma & P. Groenendijk, 2004. *STONE2.1, technical documentation, version 1.0*. National Institute for Public Health and the Environment, Bilthoven. Internal IMP report 04/04 (in Dutch).
- Beusen, A.H.W. & P. Heuberger, 2007. *Calibratie van STONE2.3 met LMM gegevens*. Milieu en Natuur Planbureau, Bilthoven. Intern Rapport
- Billon, G., B. Ouddane, J. Laureyns & A. Boughriet, 2001. Chemistry of metal sulfides in anoxic sediments. *Phys. Chem. Chem. Phys.* **3** 3586-3592.
- Blodau, C., S., Hoffmann, A. Peine, & S. Peiffer, 1998. Iron and sulfate reduction in the sediments of acidic mine lake 116 (Brandenburg, Germany): Rates and geochemical evaluation. *Wat. Air and Soil Poll.* **108**: 249-270.
- Boyer, E.W., R.B. Alexander, W.J. Parton, C. Li, K. Butterbach-Bahl, S.D. Donner, R.W. Skaggs & S.J. Del Grosso, 2006. Modeling denitrification in terrestrial and aquatic ecosystems at regional scales. *Ecological Applications* **16**: 2123–2142.
- Breve, M. A., R. W. Skaggs, J. W. Gilliam, J. E. Parsons, A. T. Mohammad, G. M. Chescheir, and R. O. Evans. 1997. Field testing of DRAINMOD–N. *Trans. ASAE* **40**: 1077–1085.
- Broers, H.P. & E.A. Buijs, 1997. *De herkomst van sporenmetalen en arseen in het waterwingebied Oostrum*. NITG-TNO, Utrecht. Rapportno. 97-189-A
- Broers, H.P., Griffioen, J., Willems, W.J., Fraters, B., 2004. *Naar een andere toetsdiepte voor nitraat in grondwater? Achtergronddocument voor de Evaluatie Meststoffenwet 2004*. Nederlands Instituut voor Toegepaste Geowetenschappen, Utrecht, TNO-rapport NITG 04-066-A.
- Brown, C.J., M.A.A. Schoonen & J.L. Candeale, 2000. Geochemical modeling of iron, sulfur, oxygen and carbon in a coastal plain aquifer. *J. of Hyd.* **237**: 147-168.
- Chapelle F.H. & P.B. McMahon, 1991. Geochemistry of dissolved inorganic carbon in a coastal plain aquifer. 1. Sulphate from confining beds as an oxidant in microbial CO<sub>2</sub> production. *J. of Hydrol.* **127**: 85-108.
- Chen, J., B. Gu, R.A. Royer & W.D. Burgos, 2003. The roles of natural organic matter in chemical and microbial reduction of ferric iron. *Sci. of the Tot. Env.* **307**: 167-178 .

- Cleveland, W.S. & J.J. Devlin, 1988. Locally weighted regression: an approach to regression analysis by local fitting. *J. Am. Stat. Ass.* **83**: 596-610.
- Davidson, E. A. & J. P. Schimel. 1995. *Microbial processes of production and consumption of nitric oxide, nitrous oxide and methane, in biogenic trace gases: measuring emissions from soil and water*. In: P.A. Matson and R.C. Harriss (Eds.). *Biogenic trace gases: measuring emissions from soil and water*. Blackwell, Cambridge, Massachusetts. pp 327–357.
- De Lange, W.J., 1999. A Cauchy boundary condition for the lumped interaction between an arbitrary number of surface waters and a regional aquifer. *J. of Hydrol.* **226**: 250-261.
- De Mulder, E.F.J., M.C. Geluk, I. Ritsema, W.E. Westerhoff & T.E. Wong, 2003. *De ondergrond van Nederland*. TNO Nederlands Instituut voor Toegepaste Geowetenschappen/Wolters Noordhoff, 379 pp.
- EU, 2003. *Draft guidelines for the monitoring required under the Nitrates Directive (91/676/EEC). Version 3, with annexes 1 through 3*. European Commission, Directorate-General XI (Environment, Nuclear Safety and Civil Protection), Directorate D (Environment, Quality and Natural Resources).
- Finke, P.A, Gruijter de J.J. and Visschers R., 2001. Status 2001 National random check of map units and applications; structured sampling and characterisation of Dutch soils. Wageningen, Alterra, Report 389 (in Dutch).
- Firestone, M. K., & E. A. Davidson. 1989. *Microbial basis of NO and N<sub>2</sub>O production and consumption in soils*. In: M.O. Andreae and D. S. Schimel (Eds). *Exchange of trace gases between terrestrial ecosystems and the atmosphere*. John Wiley, New York, Pp 7–21.
- Foppen, J.W.A. & B. van der Grift, submitted. Zinc and Cadmium Mobility in the Dommel Brook Valley in the Southern Netherlands. *Submitted to J. of Hydrol.*
- Fraters, B., L.J.M. Boumans, B.G. van Elzakker, L.F.L. Gast, J. Grittoen, G.T. Klaver, J.A. Nelemans, G.L. Velthof & H. Veld, 2006. *A new compliance checking level for nitrate in groundwater? Feasibility study on monitoring the upper five metres of groundwater*. RIVM, Bilthoven. Rapport 680100005/2006. (in Dutch).
- Frind, E.O., W.H.M. Duynisveld, O. Strelbel & J. Boettcher, 1990. Modeling of Multicomponent Transport With Microbial Transformation in Groundwater: The Fuhrberg Case. *Water Resources Research*, **26**: 1707-1719
- Galloway, J. N., *et al.* 2004. Nitrogen cycles: past, present and future. *Biogeochemistry* **70**:153–226.
- Griffioen, J., R. Heerdink, L. Maring, S. Vermooten, D. Maljers & J. Hettelaar, 2006. *Enkele lithologische en (hydro)geochemische karakteristieken van het topsysteem van de Nederlandse ondergrond t.b.v. de parametrisering van het nutriëntenmodellensysteem STONE*. TNO Bouw en Ondergrond, Utrecht. TNO rapport 2006-U-R0161/A.
- Griffioen, J. G.M.C.M. Janssen, S. Jansen, R. Mutsaers & G.L. Velthof, 2008. *A new compliance checking level for nitrate in groundwater. A field and laboratory campaign to collect geochemical data for the shallow subsurface below agricultural fields in the Central Netherlands*. TNO Built Environment and Geosciences, Utrecht. Report in press.

Groenendijk, P. & Van den Eertwegh, 2004. *Drainage-water travel times as a key factor for surface water contamination*. In: R.A. Feddes, G.H. de Rooij and J.C. van Dam (eds.). *Unsaturated zone modeling. Progress, challenges and applications*. Wageningen UR Frontis Series. Vol. 6. Kluwer Ac. Pub. Dordrecht, the Netherlands. p. 145-178.

Groenendijk, P., L.V. Renaud & J. Roelsma, 2005. *Prediction of Nitrogen and Phosphorus leaching to groundwater and surface waters; Process descriptions of the ANIMO4.0 model*. Alterra, Wageningen. Alterra report 983.

Groenendijk, P., L. V. Renaud, C. van der Salm, J. G. Kroes, O. F. Schoumans, J.G. Conijn, A.M. van Dam, A. Beusen & W.J. Willems, 2008. *Preparation of the STONE model for the assessment of the effects of the new fertilizer and manure policy*. Alterra, Wageningen, Report in prep. (in Dutch).

Groffman, P. M., M. A. Altabet, J. K. Böhlke, K. Butterbach-Bahl, M. B. David, M. K. Firestone, A. E. Giblin, T. M. Kana, L. P. Nielsen & M. A. Voytek, 2006. Methods for measuring denitrification: diverse approaches to a difficult problem. *Ecological Applications* **16**: 2091–2122.

Hansen, L.K., R. Jakobsen, & D. Postma, 2001. Methanogenesis in a shallow aquifer, Rømø, Denmark. *Geochim. et Cos.* **17**: 2925-2935.

Helwig, T.G., C.A. Madramootoo & G.T. Dodds, 2002. Modelling nitrate losses in drainage water using DRAINMOD 5.0. *Agricultural Water Management* **56** 153-168.

Huerta-Diaz, M.A. & J.A. Morse, 1990.. A Quantitative Method for Determination of Trace Metal Concentrations in Sedimentary Pyrite. *Marine Chemistry* **29** 119-144.

Huerta-Diaz, M.A. & J.W. Morse, 1992. Pyritization of trace metals in anoxic marine sediments. *Geochim. Cosmochim. Acta.* **56**: 2681-2702.

Iversen, N. & B.B. Jørgensen, 1985. Anaerobic methane oxidation at the sulfate-methane transition in marine sediments from Kattegat and Skagerrak (Denmark). *Limn. Ocean.* **30**: 944-955

Klein, J. & J. Griffioen, 2008. *Het topsysteem van de ondergrond: Een reactievat. Deelrapport 8. Pilot-studie naar de reactiecapaciteit van twee geologische formaties in Noord-Brabant*. TNO Bouw en Ondergrond, Utrecht. Rapport 2008-U-R0797/A.

Klijne, A. de, Hooijboer, A. E. J., Bakker, D. W., Schoumans, O.F., Ham, A. van den, 2007. *Milieu kwaliteit en nutriëntenbelasting. Achtergrondrapport van de Evaluatie Meststoffenwet 2007*. Bilthoven, RIVM. Rapport 680130001/2007

Korom, S.F., 1992. Natural Denitrification in the Saturated Zone: A Review. *Wat. Res. Research.* **28**: 1657-1668

Kroes, J.G., J.C. van Dam, P. Groenendijk, R.F.A. Hendriks & C.M.J. Jacobs, 2008. *SWAP version 3.2. Theory description and user manual*, Alterra, Wageningen, The Netherlands. Alterra-report 1649.

Kuivila, K.M., J.W. Murray, A.H. Devol, & P.C. Novelli, 1989. Methane production, sulfate reduction and competition for substrates in the sediments of Lake Washington. *Geo. et Cos.* **53**: 409-416.

Larsen, F. & D. Postma, 1997. Nickel Mobilization in a Groundwater Well Field: Release by Pyrite Oxidation and Desorption from Manganese Oxides. *Environ. Sci. Technol.* **31** 3589-2595.

- Ludvigsen, L., H.J. Albrechtsen, G. Heron, P.L. Bjerg & T.H. Christensen, 1998. Anaerobic microbial redox processes in a landfill leachate contaminated aquifer (Grindsted, Denmark). *J. Cont. Hydr.* **33**: 273-291.
- Luesink, H.H., & G. Kruseman, 2007. *Emission inventories*. In: Ammonia the case of the Netherlands. Academic Publishers, Wageningen. pp 45-67.
- Madramootoo, C.A., J.W. Kaluli, G.T. Dodds, 1999. Simulating nitrogen dynamics under water table management systems with DRAINMOD-N. *Transactions of the ASAE* **42**: 965-973.
- Massmann, G., A. Pekdeger & C. Merz, 2004. Redox processes in the Oderbruch polder groundwater flow system in Germany. *App. Geoch.* **19**: 863-886.
- Massop, H.Th.L., T. Kroon, P.J.T. van Bakel, W.J. de Lange, A. van der Giessen, M.J.H. Pastoors & J. Huygen, 2000. *Hydrology for STONE; schematisation and parameterisation*. Alterra, Wageningen, Report 38. (in Dutch).
- Mol, G., H.F. Passier, G.T. Klaver & P. Römkens, 2007. *Het topsysteem van de ondergrond: Een reactievat. Deelrapport 1. De geochemische en analytische aspecten van het karakteriseren van de ondergrond: Uitwerking van een geochemisch analysepakket*. TNO Bouw en Ondergrond, Utrecht. rapport 2007-U-R0323 A
- Murphy, E. M. & J.A. Schramke, 1998. Estimation of microbial respiration rates in groundwater by geochemical modeling constrained with stable isotopes. *Geoch. et Cos.* **62**: 3395-3406.
- McClain, M. E., E. W. Boyer, C. L. Dent, S. E. Gergel, N. B. Grimm, P. M. Groffman, S. C. Hart, J. W. Harvey, C. A. Johnston, E. Mayorga, W. H. McDowell & G. Pinay. 2003. Biogeochemical hot spots and hot moments at the interface of terrestrial and aquatic ecosystems. *Ecosystems* **6**: 301-312.
- MNP, 2004. *Mineralen beter geregeld. Evaluatie van de werking van de Meststoffenwet 1998-2003*. Milieu en Natuurplanbureau RIVM, Bilthoven, RIVM Rapport 500031001.
- MNP, 2002. *MINAS en Milieu. Balans en Verkenning*. Milieu en Natuurplanbureau RIVM, Bilthoven, RIVM Rapport 718201005.
- Middelburg, J.J. 1989. A simple rate model for organic matter decomposition in marine sediments. *Geoch. et Cos.* **53**: 1577-1581.
- Moore, T.R. & R. Knowles, 1990. Methane emissions from fen, bog and swamp peatlands in Quebec. *Biogeochem.* **11**: 45-61.
- Otero, X.L. & F. Macias, 2003. Spatial variation in pyritization of trace metals in salt-marsh soils. *Biogeochemistry* **62** 59-86.
- Otero, X.L., P. Vidal-Torrado, R.M. Calvo de Ante & F. Macias, 2005. Trace elements in biodeposits and sediments from mussel culture in the Ria de Arousa (Galicia, NW Spain). *Environmental Pollution* **136** 119-134.
- Parkhurst, D.L. & C.A.J. Appelo, 1999. *User's guide to PHREEQC (Version 2) – A computer program for speciation, batch-reaction, one-dimensional transport, and inverse geochemical calculations*. U.S. Geol. Survey, Water-Resour. Investigations Report 99-4259, 312 pp.

- Roden, E.E. & R.G. Wetzel, 1996. Organic carbon oxidation and suppression of methane production by microbial Fe(III) oxide reduction in vegetated and unvegetated freshwater wetland sediments. *Limnol. Oceanogr.* **41**: 1733-1748.
- Scholz, F. & T. Neumann, 2007. Trace element diagenesis in pyrite-rich sediments of the Achterwasser lagoon, SW Baltic Sea. *Marine Chemistry* **107** 516-532.
- Schoumans, O.F., 1995. *Beschrijving en validatie van de procesformulering van de abiotische fosfaatreacties in kalkloze zandgronden*, DLO-Staring Centre, Wageningen. Rapport 381
- Schoumans, O.F. & A. Breeuwsma, 1997. *The relation between accumulation and leaching of phosphorus: laboratory, field and modelling results*. In: Tunney, H., et al., (Eds) , Proceedings of a workshop held September 29-31, 1995, Wexford, Ireland. p. 361-363.
- Schröder, J.J., Aarts, H.F.M., Bode, M.J.C. de, Dijk, W. van, Middelkoop, J.C. van, Haan, M.H.A. de, Schils, R.L.M., Velthof, G.L. & Willems, W.J., 2004. *Gebruiksnormen bij verschillende landbouwkundige en milieukundige uitgangspunten*. Wageningen, Plant Research International, PRI rapport 79
- Seitzinger, S., J. A. Harrison, J. K. Böhlke, A. F. Bouwman, R. Lowrance, B. Peterson, C. Tobias & G. Van Drecht. 2006. Denitrification across landscapes and waterscapes: a synthesis. *Ecological Applications* **16**: 2064–2090.
- Skaggs, R.W., M.A. Brevé, A.T. Mohammad, J.E. Parsons & J.W. Gilliam, 1995. *Irrigation and Drainage Systems* **9**: 259-277.
- Staatscourant, 2000. Streefwaarden en interventiewaarden bodemsanering. *Staatscourant* 24 febr. 2000. nr. **39** / pag. 8.
- Ten Berge, H.F.M., J.C.M. Withagen, F.J. de Ruijter, M.J.W. Jansen & H.G. van der Meer, 2000. *Nitrogen responses in grass and selected field crops. QUADMOD parameterization and extensions for STONE-application*. Plant Research International, Wageningen. PRI report 24.
- Tiedje, J. M. 1988. *Ecology of denitrification and dissimilatory nitrate reduction to ammonium*. in: A.J.B. Zehnder (Ed). *Biology of anaerobic microorganisms*. John Wiley and Sons, New York, USA.. pp 179–244.
- Uffink, G.J.M., 2003. *Determination of denitrification parameters in deep groundwater. A pilot study for several pumping stations in the Netherlands*. RIVM, Bilthoven. Report 703717011/2003.
- Van der Aa, M., H.P. Broers, J. Griffioen & K. Verloop, 2003. Omzetting van nitraat in de ondergrond; kunnen we daarop vertrouwen? *Bodem* **5-2003**: 167-169.
- Van Bakel, P.J.T., H.Th.L. Massop, J.G. Kroes, J. Hoogewoud, M.J.H. Pastoors & T. Kroon, 2008. *Actualisatie hydrologie voor STONE2.3. Aanpassing randvoorwaarden en parameters, koppeling tussen NAGROM en SWAP, en plausibiliteitsstoets*. Wettelijke Onderzoekstaken Natuur & Milieu, Wageningen. WOT rapport 57.
- Van Beek, C.G.E.M., C. Vink, J.G.R. Beemster, 2002. *Bemesting en grondwaterwinning. Invloed van meststoffen op de kwaliteit van door waterleidingbedrijven opgepompt grondwater*. KIWA, Nieuwegein. Report No. KOA 01.116, 123 pp.

- Van Boekel, E.M.P.M., 2008. *Geochemische schematisering van de ondergrond in het STONE-model. Organisch stofgehalte*. Alterra, Wageningen. Alterra-rapport in press.
- Van Breemen, N., *et al.* 2002. Where did all the nitrogen go? Fate of nitrogen inputs to large watersheds in the northeastern USA. *Biogeochemistry* **57**: 267–293.
- Van Cappellen, P. & Y. Wang, (1996): Cycling of iron and manganese in surface sediments: a general theory for the coupled transport and reaction of carbon, oxygen, nitrogen, sulfur, iron and manganese. *Am. Jour. of Sc.* **296**: 197-243
- Van Dam, J.C., P. Groenendijk, R.F.A. Hendriks and J.G. Kroes, 2008. Advances of modeling water flow in variably saturated soils with SWAP. *Vadose Zone Journal* **7**:640-653.
- Van der Grift, B., J.C. Rozemeijer, M.E. van Vliet & H.P. Broers, 2004. *De kwaliteit van het grondwater in de provincie Noord-Brabant: rapportage over de toestand van 2003 en trends in de periode 1992 t/m 2003*. TNO-NITG, Utrecht. Rapportno. NITG 04-206-B.
- Velthof, G.L., C.L. van Beek, F. Brouwer, S.L.G.E. Burgers, B. Fraters, P. Groenendijk, M.J.D. Hack-tenBroeke, A.J. van Kekem, H.P. Oosterom, O.F. Schoumans, F. de Vries, W.J. Willems & Vermooten, J.S.A., L., Vasak, J. Griffioen, G.T. Klaver, R.W. Vernes & H.J.T. Weerts, 2005. *Afbakening van het topsysteem voor de kartering van de reactiviteit van de Nederlandse ondergrond*. TNO Bouw en Ondergrond, Utrecht. rapport NITG 05-121-A
- Vermooten, J.S.A., L. Maring, M. van Vliet & J. Griffioen, 2006. *Landsdekkende geologische karakterisering van de regionale grondwatersamenstelling in de geotop van nederland: Data rapport*. TNO Bouw en Ondergrond, Utrecht. Rapport 2006-U-R0171/A
- Vermooten, S., L. Maring, J. Hettelaar, G.J.L. van Oyen & J. Griffioen, 2007. *Landsdekkende, geologische karakterisering van de regionale grondwatersamenstelling in de geotop van Nederland*. Atlas. TNO Bouw en Ondergrond, Utrecht. rapport 2007-U-R0021/A.
- Vrolijk, H.C.J., G. Kruseman, H.H. Luesink & L.J. Mokveld, 2008. *Model voor Agrarische Mineralenstromen en Beleidsondersteuning*. LEI, Den Haag, LEI report in press.
- Wendland, F., R. Kunkel and H.-J. Voigt, 2004. Assessment of groundwater residence times in the pore aquifers of the River Elbe Basin. *Environmental Geology* **46**: 1-9.
- Wieder, R.K., J.B. Yavitt, & G.E. Lang, 1990. Methane production and sulfate reduction in two Appalachian peatlands. *Biogeochem.* **10**: 81-104.
- Willems, W.J., A.H.W. Beusen, L.V. Renaud, H.H. Luesink, J.G. Conijn, G.J. van den Born, J.G. Kroes, P. Groenendijk, O.F. Schoumans & H. van der Weerd, 2008. *Emission of nutrients to soil and water: an assessment of the effects of the new fertilizer and manure policy*. The Netherlands Environmental Assessment Agency, Bilthoven. PBL report 500124002. (in Dutch).
- Wolf, J., A. H. W. Beusen, P. Groenendijk, T. Kroon, R. Rotter & H. van Zeijts, 2003. The integrated modeling system STONE for calculating nutrient emissions from agriculture in the Netherlands, *Environmental Modelling & Software* **18**: 597-617.
- Wösten, J.H.M., F. de Vries, J. Denneboom & A.F. van Holst, 1988. *Generalisatie en bodemfysische vertaling van de Bodemkaart van Nederland, 1 : 250 000, ten behoeve van de PAWN-studie*. Stiboka, Wageningen, Rapport 2055.

Wriedt, G. 2004. *Modelling of nitrogen transport and turnover during soil and groundwater passage in a small lowland catchment of Northern Germany*. PhD dissertation, University of Potsdam.

Wriedt, G and M. Rode, 2006. Modelling nitrate transport and turnover in a lowland catchment system. *Journal of Hydrology* **328**: 157– 176.

Zwart, K.B., 2004. *Denitrificatie in de zone tussen bouwvoor en het bovenste grondwater water in zandgronden*. Alterra, Wageningen, Alterra-rapport 730.1.

Zwart, M. H., Hooijboer, A. E. J., Fraters, B., Kotte, M., Duin, R. N. M., Daatselaar, C. H. G., Olsthoorn, C. S. M., Bosma, J. N., 2008. *Agricultural practice and water quality in the Netherlands in the 1992-2006 period*. Bilthoven, RIVM. Report 680716003/2008.

## Appendix 1 Model description

### STONE

The STONE model (Wolf *et al.*, 2003) is the result of integration of knowledge and ongoing work from a large number of Dutch research institutes in the fields of plant production, land use, environment, surface waters and agricultural economics (Alterra, RIVM, RIZA, Plant Research International, LEI). The STONE model chain has the ability to

- (1) translate environmental policy measures into model input data;
- (2) apply the model at national and regional scales;
- (3) accept spatially distributed input data on land characteristics;

and consists of a chain of models with

- A number of files containing soil hydrological data generated by the detailed mechanistic the soil–water–atmosphere–plant model (SWAP)
- an optimization model for calculating the N and P input into soils from manure and inorganic fertilizer allocation,
- a metamodel for calculating the N deposition from air,
- the process-based mechanistic ANIMO model for simulation of the N and P cycling in the soil and the N and P nutrient emissions to ground and surface waters.
- QUAD-MOD (four QUADrant MODel) relating crop production to fertilizer application, fertilizer recovery fraction and soil nutrient supply) is an empirical model for calculating the nutrient uptake by crops and the yield, as based on fertilizer experiments (Ten Berge *et al.* 2000). The model consists mainly of two relationships: (1) curvy-linear relationship between biomass yield and uptake of one nutrient (N or P); (2) linear relationship between nutrient application (N or P in inorganic and organic fertilizers) and nutrient uptake which relationship bends off near the maximum biomass yield level.
- The fertilization rates are calculated by the MAMBO model (Vrolijk *et al.*, 2008). The objective of the MAMBO model is to calculate emission from several sources, manure production and -allocation, the transports of animal manure and the costs of transport and the mineral input to the soil. The transport of surplus manure is optimized by minimizing costs of distribution, export and processing... The model distinguishes a number of items: manure production, potential manure allocation, manure surplus, manure transport and input to the soil. Results of the MAMBO model are transferred at an aggregated level and disaggregated to STONE-plots by a procedure developed by Beusen *et al.* (2004).

The architecture is schematically depicted in Fig. A1.1.

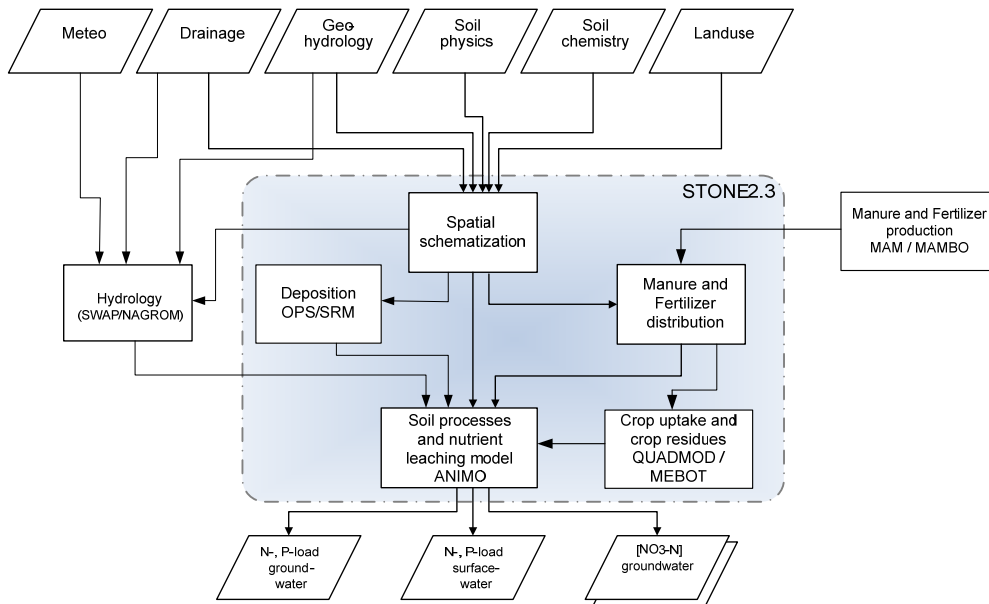


Fig. A1.1 Files and modules in the STONE model chain

## SWAP and ANIMO

The ANIMO model for simulation of nutrient leaching to groundwater and surface waters is used within the STONE model chain to assess the impact of agricultural policy measures at the national scale. In STONE (Kroes *et al.*, 2002; Wolf *et al.*, 2003), a plot is defined by a unique combination of meteorology, physical and chemical soil conditions, boundary conditions for drainage flow (defined here as local groundwater flow), and the bottom boundary conditions for regional groundwater flow. In the STONE model, the national land surface is discretized into 6405 different plots (Kroon *et al.*, 2003). Each plot consists of one or more of 6.25 ha grid cells (250 x 250 m). The spatial discretization was based on a number of data sources. The average diameter of a STONE plot ranges from 500 – 5000 m.

## Hydrologic schematization

An overlay was made using four maps. The maps are composed of:

- 6 classes of upward seepage fluxes which result from the simulations by a nation wide groundwater model (NAGROM). These seepage fluxes account for the interaction with the regional hydrological system;
- 22 hydro types as defined by Massop *et al* (2000). These hydro types characterize geo hydrological units of the subsoil;
- 6 classes of drainage resistances, derived from digitized topographical maps. These resistances account for the interaction between ground water and surface water system;
- classes of ground water table depths, taken from the national soil database. These classes are a further spatial refinement to the interaction between ground water and surface water system.

Land use and soil chemical parameters were used to further refine the spatial discretization by making another overlay with three maps:

- 4 classes of land use from Landsat satellite images (grassland, forage maize, arable land and nature);
- 21 classes of soil types (Wösten *et al.*, 1988);
- phosphate binding (3 classes), mineralisation capacity (2–3 classes) and cation exchange capacity (2–3 classes) were taken from the national soil database.

This resulted in about 120 000 units. This number was reduced to 6405 unique combinations by using so-called relation diagrams, which allowed merging of small sized units into units with analogue properties. The resolution of the final map is 250 x 250 m.

A number of items needed to be parameterized for each plot. Parameters had to be assigned to:

- 4 different crops: grassland, forage maize, arable land and nature;
- 5 different drainage systems:
  - i) primary system with a width of water courses of >3 meters;
  - ii) secondary system with a width of water courses < 3 meters;
  - iii) tertiary system existing of trenches and water courses that fall dry temporarily;
  - iv) tile drains
  - v) shallow surface drainage

Input parameters for the first three drainage systems were derived from digitised topographical maps. The presence of tile drains was based on regional inventories and expert rules. A simplified surface water balance was maintained using regional surface water target levels for a summer and a winter period. Inlet and outlet of surface water by means of weirs allowed additional infiltration to, and drainage from, the soil systems. Surface runoff was calculated when: i) the soil is saturated or ii) the rainfall intensity exceeds infiltration capacity of the soil top layer. The occurrence of irrigation was derived from regional inventories.

Besides the horizontal spatial discretization, a vertical discretization of the soils is required. This schematisation is based on the thickness of soils horizons in the national soil database, which describe the upper 1.2 m of the soil. For the deeper layers up to 13 m below soil surface, the physical properties of the layer at 1.2 m were adopted and increasing compartment thicknesses with depth were chosen.

The atmosphere forms the upper boundary of the modelled system, the lateral boundary is used to interact with surface water systems and the bottom boundary conditions describe the interaction of local groundwater with the deep groundwater system. The bottom boundary is situated a saturated soil layer at 13 m below soil surface and determines the interaction with a regional groundwater system. Results were achieved using an iterative procedure for boundary conditions of a regional groundwater model (de Lange, 1999) and the SWAP model. During each iteration step the groundwater recharge as simulated by the

SWAP model was used as input to the regional groundwater model, which returned a regional seepage or percolation flux as input to the SWAP model (Fig. A1.2).

The SWAP output included all terms of the soil water balance at a ten day time resolution for a period of more than 30 years.

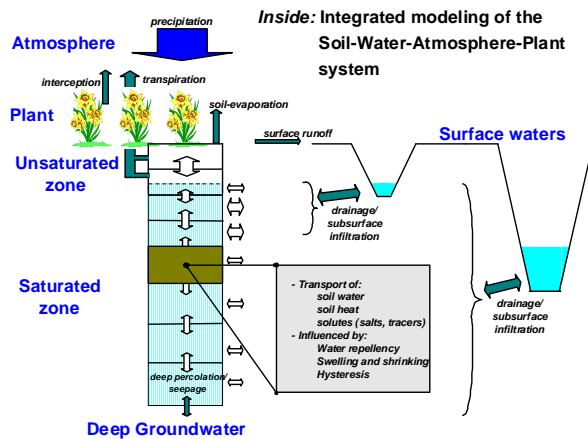


Fig. A1.2 Scheme of water flows in a soil profile and the main terms of the water balance

### Regional schematization of water flow to drains

In regions with high groundwater levels and water discharge to local surface waters, residence times are strongly influenced by the size and depth of the drainage system. For the simulation of hydrologic processes within a STONE plot, the area is considered as one large field and the simulation are conducted by the field scale model SWAP. The model compartments in the 1D model has a thickness of 5 cm – 100 cm in the vertical direction and stretches in the horizontal direction over the complete diameter of at least 250 m. Within one calculation unit, several drainage systems can be present. The three dimensional patterns of water flows to the drains are up scaled to the system of model compartments by a scheme of vertical fluxes and diffuse sink terms (Fig. A1.3). The diffuse sink terms are calculated by dividing the drainage fluxes over a certain depth. By partitioning the drainage flux over the depth-axes, the vertical drainage flux decreases with the depth. The travel time of drainage water increases then disproportional with depth. Within a compartment, the water is mixed perfectly and the concentration is uniform distributed over the complete diameter of a plot. It is shown (Groenendijk & Van den Eertwegh, 2004) that this concept is valid with regard to the partitioning of travel times of drainage water and the vertical concentration gradient. However, the concept neglects possible horizontal concentration gradients.

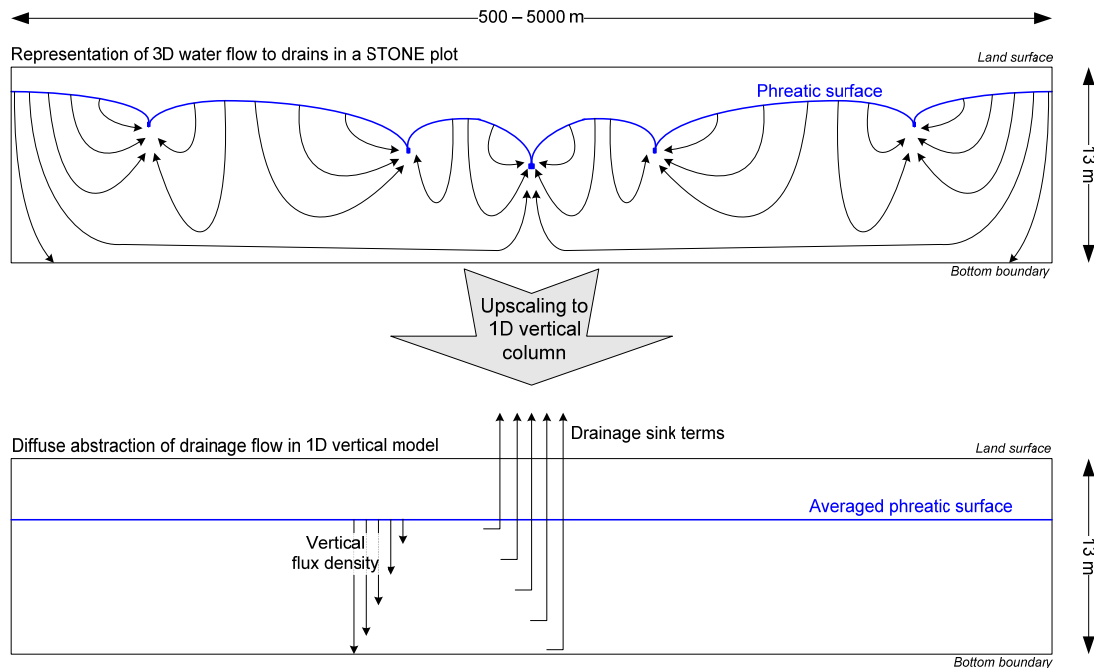


Fig. A1.3 Schematic representation of flow pattern of water conveyed to drains and the up-scaling of the drainage flow in a 1D vertical column model

### Soil nutrient cycle and leaching (ANIMO)

The ANIMO model quantifies the relation between fertilisation rates, land management and the leaching of nutrients to groundwater and surface water systems for a wide range of soil types and different hydrological conditions. Only the retention in the soil is described, the removal of nutrients in the ditch walls and in the surface water body is not considered. A detailed description of the ANIMO model is given by Groenendijk *et al* (2005).

Nutrient path ways from agricultural land are related to surface runoff, leaching to groundwater and leaching to surface water systems (Figure A1.4). Five leaching substances have been distinguished: three soluble nitrogen substances (nitrate-N, ammonium-N, dissolved organic-N) and two soluble phosphorus substances (mineral-P and dissolved organic-P). In the ANIMO model only ammonium and mineral phosphate are assumed to exhibit sorptive behaviour. Ammonium is sorbed to the negative surfaces of clay particles and humic compounds in the soil. Since the ammonium fraction in the total cation content is relatively small under field circumstances it is assumed that there is no need to consider cation exchange processes and sorption is described by a linear sorption isotherm.

Phosphate sorption is modelled by assuming a reversible adsorption reaction and an irreversible diffusion (fixation) process. The adsorption of phosphate is described by a Langmuir adsorption equation (Schoumans, 1995; Schoumans and Breeuwsma, 1997):

$$Q_P = \frac{Kc}{1 + Kc} Q_{\max}$$

where  $Q_p$  is the content of adsorbed P ( $\text{mmol M}^{-1}$ ),  $Q_{max}$  is the maximum content of adsorbed P ( $\text{mmol M}^{-1}$ ) and  $K$  is the adsorption constant ( $\text{L}^3 \text{M}^{-1}$ ). The incorporation of phosphate by diffusion is described by a time dependent Freundlich equation taking into account three types of sites with different affinities of phosphate:

$$S = \sum_{m=1}^3 (S_{0,m} e^{-\alpha_m t} + K_m c^{N_m} (1 - e^{-\alpha_m t}))$$

where  $S$  is the phosphate content in the diffusion sorption pool ( $\text{mmol M}^{-1}$ ),  $K_m$  is the Freundlich sorption coefficient for site  $m$  ( $(\text{M L}^{-3})^{1/N_m} \text{mmol M}^{-1}$ ),  $N_m$  is the Freundlich exponent for site  $m$  (-),  $\alpha_m$  is the diffusion rate constant ( $\text{T}^{-1}$ ) and  $S_{0,m}$  is the initial content of sorbed P for site  $m$  ( $\text{mmol M}^{-1}$ ). The parameters  $K_m$ ,  $N_m$ ,  $\alpha_m$  have been fitted on experimental data for a wide range of Dutch sandy soils by Schoumans (1995).

Phosphate precipitation is modelled as an instantaneous reaction. The reaction occurs immediately and complete when the solute concentration exceeds the equilibrium concentration  $c_{eq}$ . The precipitated minerals dissolve immediately when the concentration of the water phase drops below the buffer concentration. For most of the Dutch sandy soils, the parameterization of the model has been restricted to the instantaneous precipitation formulation. For establishing the equilibrium concentration a dependence on  $pH$  has been taken into account.

Additions to the soil can be introduced at the start of any time step. The properties of the added materials and the application method have to be defined in the input. If relevant, crop residues can be introduced as additions of fresh organic material to the top layer at any time step. The simulation of tillage is described by the uniform redistribution of all constituents present in the layers for which ploughing is specified in the input

When ammonium-containing material is added superficially and dry and warm weather conditions occur, a major part of it gets lost through volatilization. If, however, the material is incorporated the major part will be saved. Volatilization of  $\text{NH}_3$  has been described very simple as a fraction of the ammonium applied in manure or fertilizer additions.

The input of fresh organic matter to the soil system occurs by additions of manure, root materials, grazing and harvest losses and any other organic materials defined by the model user. In the organic carbon cycle the following processes are described (Fig. 3):

- (a) application of various organic materials, such as manure and crop residues;
- (b) decomposition of roots and root exudates;
- (c) decomposition of fresh organic materials in soils and transformation partly to humus/biomass and partly to dissolved organic matter;
- (d) decomposition of dissolved organic matter and transformation to humus/biomass
- (e) turnover of humus/biomass. Humus is a lumped pool consisting of dead soil organic matter and living biomass.

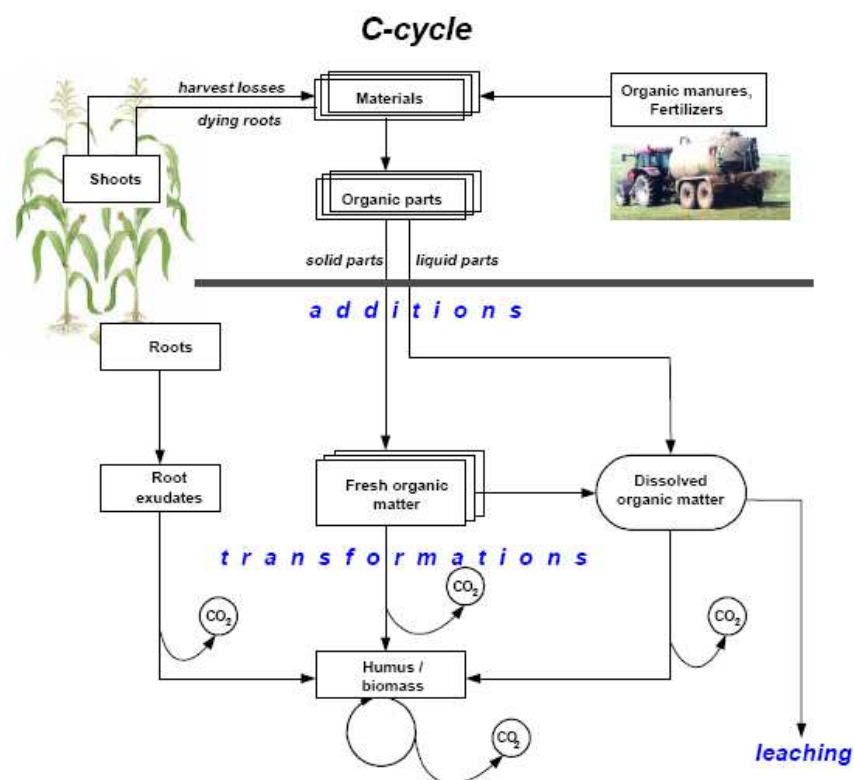


Fig. A1.4 Relational diagram of the organic matter cycle described in the ANIMO-model

Organic materials are partly lost during decomposition in soils and partly transformed to humus. For each kind of organic material, fractions are specified which have different decomposition rates, and N and P contents. For each fraction the decomposition rate is assumed to follow first-order kinetics. This approach allows the simulation of decomposition of various organic materials and to mimic the experimental results from laboratory and field research. Also dissolved organic matter (DOM) is distinguished which results from both manure application and organic matter decomposition. The organic part of both the N and the P cycle in the soil runs largely parallel to the organic C cycle. Hence, the decomposition and transformation processes of fresh organic materials (FOM) and the humus (HU) turnover determine the mineralization and immobilization of both N and P in soils. The relative N (or P) mineralization rate depends on the C/N (or C/P) ratio in decomposed fresh organic materials, the C/N (or C/P) ratio in newly formed humus, and the assimilation/dissimilation ratio. As a result of organic matter dissimilation, part of the organic N and P is transformed to the mineral status. Another part of the organic pools remains in the organic status in dead humic components. Depending on the assimilation ratio and the ratio between N or P content in parent fresh organic material and the N or P weight fraction of the humus/biomass pool, mineral N or P are released or incorporated. No immobilization of nitrate has been assumed. The mineralization rate is input to the solution of the transport and conservation equations of ammonium and mineral P.

The initial organic matter contents and the attribution to the pools determine the mineralization rates to some extent. In the STONE model, the initial contents are derived from the soil map schematization to 21 soil units (Wösten *et al.*, 1988). For each of the soil units the organic matter content per soil horizon is estimated on the basis of the available information in the Soil Information System. These contents imposed to the model for the so-called initialization run which starts in 1941. From 1941–2000 the model is run with assumed and calculated land management information. For the first period to the midst of the eighties, the information is rather coarse, but from 1986 onwards, the information on fertilization rates and crop uptake rates is detailed. The distribution of the organic matter and the accumulated phosphate over the different pools in 2000 has then, beside the assumed attribution in 1941, also become a function of the historical land management. The subsoil organic matter contents are based on the procedures described by Kroon *et al.*, (2000). It should be noticed that the topsoil and the subsoil have been schematized independently, which has led to some illogical combinations. Some of these combinations are considered as artifacts in this study.

Under (partial) aerobic conditions in the soil system, ammonium is oxidized to nitrate. Nitrification is described by first order rate kinetics. When the moisture condition in the soil leads to (partial) anaerobiosis, the rate constant is adapted by a correction factor  $f_{ae}$  to take account for the unfavourable aeration conditions. Decomposition of organic materials under anaerobic conditions can proceed if sufficient nitrate-oxygen is available to meet the oxygen demand. In the ANIMO model, it is assumed that denitrification is governed by the oxygen requirement of respiration processes or the nitrate content itself when nitrates concentration is low. The actual denitrification  $R_{den}$  rate ( $\text{kg m}^{-3} \text{d}^{-1}$ ) is calculated from the potential denitrification  $Den_{pot}$  rate ( $\text{kg m}^{-3} \text{d}^{-1}$ ), a response function for moisture saturation degree  $f_{WFPS}$  (–) and the nitrate concentration according to:

$$R_{den} = \frac{c_{NO3}}{k_{0.5} + c_{NO3}} f_{WFPS} Den_{pot}$$

Where  $c_{NO3}$  is the nitrate concentration ( $\text{kg m}^{-3}$ ). The potential denitrification  $Den_{pot}$  is determined by the decomposition rate of organic materials.

#### *Crop uptake rates*

The nutrient crop uptake rate ( $\text{kg m}^{-3} \text{d}^{-1}$ ) in a soil compartment with thickness  $\Delta z$  (m) is described proportional to the ammonium, nitrate and phosphate concentration and the transpiration flux  $q_{tr}$  ( $\text{m d}^{-1}$ ) towards plant roots:

$$R_u = \sigma \frac{q_{tr}}{\Delta z} c_i$$

The transpiration stream concentration factor  $\sigma$  (–) has been introduced to match the nutrient availability in the soil to crop requirement.

When the ANIMO model is used in combination with an external crop production model (e.g. Ten Berge *et al.*, 2000) all the input data concerning nitrogen and phosphorous uptake and crop losses are read from an input file. The following data should be specified:

- Minimum and maximum nitrogen and phosphorous content values of crop losses as a constant value for the model run.
- Nitrogen and phosphorous uptake quantities as well as dry matter, nitrogen and phosphorous quantities of crop losses per time step.

The forcing function for crop uptake is subdivided to values per soil compartment which show significant plant transpiration. From these data a transpiration stream concentration factor  $\sigma$  (–) is calculated to relate nutrient uptake to transpiration flux and to obtain a first order sink term which can be incorporated into the conservation and transport equation. If the nutrient availability in the soil is less compared to the nutrient demand the deficit is added to the demand of the next time step. Only when a certain deficit is not compensated by external sources (fertilization) or internal sources (mineralisation) during the remaining part of the growing season, the total realised uptake can stay under the total external forced uptake.

#### *Responses to environmental factors*

Both the transformation rate constants of the organic pools and the nitrification rate constant are defined by a reference value expressing the rate at optimal conditions. Environmental influences are taken into account by multiplication factors for reduced aeration at wet conditions, drought stress at dry conditions, temperature and pH.

Aeration has a major influence on transformation rates of all micro-biological processes in agricultural eco-systems. The Water Filled Pore Space (WFPS) is defined as the ratio between the actual soil moisture content and the content at saturation. The WFPS-variable affects mineralisation, nitrification and denitrification. Functional relationships have been implemented to describe the relative process rate on this WFPS-variable. The moisture response of nitrification is based on a response sigmoid function which only depends on the soil air fraction. It is assumed that the half rate value occurs at 4% air fraction and that nitrification is optimal when the soil air fraction exceeds 8%.

The relative denitrification rate in sandy soils is defined as linear relation with the WFPS-variable. When a certain WFPS-value is exceeded, the denitrification process starts and the relative rate proceeds to one at WFPS=1. The threshold value has been calibrated in the different versions of the STONE model. The value was set at 0.8 in STONE2.3. Because of the dependency of the potential denitrification rate, the variable should be calibrated after each adjustment of the organic matter cycle parameterization.

The correction factor for temperature ( $f_T$ ) is described by an Arrhenius equation:

$$f_T = \exp \left[ -\frac{\mu}{R_{gas}} \left( \frac{1}{T + 273} - \frac{1}{T_{ref} + 273} \right) \right]$$

where  $\mu$  is the molar activation energy taken ( $\text{J mol}^{-1}$ ),  $R_{gas}$  is the gas constant ( $\text{J mol}^{-1} \text{K}^{-1}$ ) and  $T_{ref}$  is the average annual temperature for the Dutch climate. Two options for obtaining soil temperature values per time step are available: a simple sinus wave model incorporated in the ANIMO model and the capability to read soil temperature data per time step from the hydrological input file.

The response of the reaction rates to the  $pH$  is one function for all micro-biological related processes. The multiplication factor  $f_{pH}$  is given as:

$$f_{pH} = \frac{1}{1 + e^{-2.5(pH - 5)}}$$

Time independent  $pH$ -values are defined by the user for each soil horizon. It has been assumed that under optimal agricultural practises, the  $pH$ -value will not change and the seasonal fluctuation has been ignored.

## Appendix 2 Literature survey of the denitrification rates in the subsoil

Many studies on the denitrification process can be found in literature (Boyer *et al* 2006), but only few of them are applicable for the sandy aquifers of the Dutch lowland landscape. Denitrification is a reduction process performed by particular groups of heterotrophic bacteria that are ubiquitous in the environment and that have the ability to use nitrate ( $\text{NO}_3$ ) as an electron acceptor during anaerobic respiration, thereby converting  $\text{NO}_3$  in soils and waters to gaseous forms (Firestone and Davidson, 1989). At low oxygen ( $\text{O}_2$ ) levels, these microbial communities may use nitrate ( $\text{NO}_3$ ), nitrite ( $\text{NO}_2$ ), or nitrous oxide ( $\text{N}_2\text{O}$ ) as alternative electron acceptors to  $\text{O}_2$ , with molecular  $\text{N}_2$  as the final product, given by the following reaction sequence:  $\text{NO}_3^- \rightarrow \text{NO}_2^- \rightarrow \text{NO} \rightarrow \text{N}_2\text{O} \rightarrow \text{N}_2$  (Davidson and Schimel, 1995). There remains uncertainty about the conditions favouring the various products of the  $\text{NO}_3$  transformation. Understanding these controlling factors is of interest because the intermediate gaseous products are important greenhouse gases whereas the  $\text{N}_2$  final product is highly inert and thus has no adverse environmental consequences.

Quantifying where, when, and how much denitrification occurs in ecosystems remains particularly vexing at virtually all spatial scales (Van Breemen *et al.* 2002, Galloway *et al.* 2004, Groffman *et al.* 2006, Seitzinger *et al.* 2006). It is difficult to detect changes in  $\text{N}_2$  in the environment attributed to denitrification amid the very large reservoir of  $\text{N}_2$  that makes up the majority (nearly 80%) of earth's atmosphere. At present, there are no scientific methods for making direct measurements of the rates of denitrification at the scale of watersheds or large regions. Even at field scales, there remain large challenges in using direct measurements of denitrification—the measurements are often sparse, sometimes unreliable, and can vary appreciably over short distances. Understanding this variability is complicated by the complex set of environmental variables that control the rates of denitrification and heterogeneity in soils and microbial communities (Firestone and Davidson 1989, Tiedje 1988). Because the dominant controlling factors are highly variable over space and time, they give rise to “hot spots” and “hot moments” of denitrification that are difficult to predict (McClain *et al.* 2003).

The vast majority of denitrification studies have been conducted for the root zone and only few studies concerning subsoil sediments and aquifers are available. Most of the research was devoted to decay rate constants of organic material and it appeared that the decay rate is dependent on the age of the organic material.

A wide range of first order rate constant values related to the denitrification process can be found in the literature. Values ranging between 2 and 400  $\text{yr}^{-1}$  have been used by Skaggs *et al.* (1995), Breve *et al.* (1997) and Helwig *et al.* (2002) for calibration of different versions of the DRAINMOD model on field plots accommodated with tile drains, however Madramootoo *et al.*, (1999) applied the DRAINMOD model using values of 0.44 – 1.3  $\text{yr}^{-1}$

for the denitrification rate constant. Wriedt (2004) took account for organic matter contents in soils in his nitrate transport and denitrification simulations in the groundwater system of the Schaugraben catchment in Northern Germany. Upper root zone denitrification rate constants were set by him to  $1.46 \text{ yr}^{-1}$  for mollic and humic gleyic soils,  $0.73 \text{ yr}^{-1}$  for gleyic soils,  $0.37 \text{ yr}^{-1}$  for luvisols and  $0.037 \text{ yr}^{-1}$  for sandy cambisols.

The rate constant for aquifers was found to be in the range of  $0.3 - 0.7 \text{ yr}^{-1}$  by Frind *et al.* (1990) for the Fuhrbergh aquifer, was assumed at  $0.37 \text{ yr}^{-1}$  by Wriedt and Rode (2006) the aquifer of the Schaugraben catchment and was set to  $0.17 - 0.56 \text{ yr}^{-1}$  by Wendland *et al.* (2001). Average values of the rate constant as found by Uffink (2003) were  $0.8 \text{ yr}^{-1}$  for a fast reacting groundwater zone and  $0.09 \text{ yr}^{-1}$  for a slowing reacting zone in a calibration of a first order rate model describing denitrification in deep groundwater in the vicinity of pumping stations in the Eastern part of the Netherlands.

In the scope of this study on the consequences of choosing an alternative depth for the nitrate compliance checking, the scientific literature has been surveyed for denitrification rates in aquifers. Because only a few specific denitrification rates have been reported, the organic matter decay rates have also been considered. When the nitrate reduction in the presence by materials containing iron and / or sulphide (pyrite, iron carbonates) reductants does not occur, the organic matter decay rates and denitrification rates are related to each other. Reported denitrification rates have been summarized in table A2.1. Most of the literature sources express the denitrification rate in mg per kg sediment per day. The order of the reaction is not reported in most of the publications. The references mentioned by Koron (1991) are consulted for additional information, for instance on the age of the material in his laboratory or field experiments. Most of the articles do not mention the geological age of the sediments. In such a case, the age has been estimated from geological mapping information.

As explained before, the decay rates of organic material in the presence of other electron acceptors has been considered beside the specific denitrification rates. We tried to obtain both quantitative and qualitative information on the band width of decay rate constant in relation with the age of the material. The decay rate of organic material in the presence of different electron acceptors as a function of the age has been depicted in Fig. A2.1. The rate is expressed milli-equivalent electrons, to be able to compare the differences of the reaction stoichiometry of the transformation processes. The organic matter originates from different environments: fresh water sediments, soils, estuaries, salt water sediments, and aquifers. The age of the organic material has been derived from geological maps (e.g. Pleistocene sediment), or has been estimated on the basis of expert judgement. The age of organic material in fresh water sediments is estimated at 100 year and for peat formations at 1000 year. Additionally, the decay rate of organic material as a function of age according to the relation derived by Middelburg (1989) has been depicted. This function describes the

decrease of organic matter in marine sediments by a first order decay process, where the rate constant ( $k_{den}$ ) is dependent on the age according to:

$$\log(k_{den}) = -0.95 \log(t) - 0.81 \quad (N = 140; \quad r = 0.987)$$

It appears from Fig. A2.1:

- The expected relation between the decay rate and the age of the organic material is confirmed.
- The function of Middelburg follows the minimum values of the observed decay rates.
- A great variation of reported rates is observed, even within the same age class. The difference between the maximum and the minimum value amount to two orders of magnitude of time intervals.
- The denitrification rates in aquifers with a residence time of more than one million year are higher than the rates of in sediments with complete anaerobic conditions.
- Denitrification rates measured under field conditions do not show a clear difference from the rates measured in the laboratory.
- The denitrification rate ranges between 10 and 1000 meq  $\Gamma^{-1}$  yr $^{-1}$ .
- At higher ages of the organic material, no clear difference can be observed for the decay rate influenced by different anaerobic electron acceptors (Fe, SO $_4$ , Mn, CH $_2$ O). It is concluded that under anaerobic circumstances, the decay rate is determined by the reactivity of organic material.

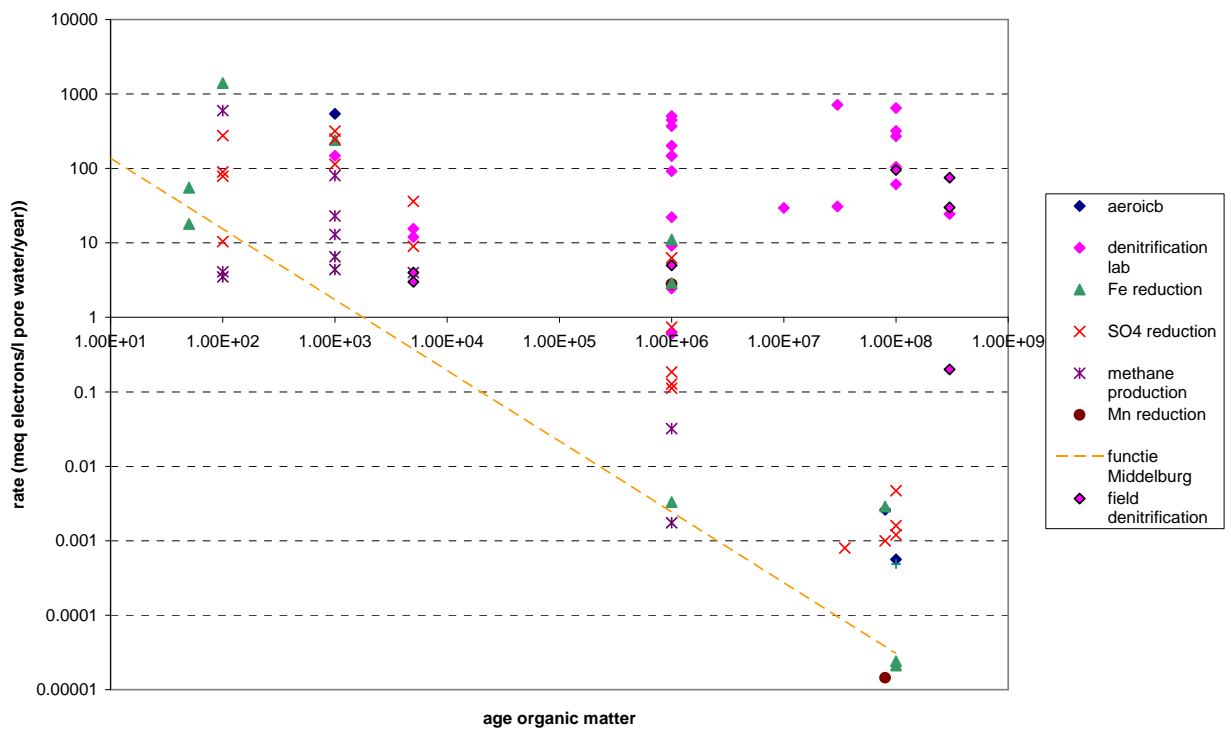


Fig. A2.1 Decay rates of organic material with different electron acceptors (meq electrons / (liter pore water·year)) as a function of the age of the organic material



Table A2.1: Denitrification rates in aquifers

Location	System	Sediment. Age	estimated age (yr)	Lab / field	Rate based on	Rate** in mmol L <sup>-1</sup> yr <sup>-1</sup>	order	Rate constant (yr <sup>-1</sup> )	remark	Reference
Skagerrak (Denmark)	continental margin sediment	Holocene	10 <sup>3</sup>	Lab / model	CH <sub>2</sub> O	37				Van Cappellen, P. & Wang, Y
Florida, USA	aquifer	Pleistocene	10 <sup>6</sup>	batch lab	CH <sub>2</sub> O	37	1 <sup>st</sup>	0.00736	first order rate based on 1% carbon	Bradley <i>et al.</i> , 1992
Herlsmagle, Denmark	aquifer, clay with stones and clay loam with stone	Jurassic & Crataceous*	10 <sup>8</sup>	lab	NO <sub>3</sub>	54.1			10 °C (initial 1000 mg NO <sub>3</sub> -N/l)	Lind (1983); from Koron (1992)
Herlsmagle, Denmark	aquifer, clay with stones and clay loam with stone	Jurassic & Crataceous*	10 <sup>8</sup>	lab	NO <sub>3</sub>	129.1			25 °C (initial 1000 mg NO <sub>3</sub> -N/l)	Lind (1983); from Koron (1992)
Bramminge, Denmark	aquifer, coarse sand and sand	Tertiar*	3.0 × 10 <sup>7</sup>	lab	NO <sub>3</sub>	6.1			10 °C (initial 1000 mg NO <sub>3</sub> -N/l)	Lind (1983); from Koron (1992)
Bramminge, Denmark	aquifer, coarse sand and sand	Tertiar*	3.0 × 10 <sup>7</sup>	lab	NO <sub>3</sub>	142.6			25 °C (initial 1000 mg NO <sub>3</sub> -N/l)	Lind (1983); from Koron (1992)
Skaelskor, Denmark	aquifer, clay with stones	Jurassic & Crataceous*	10 <sup>8</sup>	lab	NO <sub>3</sub>	12.3			10 °C (initial 1000 mg NO <sub>3</sub> -N/l)	Lind (1983); from Koron (1992)
Skaelskor, Denmark	aquifer, clay with stones	Jurassic & Crataceous*	10 <sup>8</sup>	lab	NO <sub>3</sub>	20.9			25 °C (initial 1000 mg NO <sub>3</sub> -N/l)	Lind (1983); from Koron (1992)
Upper Glacial aquifer Long Island, NY	aquifer	Pleistocene*	10 <sup>6</sup>	lab	NO <sub>3</sub>	29.5			initial 3.8 mg NO <sub>3</sub> -N/l	Slater & Capone; from Koron (1992)
Upper Glacial aquifer Long Island, NY	aquifer	Pleistocene*	10 <sup>6</sup>	lab	NO <sub>3</sub>	18.4			amended to 5.2 mg NO <sub>3</sub> -N/l	Slater & Capone; from Koron (1992)
Paris Island, South Carolina	aquifer, sand and limestone	Pleistocene-Miocene	10 <sup>7</sup>	lab	NO <sub>3</sub>	5.9			amended with 14 mg NO <sub>3</sub> -N/l	Morris <i>et al.</i> (1988); from Koron (1992)
Falmouth, Massachusetts	aquifer, sand and gravel	Pleistocene*	10 <sup>6</sup>	lab	NO <sub>3</sub>	100.8			7.3 mg NO <sub>3</sub> -N/l	Smith & Duff (1988); from Koron (1992)
Falmouth, Massachusetts	aquifer, sand and gravel	Pleistocene*	10 <sup>6</sup>	lab	NO <sub>3</sub>	40.6			15.7 mg NO <sub>3</sub> -N/l	Smith & Duff (1988); from Koron (1992)

Location	System	Sediment. Age	estimated age (yr)	Lab / field	Rate based on	Rate** in mmol L <sup>-1</sup> yr <sup>-1</sup>	order	Rate constant (yr <sup>-1</sup> )	remark	Reference
Falmouth, Massachusetts	aquifer, sand and gravel	Pleistocene*	10 <sup>6</sup>	lab	NO <sub>3</sub>	1.8			1.12 mg NO <sub>3</sub> -N/l	Smith & Duff (1988) from Koron (1992)
Falmouth, Massachusetts	aquifer, sand and gravel	Pleistocene*	10 <sup>6</sup>	lab	NO <sub>3</sub>	0.5			0.49 mg NO <sub>3</sub> -N/l	Smith & Duff (1988); from Koron (1992)
Vomb, Southern Sweden	aquifer	Jurassic & Crataceous*	10 <sup>8</sup>	lab	NO <sub>3</sub>	63.9			2.5 mg NO <sub>3</sub> -N/l	Bengtsson & Annadotter (1989); from Koron (1992)
Savannah River site, South Carolina	aquifer, sand, clayey sands and sandy clays	Pleistocene*	10 <sup>6</sup>	lab	NO <sub>3</sub>	1.8			<0.21 mg NO <sub>3</sub> -N/l	Fransis <i>et al.</i> (1989); from Koron (1992)
Savannah River site, South Carolina	aquifer, sand, clayey sands and sandy clays	Pleistocene*	10 <sup>6</sup>	lab	NO <sub>3</sub>	89.7			amended with 4.2 mg NO <sub>3</sub> -N/l	Fransis <i>et al.</i> (1989); from Koron (1992)
Savannah River site, South Carolina	aquifer, <50% sand; >30% clay	Pleistocene*	10 <sup>6</sup>	lab	NO <sub>3</sub>	0.0			0.15 mg NO <sub>3</sub> -N/l	Fransis <i>et al.</i> (1989); from Koron (1992)
Savannah River site, South Carolina	aquifer, <50% sand; >30% clay	Pleistocene*	10 <sup>6</sup>	lab	NO <sub>3</sub>	73.7			amended with 4.2 mg NO <sub>3</sub> -N/l	Fransis <i>et al.</i> (1989); from Koron (1992)
Falmouth, Massachusetts	aquifer, sand and gravel	Pleistocene*	10 <sup>6</sup>	lab	NO <sub>3</sub>	4.4			corrected to 12 °C, 11 mg NO <sub>3</sub> -N/l	Smith <i>et al.</i> (1991); from Koron (1992)
dunes in wester Netherlands	aquifer, coarse sand with shells	Holocene	5.0 x 10 <sup>3</sup>	field	NO <sub>3</sub>	3.1–5.2			10 °C (initial 2.1 mg NO <sub>3</sub> -N/l)	Van Beek & Van Puffelen (1987); from Koron (1992)
dunes in wester Netherlands	aquifer, coarse sand with gravel	Holocene	5.0 x 10 <sup>3</sup>	field	NO <sub>3</sub>	2.4–3.9			10 °C (initial 2.1 mg NO <sub>3</sub> -N/l)	Van Beek & Van Puffelen (1987); from Koron (1992)
Grindsted landfill, Denmark	aquifer, landfill leachate	Pleistocene	10 <sup>6</sup>	field	NO <sub>3</sub>	0.12–21.6				Ludvigsen <i>et al.</i> (1998)
Hannover, northern Germany	aquifer, limestone	Tertiar*	3.0 x 10 <sup>7</sup>	field	NO <sub>3</sub>		1 <sup>st</sup>	1.2–2.1	10 °C (initial to 40 mg NO <sub>3</sub> -N/l)	Kölle <i>et al.</i> (1985) and Böttcher <i>et al.</i> (1989); from Koron (1992)
Rodney, Ontario, Canada	aquifer, sand	Paleozoic*	3.0 x 10 <sup>7</sup>	field	NO <sub>3</sub>	4.9–80.9			initial 13.0 mg NO <sub>3</sub> -N/l	Trudell <i>et al.</i> (1986)
Rodney, Ontario, Canada	aquifer, sand	Paleozoic*	3.0 x 10 <sup>7</sup>	field	NO <sub>3</sub>	15.1			initial about 6.4 mg NO <sub>3</sub> -N/l	Starr and Gillham (1989); from Koron (1992)

Location	System	Sediment. Age	estimated age (yr)	Lab / field	Rate based on	Rate** in mmol L <sup>-1</sup> yr <sup>-1</sup>	order	Rate constant (yr <sup>-1</sup> )	remark	Reference
Alliston, Ontario, Canada	aquifer	Paleozoic*	3.0 × 10 <sup>7</sup>	field	NO <sub>3</sub>	0.04			initial about 3.8 mg NO <sub>3</sub> -N/l	Starr and Gillham (1989); from Koron (1992)
Heber, Utah	aquifer, clay, silt, sand with cobbles	Jurassic & Crataceous*	10 <sup>8</sup>	field	NO <sub>3</sub>	19.0			7 °C (initial 12.5 and 23.7 mg NO <sub>3</sub> -N/l)	Korom (1991); from Koron (1992)
a catchment area in the North German Lowlands	aquifer	Tertiar*	3.0 × 10 <sup>7</sup>	field	NO <sub>3</sub>		1 <sup>st</sup>	0.17 –0.56		H. Goßmann <i>et al.</i> , (2005); after Böttcher (1989) and Van Beek (1987)
Germany	aquifer	Tertiar*	3.0 × 10 <sup>7</sup>	field			1 <sup>st</sup> ; NO <sub>3</sub>	0.35	under denitrification conditions	Wendland <i>et. al.</i> , (1994); After Böttcher (1989)
Germany	aquifer	Tertiar*	3.0 × 10 <sup>7</sup>	field			1 <sup>st</sup> ; NO <sub>3</sub>	0.02	under insignificant dinitrification conditions	Wendland <i>et. al.</i> , (1994); After Böttcher (1989)
Abbotsford-Sumas aquifer, Fraser-Whatcom Lowlands, Br.Col., Ca	aquifer, glacial-fluvial coarse sands and gravels				NO <sub>3</sub>	<0.01–0.14			agricultural watershed, in deep unpolluted part the aquifer	Tesoriero <i>et. al.</i> (2000)
Abbotsford-Sumas aquifer, Fraser-Whatcom Lowlands, Br.Col., Ca	aquifer, glacial-fluvial coarse sands and gravels				NO <sub>3</sub>	1.0–2.7			agricultural watershed, at redo cline along shallow flow path	Tesoriero <i>et. al.</i> (2000)
Abbotsford-Sumas aquifer, Fraser-Whatcom Lowlands, Br.Col., Ca	aquifer, glacial-fluvial coarse sands and gravels				NO <sub>3</sub>	140.0			groundwater in riparian zone adjacent to the stream	Tesoriero <i>et. al.</i> (2000)

\* Sedimentary age not reported in paper but based on geological map

\*\* If rate reported were based gr sediment they were converted to l pore water by assuming that the sandy sediments had a porosity of 0.35 and a bulk density of 1,6 kg/l



## Appendix 3 Sediment analysis of aquifer samples to support refinement of regional model input

To support the regional nutrient transport model STONE used by Alterra, sediment data was collected and analysed. This could support the modelling effort by:

- providing direct input parameters for STONE;
- providing information on relevant parameters, which could help indicating whether the model outcome from STONE is plausible.

This appendix describes the data used and its relevance for denitrification. The study is restricted to the Pleistocene part of the Netherlands since this was also the area of interest of the overall study.

### A3.1 Data analysis of sediment

An analysis was performed of solid sediment parameters in order to get more insight in the geochemical background underlying the areas of interest and their influence on the fate of nitrate. Special attention was given to differences between the various areas under investigation (South, Central, North), and differences between various areas.

The following data was used:

- South Netherlands: a combination of old data (as reported in Bakker *et al.*, 2007) and recent data (Klein *et al.*, 2008);
- Central Netherlands: new samples collected and analysed (see report on field campaign Griffioen *et al.*, 2008);
- North Netherlands: recent data collected in 2006 and 2007.

A lot of these data was generated or aggregated during the last 2–3 years, and has therefore not yet been used in the discussion about the nitrate compliance checking depth.

#### A3.1.1 Data analysis

Analytical methods used to obtain the data are described in the report on the field campaign (Griffioen *et al.*, 2008). Only samples were used until at most 30 m depth. This depth was chosen because:

- it corresponds to the GEOTOP classification of TNO, and therefore many samples are present;
- this depth selection includes at least the first 5 meters of the saturated zone, which is the primary interest of this study, and addition of samples up till 30 meters depth increases the number of samples, thereby increasing the reliability of statistical figures;
- STONE has a model domain from the surface to 13 m–s.s.

Lithology was assessed by visual inspection. This classification was checked in the following way (see figure A3.1):

- Samples with an organic carbon content higher than 15% were classified as peat;

- From the remaining samples, if the lutum concentration was smaller than 8% and the fraction with a grain size of  $>63 \mu\text{m}$  was more than 50%, samples were classified as sand, otherwise as clay/loam;
- In the samples with lithology clay/loam from South-Netherlands,  $\text{Al}_2\text{O}_3$  was significantly higher than in the samples with lithology sand (Klein *et al.*, 2008). Therefore, in case of doubt, samples that had been renamed were checked again with the criteria:
  - Samples with  $\text{Al}_2\text{O}_3 > 5\%$  were classified as clay/loam;
  - Samples with  $\text{Al}_2\text{O}_3 < 7\%$  were classified as sand.

For samples with a content of  $\text{Al}_2\text{O}_3$  between 5 and 7%, the lithology class that was attributed by visual inspection was maintained.

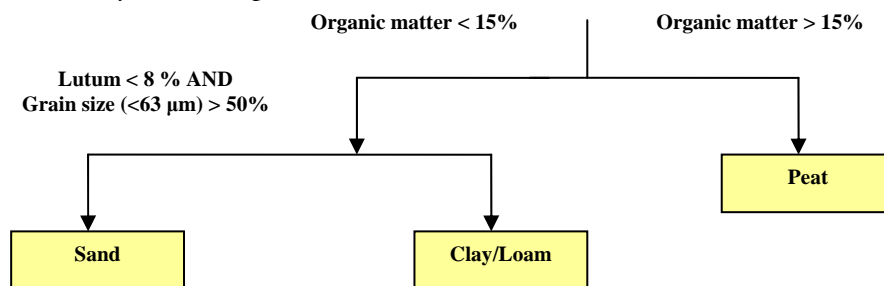


Fig. A3.1 Lithology classification method, additional to classification by visual inspection.

Patterns in organic matter and pyrite will be discussed hereafter. Therefore, the calculation of these parameters will be discussed briefly here.

### A3.1.2 Organic matter

If available, the organic matter content can be calculated from the results of two analytical techniques:

- 1) from Thermogravimetric Analysis (TGA) over the temperature range  $105 - 550^\circ\text{C}$ , including a correction for water loss from other components such as clays (after Bakker *et al.*, 2007):

$$\text{Organic matter (\% d.w.)} = (\text{loss on ignition } 105\text{--}550^\circ\text{C}) - 0.07 * \text{lutum (\%d.w.)} \quad (\text{A3.1})$$

- 2) direct analysis of organic carbon content using a CS-analyzer, from which the organic matter content was calculated according to equation A3.2:

$$\text{Organic matter (\%d.w.)} = \text{Organic carbon (\% d.w.)} * 2 \quad (\text{A3.2}).$$

In case both TGA- and CS-analyzer-results were available, the latter were used, because the former has a larger error due to the release of other components over the temperature range, such as water from clays. This contribution is sample and matrix dependent.

### A3.1.3 Pyrite

Pyrite ( $\text{FeS}_2$ ) was calculated according to Bakker *et al.*, 2007:

$$\text{FeS}_2(\%d.w.) = \frac{\text{FeS}_{2, \text{massa}} * S(\%d.w.)}{S_{2, \text{massa}}} \quad (\text{A3.3}).$$

It was assumed that all S measured is present as pyrite. Using this assumption, the total sulphur content is converted to the pyrite content on the basis of the stoichiometry, as can be seen in equation A3.3.

If possible, the sulphur content was determined using XRF or CS-analyzer (see also Mol *et al.*, 2006). In case both were available, data obtained with the CS-analyzer were preferred, because XRF gives a rougher estimate of the sulphur content (Bakker *et al.*, 2007).

## A3.2 Regional differences and depth profiles

Clear differences were found in the organic matter and pyrite contents for South, Central and North Netherlands (fig. A3.2 and A3.3). For both organic matter and pyrite, highest concentrations were found in North Netherlands, followed by South Netherlands, and in Central Netherlands concentrations were smallest (or even below detection limit). This pattern was found for various formations considered (fig. A3.2 and A3.3 show the formations of Boxtel, Drente and Kreftenheije as examples). The formation of Boxtel is most relevant here: it is present at the surface and has a thickness of a few meters (fig. A3.4). Data for sand samples only (fig. A3.3) show the difference less distinctively than the data for all lithology classes (fig. A3.2). This was to be expected, because the clay/loam and peat samples, which contain most organic matter and pyrite, were removed. However, even when considering the sand samples only, the patterns described above remain the same. Thus, within formations, differences exist between North, Central and South Netherlands, and these will have to be parameterized separately.

Figure A3.5 gives an example of the differences between formations, for North of the Netherlands. It makes clear that differences between formations can be larger and smaller. The difference gets smaller but remains when limiting the scope to only sands or Pleistocene sands.

Depth profiles for pyrite and organic matter (fig. A3.6) show similar patterns as described above. The difference between the various regions is more pronounced for organic matter than for pyrite. The combination of data does not show a very clear depth pattern, although pyrite content does seem to increase with depth. This increase occurs at the most for the shallow groundwater in the Northern sand district.

Overall, the organic matter and pyrite data indicate that the subsurface of North Netherlands is most reduced, followed by South Netherlands and finally Central Netherlands. These findings correspond well to the patterns found for nitrate and iron in groundwater (appendix 4). They are expected to have consequences for denitrification: under more reduced conditions, denitrification is more likely to occur.

### **A3.3 Data parameterization for STONE**

For use in STONE, data of organic matter and pyrite were parameterized. The data was grouped according to classification in GEOTOP units (Vermooten *et al.*, 2005), sand districts (North, Central, South), and geological formations (Mulder *et al.*, 2003). South-Limburg was excluded from the dataset. The aim was mainly to obtain averages and to have a firm basis for general statistics (average, 10-, 50-, 90-percentile of organic matter and pyrite). Furthermore, data groups that were not significantly different were combined to minimize the amount of input to work with.

GEOTOP areas (A3.7) were selected which have Pleistocene formation at the surface:

- 4a1, 4b, 4c, 4d1 (South Netherlands);
- 2b, 3a, 3b, 6a, 6b (Central Netherlands);
- 5a1, 5b1, 5c1, 5c3 (North Netherlands).

Sand and clay/loam were combined; peat was not included. The reason for this is that the peat samples, although present in small numbers, are expected to contribute in an atypical way to the total concentrations because of their high concentrations of organic matter and pyrite. Because the percentage of peat in each GEOTOP unit is known, it is still possible to include the regional presence of peat in a spatial unit. With respect to the contribution of clay/loam or peat it is noteworthy to remark that it remains an open question whether groundwater will really pass the pore matrix having these lithologies; generally, clay/loam is less permeable and thus the groundwater will preferentially flow around it. This will also mean that denitrification might take place in these parts to a smaller extent. Flow around impermeable layers is, however, more likely when these layers are local and do not occur at larger scale.

To give a first answer to the question whether data groups differed significantly, percentile plots (fig. A3.8A-I) were compared. Groups were made according to combinations of sand district, formation and GEOTOP. For example, samples from GEOTOP 4a1 from the Formation of Boxtel from South-Netherlands form one group. Percentile plots were only compared per geological formation in a combined sand district in case two or more lines consisted of 20 or more data points each; otherwise, meaningful comparison would not be possible. When percentile plots of two or more GEOTOP areas (within a formation, within a sand district) already differ significantly from less than the 75-percentile onward, the averages calculated for these various GEOTOP areas are also different. In that case, for parameterization method 1 is applicable (see below).

When percentile plots of a geological formation for two or more GEOTOP areas (within a sand district) do not differ much until > 75 percentile, the mean calculated for these various GEOTOP areas is also not very different. In that case, method 2 can be used for parameterisation, and GEOTOP areas within a formation and within a sand district can be aggregated: within a formation and within a sand district the same geochemical values are attributed to various GEOTOP areas (average, 10-, 50-, 90-percentile of organic matter and pyrite).

Two methods are used to parameterize:

*Method 1* is applicable for samples from GEOTOP units that differ significantly. Therefore, using this method, statistical parameters (number of samples (n), average, 10-, 50-, and 90-percentile) are calculated for all combinations of GEOTOP, formation and sand district separately. Sand fraction and clay/loam fraction were calculated using the Voxel model of 250 x 250 x 1 m of lithological class of sediment for the Netherlands, where three classes are distinguished (sand, clay + loam and peat). The statistical parameters were calculated as follows:

- number of samples (n) = number of samples 'sand' + number of samples 'clay/loam';
- average = average 'sand' from GEOTOP unit \* sand content in GEOTOP unit + average 'clay/loam' from GEOTOP unit \* clay/loam content in GEOTOP unit;
- 10-percentile = 10-percentile 'sand' from GEOTOP unit;
- 50-percentile = 50-percentile of all samples, both 'sand' and 'clay/loam' from GEOTOP unit;
- 90-percentile = 90-percentile 'clay/loam' from GEOTOP unit.

*Method 2* is applicable for samples from GEOTOP units (within formation, within sand district) that do not differ significantly. The same statistical parameters are calculated as in case of method 1 (number of samples (n), average, 10-, 50-, and 90-percentile). However, in this case GEOTOP units (within a sand district, within a formation) that are similar are combined and given the same values for the statistical parameters mentioned. For a formation within each GEOTOP within a sand district, the fraction of sand and the fraction of clay/loam were calculated using the Voxel model. The statistical parameters were calculated as follows:

- number of samples (n) = number of samples 'sand' + number of samples 'clay/loam';
- average = average 'sand' from formation \* content of sand in GEOTOP unit + average 'clay/loam' from formation \* content 'clay/loam' in GEOTOP unit;
- 10-percentile = 10-percentile 'sand' from formation;
- 50-percentile = 50-percentile of all samples, both 'sand' and 'clay/loam' from formation;
- 90-percentile = 90-percentile 'clay/loam' from formation.

On the basis of the percentile plots and the comparison methods described earlier, the following geological units were found to differ significantly between the GEOTOP areas within a sand district for either pyrite or organic matter:

*Table A3.1: Datasets found to give different values between the GEOTOP units in the various sand districts.*

District	Pyrite	Organic Matter		
North	DRGI	clay/loam		
	DRGIDRGIGADRSC	clay/loam		
	URURTYURVE	clay/loam		
Central				
South	BX	sand	WA	clay/loam
	BXBXBSBXLMBXLSBXWI	sand	ST	sand
	OO	sand	WA	sand
	WA	sand		
	BE	sand		
	BEBERO	sand		
	SY	clay/loam		
	WA	clay/loam		

Percentile plots are given in a subsequent paragraph. The statistical characteristics (average, 10–, 50– and 90–percentile) calculated for the spatial units according to the two methods are given in tables A3.2A-I, where the preferable method per group is also indicated. Note that the differences in, for example, the average can be a factor 3 or more between the two methods for a group, especially when a group is considered in which one of the units presented in Table A3.1 is involved.

Comparing the figures for the average, 10–, 50– and 90–percentile with data obtained previously (Griffioen *et al.*, 2006; Vermooten *et al.*, 2006) shows that many of these figures are different (e.g.: organic matter content for GEOTOP unit 4a1, Beegden formation, GEOTOP unit 4b, Boxtel formation). Probably this is mainly caused by the separation over the various sand districts (South, Central, North), which were shown to differ strongly (fig. A3.2. and fig A3.3.). This emphasizes the importance of taking into account regional differences. In this study, a much larger amount for various regional data was taken into account, enabling a more complete picture.

The data presented give a good indication of the distribution of organic matter and pyrite, which, as stated before, will have consequences for denitrification. This link however is not straightforward. Especially the nature of the organic matter deserves further attention: it is expected that the reactivity of the organic matter, which can vary, will influence the denitrification to a large extent.

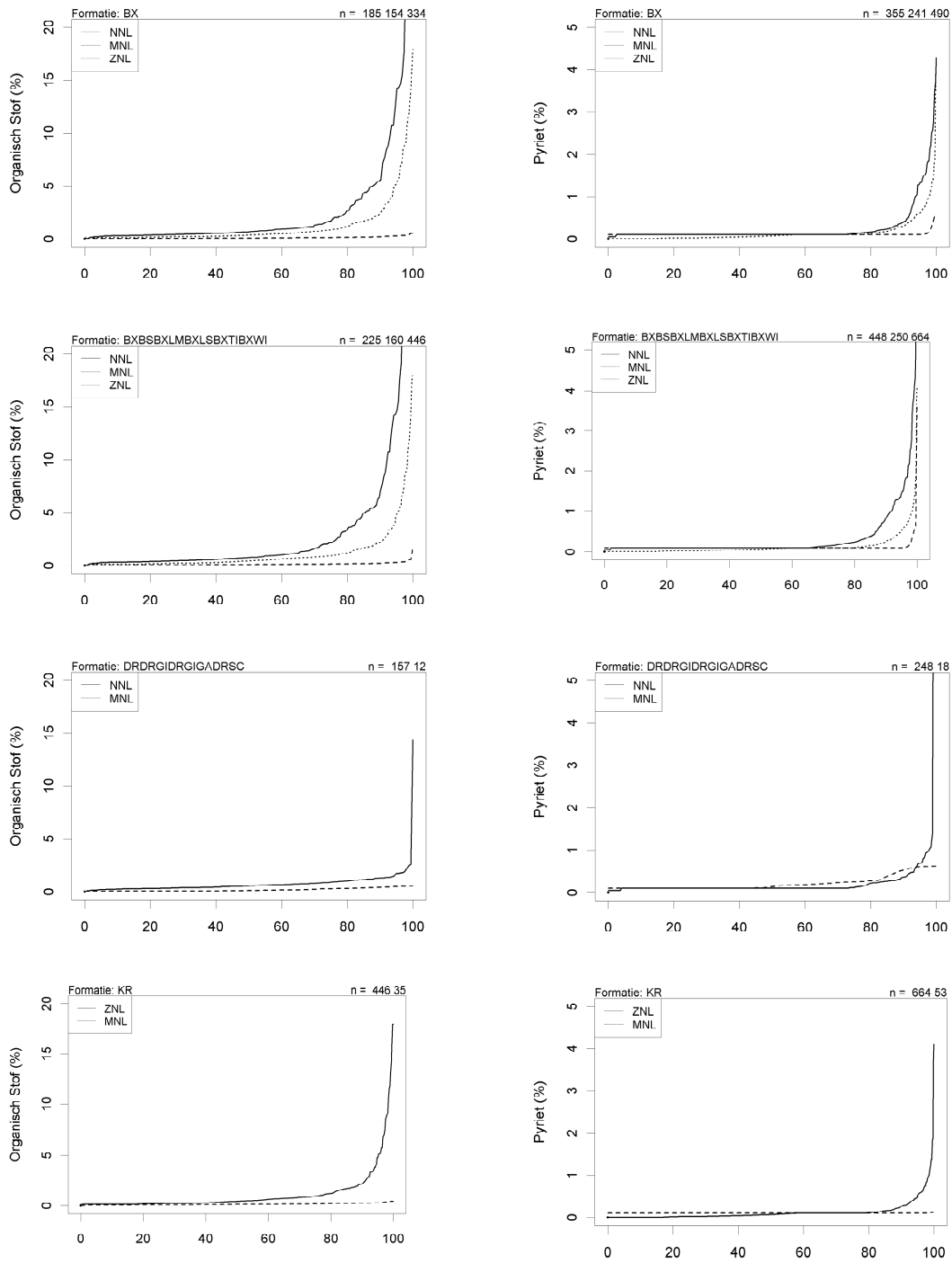


Fig. A3.2 Comparison of sedimentary content of organic matter (left) and pyrite (right) between South (Z), Central (M) and North (N) Netherlands for some selected geological formations: Boxtel (BX), Boxtel undifferentiated (BXBSBXLMBXLXSBXTIBXWI), Drentbe undifferentiated (DRDRGIDRGIGADRSC) and Kreftenbeije (KR).

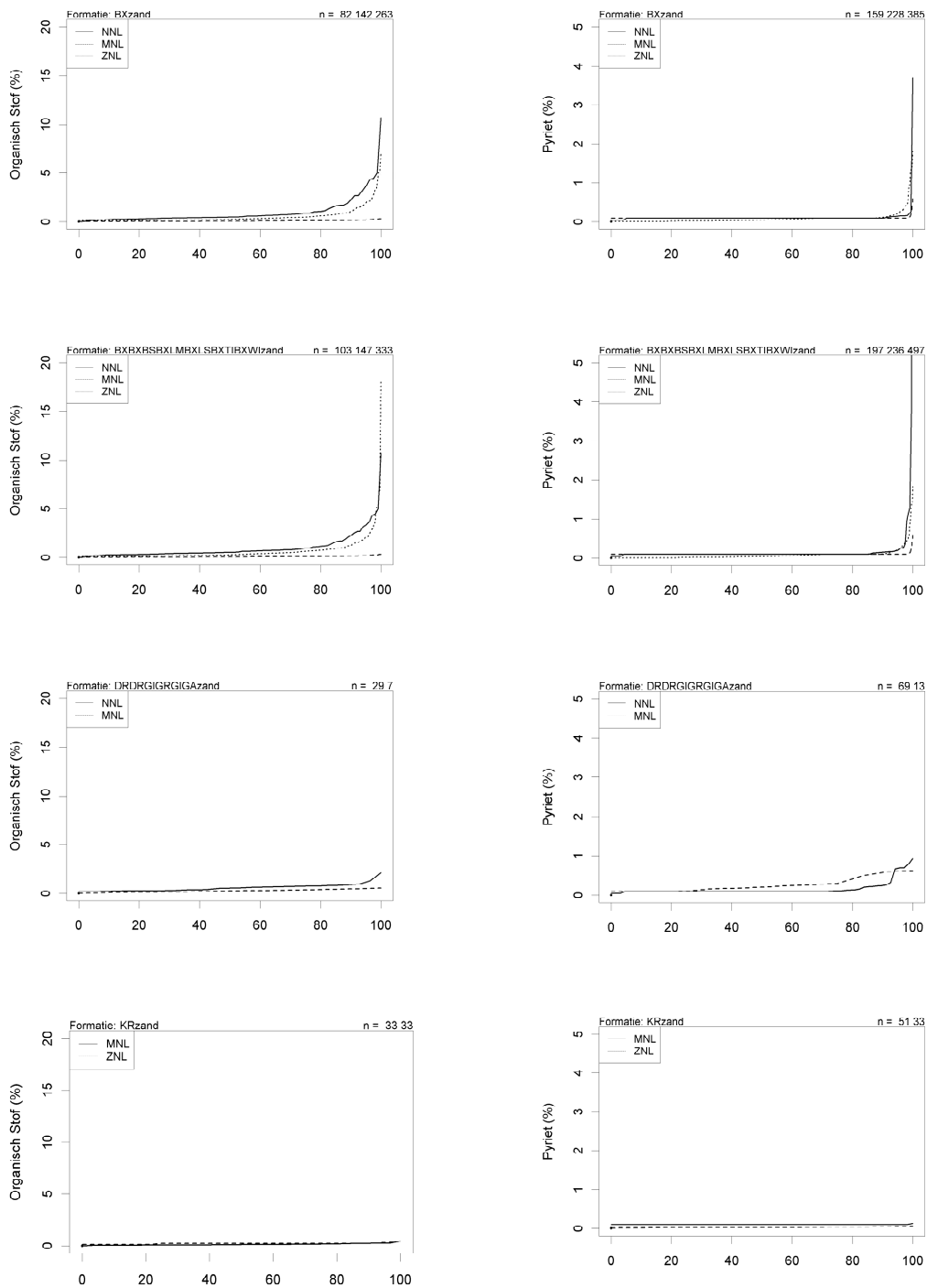
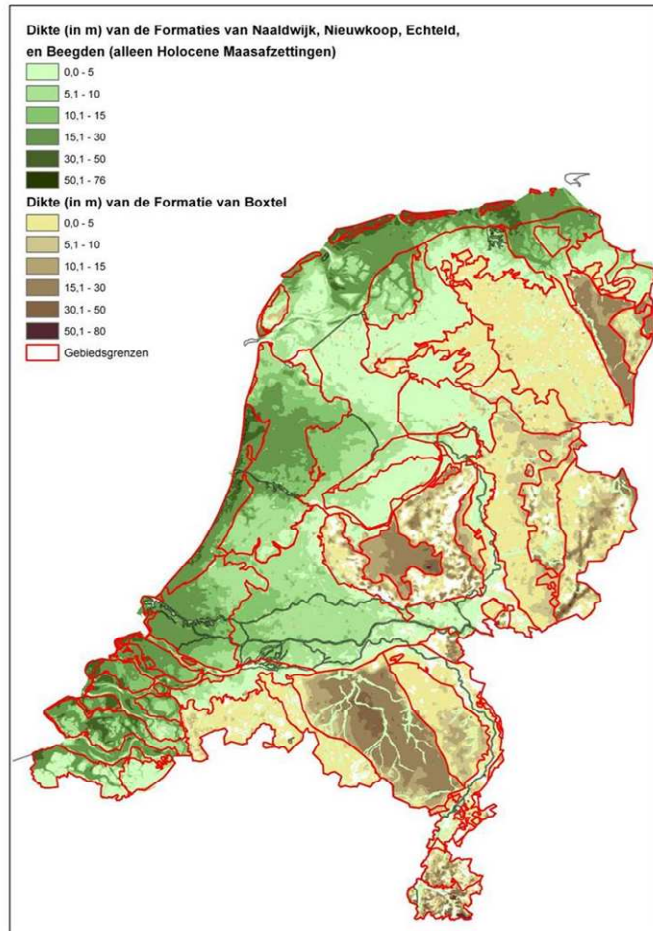


Fig. A3.3 Comparison of sedimentary content of organic matter (left) and pyrite (right) between South (Z), Central (M) and North (N) Netherlands for some selected geological formations: Boxtel (BX), Boxtel undifferentiated (BXBXLMBXLXBTIBXWI), Drenthe undifferentiated (DRDRGIGRIGIGADRSC) and Kreftenbeije (KR), selection for only sand samples (no clay/loam or peat)



*Fig. A3.4 Thickness of formations at the surface of the Netherlands, showing the presence of the Formation of Boxtel at the surface in the largest part of the study area.*

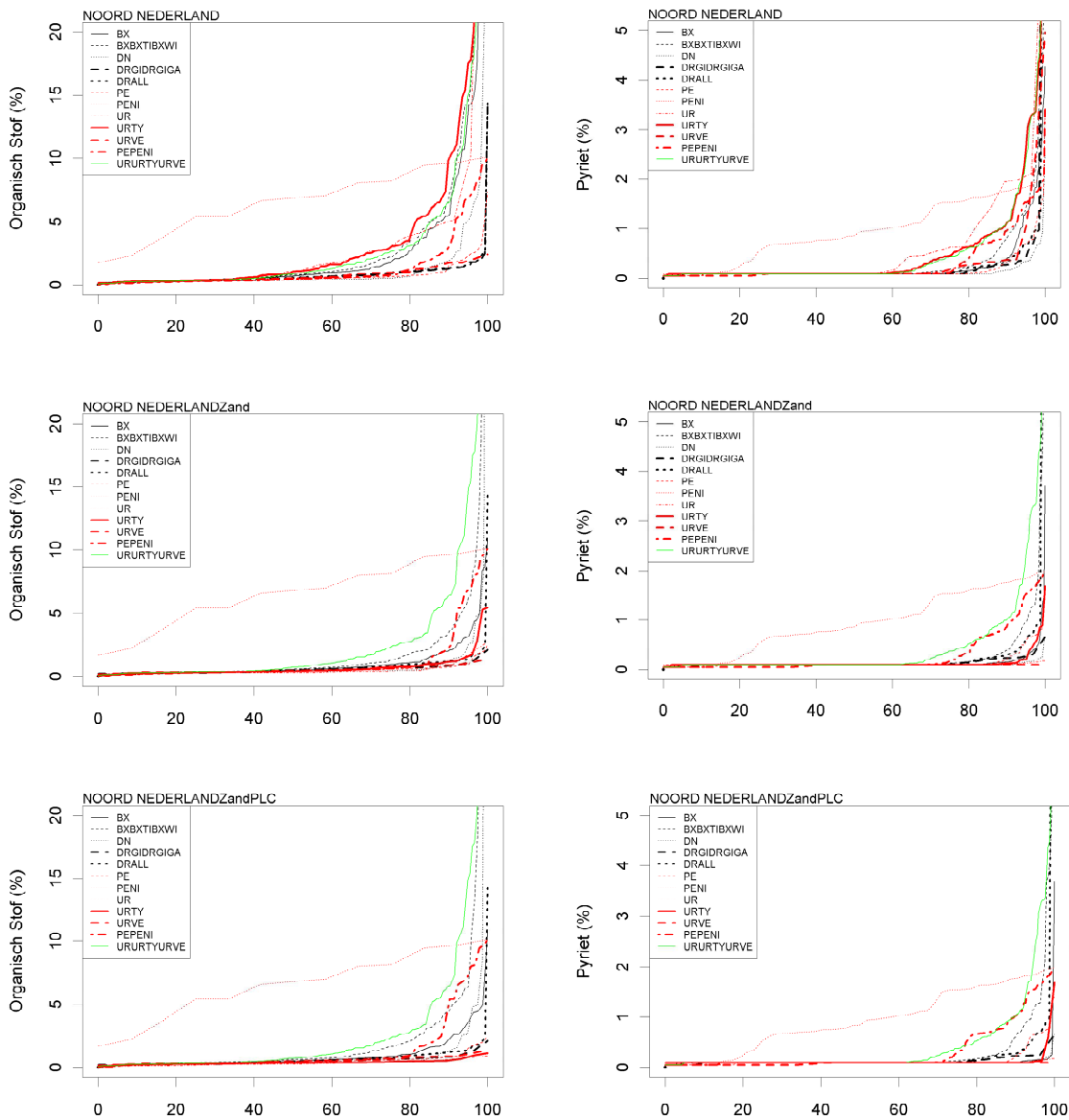


Fig. A3.5 Comparison of sedimentary content of organic matter (left) and pyrite (right) between various geological formations in North Netherlands. The figures show data for all samples (top figures), only sand samples (clay/ loam and peat left out, middle figures), and only Pleistocene sand samples (bottom figures).

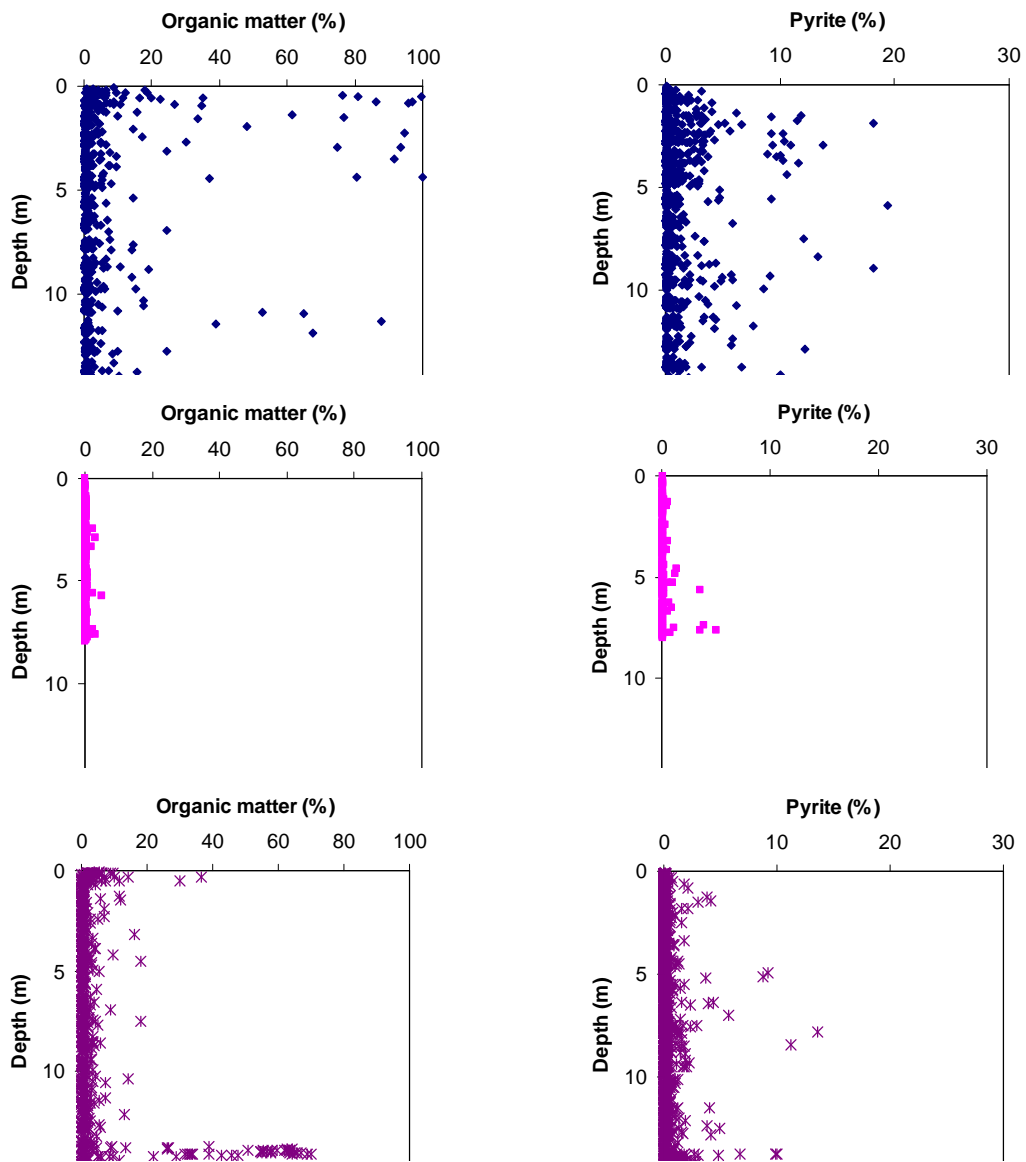


Fig. A3.6 Depth profiles of organic matter (left hand side) and pyrite (right hand side) for North, Central and South Netherlands

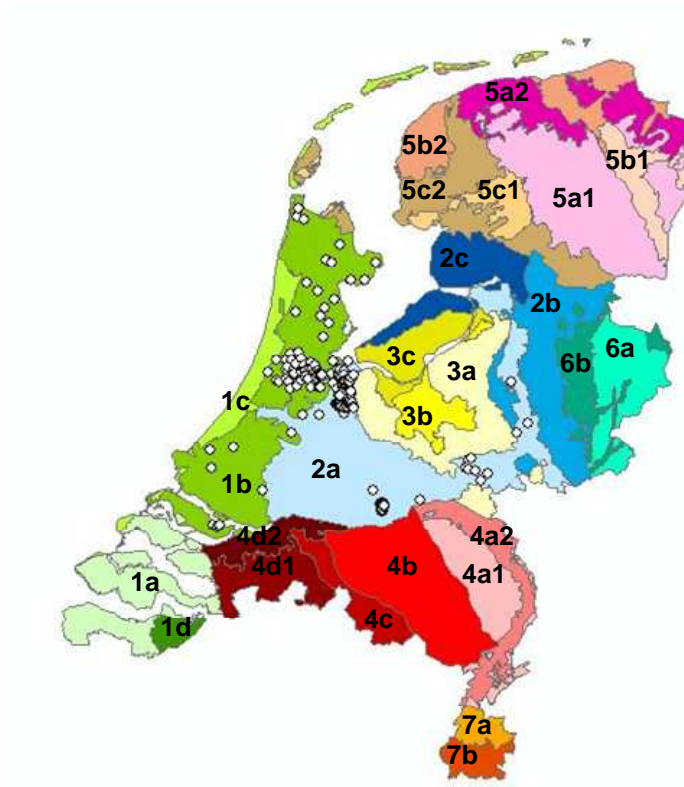


Fig. A3.7 Distribution of the Netherlands into 27 GEOTOP units

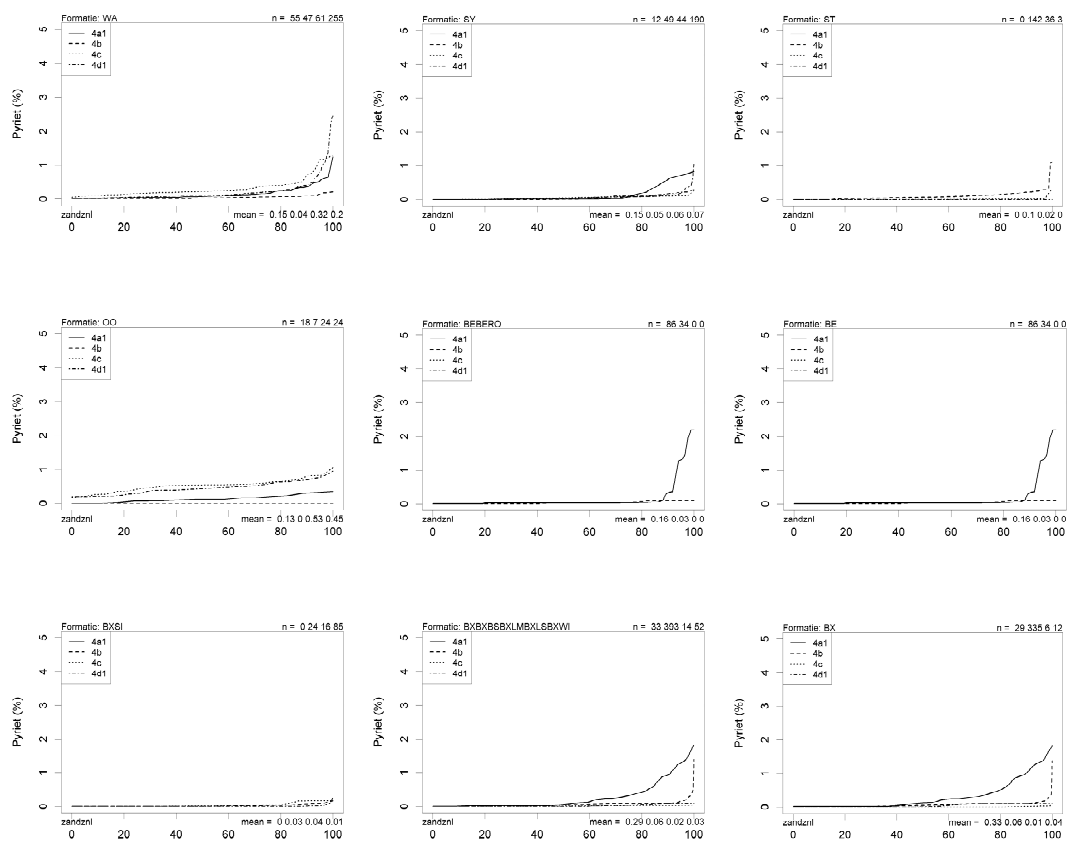


Fig. A3.8.A. Comparison percentile lines pyrite, South Netherlands, sand

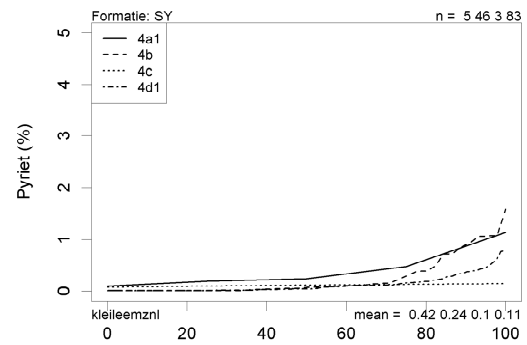
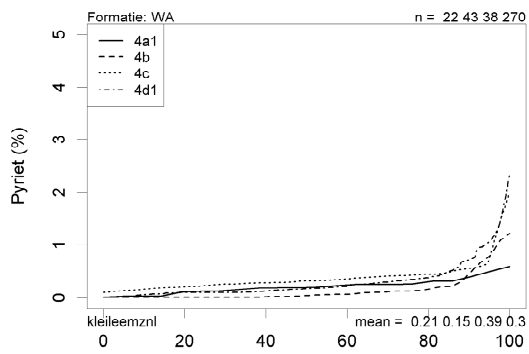


Fig. A3.8B. Comparison percentile lines pyrite, South Netherlands, clay/loam

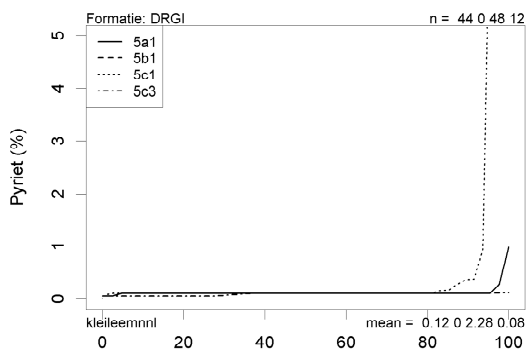
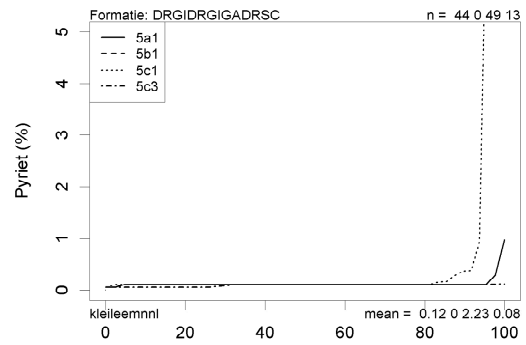
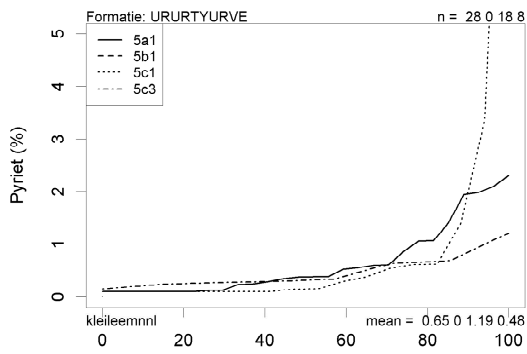


Fig. A3.8C. Comparison percentile lines pyrite, North Netherlands, clay/loam

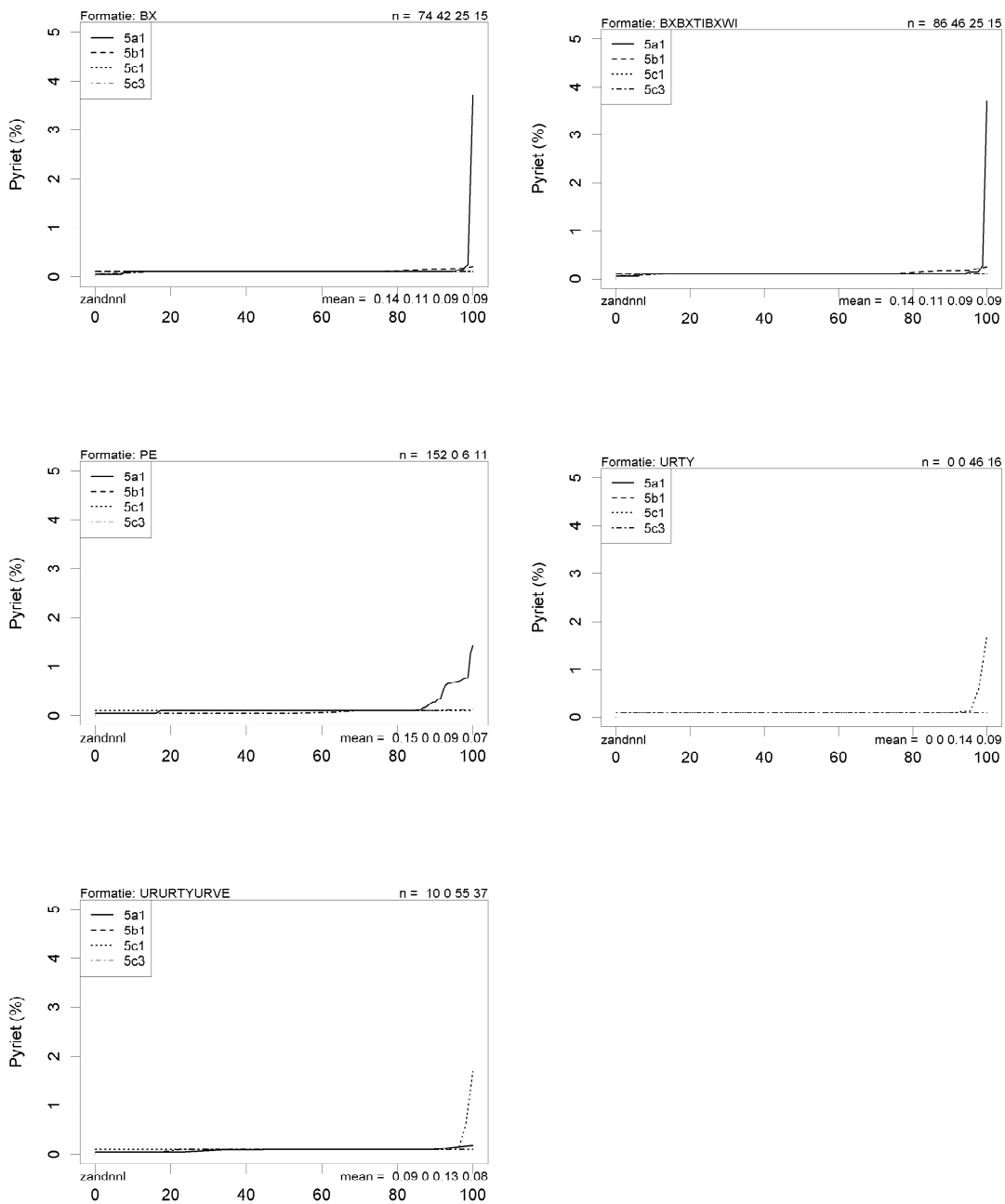


Fig. A3.8D. Comparison percentile lines pyrite, North Netherlands, sand

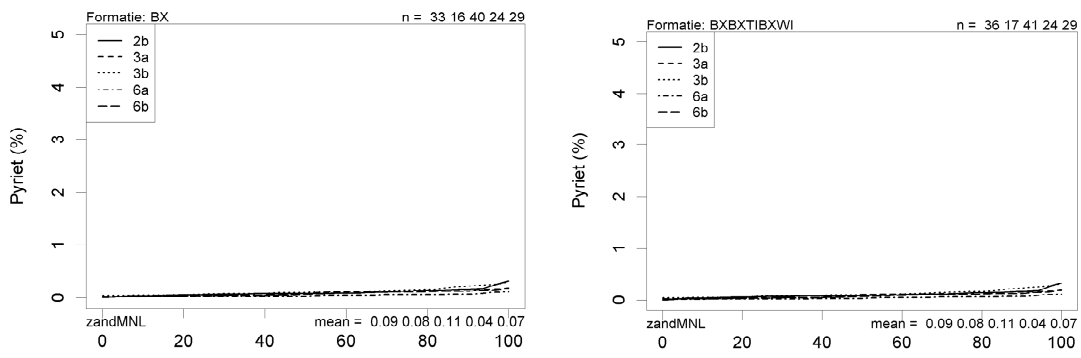


Fig. A3.8E. Comparison percentile lines pyrite, Central Netherlands, sand

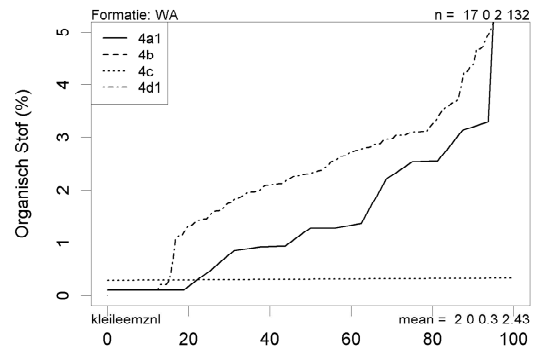
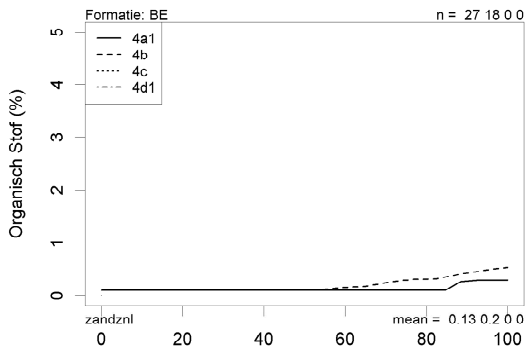
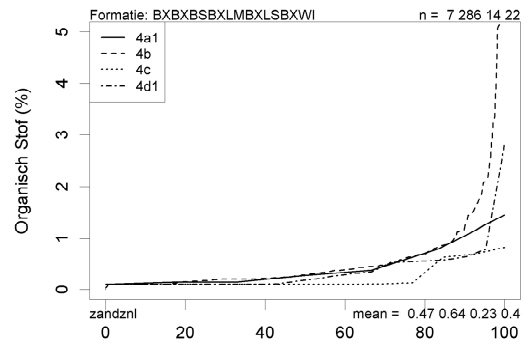
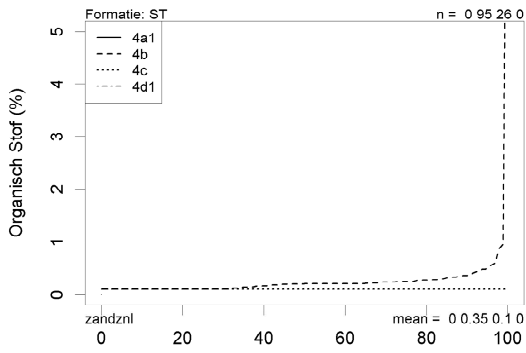
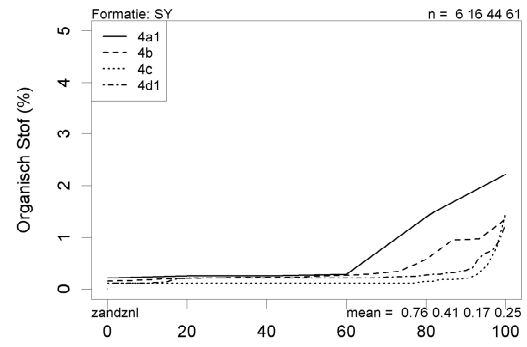
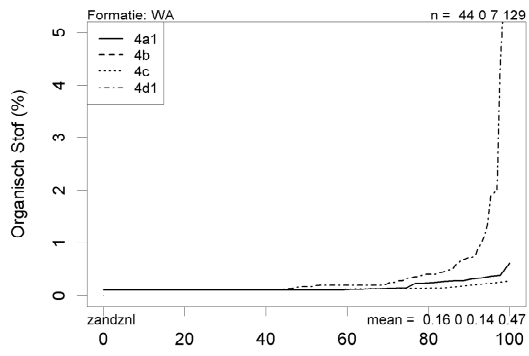


Fig. A3.8F. Comparison percentile lines Organic matter, South Netherlands

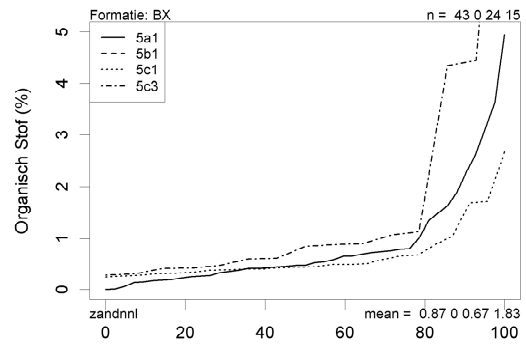
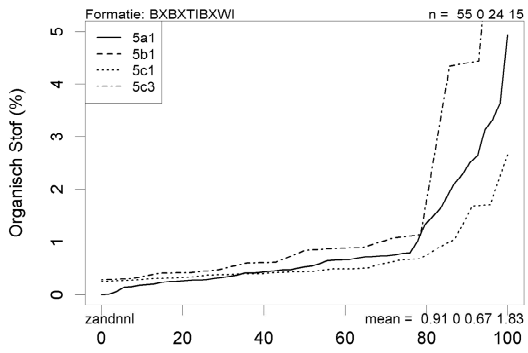
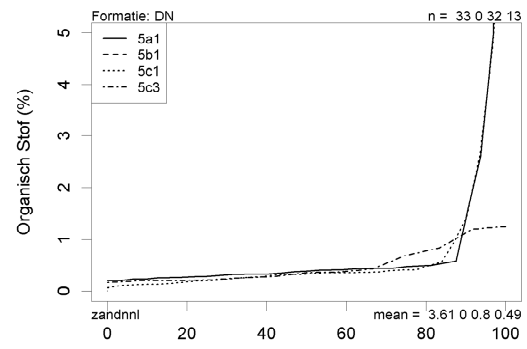
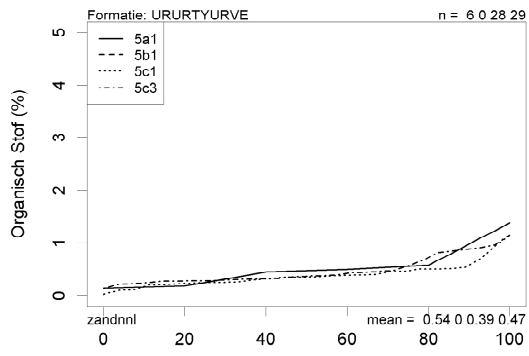


Fig. A3.8G. Comparison percentile lines organic matter, North Netherlands

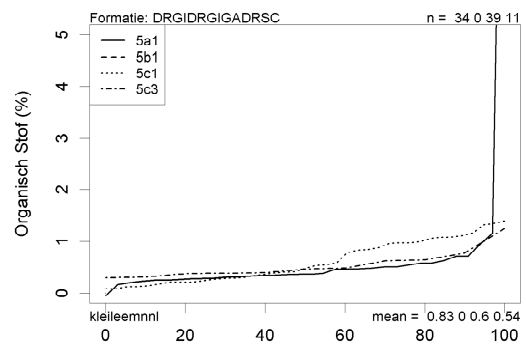
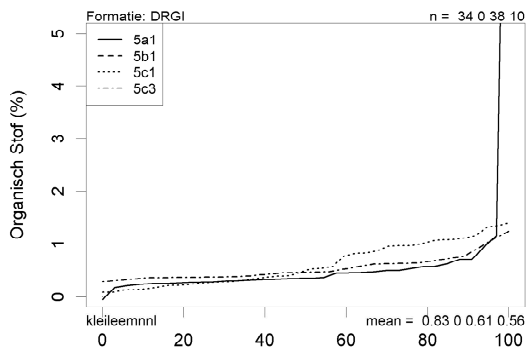


Fig. A3.8H. Comparison percentile lines organic matter, clay/loam, North Netherlands

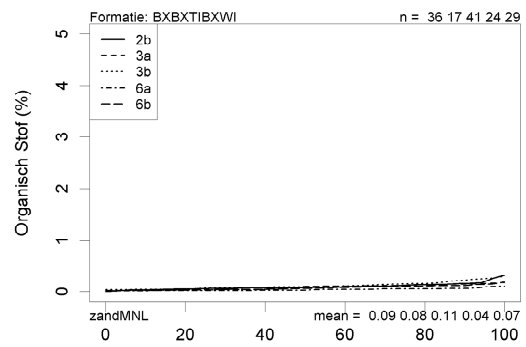
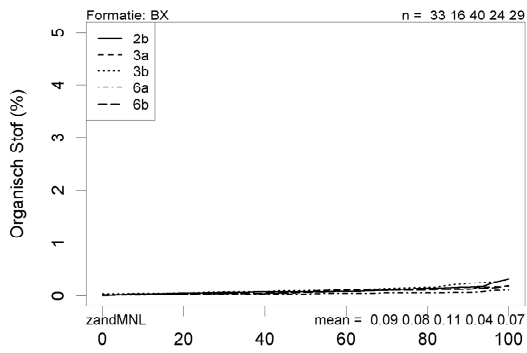


Fig. A3.8I. Comparison percentile lines organic matter, sand, Central Netherlands

Table A3.2. Statistical characteristics (amount of samples, average, 10-, 50- and 90- percentile) calculated using method 1 or 2 (see Chapter 5). For data groups containing less than 20 samples, the 10-percentile and 90-percentile were left out. In case of method 2, geotop units were combined for calculation of the 10-, 50- and 90-percentile per sand district, but the averages were calculated separately for each geotop unit, taking into account fractions of sand and clay+loam. Preferred statistical figures are indicated in bold and shaded background.

Table A3.2A. Statistical characteristics for South Netherlands, organic matter, method 1.

	Number of samples	Average	10-percentile	50-percentile	90-percentile	Formation	Geotop
		Wt%	Wt%	Wt%	Wt%		
1	27	0.13	0.10	0.10	0.26	BE	4a1
2	25	0.25	0.10	0.24	1.08	BE	4b
6	3	1.74		1.77		BERO	4b
9	36	0.50	0.10	0.22	1.40	BR	4a1
13	4	0.47		0.32		BX	4a1
14	298	0.72	0.10	0.31	4.77	BX	4b
15	6	0.22		0.10		BX	4c
16	8	0.78		0.55		BX	4d1
18	42	0.65	0.22	0.89	2.12	BXBS	4b
22	24	3.37	0.63	0.71	1.68	BXLM	4b
26	3	4.10		5.13		BXLS	4b
30	6	0.30		0.10		BXSI	4b
33	4	0.46		0.15		BXWI	4a1
34	12	0.56		0.41		BXWI	4b
35	8	0.24		0.10		BXWI	4c
36	17	0.40		0.10		BXWI	4d1
41	30	0.58	0.15	0.50	1.65	KI	4a1
46	8	0.21		0.20		KR	4b
53	18	0.86		0.90		OO	4a1
<b>58</b>	<b>107</b>	<b>0.56</b>	<b>0.10</b>	<b>0.20</b>	<b>3.40</b>	<b>ST</b>	<b>4b</b>
<b>59</b>	<b>27</b>	<b>0.10</b>	<b>0.10</b>	<b>0.10</b>	<b>0.10</b>	<b>ST</b>	<b>4c</b>
61	11	0.84		0.70		SY	4a1
62	29	0.79	0.17	0.57	7.68	SY	4b
63	47	0.16	0.10	0.10	0.10	SY	4c
64	74	0.33	0.10	0.20	1.96	SY	4d1
<b>65</b>	<b>61</b>	<b>0.28</b>	<b>0.10</b>	<b>0.11</b>	<b>3.21</b>	<b>WA</b>	<b>4a1</b>
66	1	0.47		0.47		WA	4b
67	9	0.14		0.13		WA	4c
<b>68</b>	<b>261</b>	<b>0.72</b>	<b>0.10</b>	<b>0.48</b>	<b>4.38</b>	<b>WA</b>	<b>4d1</b>
69	27	0.13	0.10	0.10	0.26	BEBERO	4a1
70	28	0.30	0.10	0.30	1.81	BEBERO	4b
73	8	0.45		0.26		BXBXBSBXLMBXLSBXWI	4a1
74	379	0.76	0.10	0.39	3.51	BXBXBSBXLMBXLSBXWI	4b
75	14	0.23		0.10		BXBXBSBXLMBXLSBXWI	4c
76	25	0.79	0.10	0.26	5.86	BXBXBSBXLMBXLSBXWI	4d1

Table A3.2B. Statistical characteristics for South Netherlands, organic matter, method 2 (legend as Table A3.2A).

	Number of samples	Average	10–percentile	50–percentile	90–percentile	Formation	Geotop
		Wt%	Wt%	Wt%	Wt%		
1	27	0.18	0.10	0.10	1.08	BE	4a1
2	25	0.21	0.10	0.10	1.08	BE	4b
6	3	1.74		1.77		BERO	4b
9	36	0.50	0.10	0.22	1.40	BR	4a1
13	4	0.61		0.31		BX	4a1
14	298	0.72	0.10	0.31	4.79	BX	4b
15	6	0.59		0.31		BX	4c
16	8	0.71		0.31		BX	4d1
18	42	0.65	0.22	0.89	2.12	BXBS	4b
22	24	3.37	0.63	0.71	1.68	BXLM	4b
26	3	4.10		5.13		BXLS	4b
30	6	0.30		0.10		BXSI	4b
33	4	0.42		0.13		BXWI	4a1
34	12	0.42		0.13		BXWI	4b
35	8	0.42		0.13		BXWI	4c
36	17	0.42		0.13		BXWI	4d1
41	30	0.58	0.15	0.50	1.65	KI	4a1
46	8	0.21		0.20		KR	4b
53	18	0.86		0.90		OO	4a1
58	107	0.50	0.10	0.17	3.39	ST	4b
59	27	0.37	0.10	0.17	3.39	ST	4c
61	11	0.37		0.20		SY	4a1
62	29	0.49	0.10	0.20	4.17	SY	4b
63	47	0.35	0.10	0.20	4.17	SY	4c
64	74	0.48	0.10	0.20	4.17	SY	4d1
65	61	0.50	0.10	0.29	4.34	WA	4a1
66	1	0.64		0.29		WA	4b
67	9	0.47		0.29		WA	4c
68	261	0.63	0.10	0.29	4.34	WA	4d1
69	27	0.20	0.10	0.10	1.81	BEBERO	4a1
70	28	0.26	0.10	0.10	1.81	BEBERO	4b
73	8	0.66		0.37		BXBBSBXLMBXLSBXWI	4a1
74	379	0.74	0.10	0.37	3.64	BXBBSBXLMBXLSBXWI	4b
75	14	0.65		0.37		BXBBSBXLMBXLSBXWI	4c
76	25	0.73	0.10	0.37	3.64	BXBBSBXLMBXLSBXWI	4d1

Table A3.2C. Statistical characteristics for Central Netherlands, organic matter, method 1 (legend as Table A3.2A).

Number of samples		Average	10–percentile	50–percentile	90–percentile	Formation	Geotop
		Wt%	Wt%	Wt%	Wt%		
4	5	0.44		0.24		BREI	6a
6	35	0.10	0.03	0.07	0.50	BX	2b
7	16	0.08		0.07		BX	3a
8	41	0.12	0.04	0.09	0.23	BX	3b
9	24	0.04	0.01	0.03	0.06	BX	6a
10	32	0.08	0.02	0.07	0.22	BX	6b
12	1	0.10		0.10		BXTI	3a
16	3	0.11		0.10		BXWI	2b
18	1	0.16		0.16		BXWI	3b
24	6	0.81		0.78		DO	6a
29	6	0.02		0.07		DR	6a
34	6	0.29		0.27		DRSC	6a
36	31	0.13	0.05	0.11	0.30	KR	2b
40	4	0.05		0.05		KR	6b
44	3	0.89		0.92		RU	6a
46	38	0.10	0.03	0.07	0.50	BXBXTIBXWI	2b
47	17	0.08		0.09		BXBXTIBXWI	3a
48	42	0.12	0.04	0.09	0.23	BXBXTIBXWI	3b
49	24	0.04	0.01	0.03	0.06	BXBXTIBXWI	6a
50	32	0.08	0.02	0.07	0.22	BXBXTIBXWI	6b
54	12	0.22		0.10		DRDRSC	6a

Table A3.2D. Statistical characteristics for Central Netherlands, organic matter, method 2 (legend as Table A3.2A).

Number of samples		Average	10–percentile	50–percentile	90–percentile	Formation	Geotop
		Wt%	Wt%	Wt%	Wt%		
4	5	0.44		0.24		BREI	6a
6	35	0.09	0.02	0.07	0.41	BX	2b
7	16	0.09		0.07		BX	3a
8	41	0.09	0.02	0.07	0.41	BX	3b
9	24	0.11	0.02	0.07	0.41	BX	6a
10	32	0.10	0.02	0.07	0.41	BX	6b
12	1	0.10		0.10		BXTI	3a
16	3	0.12		0.12		BXWI	2b
18	1	0.12		0.12		BXWI	3b
24	6	0.81		0.78		DO	6a
29	6	0.02		0.07		DR	6a
34	6	0.29		0.27		DRSC	6a
36	31	0.12	0.05	0.10	0.30	KR	2b
40	4	0.13		0.10		KR	6b
44	3	0.89		0.92		RU	6a
46	38	0.09	0.02	0.07	0.41	BXBXTIBXWI	2b
47	17	0.09		0.07		BXBXTIBXWI	3a
48	42	0.09	0.02	0.07	0.41	BXBXTIBXWI	3b
49	24	0.11	0.02	0.07	0.41	BXBXTIBXWI	6a
50	32	0.10	0.02	0.07	0.41	BXBXTIBXWI	6b
54	12	0.22		0.10		DRDRSC	6a

Table A3.2E. Statistical characteristics for North Netherlands, organic matter, method 1 (legend as Table A3.2A).

	Number of samples	Average	10– percentile	50– percentile	90– percentile	Formation	Geotop
		Wt%	Wt%	Wt%	Wt%		
4	3	0.17		0.18		AP	5c3
9	47	0.99	0.15	0.49	3.85	BX	5a1
11	25	1.51	0.29	0.44	4.59	BX	5c1
12	17	2.33		0.88		BX	5c3
13	1	5.76		5.76		BXSI	5a1
17	18	1.15		1.04		BXTI	5a1
25	35	3.51	0.23	0.38	4.89	DN	5a1
27	32	0.80	0.12	0.32	1.41	DN	5c1
28	13	0.49		0.34		DN	5c3
33	46	0.55	0.20	0.35	0.71	DRGI	5a1
35	41	0.41	0.19	0.47	1.12	DRGI	5c1
36	18	0.58		0.52		DRGI	5c3
39	1	0.21		0.21		DRGIGA	5c1
40	1	0.30		0.30		DRGIGA	5c3
41	2	0.31		0.31		DRSC	5a1
45	76	0.68	0.18	0.41	5.64	PE	5a1
47	3	0.14		0.16		PE	5c1
48	17	0.81		0.63		PE	5c3
49	12	6.71		6.91		PENI	5a1
53	5	1.77		1.69		UR	5a1
55	11	1.04		0.36		UR	5c1
57	17	6.50		3.03		URTY	5a1
59	29	0.53	0.21	0.39	1.82	URTY	5c1
60	13	1.41		0.35		URTY	5c3
61	7	0.63		0.49		URVE	5a1
64	24	0.81	0.28	0.47	2.25	URVE	5c3
65	65	1.04	0.18	0.64	3.37	BXBXTIBXWI	5a1
67	25	1.51	0.29	0.44	4.59	BXBXTIBXWI	5c1
68	17	2.33		0.88		BXBXTIBXWI	5c3
69	48	0.52	0.21	0.35	0.71	DRGIDRGIGADRSC	5a1
71	42	0.41	0.19	0.43	1.12	DRGIDRGIGADRSC	5c1
72	19	0.58		0.49		DRGIDRGIGADRSC	5c3
73	88	1.07	0.18	0.47	9.45	PEPENI	5a1
75	3	0.14		0.16		PEPENI	5c1
76	17	0.81		0.63		PEPENI	5c3
77	29	1.18	0.17	2.11	14.97	URURTYURVE	5a1
79	40	0.70	0.18	0.38	4.65	URURTYURVE	5c1
80	37	1.13	0.24	0.43	7.42	URURTYURVE	5c3

Table A3.2F. Statistical characteristics for North Netherlands, organic matter, method 2 (legend as Table A3.2A).

	Amount of samples	Average	10–percentile	50–percentile	90–percentile	Formation	Geotop
		Wt%	Wt%	Wt%	Wt%		
4	3	0.17		0.18		AP	5c3
9	47	1.25	0.23	0.50	4.98	BX	5a1
11	25	1.40	0.23	0.50	4.98	BX	5c1
12	17	1.38		0.50		BX	5c3
13	1	5.76		5.76		BXSI	5a1
17	18	1.16		1.04		BXTI	5a1
25	35	2.06	0.18	0.34	4.89	DN	5a1
27	32	2.14	0.18	0.34	4.89	DN	5c1
28	13	2.13		0.34		DN	5c3
33	46	0.53	0.20	0.45	1.08	DRGI	5a1
35	41	0.55	0.20	0.45	1.08	DRGI	5c1
36	18	0.55		0.45		DRGI	5c3
39	1	0.25		0.25		DRGIGA	5c1
40	1	0.25		0.25		DRGIGA	5c3
41	2	0.31		0.31		DRSC	5a1
45	76	0.69	0.17	0.46	4.16	PE	5a1
47	3	0.80		0.46		PE	5c1
48	17	0.79		0.46		PE	5c3
49	12	6.71		6.91		PENI	5a1
53	5	0.65		1.00		UR	5a1
55	11	0.83		1.00		UR	5c1
57	17	0.99		0.51		URTY	5a1
59	29	1.35	0.21	0.51	13.65	URTY	5c1
60	13	1.30		0.51		URTY	5c3
61	7	0.69		0.48		URVE	5a1
64	24	0.78	0.25	0.48	2.22	URVE	5c3
65	65	1.19	0.24	0.59	4.86	BXBXTIBXWI	5a1
67	25	1.31	0.24	0.59	4.86	BXBXTIBXWI	5c1
68	17	1.29		0.59		BXBXTIBXWI	5c3
69	48	0.52	0.21	0.40	1.08	DRGIDRGIGADRSC	5a1
71	42	0.53	0.21	0.40	1.08	DRGIDRGIGADRSC	5c1
72	19	0.53		0.40		DRGIDRGIGADRSC	5c3
73	88	0.98	0.17	0.49	8.54	PEPENI	5a1
75	3	1.25		0.49		PEPENI	5c1
76	17	1.21		0.49		PEPENI	5c3
77	29	0.92	0.21	0.50	10.21	URURTYURVE	5a1
79	40	1.21	0.21	0.50	10.21	URURTYURVE	5c1
80	37	1.17	0.21	0.50	10.21	URURTYURVE	5c3

Table A3.2G. Statistical characteristics for South Netherlands, pyrite, method 1 (legend as Table A3.2A).

	Number of samples	Average	10– percentile	50– percentile	90– percentile	Formation	Geotop
		Wt%	Wt%	Wt%	Wt%		
<b>1</b>	<b>91</b>	<b>0.15</b>	<b>0.00</b>	<b>0.02</b>	<b>0.17</b>	<b>BE</b>	<b>4a1</b>
<b>2</b>	<b>41</b>	<b>0.04</b>	<b>0.00</b>	<b>0.03</b>	<b>0.18</b>	<b>BE</b>	<b>4b</b>
6	3	0.09		0.09		BERO	4b
9	78	0.58	0.04	0.35	1.29	BR	4a1
<b>13</b>	<b>30</b>	<b>0.36</b>	<b>0.02</b>	<b>0.13</b>	<b>0.74</b>	<b>BX</b>	<b>4a1</b>
<b>14</b>	<b>407</b>	<b>0.09</b>	<b>0.00</b>	<b>0.06</b>	<b>0.62</b>	<b>BX</b>	<b>4b</b>
15	6	0.01		0.00		BX	4c
16	15	0.05		0.07		BX	4d1
18	65	0.07	0.00	0.09	0.30	BXBS	4b
22	32	0.13	0.00	0.09	0.13	BXLM	4b
26	3	0.29		0.20		BXLS	4b
30	26	0.03	0.00	0.01	0.08	BXSI	4b
31	18	0.05		0.02		BXSI	4c
32	92	0.01	0.00	0.00	0.00	BXSI	4d1
33	4	0.01		0.00		BXWI	4a1
34	17	0.04		0.03		BXWI	4b
35	8	0.02		0.02		BXWI	4c
36	43	0.02	0.00	0.00	0.01	BXWI	4d1
41	74	0.17	0.00	0.06	0.39	KI	4a1
46	8	0.03		0.02		KR	4b
50	26	0.00	0.00	0.00	0.00	MS	4b
52	21	0.29	0.13	0.22	0.55	MS	4d1
53	18	0.13		0.11		OO	4a1
54	8	0.00		0.00		OO	4b
<b>55</b>	<b>24</b>	<b>0.53</b>	<b>0.26</b>	<b>0.54</b>	<b>0.79</b>	<b>OO</b>	<b>4c</b>
<b>56</b>	<b>39</b>	<b>0.46</b>	<b>0.21</b>	<b>0.39</b>	<b>1.34</b>	<b>OO</b>	<b>4d1</b>
58	168	0.15	0.00	0.08	1.34	ST	4b
59	37	0.02	0.00	0.01	0.04	ST	4c
60	3	0.00		0.00		ST	4d1
61	17	0.17		0.04		SY	4a1
<b>62</b>	<b>95</b>	<b>0.07</b>	<b>0.00</b>	<b>0.03</b>	<b>0.90</b>	<b>SY</b>	<b>4b</b>
<b>63</b>	<b>47</b>	<b>0.06</b>	<b>0.01</b>	<b>0.05</b>	<b>0.12</b>	<b>SY</b>	<b>4c</b>
<b>64</b>	<b>273</b>	<b>0.08</b>	<b>0.00</b>	<b>0.03</b>	<b>0.36</b>	<b>SY</b>	<b>4d1</b>
<b>65</b>	<b>77</b>	<b>0.15</b>	<b>0.01</b>	<b>0.10</b>	<b>0.39</b>	<b>WA</b>	<b>4a1</b>
<b>66</b>	<b>90</b>	<b>0.05</b>	<b>0.00</b>	<b>0.02</b>	<b>0.45</b>	<b>WA</b>	<b>4b</b>
<b>67</b>	<b>99</b>	<b>0.32</b>	<b>0.09</b>	<b>0.26</b>	<b>0.55</b>	<b>WA</b>	<b>4c</b>
<b>68</b>	<b>525</b>	<b>0.22</b>	<b>0.01</b>	<b>0.12</b>	<b>0.71</b>	<b>WA</b>	<b>4d1</b>
<b>69</b>	<b>91</b>	<b>0.15</b>	<b>0.00</b>	<b>0.02</b>	<b>0.17</b>	<b>BEBERO</b>	<b>4a1</b>
<b>70</b>	<b>44</b>	<b>0.04</b>	<b>0.00</b>	<b>0.04</b>	<b>0.16</b>	<b>BEBERO</b>	<b>4b</b>
<b>73</b>	<b>34</b>	<b>0.32</b>	<b>0.01</b>	<b>0.08</b>	<b>0.74</b>	<b>BXBXSBXLMBXL</b> <b>SBXWI</b>	<b>4a1</b>
<b>74</b>	<b>524</b>	<b>0.08</b>	<b>0.00</b>	<b>0.07</b>	<b>0.46</b>	<b>BXBXSBXLMBXL</b> <b>SBXWI</b>	<b>4b</b>
75	14	0.02		0.01		BXBXSBXLMBXL SBXWI	4c
<b>76</b>	<b>58</b>	<b>0.03</b>	<b>0.00</b>	<b>0.00</b>	<b>0.13</b>	<b>BXBXSBXLMBXL</b> <b>SBXWI</b>	<b>4d1</b>

Table A3.2H. Statistical characteristics for South Netherlands, pyrite, method 2 (legend as Table A3.2A).

Number of samples		Average	10–percentile	50–percentile	90–percentile	Formation	Geotop
		Wt%	Wt%	Wt%	Wt%		
1	91	0.12	0.00	0.02	0.23	BE	4a1
2	41	0.12	0.00	0.02	0.23	BE	4b
<b>6</b>	<b>3</b>	<b>0.09</b>		<b>0.09</b>		<b>BERO</b>	<b>4b</b>
<b>9</b>	<b>78</b>	<b>0.58</b>	<b>0.04</b>	<b>0.35</b>	<b>1.29</b>	<b>BR</b>	<b>4a1</b>
13	30	0.09	0.00	0.06	0.65	BX	4a1
14	407	0.10	0.00	0.06	0.65	BX	4b
<b>15</b>	<b>6</b>	<b>0.09</b>		<b>0.06</b>		<b>BX</b>	<b>4c</b>
<b>16</b>	<b>15</b>	<b>0.10</b>		<b>0.06</b>		<b>BX</b>	<b>4d1</b>
<b>18</b>	<b>65</b>	<b>0.07</b>	<b>0.00</b>	<b>0.09</b>	<b>0.30</b>	<b>BXBS</b>	<b>4b</b>
<b>22</b>	<b>32</b>	<b>0.13</b>	<b>0.00</b>	<b>0.09</b>	<b>0.13</b>	<b>BXLM</b>	<b>4b</b>
<b>26</b>	<b>3</b>	<b>0.29</b>		<b>0.20</b>		<b>BXLS</b>	<b>4b</b>
<b>30</b>	<b>26</b>	<b>0.02</b>	<b>0.00</b>	<b>0.00</b>	<b>0.15</b>	<b>BXSI</b>	<b>4b</b>
<b>31</b>	<b>18</b>	<b>0.02</b>		<b>0.00</b>		<b>BXSI</b>	<b>4c</b>
<b>32</b>	<b>92</b>	<b>0.02</b>	<b>0.00</b>	<b>0.00</b>	<b>0.15</b>	<b>BXSI</b>	<b>4d1</b>
<b>33</b>	<b>4</b>	<b>0.03</b>		<b>0.01</b>		<b>BXWI</b>	<b>4a1</b>
<b>34</b>	<b>17</b>	<b>0.03</b>		<b>0.01</b>		<b>BXWI</b>	<b>4b</b>
<b>35</b>	<b>8</b>	<b>0.03</b>		<b>0.01</b>		<b>BXWI</b>	<b>4c</b>
<b>36</b>	<b>43</b>	<b>0.03</b>	<b>0.00</b>	<b>0.01</b>	<b>0.01</b>	<b>BXWI</b>	<b>4d1</b>
<b>41</b>	<b>74</b>	<b>0.18</b>	<b>0.00</b>	<b>0.06</b>	<b>0.39</b>	<b>KI</b>	<b>4a1</b>
<b>46</b>	<b>8</b>	<b>0.03</b>		<b>0.02</b>		<b>KR</b>	<b>4b</b>
<b>50</b>	<b>26</b>	<b>0.13</b>	<b>0.00</b>	<b>0.00</b>	<b>0.00</b>	<b>MS</b>	<b>4b</b>
<b>52</b>	<b>21</b>	<b>0.13</b>	<b>0.00</b>	<b>0.00</b>	<b>0.00</b>	<b>MS</b>	<b>4d1</b>
<b>53</b>	<b>18</b>	<b>0.37</b>		<b>0.33</b>		<b>OO</b>	<b>4a1</b>
<b>54</b>	<b>8</b>	<b>0.38</b>		<b>0.33</b>		<b>OO</b>	<b>4b</b>
55	24	0.37	0.00	0.33	1.26	OO	4c
56	39	0.38	0.00	0.33	1.26	OO	4d1
<b>58</b>	<b>168</b>	<b>0.13</b>	<b>0.00</b>	<b>0.06</b>	<b>1.34</b>	<b>ST</b>	<b>4b</b>
<b>59</b>	<b>37</b>	<b>0.10</b>	<b>0.00</b>	<b>0.06</b>	<b>1.34</b>	<b>ST</b>	<b>4c</b>
<b>60</b>	<b>3</b>	<b>0.13</b>		<b>0.06</b>		<b>ST</b>	<b>4d1</b>
<b>61</b>	<b>17</b>	<b>0.08</b>		<b>0.04</b>		<b>SY</b>	<b>4a1</b>
62	95	0.08	0.00	0.04	0.47	SY	4b
63	47	0.07	0.00	0.04	0.47	SY	4c
64	273	0.08	0.00	0.04	0.47	SY	4d1
65	77	0.21	0.00	0.12	0.67	WA	4a1
66	90	0.21	0.00	0.12	0.67	WA	4b
67	99	0.20	0.00	0.12	0.67	WA	4c
68	525	0.21	0.00	0.12	0.67	WA	4d1
69	91	0.12	0.00	0.02	0.20	BEBERO	4a1
70	44	0.12	0.00	0.02	0.20	BEBERO	4b
73	34	0.08	0.00	0.06	0.46	BXBBSBXLMBXLSBXWI	4a1
74	524	0.08	0.00	0.06	0.46	BXBBSBXLMBXLSBXWI	4b
<b>75</b>	<b>14</b>	<b>0.08</b>		<b>0.06</b>		<b>BXBBSBXLMBXLSBXWI</b>	<b>4c</b>
76	58	0.08	0.00	0.06	0.46	BXBBSBXLMBXLSBXWI	4d1

Table A3.2I. Statistical characteristics for Central Netherlands, pyrite, method 1 (legend as Table A3.2A).

Number of samples		Average	10–percentile	50–percentile	90–percentile	Formation	Geotop
		Wt%	Wt%	Wt%	Wt%		
4	5	0.99		0.70		BREI	6a
6	55	0.10	0.09	0.09	0.17	BX	2b
7	33	0.09	0.09	0.09	0.09	BX	3a
8	62	0.10	0.09	0.09	0.09	BX	3b
9	39	0.09	0.09	0.09	0.09	BX	6a
10	45	0.10	0.09	0.09	0.11	BX	6b
12	1	0.09		0.09		BXTI	3a
16	4	0.09		0.09		BXWI	2b
18	3	0.09		0.09		BXWI	3b
24	6	1.24		1.16		DO	6a
29	6	0.09		0.09		DR	6a
34	12	0.27		0.21		DRSC	6a
36	49	0.09	0.09	0.09	0.09	KR	2b
40	4	0.09		0.09		KR	6b
44	3	0.96		0.94		RU	6a
46	59	0.10	0.09	0.09	0.17	BXBXTIBXWI	2b
47	34	0.09	0.09	0.09	0.09	BXBXTIBXWI	3a
48	65	0.10	0.09	0.09	0.09	BXBXTIBXWI	3b
49	39	0.09	0.09	0.09	0.09	BXBXTIBXWI	6a
50	45	0.10	0.09	0.09	0.11	BXBXTIBXWI	6b
54	18	0.23		0.13		DRDRSC	6a

Table A3.2J. Statistical characteristics for Central Netherlands, pyrite, method 2 (legend as Table A3.2A).

	Number of samples	Average	10–percentile	50–percentile	90–percentile	Formation	Geotop
		Wt%	Wt%	Wt%	Wt%		
4	5	0.99		0.70		BREI	6a
6	55	0.10	0.09	0.09	0.15	BX	2b
7	33	0.10	0.09	0.09	0.15	BX	3a
8	62	0.10	0.09	0.09	0.15	BX	3b
9	39	0.10	0.09	0.09	0.15	BX	6a
10	45	0.10	0.09	0.09	0.15	BX	6b
12	1	0.09		0.09		BXTI	3a
16	4	0.09		0.09		BXWI	2b
18	3	0.09		0.09		BXWI	3b
24	6	1.24		1.16		DO	6a
29	6	0.09		0.09		DR	6a
34	12	0.27		0.21		DRSC	6a
36	49	0.09	0.09	0.09	0.09	KR	2b
40	4	0.09		0.09		KR	6b
44	3	0.96		0.94		RU	6a
46	59	0.10	0.09	0.09	0.15	BXBXTIBXWI	2b
47	34	0.10	0.09	0.09	0.15	BXBXTIBXWI	3a
48	65	0.10	0.09	0.09	0.15	BXBXTIBXWI	3b
49	39	0.10	0.09	0.09	0.15	BXBXTIBXWI	6a
50	45	0.10	0.09	0.09	0.15	BXBXTIBXWI	6b
54	18	0.23		0.13		DRDRSC	6a

Table A3.2K. Statistical characteristics for North Netherlands, pyrite, Method 1 (legend as in Table A3.2A).

	Number of samples	Average	10–percentile	50–percentile	90–percentile	Formation	Geotop
		Wt%	Wt%	Wt%	Wt%		
4	3	0.09		0.09		AP	5c3
9	82	0.14	0.09	0.09	0.20	BX	5a1
10	47	0.12	0.09	0.09	0.35	BX	5b1
11	26	0.09	0.09	0.09	0.09	BX	5c1
12	18	0.11		0.09		BX	5c3
13	1	0.09		0.09		BXSI	5a1
17	19	0.15		0.09		BXTI	5a1
18	7	0.19		0.25		BXTI	5b1
22	2	0.09		0.09		BXWI	5b1
25	38	0.13	0.09	0.09	0.43	DN	5a1
27	48	0.10	0.09	0.09	0.09	DN	5c1
28	14	0.09		0.09		DN	5c3
<b>33</b>	<b>57</b>	<b>0.12</b>	<b>0.09</b>	<b>0.09</b>	<b>0.09</b>	<b>DRGI</b>	<b>5a1</b>
<b>35</b>	<b>52</b>	<b>0.57</b>	<b>0.09</b>	<b>0.09</b>	<b>0.36</b>	<b>DRGI</b>	<b>5c1</b>
<b>36</b>	<b>20</b>	<b>0.09</b>	<b>0.04</b>	<b>0.09</b>	<b>0.09</b>	<b>DRGI</b>	<b>5c3</b>
39	1	0.09		0.09		DRGIGA	5c1
40	1	0.09		0.09		DRGIGA	5c3
41	6	0.09		0.09		DRSC	5a1
42	4	0.09		0.09		DRSC	5b1
45	170	0.18	0.04	0.09	1.19	PE	5a1
47	6	0.09		0.09		PE	5c1
48	18	0.07		0.09		PE	5c3
49	43	0.98	0.09	0.98	1.76	PENI	5a1
53	8	0.34		1.24		UR	5a1
55	13	0.17		0.09		UR	5c1
57	17	0.44		0.29		URTY	5a1
59	60	0.41	0.09	0.09	2.78	URTY	5c1
60	20	0.21	0.09	0.09	1.05	URTY	5c3
61	13	0.11		0.09		URVE	5a1
64	25	0.12	0.04	0.09	0.32	URVE	5c3
65	101	0.16	0.09	0.09	0.61	BXBXTIBXWI	5a1
66	56	0.12	0.09	0.09	0.73	BXBXTIBXWI	5b1
67	26	0.09	0.09	0.09	0.09	BXBXTIBXWI	5c1
68	18	0.11		0.09		BXBXTIBXWI	5c3
<b>69</b>	<b>63</b>	<b>0.12</b>	<b>0.09</b>	<b>0.09</b>	<b>0.09</b>	<b>DRGIDRGIGADRSC</b>	<b>5a1</b>
70	4	0.09		0.09		DRGIDRGIGADRSC	5b1
<b>71</b>	<b>53</b>	<b>0.56</b>	<b>0.09</b>	<b>0.09</b>	<b>0.36</b>	<b>DRGIDRGIGADRSC</b>	<b>5c1</b>
<b>72</b>	<b>21</b>	<b>0.09</b>	<b>0.04</b>	<b>0.09</b>	<b>0.09</b>	<b>DRGIDRGIGADRSC</b>	<b>5c3</b>
73	213	0.24	0.04	0.09	1.70	PEPENI	5a1
75	6	0.09		0.09		PEPENI	5c1
76	18	0.07		0.09		PEPENI	5c3
<b>77</b>	<b>38</b>	<b>0.16</b>	<b>0.04</b>	<b>0.21</b>	<b>1.95</b>	<b>URURTYURVE</b>	<b>5a1</b>
<b>79</b>	<b>73</b>	<b>0.36</b>	<b>0.09</b>	<b>0.09</b>	<b>1.99</b>	<b>URURTYURVE</b>	<b>5c1</b>
<b>80</b>	<b>45</b>	<b>0.16</b>	<b>0.04</b>	<b>0.09</b>	<b>0.85</b>	<b>URURTYURVE</b>	<b>5c3</b>

Table A3.2L. Statistical characteristics for North Netherlands, pyrite, method 2 (legend as in Table A3.2A).

	Amount of samples	Average	10–percentile	50–percentile	90–percentile	Formation	Geotop
		Wt%	Wt%	Wt%	Wt%		
4	3	0.09		0.09		AP	5c3
9	82	0.13	0.09	0.09	0.33	BX	5a1
10	47	0.12	0.09	0.09	0.33	BX	5b1
11	26	0.13	0.09	0.09	0.33	BX	5c1
12	18	0.13		0.09		BX	5c3
13	1	0.09		0.09		BXSI	5a1
17	19	0.16		0.09		BXTI	5a1
18	7	0.13		0.09		BXTI	5b1
22	2	0.09		0.09		BXWI	5b1
25	38	0.12	0.09	0.09	0.43	DN	5a1
27	48	0.14	0.09	0.09	0.43	DN	5c1
28	14	0.14		0.09		DN	5c3
33	57	0.25	0.06	0.09	0.13	DRGI	5a1
35	52	0.33	0.06	0.09	0.13	DRGI	5c1
36	20	0.31	0.06	0.09	0.13	DRGI	5c3
39	1	0.09		0.09		DRGIGA	5c1
40	1	0.09		0.09		DRGIGA	5c3
41	6	0.09		0.09		DRSC	5a1
42	4	0.09		0.09		DRSC	5b1
45	170	0.16	0.04	0.09	0.98	PE	5a1
47	6	0.17		0.09		PE	5c1
48	18	0.17		0.09		PE	5c3
49	43	0.98	0.09	0.98	1.76	PENI	5a1
53	8	0.24		0.09		UR	5a1
55	13	0.33		0.09		UR	5c1
57	17	0.23		0.09		URTY	5a1
59	60	0.29	0.09	0.09	1.32	URTY	5c1
60	20	0.28	0.09	0.09	1.32	URTY	5c3
61	13	0.11		0.09		URVE	5a1
64	25	0.12	0.04	0.09	0.45	URVE	5c3
65	101	0.14	0.09	0.09	0.70	BXBXTIBXWI	5a1
66	56	0.13	0.09	0.09	0.70	BXBXTIBXWI	5b1
67	26	0.16	0.09	0.09	0.70	BXBXTIBXWI	5c1
68	18	0.16		0.09		BXBXTIBXWI	5c3
69	63	0.24	0.09	0.09	0.12	DRGIDRGIGADRSC	5a1
70	4	0.16		0.09		DRGIDRGIGADRSC	5b1
71	53	0.32	0.09	0.09	0.12	DRGIDRGIGADRSC	5c1
72	21	0.31	0.09	0.09	0.12	DRGIDRGIGADRSC	5c3
73	213	0.22	0.04	0.09	1.69	PEPENI	5a1
75	6	0.27		0.09		PEPENI	5c1
76	18	0.26		0.09		PEPENI	5c3
77	38	0.20	0.07	0.09	1.78	URURTYURVE	5a1
79	73	0.26	0.07	0.09	1.78	URURTYURVE	5c1
80	45	0.25	0.07	0.09	1.78	URURTYURVE	5c3

## **Appendix 4 Investigation and analysis of groundwater quality monitoring results to support model validation**

### **A4.1 Data analysis groundwater**

An extensive analysis of available groundwater data was performed in order to get a better idea of the geochemical conditions in the areas under consideration and the fate of nitrate depending on these conditions. Special attention is given to whether differences in the fate of nitrate can be found between the various “sand districts” (south, central and north Netherlands) and groundwater classes (low, intermediate and high groundwater levels), and how these differences can be explained. Moreover, the variability and the resulting uncertainty surrounding the fate of nitrate are evaluated, by explicitly quantifying and visualizing the variability in the data sets of the relevant geochemical parameters. The improved insights mainly serve a better parameterization of the used groundwater flow and transport model STONE, by providing a means to validate its results.

For the data analysis described here it sufficed to limit the data acquisition to the following compounds: NO<sub>3</sub>, Fe, SO<sub>4</sub>, Cl, and pH. Several databases were used to get an as high a data density as possible, both areal and in the vertical. These databases included:

- 1) The groundwater quality database of DINO (Data and Information of the Subsurface of The Netherlands), DINOQua;
- 2) The national and provincial soil quality monitoring networks. These networks sample the upper groundwater (0–1m below groundwater level);
- 3) The national and provincial groundwater quality networks, sampling the deeper groundwater (> 8m below soil surface)
- 4) The national monitoring network that belongs to the National Program for Monitoring the Effectiveness of the Minerals Policy (LMM). This network also samples the upper groundwater (0–1m below groundwater level), although mainly in the Holocene part of the Netherlands. Drain and ditch water samples of the LMM were excluded from this study.

For the greater part, the monitoring networks mentioned under 2) and 3) are available through DINOQua. However, the most recent data of the networks had to be checked and added to the database separately, as part of this study.

Table A4.1. Characteristics of the differentiated sand types. *Gt* = numeric indication of groundwater level regime. *MHG* = mean highest groundwater level. *MLG* = mean lowest groundwater level.

Sand Type	<i>Gt</i>	<i>MHG</i> (cm – soil surface)	<i>MLG</i> (cm – soil surface)
High groundwater levels	I,II,II*,III,III*,IV	< 40 / > 40	< 120
Intermediate groundwater levels	V,V*,VI	< 80	> 120
Low groundwater levels	VII,VIII	> 80	> 120

The data analysis is performed separately for the different “sand districts” and “groundwater classes” differentiated between in this study. With respect to the “sand districts”, a differentiation is applied between the north of the Netherlands (North-NL), the central part of the Netherlands (Central-NL) and the south of the Netherlands (South-NL). With respect to the “groundwater classes”, we differentiate between sandy soils with high, intermediate, and low groundwater tables. The classification of sandy soils follows the classification of Fraters *et al.* (2006), who implemented the differentiation based on so called *Gt*'s (a Dutch numeric classification of groundwater level regimes) which on their turn depend on the combination of the highest average groundwater level (Dutch abbreviation: *MHG*) and lowest average groundwater levels (see Table A4.1). The *Gt*'s were taken from the hydrological base information underlying STONE, which contains a 250x250m *Gt*-grid. Figure A4.1 shows the result of the subdivision of the sandy areas in the Netherlands that are part of the study in the abovementioned categories.

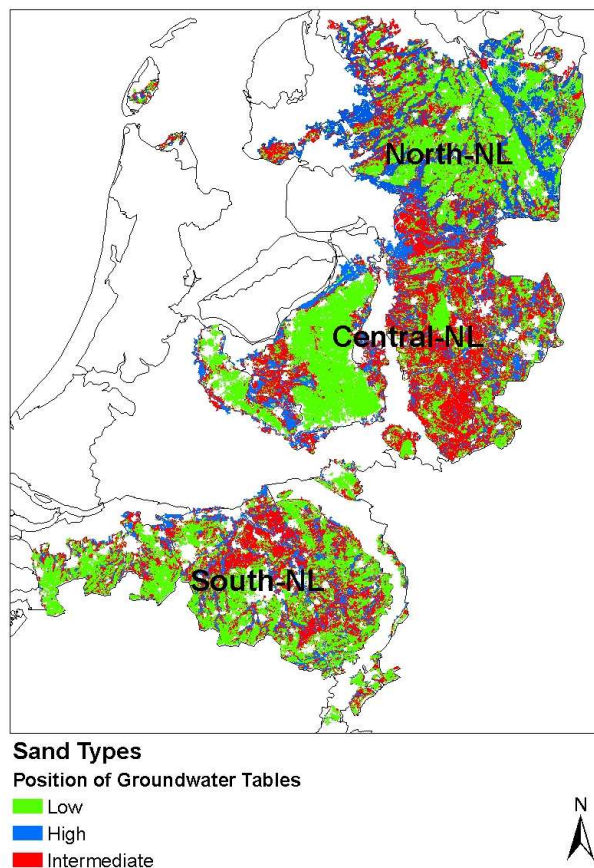


Figure A4.1. Division of the Pleistocene sandy areas in The Netherlands in sand districts (North-NL, Central-NL and South-NL) and groundwater classes (areas with low, high and intermediate groundwater tables).

## A4.2 Determination of redox clines

### A4.2.1 Introduction

Nitrate is a redox-sensitive substance, which means that the prevailing redox conditions at a certain depth in the groundwater have predictive value with respect to the fate of nitrate at that depth. In an anoxic environment nitrate can be expected to be either fully removed already or at least in the process of being removed by denitrification. In an oxic environment, denitrification will not occur.

Thus, gaining insight in the depth at which redox conditions in the groundwater change is important for getting a feeling of the depth at which nitrate concentration will start to decrease due to denitrification. With this in mind, the database composed from the several sources described above was used to see whether typical depths of the redox cline can be found per sand district / groundwater class combination, and what the ranges involved are.

#### **A4.2.2 Data selection**

For the determination of the redox clines we restricted ourselves to the groundwater quality data from 1970 to present. The choice for 1970 is somewhat arbitrary but at the same time constitutes a compromise between data availability and representativity (for the current situation). Prior to choosing 1970 as starting year, an attempt was made to build a workable dataset from groundwater analyses from 1990 to present. However, this resulted in a set with too low a data density to perform a useful analysis. Going back as far as 1970 can be (at least partially) justified by the fact that during the period from 1980 and now hardly ever a clear switch from oxic to anoxic redox conditions, or vice versa, was observed in provincial groundwater quality monitoring filters (pers. commun. A. Visser, University of Utrecht).

Naturally, the set of groundwater analyses from 1970 to present contains multiple data from the same filter that is or has been monitored more than once (especially the filters from the provincial and national groundwater and soil quality networks). For the determination of redox classes, only the last analysis in time per filter was selected. This way, the most recent redox status known is used and mixing of different redox conditions occurring over time (should that occur), for example by averaging concentrations, is avoided.

Finally, groundwater quality analyses on which the redox classification described below could not be performed (simply because not all elements and substances needed for this classification had been analyzed), had to be discarded. The same holds for recent data from the national and provincial soil and groundwater quality monitoring networks, for which no quality check could be performed because not all relevant elements necessary for an electro neutrality test had been analyzed.

The selections described above resulted in a dataset of 2080 useable groundwater quality analyses. Their distribution over the different sand district/groundwater class combinations is presented jointly with the results of the redox classification in Figure A4.3 (discussed below).

#### **A4.2.3 Redox classification**

For the classification of the groundwater samples from the final database the decision tree presented by Vermooten *et al.* (2007) was used (see Figure A4.2). Following this decision tree, the concentrations of NO<sub>3</sub>, Fe, SO<sub>4</sub> and Cl are used to divide the groundwater samples into 5 redox classes:

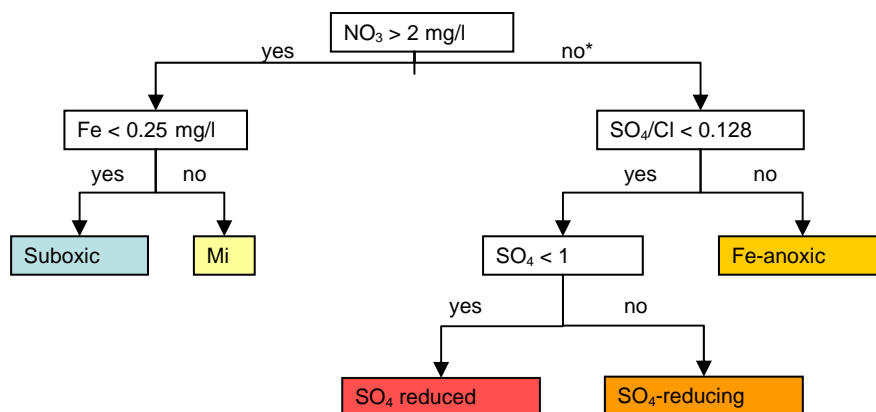
- suboxic (nitrate-containing) groundwater
- mix (groundwater containing both Fe and NO<sub>3</sub>)
- Fe-anoxic groundwater
- SO<sub>4</sub>-reducing groundwater
- SO<sub>4</sub>-reduced groundwater

These redox classes are now described in more detail, in an explanation that is in large a translation of the same explanation given by Vermooten *et al.* (2007). The criteria for nitrate

and iron refer to detection limits below which one can speak of nitrate-free or iron-free groundwater, a distinction that can be regarded as an indicator for the redox condition of the groundwater. If both substances are present simultaneously, the groundwater composition is not in a state of thermodynamic equilibrium. This can be the result of mixing of different water types over the filter or non-ideal kinetically controlled behaviour of the pore water and the soil matrix.

The criterion for the  $\text{SO}_4/\text{Cl}$  ratio refers to 0.9 times the seawater ratio of  $\text{SO}_4$  and  $\text{Cl}$ . If the ratio in the groundwater is below the seawater ratio, with a correction factor for measurement error, generally  $\text{SO}_4$  reduction can be expected to have played a role (with the exception of point pollutions with  $\text{Cl}$ ): rain water and river water, as sources for groundwater recharge, have higher  $\text{SO}_4/\text{Cl}$  ratios than seawater. Moreover, direct or indirect anthropogenic enrichment with  $\text{SO}_4$  in groundwater is almost always bigger than the enrichment with  $\text{Cl}$ .

The criterion for  $\text{SO}_4$  refers to the most frequently encountered detection limit for  $\text{SO}_4$ . The database shows a wide range of detection limits for  $\text{SO}_4$ , from  $5 \text{ mg l}^{-1}$  to tenths of  $\text{mg}$  per litre. The detection limit of  $1 \text{ mg l}^{-1}$  was used as the threshold below which sulphate was assumed completely reduced.



\*  $\text{NO}_3 < 2 \text{ mg/l}$  of  $\text{NO}_3$  not measured

Figure A4.2. Criteria for redox classification of groundwater samples (from Vermooten et al, 2007).

#### A4.2.4 Results

Results of the redox classification of the groundwater samples from the final dataset described in the previous section are presented per sand district / groundwater class combination in Figure A4.3. For every soil layer of 1 meter depth and for all groundwater samples belonging to that layer the relative occurrence of the different redox classes was calculated. If the number of groundwater analyses within a layer was less than 10, this layer was aggregated with the next, deeper, layer. This was repeated until the sum of groundwater analyses of the aggregated transect was equal to or larger than 10. This

aggregation procedure was applied because calculating percentages over a total number of samples less than 10 was considered non-informative. The classification per layer of 1 meter thickness corresponds with the 1 meter thick model layers of STONE.

For many shallow samples, i.e., those originating from the soil quality monitoring networks and the LMM-network, the depth below the soil surface are not known exactly. However, we know that these networks sample the upper groundwater, i.e., the first meter. Therefore, these samples were all allocated to the first groundwater layer. The position of this first groundwater layer (or, in other words, the thickness of the unsaturated zone) was linked to the average lowest groundwater level (MLG). The MLG of a soil type was, on its own turn, derived from the STONE map of Gt's (groundwater level regimes): per soil type the average MLG of all STONE plots belonging to that soil type was calculated, and this average MLG was used as a virtual phreatic level. Thus, the first STONE-groundwater layer for which statistics were calculated is the groundwater layer that contains this virtual phreatic level.

On the right side of the “100% stacked bar” graphs showing the results of the redox classifications (Fig. A4.3.), the number of analyses each bar is based on is given in a separate stacked bar graph. The “empty” bars indicate that the number of samples of the corresponding groundwater layer is aggregated with the samples from the groundwater layer above. The given numbers indicate the aggregated totals. It is clear that by far most of the groundwater samples are taken from the upper meter of the groundwater. A second peak is often observed around 8–9 meters below soil surface, the depth interval in which many provincial and national groundwater monitoring filters are found.

All graphs in Figure A4.3 show large numbers of samples in the first meter below MLG classified as “Mix”. This is due to the fact that all samples from the soil quality monitoring networks and from the LMM are composite samples, usually from 2 to 4 subsamples. It is therefore possible that anoxic samples (iron present, but no nitrate) are mixed with oxic samples (nitrate, no iron) to make a composite sample that contains both iron and nitrate, which is thus classified as “Mix”. The number of “Mix” samples is therefore very likely to be overestimated for this first groundwater layer.

The implications of the graphs for model validation will be treated individually for each sand district / groundwater class in Section A4.4. Here we will restrict the discussion of the redox clines to the general picture.

This general picture shows that:

- in general, a decrease of the occurrence of (sub)oxic or nitrate-containing conditions can be observed with depth;
- in areas with low groundwater tables, (sub)oxic groundwater conditions penetrate deeper than in areas with high groundwater levels. This is in accordance with the conclusions from Fraters *et al.* (2006), and can be explained by realizing that the areas with low groundwater tables are likely to be infiltration areas, where oxygen-rich

rainwater travels via deeper flow paths towards regional drainage features, whereas areas with higher groundwater tables are likely to be locally drained, forcing oxygen-rich recharge to travel along shorter and shallower flow paths. The areas with intermediate groundwater tables show intermediate behaviour. Another part of the explanation is found in the differences in soil composition between wet and dry soils. Wet soils are generally richer, e.g. contain more organic matter, thereby more rapidly consuming infiltrating oxygen.

- penetration of (sub)oxic (or nitrate containing) water is most effectively restricted in the sandy areas in the north of the Netherlands. This is also the part of the Netherlands where the observed organic matter and pyrite contents are highest (see Chapter 5), and it is likely that these higher contents explain the more rapid removal of oxygen and nitrate. The central part of the Netherlands, having the lowest organic matter and pyrite contents (Chapter 5), shows the deepest penetration of suboxic / nitrate containing water.
- as expected, no clear redox clines could be observed, due to the heterogeneity of the geohydrological and hydrogeochemical conditions. From the graphs in Figure 4.3, occurrence of (sub)oxic conditions and nitrate-containing water deeper than 5 meters below MLG cannot be excluded in any of the nine situations. This even holds for the largest depth investigated of 16 meters below soil surface.

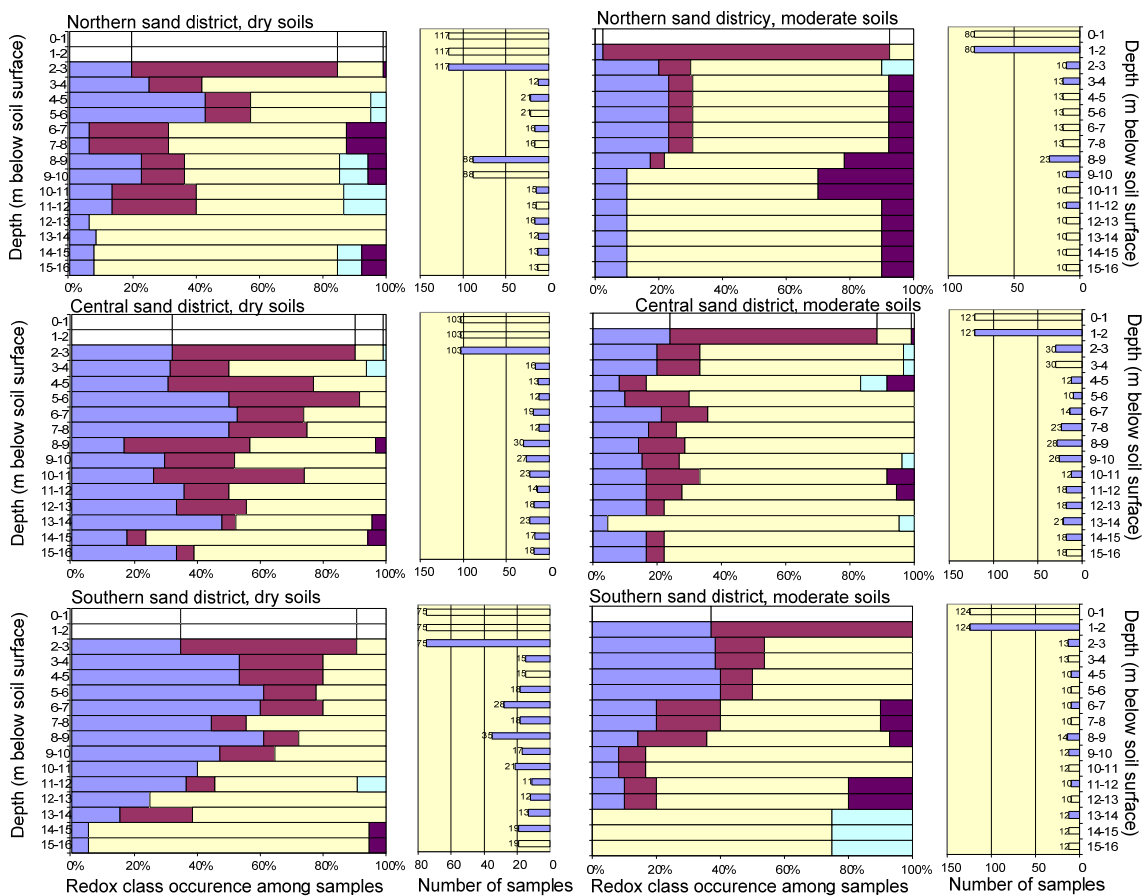


Figure A4.3. Development of the redox conditions encountered with depth for the dry soils (left) and the moderate soils (right) per sand district

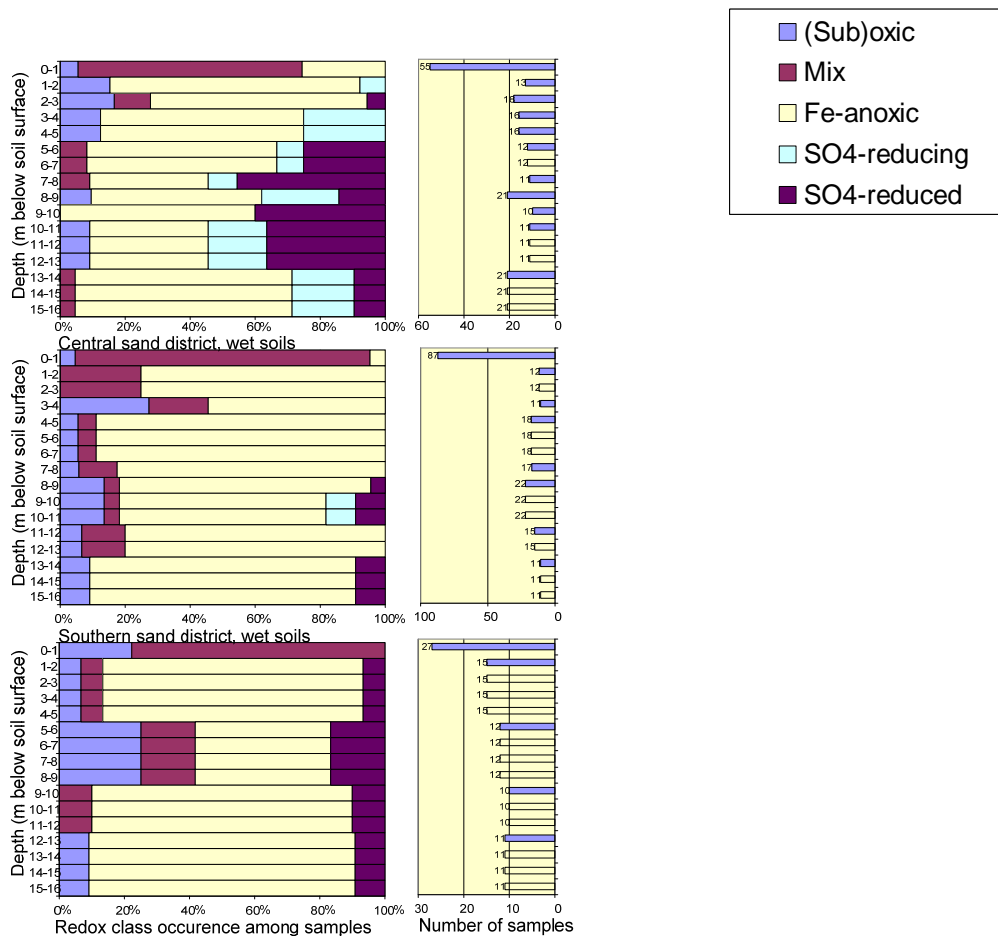


Figure A4.3 (continued). Development of the redox conditions encountered with depth for the wet soils per sand district

## A4.3 Nitrate profiles

### A4.3.1 Introduction

As mentioned in the previous section, redox clines can provide information on the reactive capacity of the subsurface and thus provide indirect information on the expected fate of nitrate. However, the most direct information on the extent to which nitrate is transported from the upper groundwater to greater depths is of course provided by evaluation of the changes in nitrate concentration itself with depth, i.e. nitrate profiles. Note, though, that both sources of information are complementary: without knowledge about the reactive capacity of the subsurface, one cannot unambiguously explain the nitrate behaviour as observed in the nitrate profiles, i.e., attribute nitrate loss to denitrification. If nitrate loss is observed at depths where anoxic conditions prevail, denitrification is a reasonable explanation. Otherwise, other causes are more likely, for example a transfer of the nitrate load onto the surface water system by lateral flow.

### A4.3.2 Data selection

A different set of data was selected for the construction of nitrate profiles compared to the set used for the determination of the redox clines. First of all, only data as recent as 1997 or later were used. The main reason for this is to avoid, as much as possible, effects of high nitrate inputs from the period before manure legislation<sup>10</sup> on the nitrate concentrations in the deeper groundwater samples.

Second, since nitrate input in nature areas is much lower than in agricultural areas and their contribution to an average idea of a nitrate profile per sand district / groundwater class combination will lead to an underestimation of nitrate concentrations in agricultural areas, only filters from agricultural areas were used.

For every filter in the dataset resulting from the selections described above, the median (615 in total) of the measured groundwater concentrations in time was calculated. An exception was made for the LMM data, of which the most recent sample was used instead of taking the median over multiple sampling rounds (if available). This exception was made because in the LMM there is no guarantee that in subsequent sampling rounds the exact same locations were sampled.

### A4.3.3 Results

The median values were plotted against the depth of the corresponding sampling filters. In order to get a sampling depth for the groundwater samples for which this depth is not recorded explicitly (as mentioned above, these are mainly the samples from the soil quality networks and the LMM), the following procedure was followed: for the LMM data, an estimation of the average groundwater level at the locations of the subsamples contributing to the analyzed composite sample is known. The depth of sampling for the LMM filters was assumed to be 0.5 m below this estimated groundwater level. For the other data (for which no estimate of the groundwater level at the time of sampling was known), the depth of sampling was assumed to be at the estimated MLG (estimated as explained in section 4.2.4).

The resulting nitrate scatter plots are shown in Figure 4.4. In order to extract an average idea of the nitrate depth profile, a “locally weighted scatter plot smoothing” (LOWESS; Cleveland & Devlin, 1988) is applied to the plots. The major advantage of using a LOWESS analysis over the use of a regression analysis is that a priori no assumptions are needed on the model to be applied (Griffioen *et al.*, 2006). The current problem lacks a theoretical foundation for such assumptions. Data from the soil quality networks and LMM are indicated by red dots. This was done because their depths have not been recorded and had to be estimated.

---

<sup>10</sup> In the Netherlands, effective manure legislation started in the late 1980's.

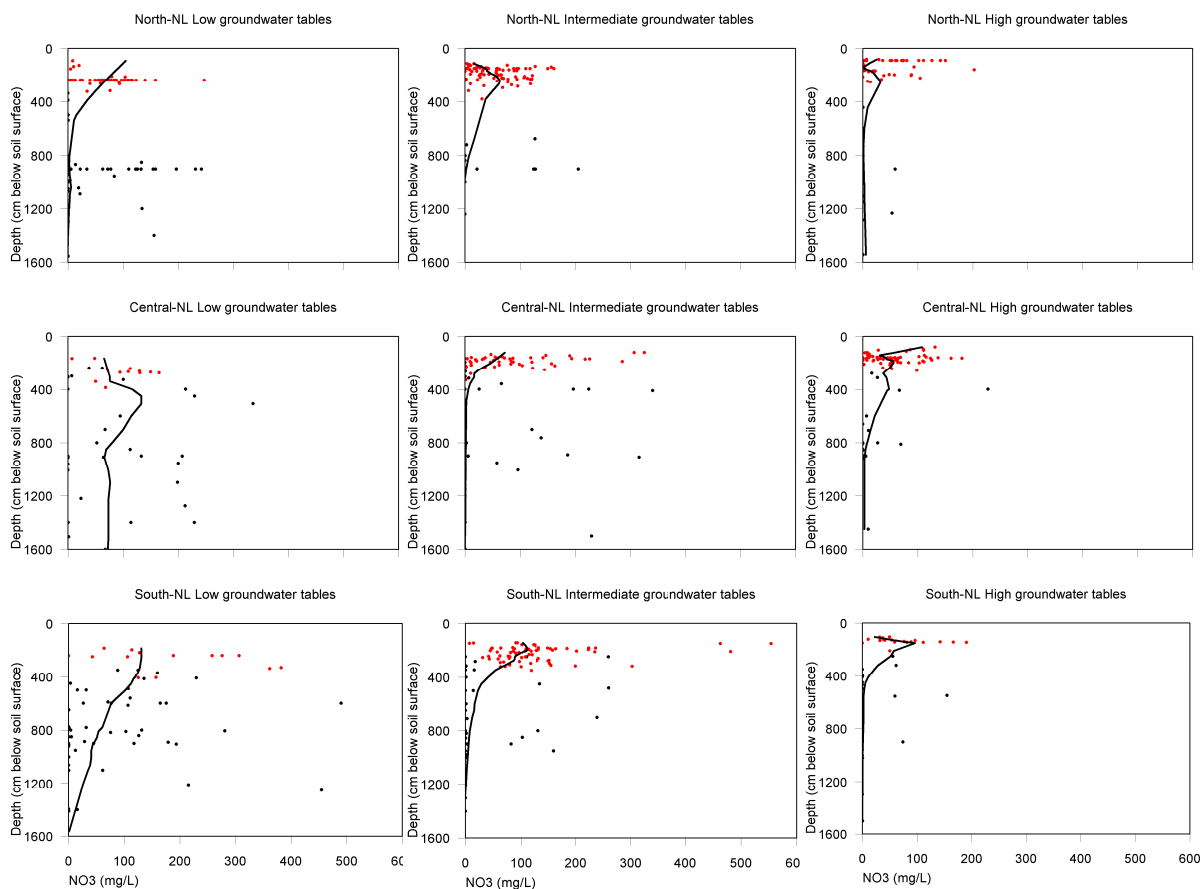


Fig. A4.4. Nitrate profiles with depth (red dots indicate the LMM observations, black dots refer to other monitoring networks)

The procedure followed to produce the scatter plots for nitrate was repeated for Fe and the pH.

A more detailed statistical characterization of the nitrate profiles is given in Table A4.2, where for three relevant depth intervals (near MLG, near MLG–5m, near MLG–10m) the minimum and maximum nitrate concentration observed is given, as well as the 25-, 50-, and 90-percentiles, for every combination of sand district and groundwater class.

The general picture that arises from the nitrate profiles in Figure A4.4 is comparable with that described for Figure A4.3. The general picture is that:

- nitrate concentrations generally decrease with depth. This decrease is generally accompanied by an increase in the occurrence of anoxic conditions (Fig. A4.3) and an increase in iron concentrations (Fig. A4.4) and is, therefore, at least partly explained by redox activity (in this case denitrification);
- nitrate concentrations decline most strongly (with depth) in areas with high groundwater tables. Nitrate penetrates deepest in areas with low groundwater tables, and areas with intermediate groundwater level act in an intermediate manner;
- in the sand areas in the north of the Netherlands, the nitrate concentrations decline fastest with depth, and in the central part this decline is generally the slowest.

Table A4.2. Quantitative characterization of the nitrate scatter plots of Fig. 4.4. For three depth intervals, representative of depths around the GLG, around 5 meters below GLG, and around 10 meters below GLG (choice of intervals was made depending on data availability), the minimum nitrate concentration (MIN), the 25-percentile (25-PERC.), the median, the 90-percentile (90-PERC.) and the maximum nitrate concentration found per sand district and groundwater class are presented. N = number of samples on which the statistical indicators are based (= number of available samples within the given depth interval).

Sand district / groundwater class and depth category	Depth (m. below soil surface)	N	MIN	25-PERC.	50-PERC. (MEDIAN)	90-PERC.	MAX
<b>South, Low (dry soils)</b>							
GLG	1.8 – 2.5	11	0.02	53.45	113.90	276.33	306.50
GLG–5m	6.0 – 8.0	12	0.04	3.05	54.33	174.76	490.05
GLG–10m	10.0 – 15.6	10	0.07	0.15	0.41	180.45	455.00
<b>South, Intermediate (moderate soils)</b>							
GLG	1.5 – 2.0	28	7.20	89.93	124.80	227.65	554.13
GLG–5m	6.0 – 8.0	7	0.04	0.20	1.35	174.59	238.82
GLG–10m	10.0 – 14.0	7	0.04	0.09	0.24	0.29	0.36
<b>South, High (wet soils)</b>							
GLG	1.0 – 1.5	19	0.02	35.00	53.60	147.38	190.70
GLG–5m	4.0 – 5.5	7	0.04	0.08	0.31	97.78	154.91
GLG–10m	9.6 – 15.0	7	0.04	0.12	0.18	0.35	0.50
<b>Central, Low (dry soils)</b>							
GLG	1.7 – 3.1	16	0.07	7.23	66.99	140.20	165.50
GLG–5m	6.0 – 9.0	7	0.04	60.04	94.71	162.83	207.53
GLG–10m	11.0 – 14.0	7	0.00	11.93	114.29	219.27	229.21
<b>Central, Intermediate (moderate soils)</b>							
GLG	1.2 – 1.8	26	0.80	34.60	67.10	222.25	325.60
GLG–5m	5.2 – 8.0	8	0.04	0.06	0.09	126.60	138.39
GLG–10m	10.0 – 12.1	9	0.04	0.12	0.12	19.65	96.37
<b>Central, High (wet soils)</b>							
GLG	0.8 – 1.6	25	4.00	13.80	45.00	114.04	137.10
GLG–5m	4.0 – 7.0	5	0.07	6.68	10.40	163.25	227.69
GLG–10m	9.0 – 9.2	6	0.04	0.04	0.04	3.16	5.72
<b>North, Low (dry soils)</b>							
GLG	0.9 – 2.7	53	0.53	39.78	68.51	114.57	247.52
GLG–5m	8.0 – 9.0	49	0.04	0.44	0.53	135.61	242.38
GLG–10m	10.9 – 13.0	7	0.04	0.22	0.44	66.85	134.37
<b>North, Intermediate (moderate soils)</b>							
GLG	1.1 – 2.0	56	0.00	11.78	36.35	103.87	161.33
GLG–5m	–	–	–	–	–	–	–
GLG–10m	9.0 – 12.4	19	0.04	0.19	0.44	125.22	205.53
<b>North, High (wet soils)</b>							
GLG	0.8 – 1.1	32	0.000	0.81	18.15	109.62	150.28
GLG–5m	6.8 – 8.00	7	0.111	0.34	0.39	0.52	0.53
GLG–10m	10.0–15.6	7	0.044	0.04	0.23	21.58	53.16

- In case of low groundwater tables, no significant decrease could be observed at all in the central part of the Netherlands.

The resulting profiles for Fe are shown in Figure A4.5 and A4.6, respectively. Iron profiles can provide complementary information about the fate of nitrate. If measured dissolved Fe concentrations are assumed to be concentrations of Fe(II), which is a valid assumption if pH values are not too low, under conditions of an infiltrating electron acceptor (nitrate) these concentrations are likely to be caused by pyrite oxidation. Almost every plot in Figure A4.5 shows increasing Fe concentrations with depth, suggesting progressing mobilization of Fe, and supporting the notion that decreasing nitrate concentrations are at least partially caused by denitrification, with pyrite as electron donor. Exceptions are the areas in the central part of the Netherlands. This is consistent with the sediment analysis described in Appendix 3.

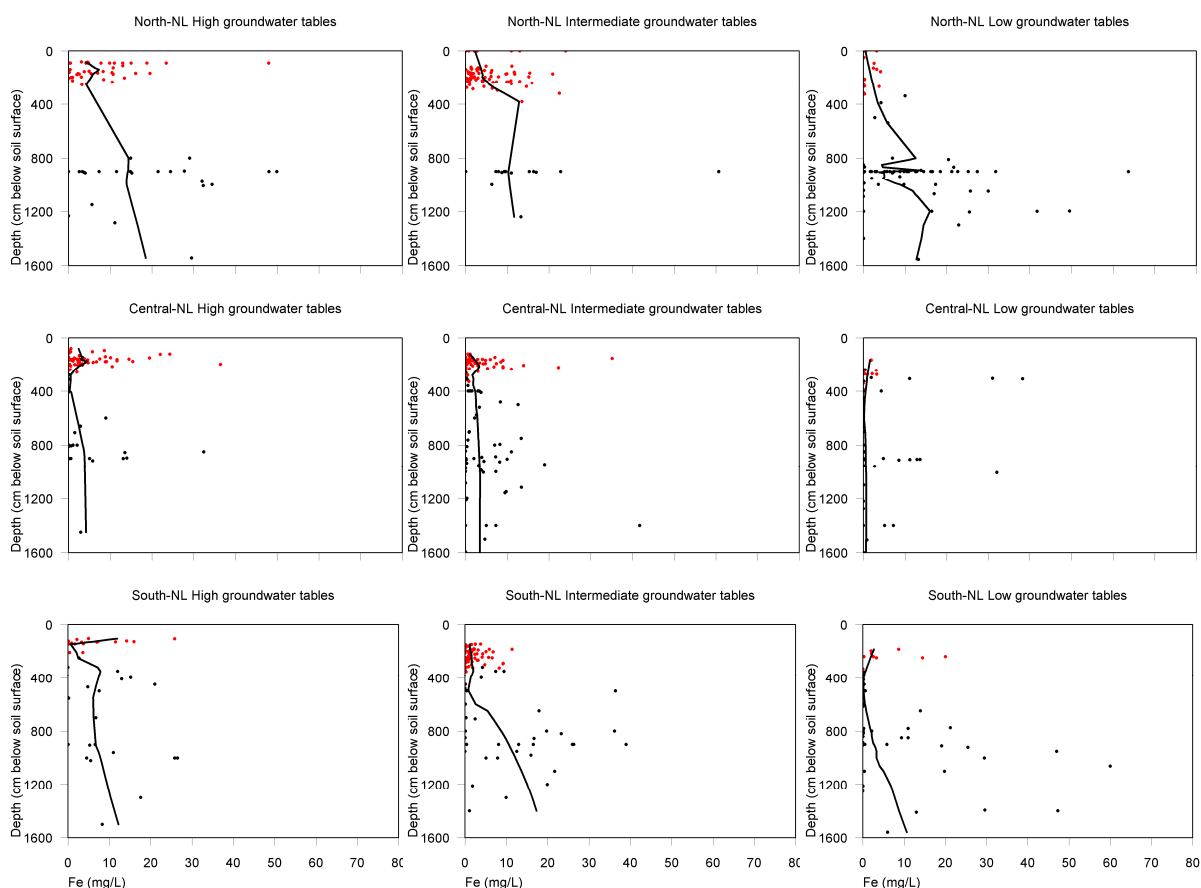


Fig. A4.5. Iron profiles with depth (red dots indicate the LMM observations, black dots refer to other monitoring networks)

Substantiation of the assumption that measured Fe concentrations are in large due to Fe(II) can be provided by looking at the pH profiles. Two examples of these pH profiles are given in Figure A4.6a and b, for intermediate groundwater levels in the central and southern part of the Netherlands, respectively. Most other areas generally show the behaviour of these depicted areas also. This general behaviour is an increase of pH values with depth from values that are clearly influenced by rain water and manure application

(pH 5–6) to near-neutral values, the increase conceivably being caused by the buffering capacity of the soil matrix and the dilution and buffering effect of seepage.

Over the largest part of the profile the pH values are such that the assumption that measured Fe is due to Fe(II) is warranted. Exceptions are found in the upper meters of the profile, mostly in the red dots. These data points contain data from samples with low pH values which do not exclude presence of dissolved Fe(III). The same group of data points also contains high Fe concentrations. The assumption could be formulated that these higher Fe concentrations are not necessarily due to pyrite oxidation, but perhaps to dissolution of Fe(III) from iron oxides under influence of low pH, and/or aqueous complexation between Fe(III) and dissolved organic acids. Then, the LOWESS curve of Fe excluding Fe(III) would lie even more towards zero in the “red dots zone”. However, no correlation could be found between Fe concentration and pH within this data group, see Figure 4.7, meaning that high Fe-concentrations are not exclusively related to low groundwater pH. Another explanation has to be searched for the higher Fe concentrations, possibly higher organic matter contents leading to reduced conditions and reduction of iron oxides, or still pyrite oxidation. This is, however, hard to substantiate because of the presence of many composite samples within this data group, making that, for example  $\text{NO}_3\text{-Fe}$  plots do not yield a clear picture of what is happening in the upper meters of the groundwater.

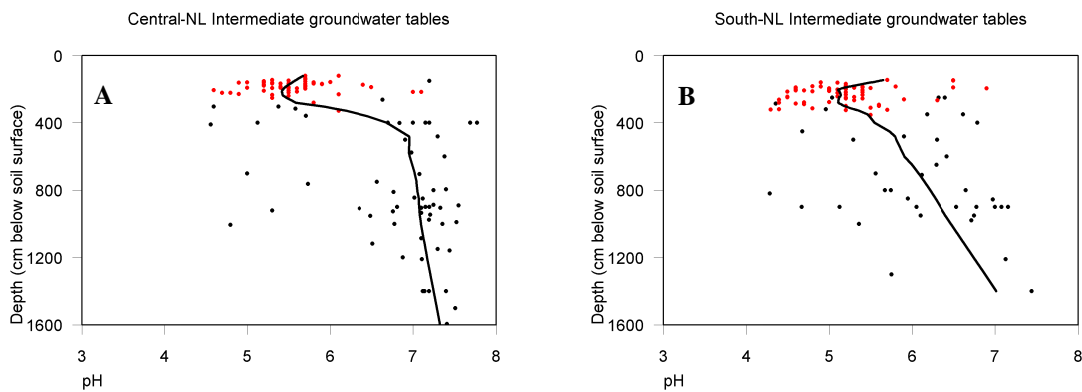


Fig. A4.6. pH profile as calculated for the class of intermediate groundwater tables in the central (A) and south (B) part of the Netherlands (red dots indicate the LMM observations, black dots refer to other monitoring networks).

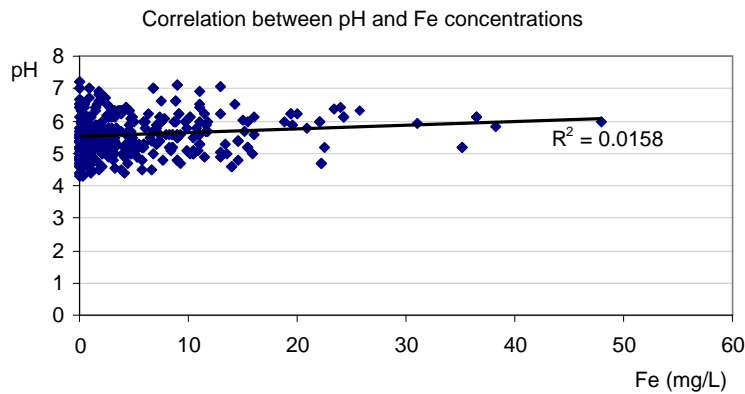


Fig. A4.7. Correlation between pH and total dissolved Fe concentrations for the data from the soil quality networks and the LMM (the “red dots” in Figures 4.3-4.6).

#### A4.4 Model validation criteria

The results obtained above have to be translated towards a set of criteria that is used for model validation. The table in Appendix 4 with statistical indicators of the nitrate profiles can be used directly to assess the plausibility of calculated nitrate concentrations per sand district and groundwater class. In addition, Table 4.2 presents, for every sand district / groundwater class combination, some assessments related to the nitrate removal potential and nitrate removal as observed in the results described above.

Table A4.2. Assessment of nitrate removal (potential) per sand district / groundwater class combination. N = North Netherlands, C = Central Netherlands, S = South Netherlands. Low, Interm. (=Intermediate) and High refer to the position of the groundwater tables and thus indicate groundwater class.

Sand area/ Sand types	Increase of anoxic conditions within the first meter below MLG	Increase of anoxic conditions within the first 5 meters below MLG	Depth at which percentage of anoxic samples > 90% (m below soil surface)	Nitrate removal within first 5 meters below groundwater level	Depth at which nitrate removal is virtually complete according to LOWESS curve (m – s.s.)	Nitrate removal at 5 meters below MLG
N, Low	Weak	Not evident	12	Strong	8	Ongoing
C, Low	Not evident	Not evident	nowhere	Not evident	nowhere	Not occurring
S, Low	Not evident	None	14	Not evident	16	Ongoing
N, Interm.	Strong	None	9	Strong	9	Ongoing
C, Interm.	Strong	Gradual	nowhere	Strong	5	Complete
S, Interm.	Strong	None	13	Strong	11	Ongoing
N, High	Strong	Not relevant	5	Strong	6	Complete
C, High	Strong	Not evident	13	Strong	9	Ongoing
S, High	Strong	Not relevant	9	Strong	5	Complete

## Appendix 5 Comparison of flux weighted concentrations at MLG level with concentrations in the first meter below a fluctuating groundwater level

The output of the STONE model comprises nitrate concentrations and nitrate and Total N balances. The nitrate concentrations are derived for a layer of  $m$  thickness just below the groundwater level. Since the groundwater level is a dynamic variable, the depth for assessing the averaged nitrate concentration varies with time. For the estimation of balances, a fixed depth is required. The top of the zone for which the balances are calculated is set at the mean lowest groundwater level. This indicator is a soil characteristic. The bottom of the zone is set at 5 m below the mean lowest groundwater level. Since the alternative definition of the upper groundwater may lead to deviations of the nitrate concentrations assessed according to the nitrate compliance checking procedure, the nitrate concentrations calculated by both methods have been plotted as X-Y scatter plots (Fig. A5.1).

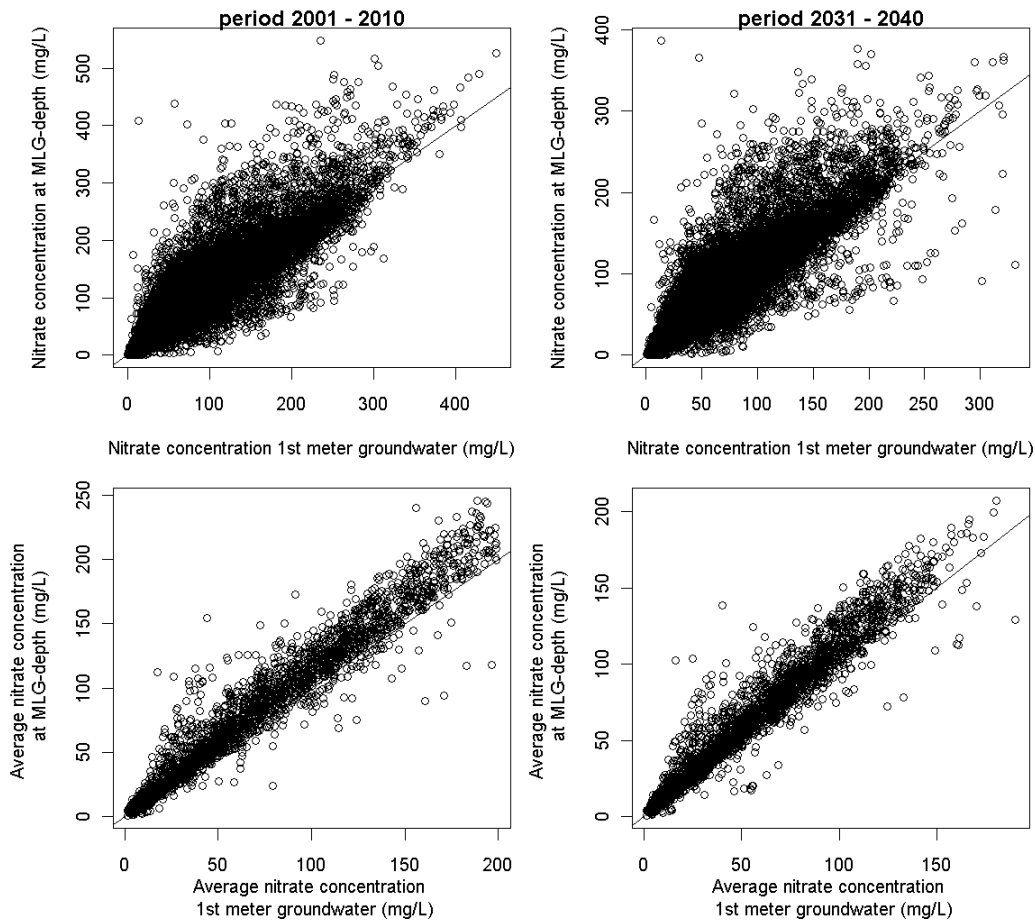


Fig. A5.1 Flux weighted nitrate concentration at the depth of the mean lowest groundwater level as a function of the nitrate concentration assessed according to the compliance checking procedure for plots with a maximum average concentration of  $200 \text{ mg l}^{-1}$  on sandy soils with a GWT  $\geq$  III. Left for the first period 2001–2010 and right for the second period 2031–2040.

The nitrate concentration at the top of the 5 m zone below the mean lowest groundwater level is calculated by dividing the annual nitrate load by the annual water flux. The comparison of the nitrate concentration calculated by both methods may yield a correction factor of the nitrate balances.

Nitrate concentrations calculated as the flux weighted average at depth of the mean lowest groundwater level are plotted against the concentration assessed according to the nitrate compliance checking procedure. Fig. 7.1 depicts the results of the two periods (left and right). At the upper row the annual results are shown and at the lower row the 10 year averaged results are shown.

The figures in the upper row show a scatter diagram of annual values. The variability of the meteorological conditions does affect the nitrate concentrations at the two depths in a different way. The figures at the lower which show the temporal averaged concentration do exhibit a less scattered pattern. The correlation coefficient has a high value ( $R^2=0.95$  en  $0.94$ ) and the intercept approaches to zero. The ratio between the concentrations calculated by both definitions amounts to 1.11 for the first period and 1.09 for the second period. The flux weighted nitrate concentrations at MLG-depth are on average 11% and 9% higher than the concentrations derived the compliance checking procedure. If one wants to derive concentration standards for the upper groundwater on the basis of balances and surface water loads, this factor could be taken into account for correcting to concentrations levels which comply with the normal procedures.

## Appendix 6 Calibration of SWAP and ANIMO on observed groundwater levels and nitrate concentrations at four dairy farms

### A6.1 Characterization of the farms

In a previous study reported by Fraters *et al.*, 2006, four farms were selected from the LMM participants (Figure A6.1) of which three farms were participating in the ‘Cows and Opportunities’ project (C&O). The nitrate concentrations measured in previous years at the farms had an average more than 25 mg l<sup>-1</sup> (see Table 6.1). The locations of the farms are depicted in Fig. A6.1.

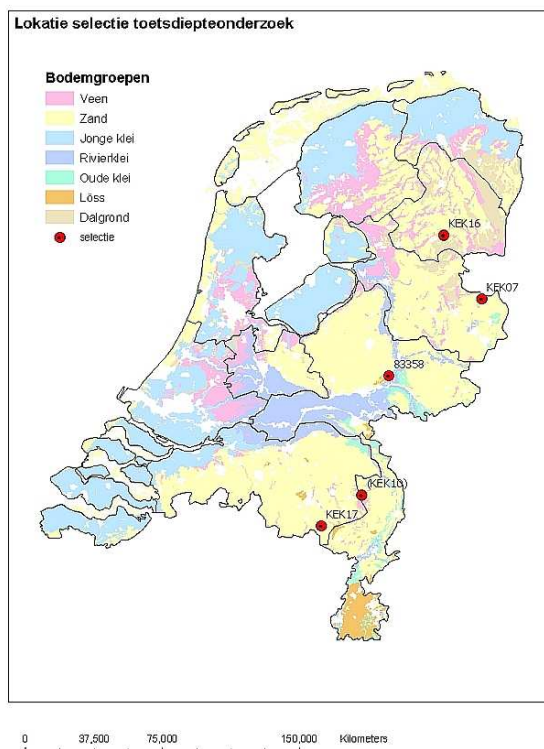


Figure A6.1 Farms selected for the field study in Fraters *et al.*, 2006. The farms are located at Maarheeze (KEK17), Spankeren (83358), Nutter (KEK07), and Nieuweroord (KEK16).

A preliminary geological study was carried out by TNO Built Environment and Geosciences. Series of groundwater level data were also supplied for piezometric wells in the vicinity of the farms, including the mean highest groundwater level (MHG) and mean lowest groundwater level (MLG) calculated from these data for these wells.

The preliminary geological study was based on descriptions of bore holes in the vicinity of the farms and what is known about the area by the TNO regional expert and provides insight into the occurrence of the lateral continuity of clay/loam layers or layers with a coarse texture (soil layers and coarse sand layers) in the shallow subsoil (to 10 meters below MLG).

The soil structure of the sedimentary deposits in the upper five meters of the groundwater body is heterogeneous (A6.2). The sediments at most of the locations consist of sand with thin clay and/or loam layers in it. The locations at Nieuweroord and one location at Nutter (28F0473) and Spankeren (33G0414) are exceptions. The sediments here consist primarily of loam containing (thin) sandy layers. At the location 33G0412 the bottom of the deposit consists of gravel layers. Peat layers occur at a number of locations (57E0335, 57E0338 and 33G0414). A layer of (organic-rich) detritus occurs in the sediments at two locations at Spankeren (33G0413 and 33G0415). The locations at Spankeren contain carbonate, the others do not. The carbonate contains siderite ( $\text{FeCO}_3$ ). Two of the locations at Maarheeze may contain layers in which some pyrite occurs (57E0335, 57E0338) in addition to a few other reactive iron compounds.

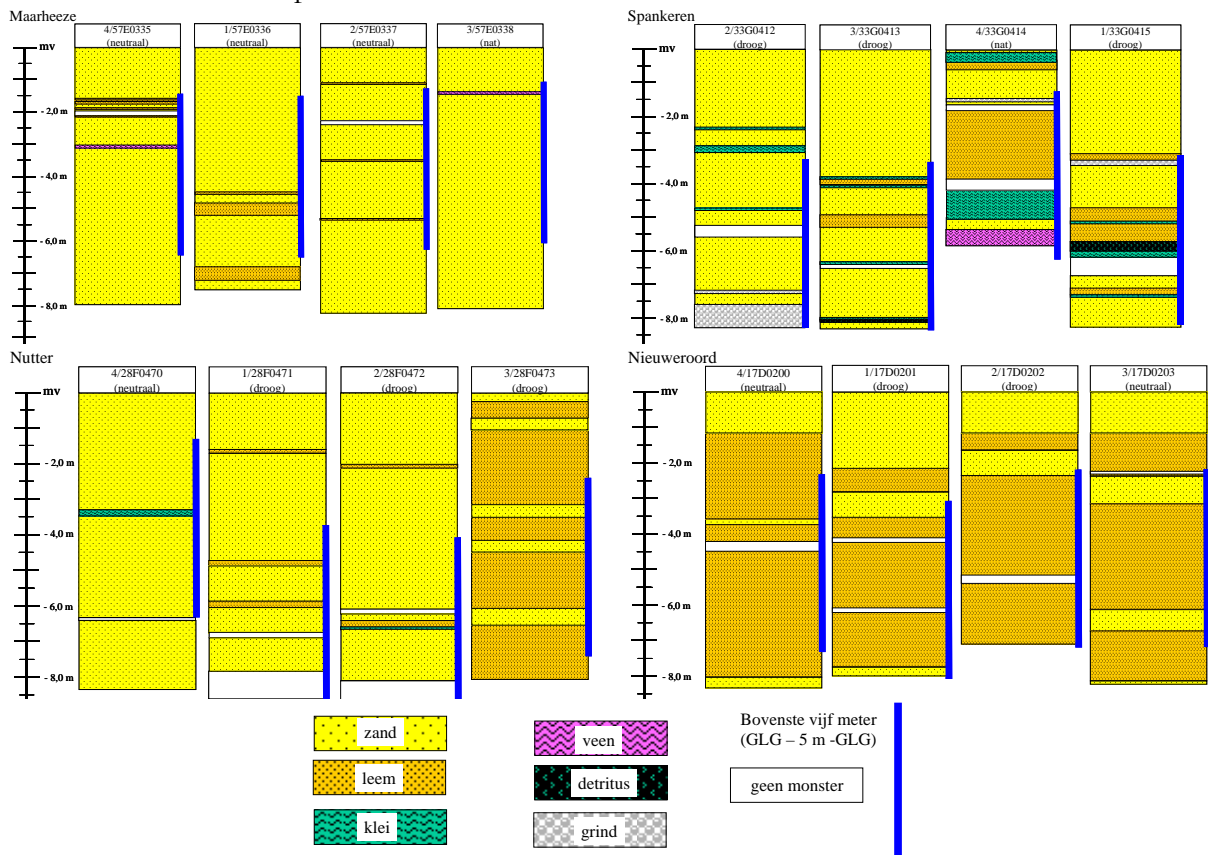


Figure A6.2 Simplified diagram of the soil layers from MLG to five meters below MLG for the locations examined at the four dairy farms, based on the description of the subsoil by TNO, and of the topsoil by Utrecht University. Top left Maarheeze (57E), top right Spankeren (33G), below left Nutter (28F) and below right Nieuweroord (17D).

Most layers in the sedimentary deposits at the Nutter locations contain varying amounts of reactive iron in the form of glauconite and, possibly, iron oxides. Location 28F0473 is the only one to contain some pyrite at the bottom of the sedimentary deposits. The locations at Nieuweroord do not contain any reactive iron with the exception of one sample from location 17D0200. Pyrite does not play an important role in the denitrifying capacity of the sediments at Nieuweroord.

The distribution of the groundwater classes of the fields for each farm is given in Table A6.1.

*Table A6.1 Characteristics of the four dairy farms and the numbers of locations for each drainage class; wet (GWTs I through IV), moderate (GWTs V, V\* and VI) and dry (GWTs VII and VIII).*

Farm	Code	Sandy area	Soil type	Type	Wet	Moderate	Dry
Maarheeze	57E	South	Sand	Large push- moraine	1	3	–
Spankeren	33G	Central	Sand	Carbonate -free pyrite	1	–	3
Nieuweroord	17D	North	Reclaimed peat soils	Boulder clay	–	2	2
Nutter	28F	East	Sand	Carbonate-free pyrite	–	1	3

Table A6.2 shows the average nitrate concentrations for the first meter of the groundwater column averaged for the farms as observed in the regular LMM monitoring samplings.

*Table A6.2 Nitrate concentrations ( $mg\ l^{-1}$ ) in the upper meter of the groundwater on the farms selected for the field study in the period 1999–2004 (– means that no groundwater samples were taken).*

	Farm book	1998	1999	2000	2001	2002	2003	2004	2005
	keeping year								
	Observation	1999	2000	2001	2002	2003	2004	2005	2006
	year								
Maarheeze		–	82	112	93	67	64	80	87
Spankeren		–	116	–	–	36	–	56	91
Nutter		129	94	81	75	69	88	108	76
Nieuweroord		–	51	35	24	12	27	14	9

During the field study by Fraters *et al* (2006), samples were taken at some dates and at different depths. The results of the final sampling round are depicted in Fig. A6.3. The results clearly show that the upper groundwater at the farm on reclaimed peat soil (Nieuweroord) contains very little nitrate, if any, despite the fact that the locations at this farm are classified as being in a moderate or dry drainage class. The locations with a dry drainage class at the other farms (three at Spankeren and one at Nutter) show both a decrease (28F0472 and 33G0413) and an increase (33G0412 and 33G0415) with depth. The locations with a moderate drainage class at Maarheeze (57E) show a decrease, the location at Nutter (28F0470) on the other hand, an increase.

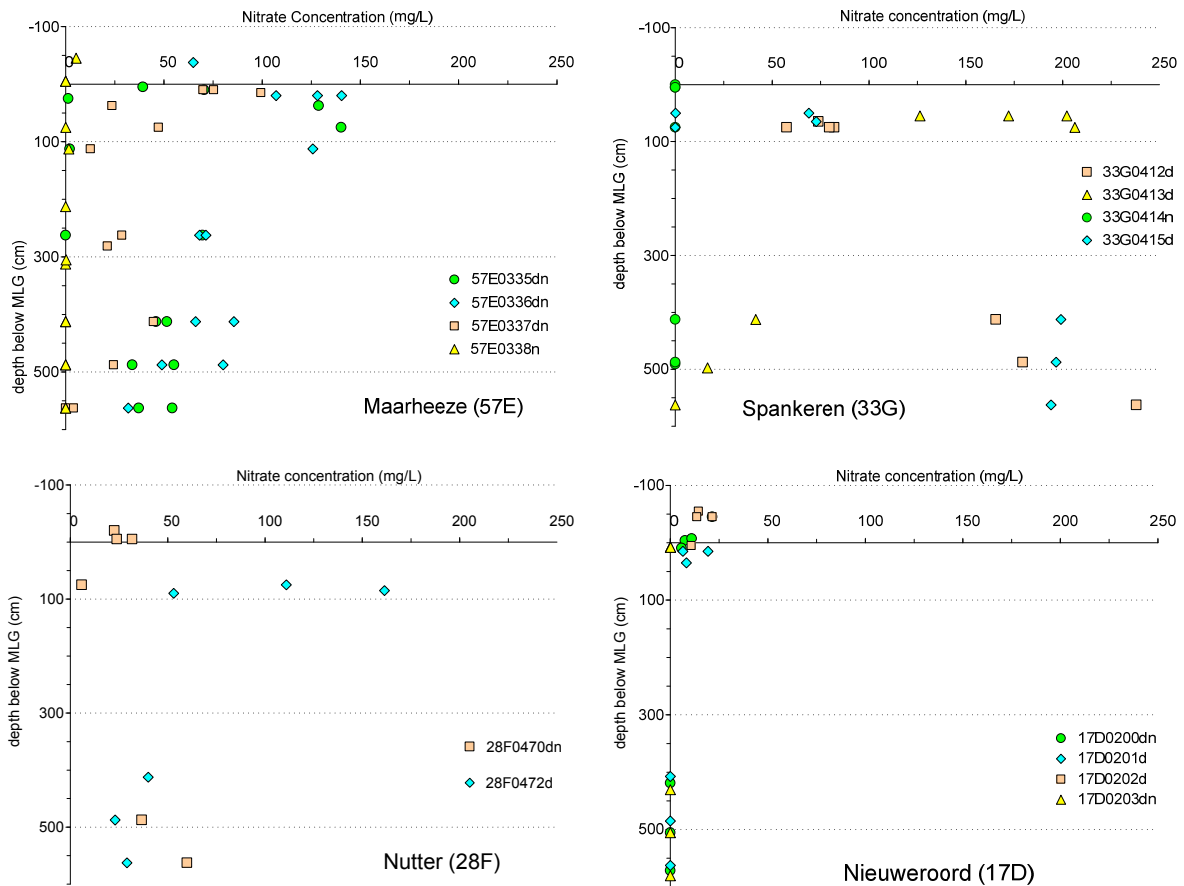


Figure A6.3 Nitrate concentrations at various depths at the four dairy farms for the final sampling round as reported by Fraters *et al* (2006). Drainage classes: d = dry, dn = moderate, n = wet.

The study of Fraters *et al* (2006) made clear that the subsoil of the sandy areas in the Netherlands is highly heterogeneous. At least one aberrant (non-sandy) layer is observed at every location. In most cases, the locations at any one particular farm also vary from one another in terms of the structure of the upper part of the aquifer. A notable point is that the locations at Spankeren contain carbonate, which is atypical for this area (Van Beek, 2002). The same applies to the lack of pyrite at the locations at Nutter (area with carbonate-free pyrite). As a result, large differences can arise within short distances in groundwater flow and whether denitrification occurs or not.

The nitrate concentrations are (not-significantly) lower in the fifth metre than in the first metre. There are differences between drainage classes as was the case in the previous study. On average, the soils with dry classes do not show a decrease, and those with neutral classes do, although this is not significant. The soils with a wet class do not contain any nitrate in either the first metre or the fifth.

## A6.2 Calibration approach

The following actions are taken for the calibration of the SWAP/ANIMO model.

1. Despite a number of model inputs are available from field investigations, a great number of other inputs are not available. To fill this data gap, the model input of STONE plots is used. The selection of STONE-plots is done on the basis of similarity with respect to land use, soil mapping unit, geo-chemical characteristics of the sub-soil, groundwater class in the near vicinity with similar characteristics to derive model input.
2. The distribution between grassland and maize is not exactly known at each of the observation points and the land use can change every year. For each location a grassland and a maize plot has been selected from the STONE database.
3. The hydrological model SWAP has been applied to evaluate the performance of the groundwater level simulations. In addition the ANIMO was run to obtain nitrate concentrations for the not-calibrated models.
4. A comparison is made between the observed and simulated groundwater levels and the observed and simulated nitrate concentrations.
5. The SWAP model was attuned by:
  - o Imposing the rainfall figures of the most nearby rainfall station instead the regionally up scaled rainfall figures of the STONE model
  - o Examination of the drainage levels and drainage resistances on the basis of a description of the local geo-hydrological system.
  - o Calibration by adjusting the boundary bottom flux (upward / downward seepage)
  - o Comparison with groundwater level observations at the field and with time series in nearby monitoring wells
6. The application of the ANIMO model based on inputs of the STONE-model schematization and based on the results of the calibrated SWAP-model but the non-calibrated ANIMO model.
7. Refinement of the input data to the ANIMO model by using farm specific data on fertilization rates and nitrogen excesses.
8. Refinement of the input data to the ANIMO model by making use of the potential denitrification rates as observed in the borings at the farms.
9. Evaluation of the model results.
10. Sensitivity analysis of the ANIMO model with respect to the decay rate constants of organic matter pools and the associated potential denitrification rate in the groundwater zone (see §5.1.3).

## A6.3 Results

### A6.3.1 Maarheeze results

For three of the four fields the groundwater levels in 2005 simulated by the non-calibrated SWAP model approached the observed values. In field 57E0337 the model overestimated the field measurements. Two of the three observed groundwater levels in field 57E0338 have been measured in a period with heavy rainfall. After imposing region specific rainfall data and calibration of the bottom boundary flux condition, the simulated groundwater level fit the observed values satisfactorily. It can be seen that the measurements apply to normal and low values of the groundwater course with that and that no observations of high groundwater events are available.

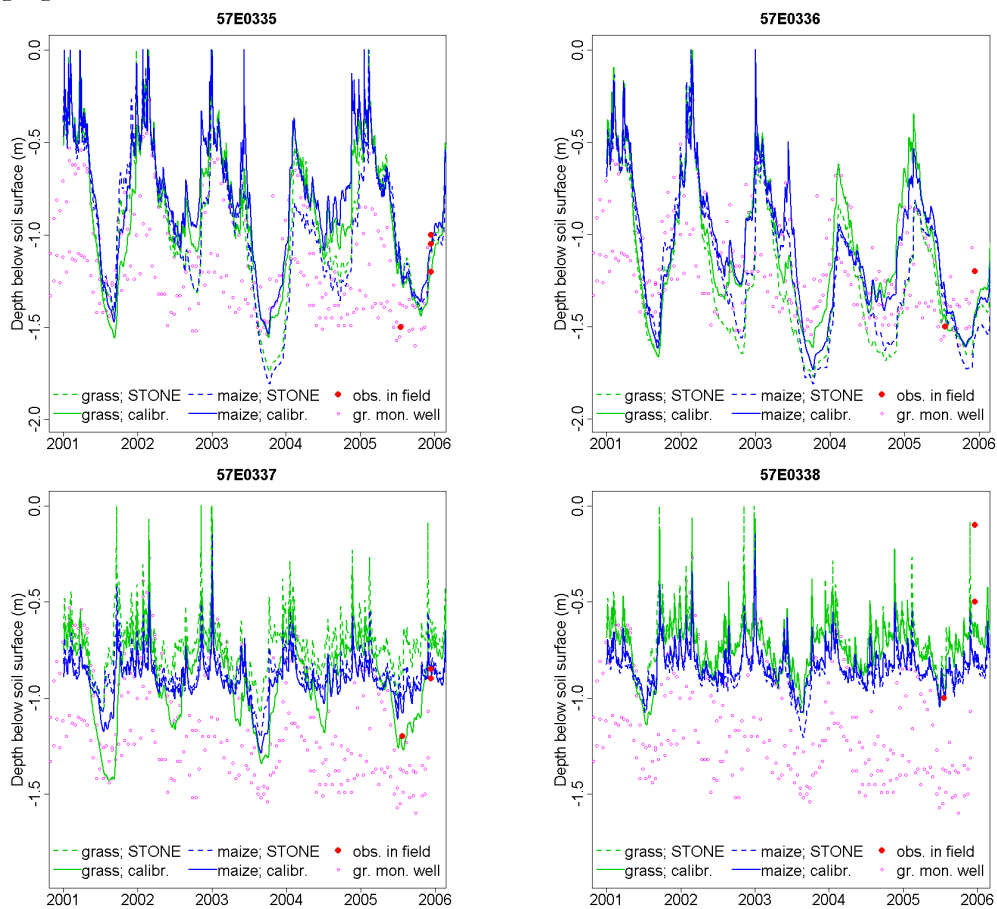


Fig. A6.4 Observed and simulated groundwater levels at the 4 locations of the Maarheeze farm. The dashed lines represent the non-calibrated SWAP model results and the solid line refers to the calibrated SWAP model results.

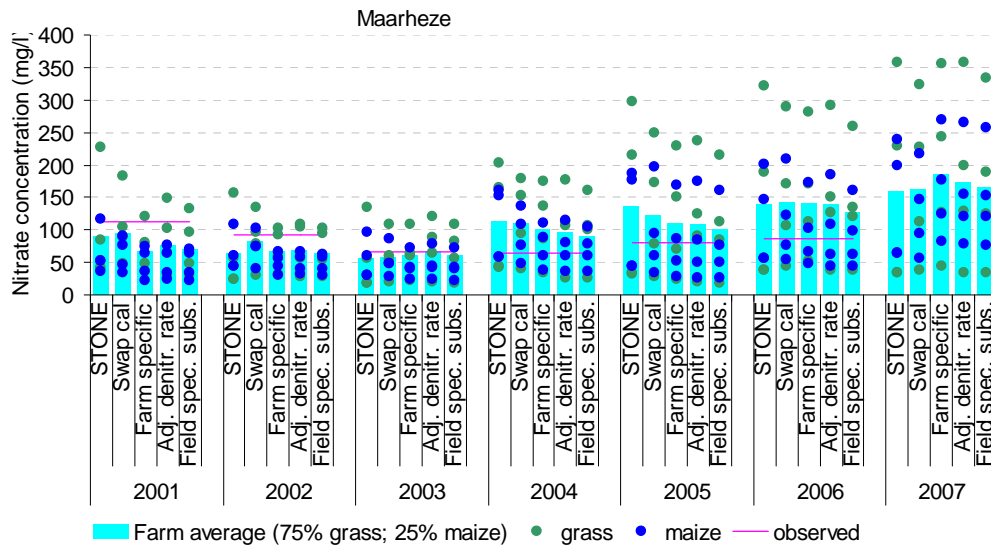


Fig. A6.5 Annual averaged nitrate concentrations at farm level of the Maarbeze farm resulting from successive model adjustments. Green and blue dots are the results of the individual fields.

Results of the model evaluation for field specific nitrate concentrations are depicted in Fig. A6.6.

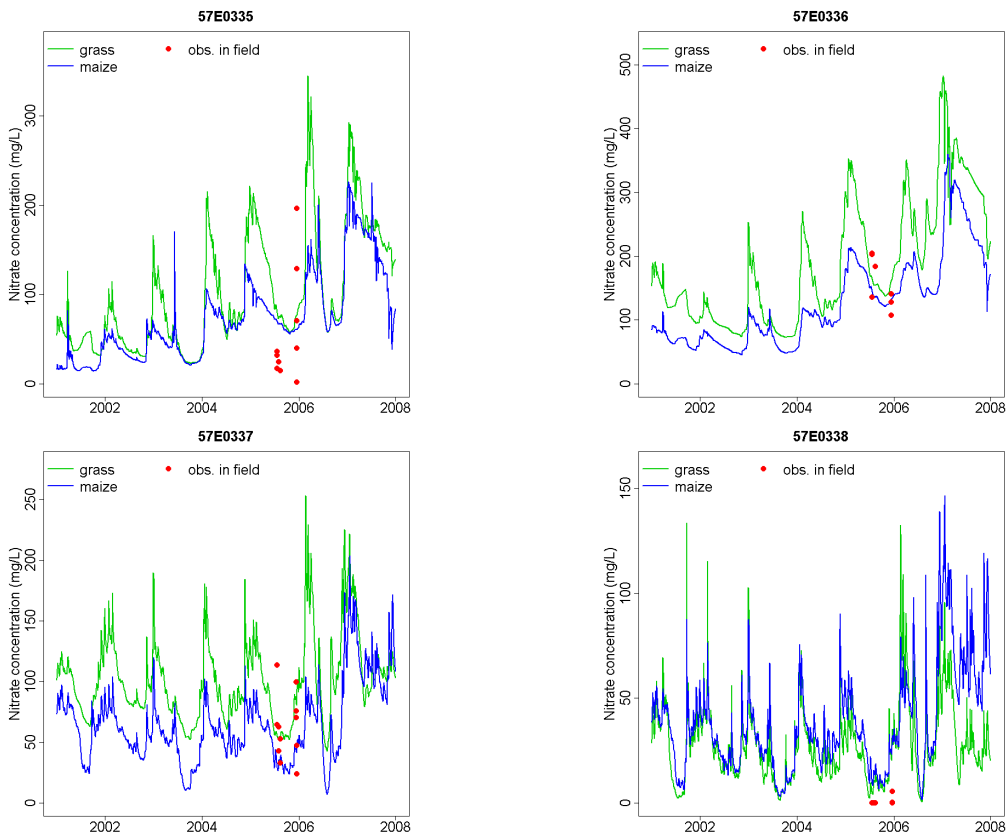


Fig. A6.6 Observed and simulated nitrate concentrations at the four locations of the Maarbeze farm.

The nitrate concentrations as depicted in Fig A6.5 show an increase with time after 2003. Both the simulated and observed concentrations increase, but the increase rate for the simulated values is higher. It can be seen from Fig. A6.6 that only field 57E0335 and field E0336 are responsible for this trend. In the first years the model underestimates the observed nitrate concentrations, but in the last years the simulated concentrations are higher than the observed ones. Probably the initial conditions in the model disagree with the field conditions. No data was available with respect to the organic and nitrogen pools in the soil and the historic land management.

The farm averaged concentration is surrounded by a large band width of individual observations (Fig. A6.6). The nitrate simulations in field 57E0336 and 57E0337 fit quiet well with the measured concentrations. It can be seen that the simulated concentration amplitude is larger than the band width of field observations. The number of field observations is too limited to evaluate the performance of the concentration dynamics.

The model adjustments with respect to input and parameterization resulted from 2003 and later years to only a minor decrease of the concentration levels (Fig. A6.5). Only in the first simulation year the adaptations resulted to a significant reduction of the concentrations.

*Maarbeeze farm: influence of field specific organic matter contents*

*Maarbeeze 57E0335*

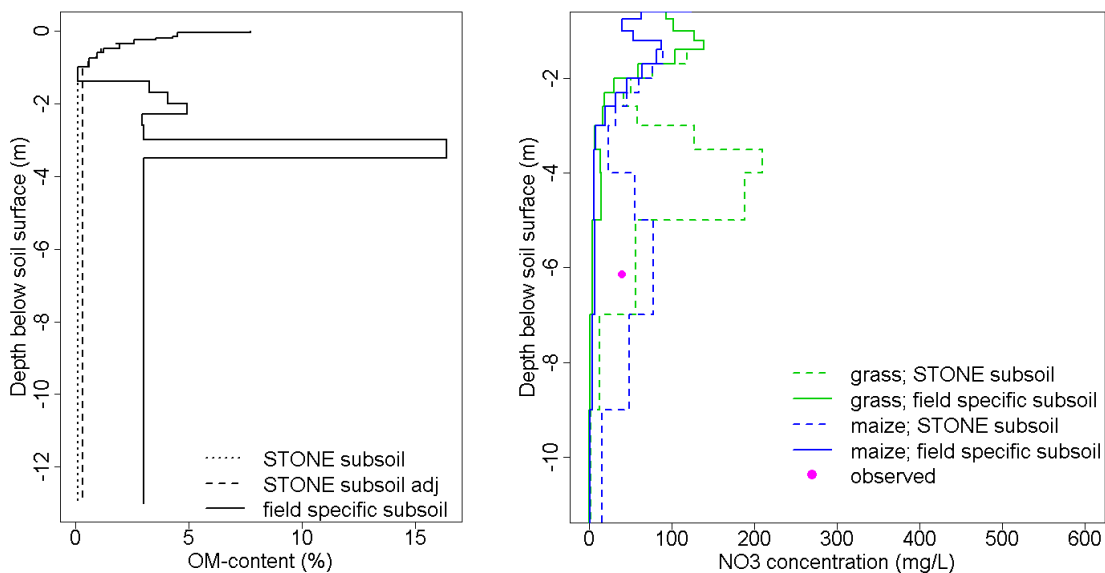


*Fig. A6.7 Solid organic matter contents in the regional STONE model and in the field study (left figure) and observed and simulated nitrate concentrations for grassland and silage maize as a function of depth for fields of the Maarbeeze farm, location 57E0335 (right figure). Results for the STONE schematization are indicated by interrupted lines and results for the schematization on the basis of observed OM-contents are given by solid lines.*

Maarbeeze 57E0337

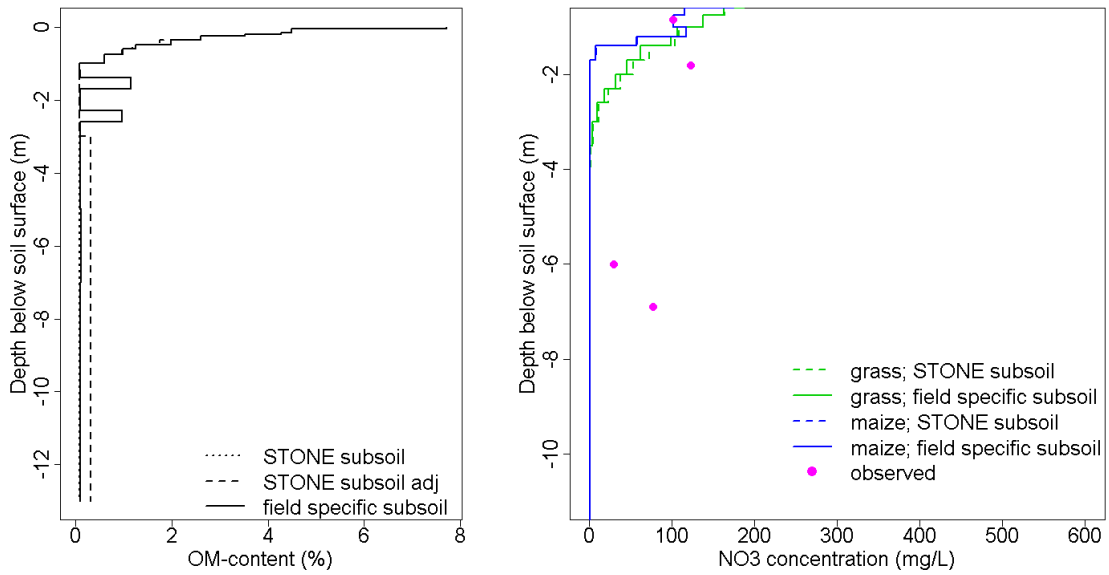


Fig. A6.8 Solid organic matter contents in the regional STONE model and in the field study (left figure) and observed and simulated nitrate concentrations for grassland and silage maize as a function of depth for fields of the Maarbeeze farm, location 57E0337 (right figure). Results for the STONE schematization are indicated by interrupted lines and results for the schematization on the basis of observed OM-contents are given by solid lines.

Maarbeeze 57E0338

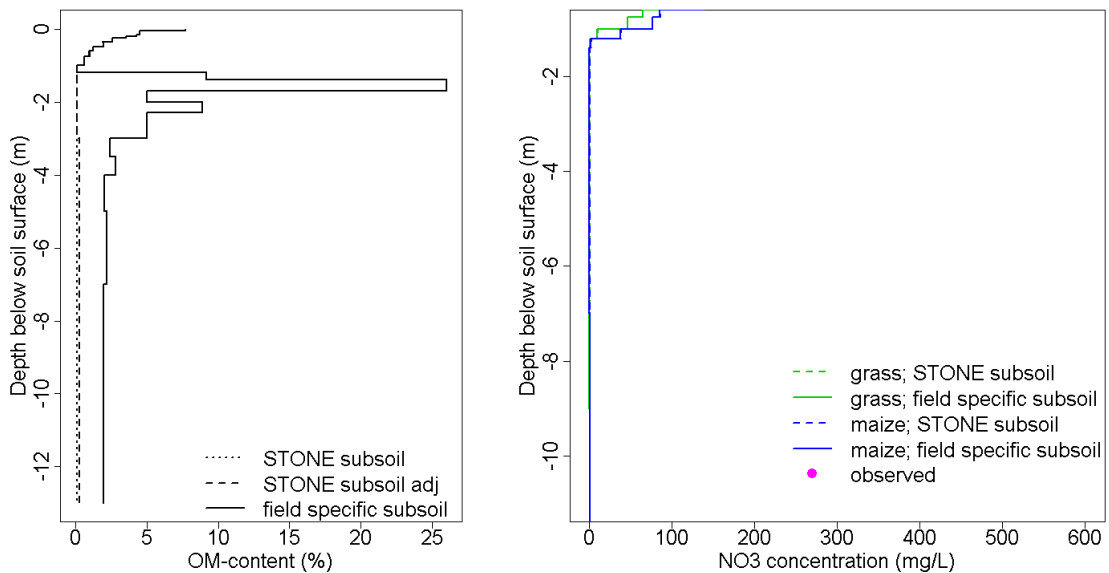


Fig. A6.9 Solid organic matter contents in the regional STONE model and in the field study (left figure) and observed and simulated nitrate concentrations for grassland and silage maize as a function of depth for fields of the Maarbeeze farm, location 57E0338 (right figure). Results for the STONE schematization are indicated by interrupted lines and results for the schematization on the basis of observed OM-contents are given by solid lines.

### Spankeren results

The non-calibrated groundwater simulations resulted to an underestimation of the groundwater depth for three of the four fields (Fig. A6.10). After imposing regional specific rainfall data and calibration, the simulated groundwater levels fit well with the few measured data. It should be noted that the number of observation is very limited.

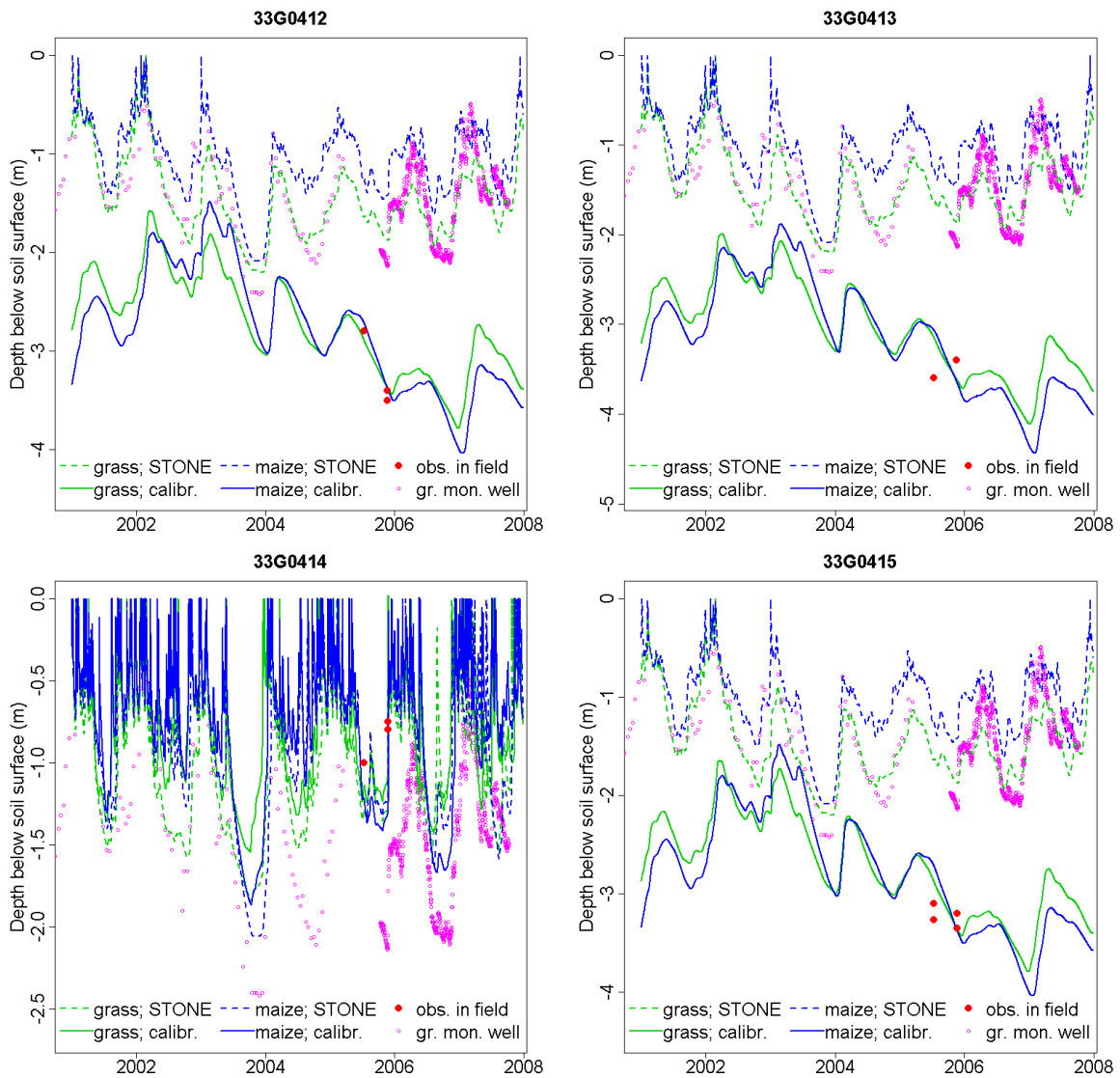


Fig. A6.10 Observed and simulated groundwater levels at the 4 locations of the Spankeren farm. The dashed lines represent the non-calibrated SWAP model results and the solid line refers to the calibrated SWAP model results.

Three fields having the lowest groundwater levels show a decrease with time. Inspection by considering a longer time series showed that this is due to the choice of the time frame depicted and that the long term time series do not show a decrease.

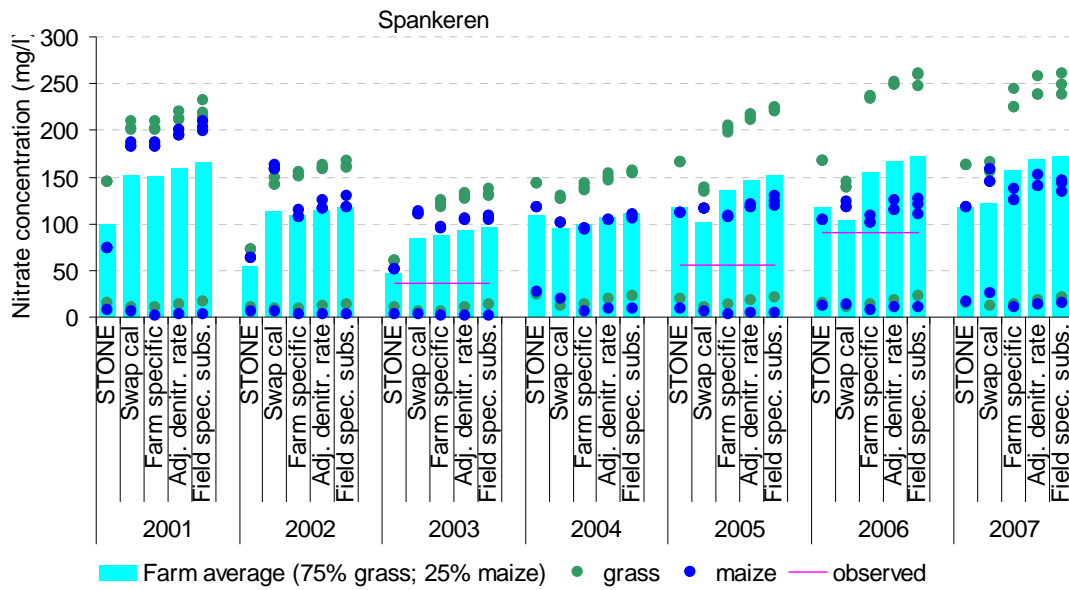


Fig. A6.1 Annual averaged nitrate concentrations at farm level of the Spankeren farm resulting from successive model adjustments. Green en blue dots are the results of the individual fields.

Results of the model evaluation for field specific nitrate concentrations are depicted in Fig. A6.12.

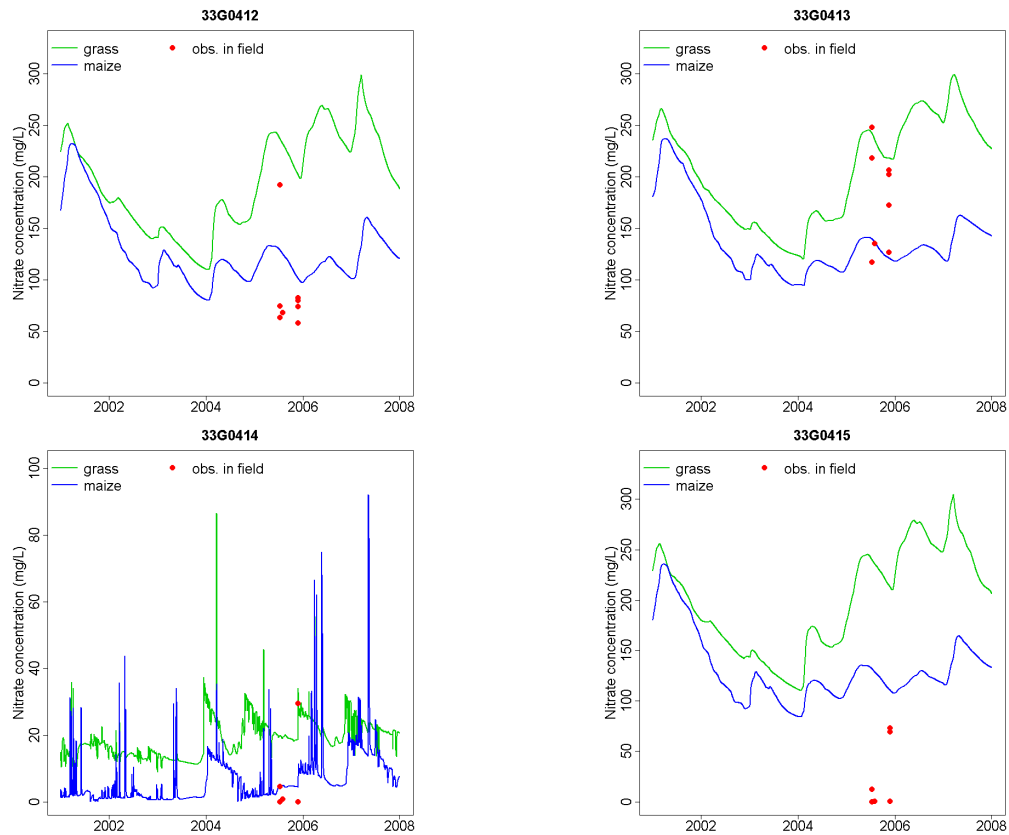


Fig. A6.12 Observed and simulated nitrate concentrations at the four locations of the Spankeren farm.

The majority of the simulations at field scale resulted to higher concentrations than the farm averaged value. Information on the position of the samples taken for determining the farm averaged value is missing. One of the fields (33G0414) encounters high groundwater levels which lead to low concentrations. The distribution of the farm samples over the different fields is unknown. The first step of the model adjustment (refinement and calibration of SWAP) yielded an increase of the nitrate concentrations during the first three years. Later on, the refinement of the farm specific fertilization rates resulted to increased nitrate concentrations. Imposing field specific subsoil organic matter contents had a minor effect on the nitrate concentration in the first meter of the groundwater body

*Spankeren farm: influence of field specific organic matter contents*

*Spankeren 33G0412*

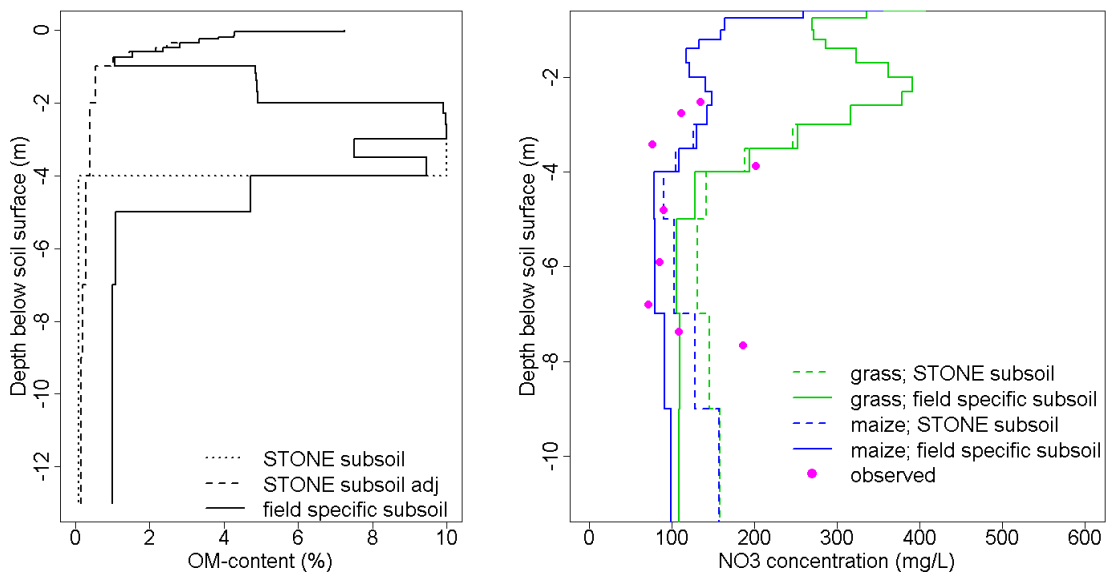


Fig. A6.13 Solid organic matter contents in the regional STONE model and in the field study (left figure) and observed and simulated nitrate concentrations for grassland and silage maize as a function of depth for fields of the Spankeren farm, location 33G0412 (right figure). Results for the STONE schematization are indicated by interrupted lines and results for the schematization on the basis of observed OM-contents are given by solid lines.

Spankeren 33G0414

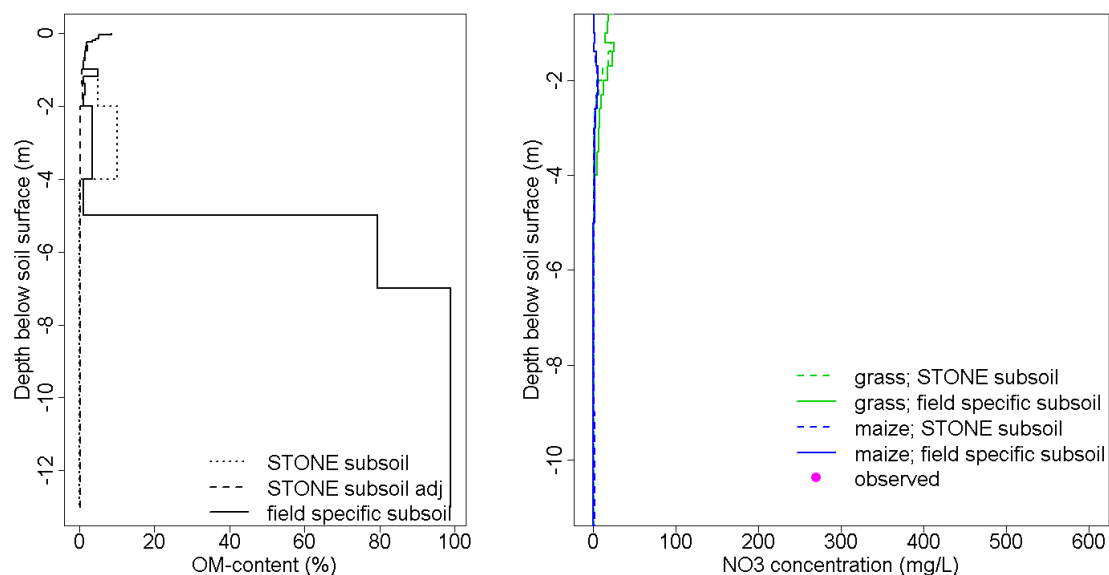


Fig. A6.14 Solid organic matter contents in the regional STONE model and in the field study (left figure) and observed and simulated nitrate concentrations for grassland and silage maize as a function of depth for fields of the Spankeren farm, location 33G0414 (right figure). Results for the STONE schematization are indicated by interrupted lines and results for the schematization on the basis of observed OM-contents are given by solid lines.

Spankeren 33G0415

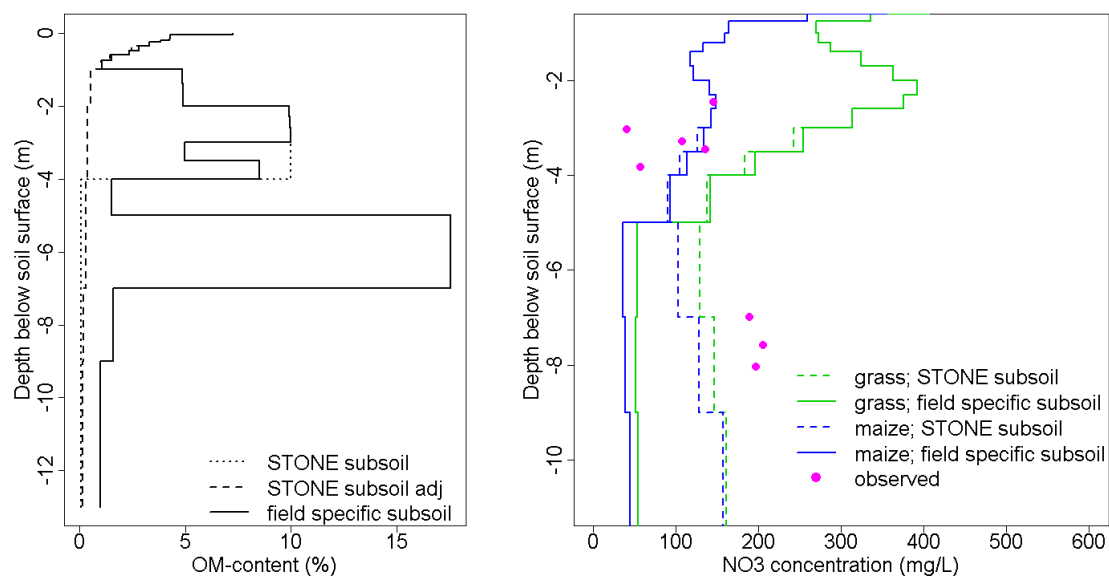


Fig. A6.15 Solid organic matter contents in the regional STONE model and in the field study (left figure) and observed and simulated nitrate concentrations for grassland and silage maize as a function of depth for fields of the Spankeren farm, location 33G0415 (right figure). Results for the STONE schematization are indicated by interrupted lines and results for the schematization on the basis of observed OM-contents are given by solid lines.

*Nutter results*

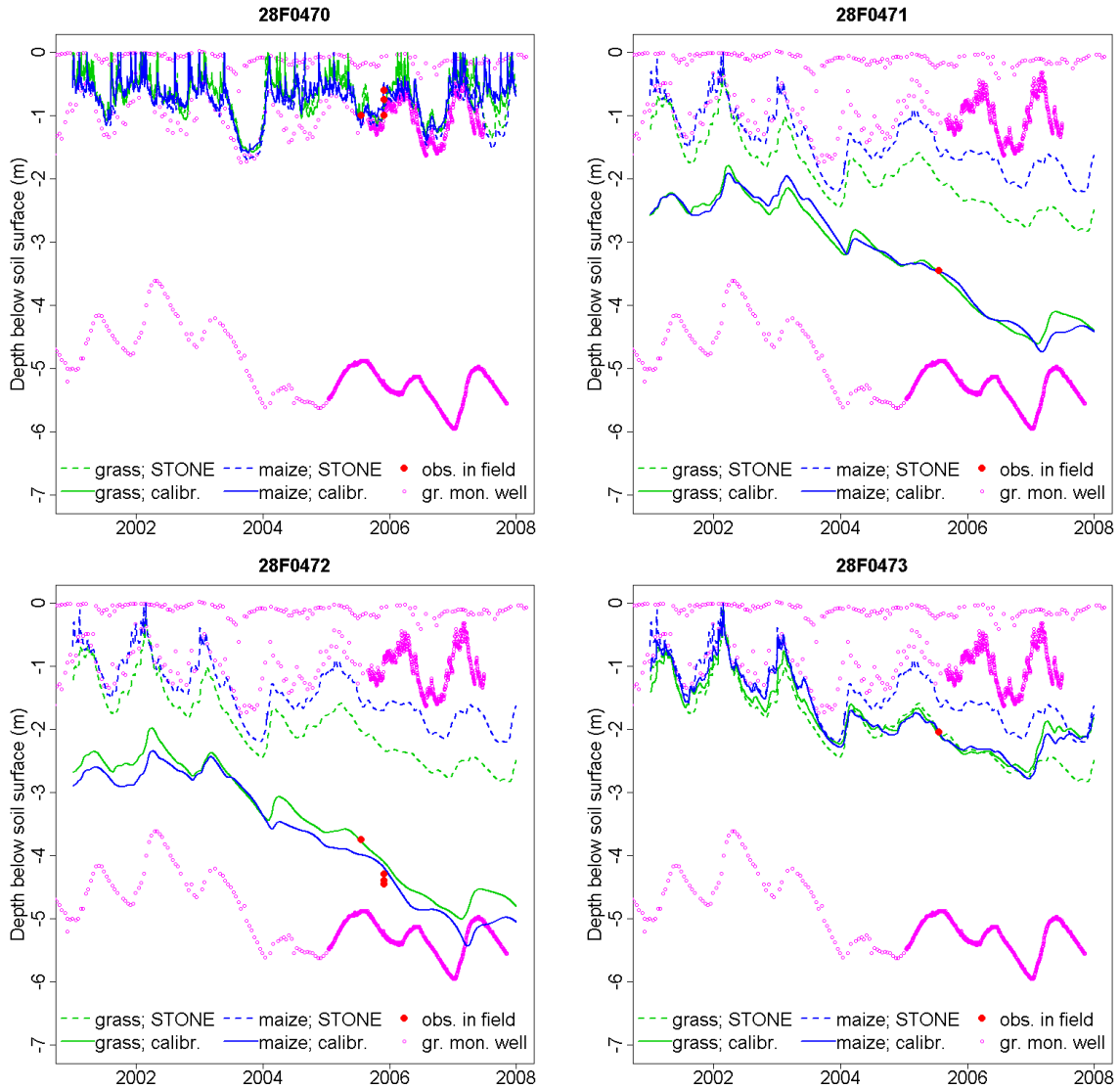


Fig. A6.16 Observed and simulated groundwater levels at the 4 locations of the Nutter farm. The dashed lines represent the non-calibrated SWAP model results and the solid line refers to the calibrated SWAP model results.

The groundwater levels simulated with the non-calibrated SWAP model were in general too high at the Nutter farm for three of the four fields (Fig. A6.16). Only the “wet” field showed initially satisfactorily groundwater levels. After adjustment of the rainfall time series and the bottom boundary condition the groundwater level fitted well the observed values, but showed a discrepancy with the dynamic behaviour of the time series observed in the groundwater monitoring wells of the regular network in 2005 and 2006. Inspection by evaluating a longer time series showed that the decrease is due to the choice of the time frame depicted and that the long term time series do not show a decrease.

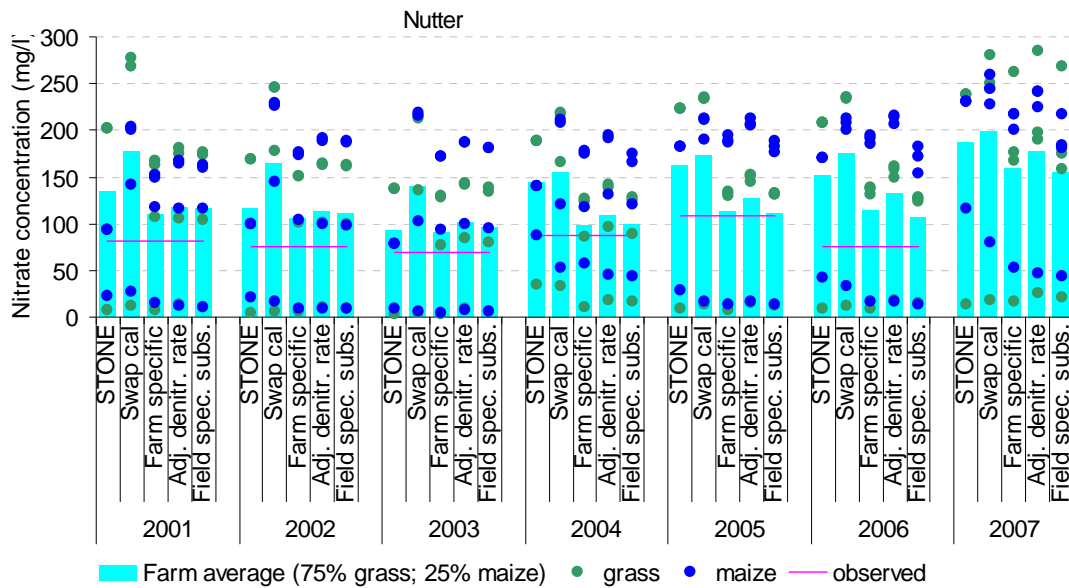


Fig. A6.17 Annual averaged nitrate concentrations at farm level of the Nutter farm resulting from successive model adjustments. Green en blue dots are the results of the individual fields.

The majority of the field simulation results overestimate the farm averaged observations (Fig. A6.17). Only the concentrations at the wet field are lower than the observed average value. After the calibration of the SWAP model, the average of the field simulations fits well with the observed concentrations in 2004 and 2005, but overestimates the measured values in the other years. The field scale concentrations have been up scaled to the farm scale by weighing the grass fields and the maize fields and assuming 75% land covered with grassland and 25% with silage maize. Imposing farm specific fertilization date affects the nitrate concentration with approximately 50 mg l<sup>-1</sup> in 2004, 2005 and 2006. The improved subsoil organic matter contents derived from field specific data had hardly any effect on the nitrate concentrations in the upper groundwater. The concentrations at greater depth, however, show a response to the adjusted organic matter contents.

Results of the model evaluation for field specific nitrate concentrations are depicted in Fig. A6.18.

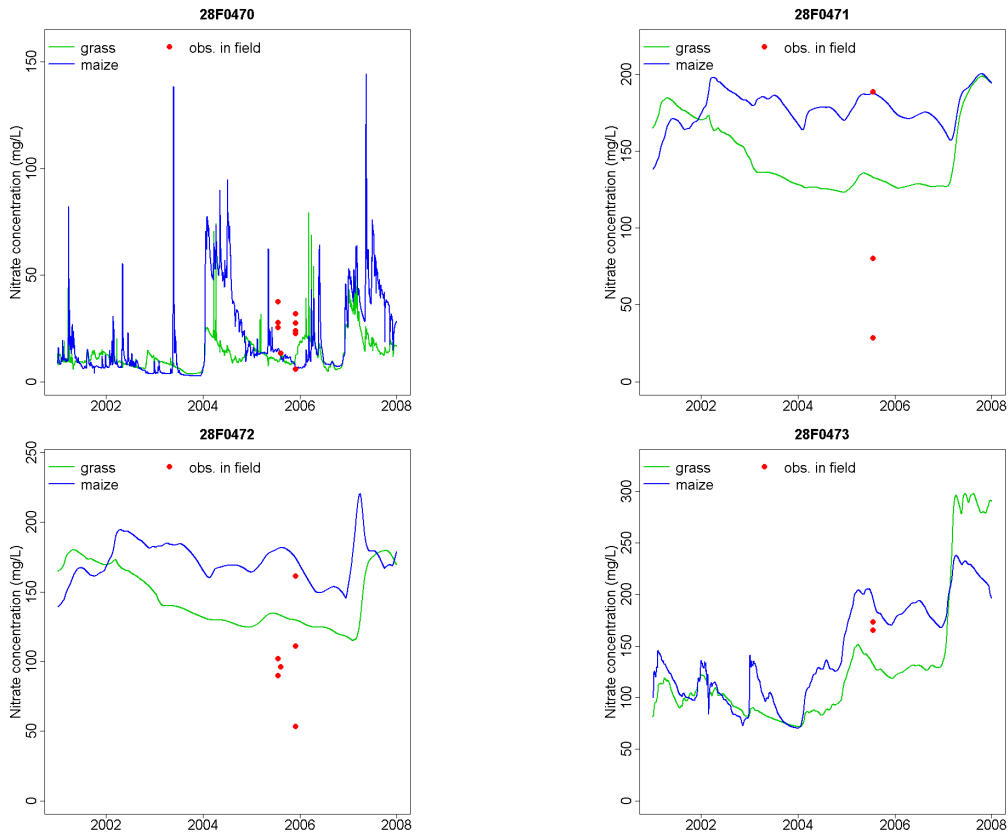


Fig. A6.18 Observed and simulated nitrate concentrations at the four locations of the Nutter farm.

The simulated nitrate concentrations exceed the observed concentrations for two of the four fields (Fig. A6.18). The concentration dynamics in the wet field (28F0470) is high. The performance for the 28F043 is good. It appears that an increase trend is predicted for the 28F043 field, mainly due to the initial conditions based on the regional STONE schematization which do not comply with the specific field conditions. The initial concentrations in 2001 were estimated too low for this field. Another reason for this trend is the lowering of the groundwater level in the years 2004–2007 due to the succession of relative dry years.

It should be noted that only a few observations are available. The scarce available measurements refer only to one year and show a high variability at field scale.

Nutter farm: influence of field specific organic matter contents

Nutter 28F0470

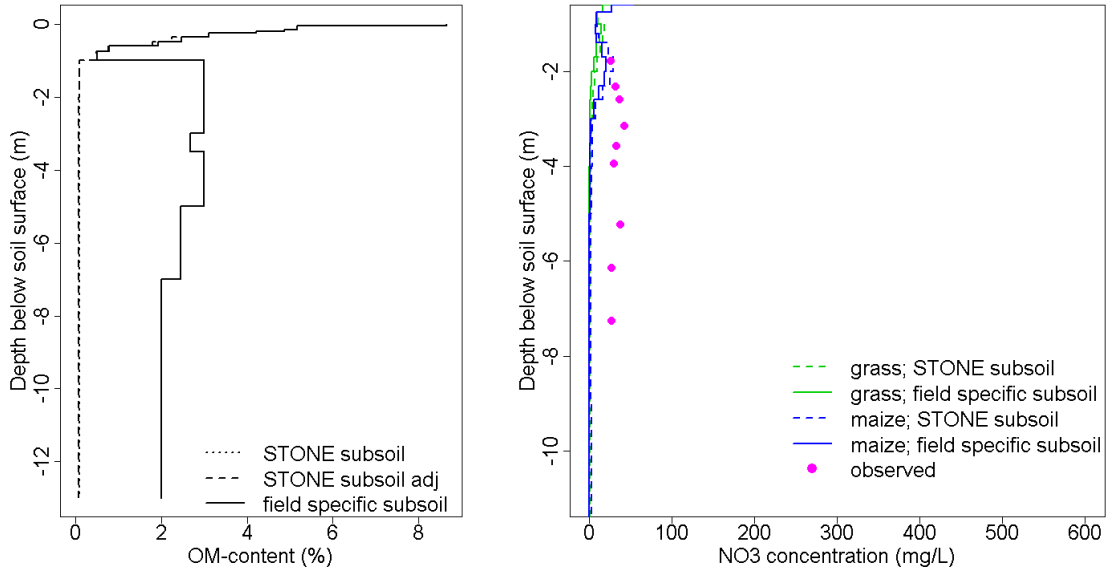


Fig. A6.19 Solid organic matter contents in the regional STONE model and in the field study (left figure) and observed and simulated nitrate concentrations for grassland and silage maize as a function of depth for fields of the Nutter farm, location 28F0470 (right figure). Results for the STONE schematization are indicated by interrupted lines and results for the schematization on the basis of observed OM-contents are given by solid lines.

Nutter 28F0472

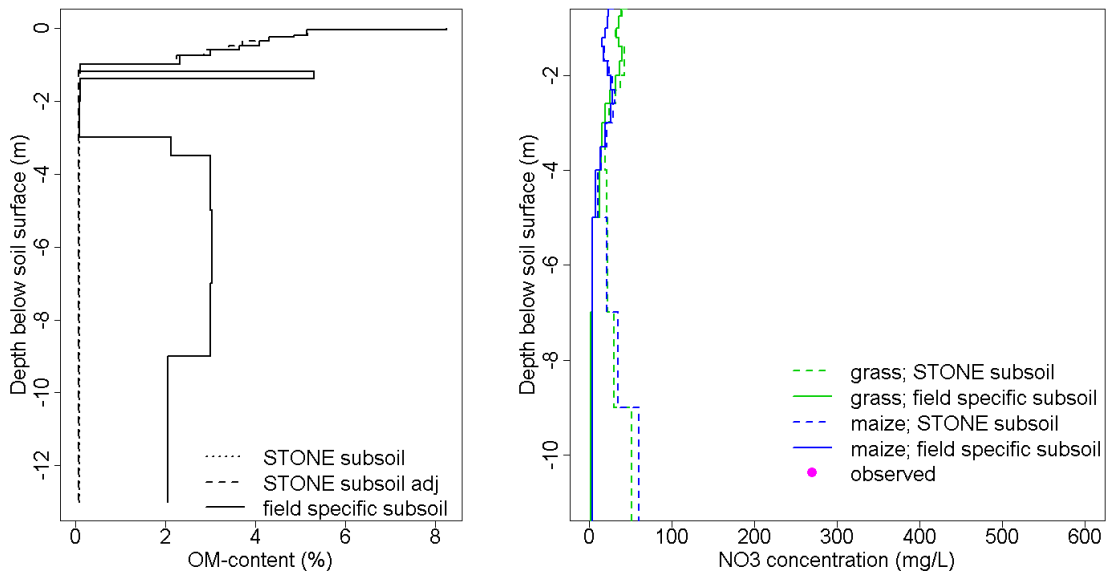


Fig. A6.20 Solid organic matter contents in the regional STONE model and in the field study (left figure) and observed and simulated nitrate concentrations for grassland and silage maize as a function of depth for fields of the Nutter farm, location 28F0472 (right figure). Results for the STONE schematization are indicated by interrupted lines and results for the schematization on the basis of observed OM-contents are given by solid lines.

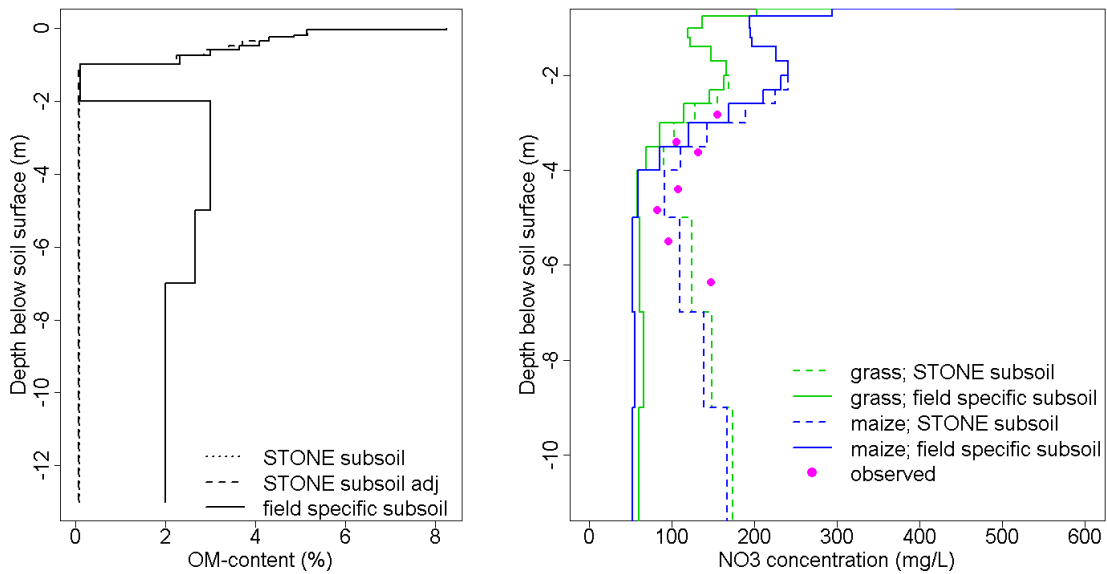


Fig. A6.21 Solid organic matter contents in the regional STONE model and in the field study (left figure) and observed and simulated nitrate concentrations for grassland and silage maize as a function of depth for fields of the Nutter farm, location 28F0473 (right figure). Results for the STONE schematization are indicated by interrupted lines and results for the schematization on the basis of observed OM-contents are given by solid lines.

*Nieuweroord results*

The simulated groundwater levels based on the STONE plots selected as being representative for the fields were higher than the observed levels in three of the four fields of the Nieuweroord farm (Fig. A6.22). After refinement of the rainfall data and calibration of the bottom boundary flux, a decreasing trend is visible in three of the four fields. The time series of the ground water monitoring wells at some distance do not indicate such a trend. Inspection by looking at a longer time series showed that this is due to the choice of the time frame depicted and that the long term time series do not show a decrease.

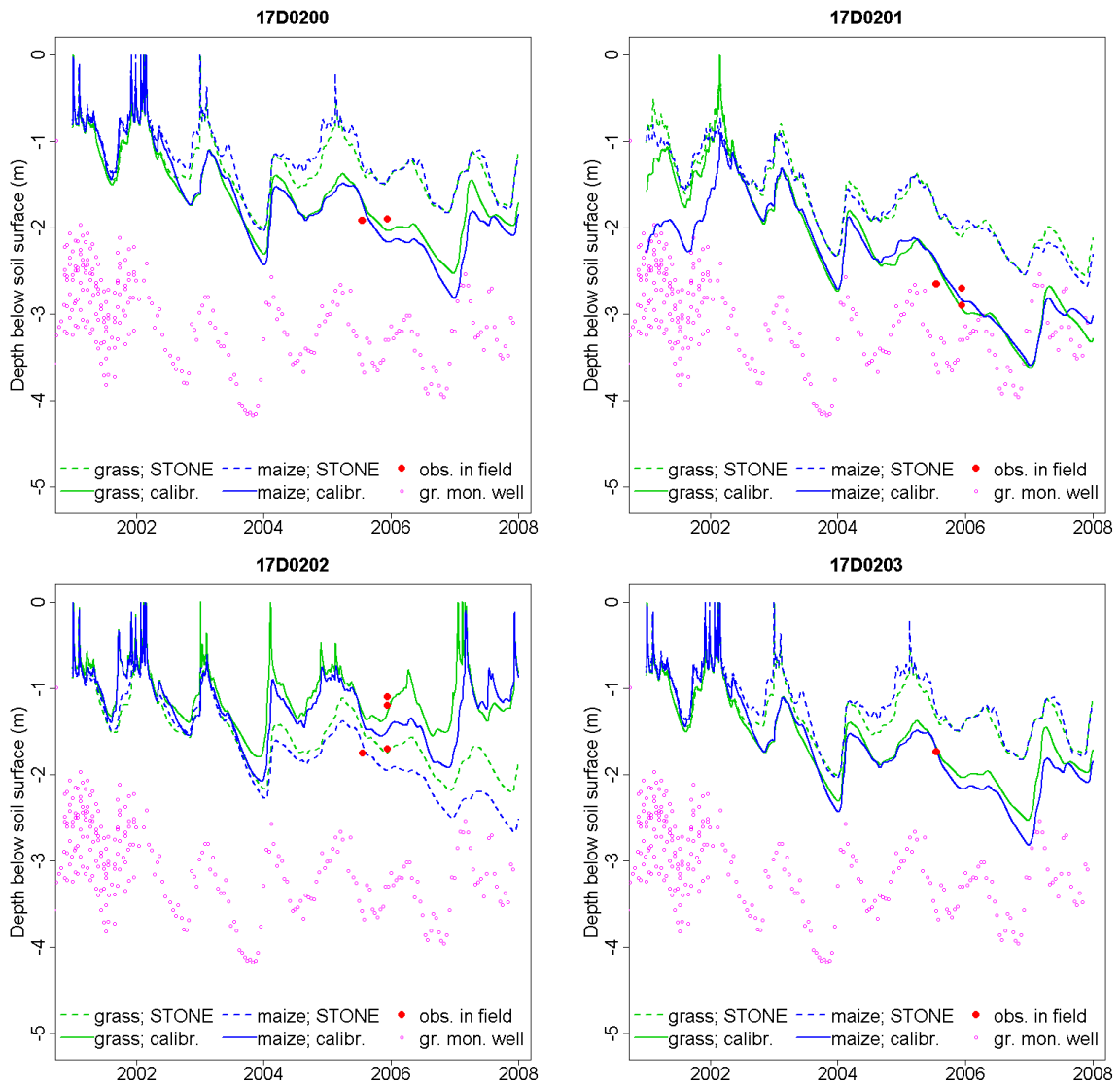


Fig. A6.22 Observed and simulated groundwater levels at the 4 locations of the Nieuweoord farm. The dashed lines represent the non-calibrated SWAP model results and the solid line refers to the calibrated SWAP model results.

The decrease of groundwater levels in the period 2004–2007 manifests itself in the increasing trend of nitrate concentrations (Fig. A6.23). The increasing trend is not visible for the observed farm averaged concentrations. In 2001–2002 some simulated concentrations were lower than the farm averaged observations and other were higher, but in the second part of the simulation period all the simulated concentrations were higher than the observed farm averages.

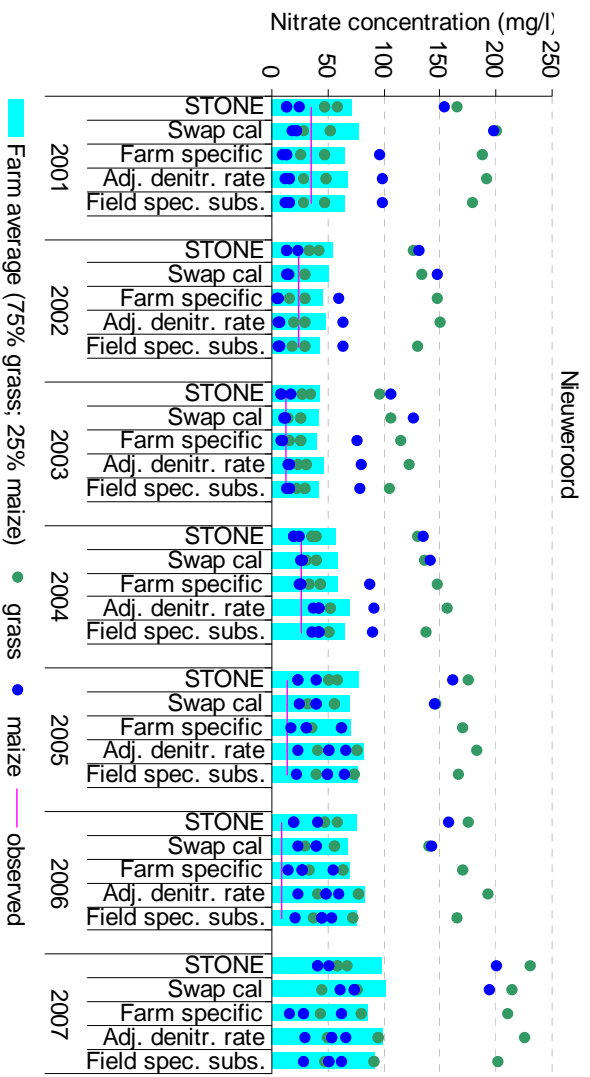


Fig. 16.23 Annual averaged nitrate concentrations at farm level of the Nieuwerwaard farm resulting from successive model adjustments. Green en blue dots are the results of the individual fields.

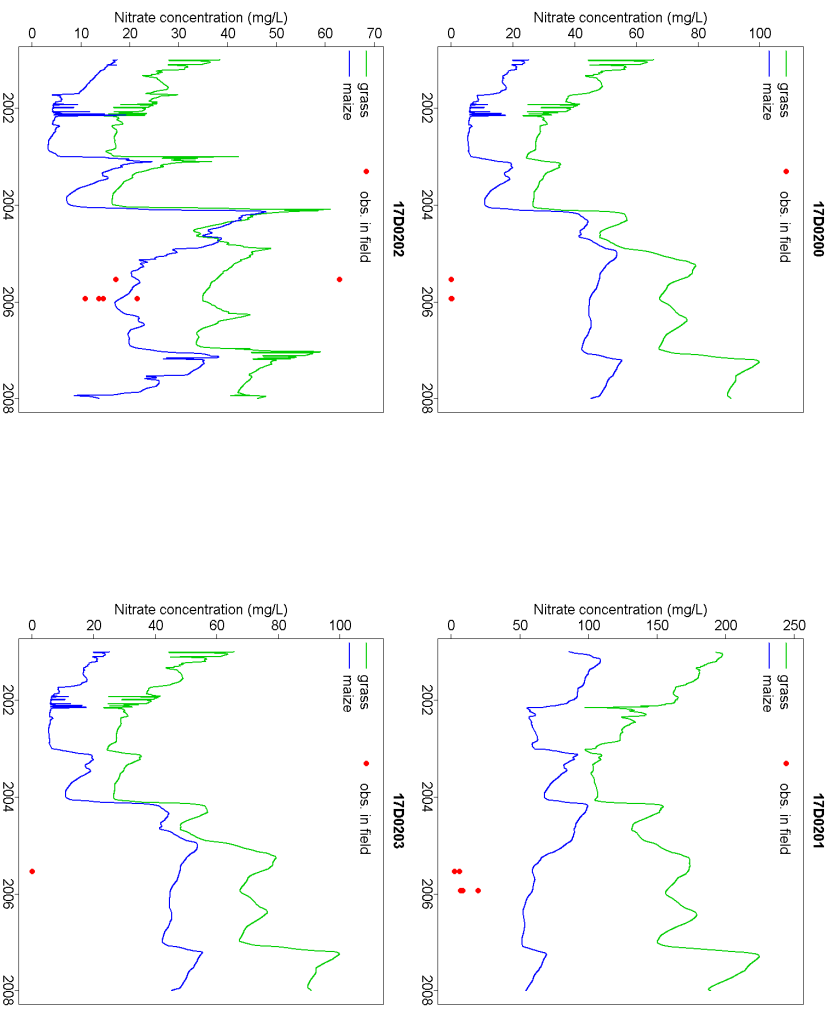


Fig. 16.24 Observed and simulated nitrate concentrations at the four locations of the Nieuwerwaard farm.

The band width of the concentrations is large: the lowest value equals ca. 10 mg l<sup>-1</sup> and the highest is ca. 200 mg l<sup>-1</sup>. The refinement of farm specific input data has the greatest impact on the nitrate simulations for one maize field. The other adaptations have less impact. The hydrology appears to be an important driving force in the behaviour of nitrate concentrations.

Also for the Nieuweoord farm only little field specific nitrate concentrations were available for the evaluation of the model performance at field scale (Fig. A6.24). In all fields the model overestimated the nitrate concentrations of the water samples taken in 2005. The results for maize based on hydrologic and soil conditions of field 17D0202 match quiet well, but for the other combinations the model overestimates the measurements. A relatively large difference between grassland and maize fields appears, due to the difference of nitrogen losses.

*Nieuweoord farm: influence of field specific organic matter contents*

*Nieuweoord 17D0200*

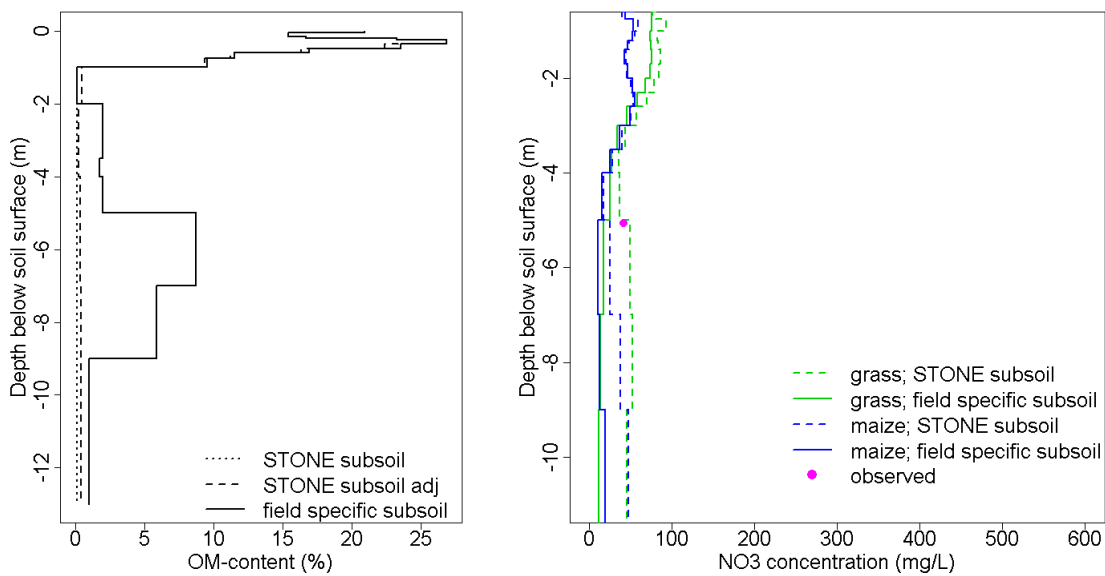


Fig. A6.25 Solid organic matter contents in the regional STONE model and in the field study (left figure) and observed and simulated nitrate concentrations for grassland and silage maize as a function of depth for fields of the Nieuweoord farm, location 17D0200 (right figure). Results for the STONE schematization are indicated by interrupted lines and results for the schematization on the basis of observed OM-contents are given by solid lines.

Nieuweroord 17D0202

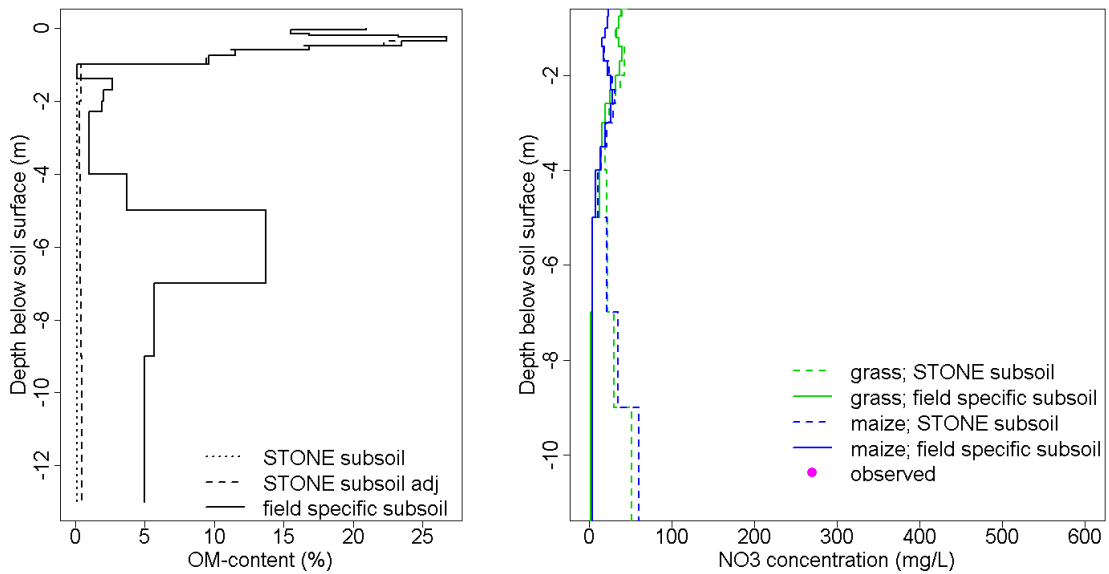


Fig. A6.26 Solid organic matter contents in the regional STONE model and in the field study (left figure) and observed and simulated nitrate concentrations for grassland and silage maize as a function of depth for fields of the Nieuweroord farm, location 17D0202 (right figure). Results for the STONE schematization are indicated by interrupted lines and results for the schematization on the basis of observed OM-contents are given by solid lines.

Nieuweroord 17D0203

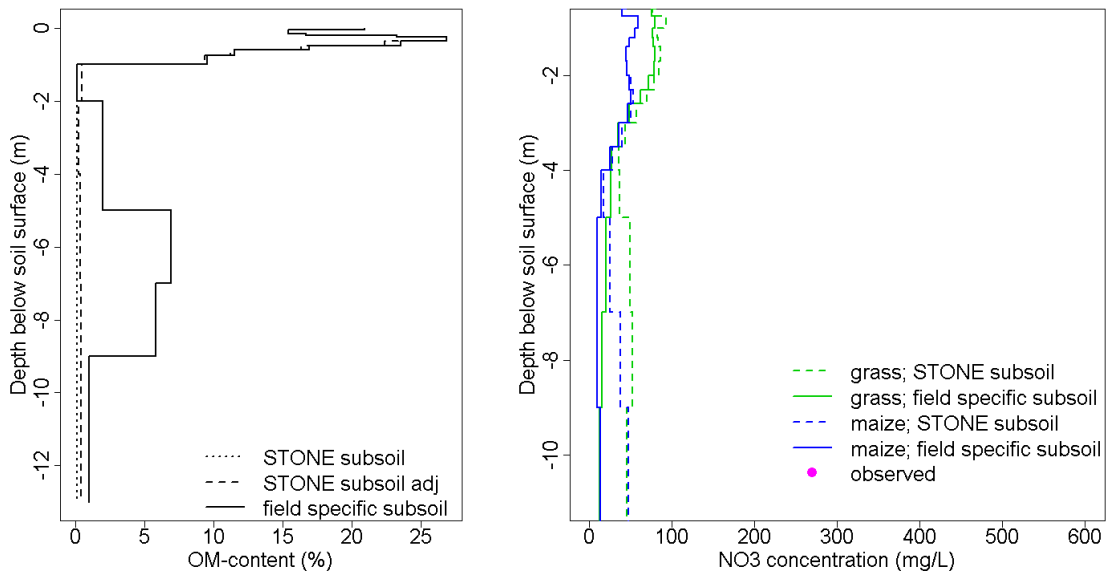


Fig. A6.27 Solid organic matter contents in the regional STONE model and in the field study (left figure) and observed and simulated nitrate concentrations for grassland and silage maize as a function of depth for fields of the Nieuweroord farm, location 17D0203 (right figure). Results for the STONE schematization are indicated by interrupted lines and results for the schematization on the basis of observed OM-contents are given by solid lines.

## A6.4 Synthesis

The rainfall data was refined in the hydrological simulations and the bottom boundary condition was calibrated on scarce groundwater observations. This resulted in an agreement between simulated and observed groundwater levels, but also in an apparent decreasing trend in some fields of the Spankeren, Nutter and Nieuweroord farm. Inspection of groundwater results over a longer period revealed that the decrease is not a real trend but is due to the succession of relative dry years in 2004–2007. The response to the dry conditions is overestimated, which can be due to an imbalance between the drainage relation and the bottom boundary condition. The hydrological simulations are considered as sub-optimal with respect to the performance evaluation of the leaching model. The apparent decreasing trend of the simulated groundwater levels affects the nitrate concentrations.

Although the STONE information with respect to rainfall and fertilization was refined and the groundwater levels were calibrated on a few data, the parameterization of the ANIMO as such was not adjusted. After the refinement, no calibration was performed to remain close to the original STONE model. The results of the ANIMO model appeared to overestimate the nitrate concentration for one of the four fields of Maarheeze, two of the four fields of the Spankeren and the Nutter farm and three of the four field of the Nieuweroord farm.

The evaluation of the model performance is difficult due to the scarce data availability. Only some data on groundwater levels and nitrate concentrations were available for a few dates. Groundwater levels and nitrate concentrations can fluctuate to some extent within a month and it should be realized that the choice of the sampling dates influence the results of the field campaign.

The adjustments of the model input had only a minor impact on the simulated nitrate concentrations (Fig. A6.5; A6.11; A6.17; A6.23). The position of the groundwater level (dry, moderate or wet) has a larger influence just as the initial amounts of mineral and organic nitrogen in the soil. The attribution to the different organic pools also affects the nitrate concentrations. The access to historic land management data at field will improve the estimates for the pools mentioned and will contribute to a better model performance.

The trend in the nitrate concentrations as depicted in Fig. A6.6, A6.12, A6.18 and A6.24 is mainly a response to the fertilization rates assumed and the courses with time of the fertilization rate. Information on the fertilization rates is only available at farm scale and assumption had to be made for the attribution to the individual fields.

The comparison of annual averaged prediction results with occasional observations may lead to a mismatch. Field observations with a higher time resolution can support a better

understanding of similarities and differences between predictions and observations. The variability of the predicted concentrations at field scale is large. For the interpretation of farm scale averaged concentrations for model validation studies, accurate information on the land management practice and history, the soils and the hydrological regimes of each of the fields is required.

The weak validation results for the nitrate concentrations in the upper meter at field scale do not restrain the model application at regional scale, due to a large number of uncertainties involved in this study. This conclusion is supported by the predicted nitrate concentrations at greater depth.

## Appendix 7 Flux averaged nitrate concentrations in groundwater

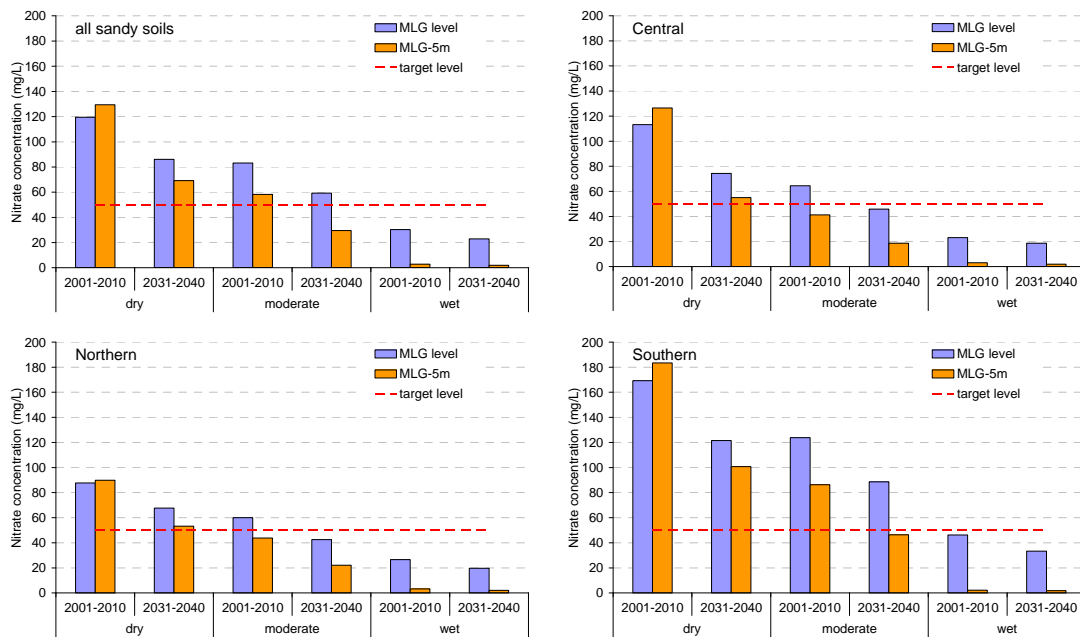


Fig. A7.1 Flux weighted nitrate concentrations at MLG depth and 5m below MLG depth for two periods, three groundwater classes and for the main sand districts

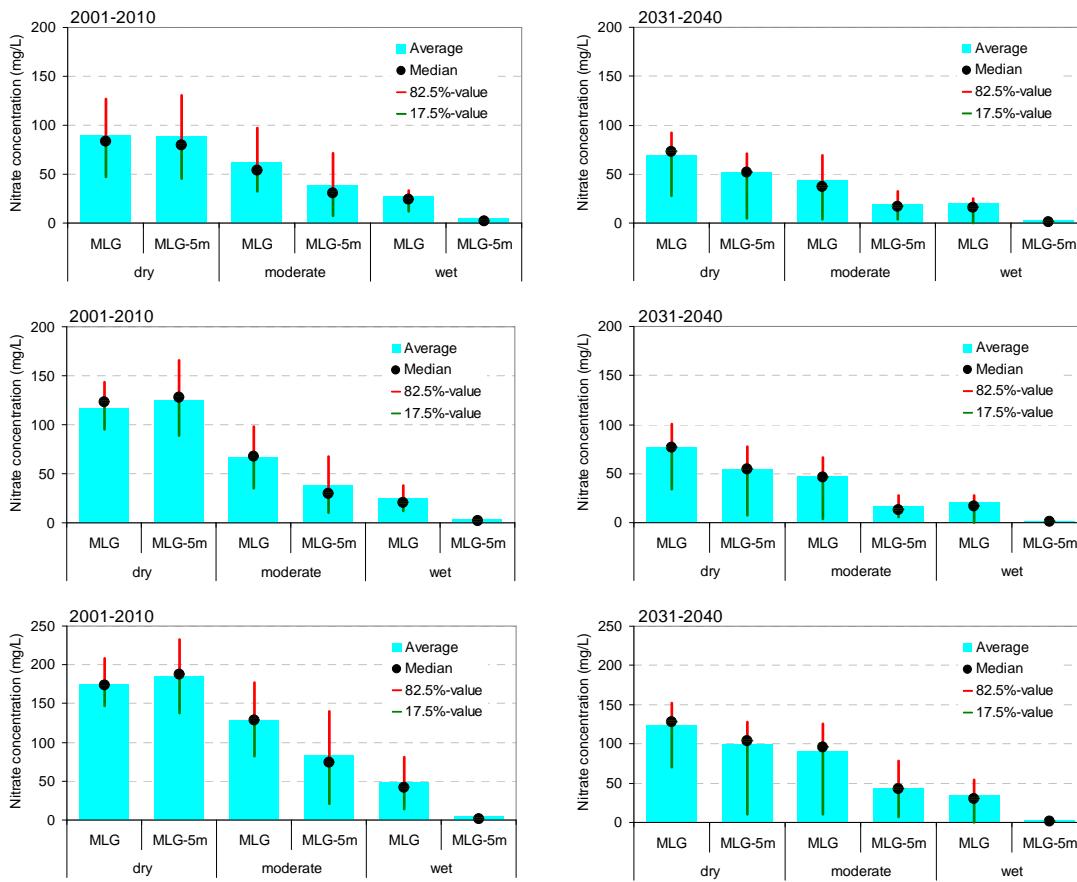


Fig. A7.2 Statistical properties of the flux weighted nitrate concentrations at MLG depth and 5m below MLG depth for two periods, three groundwater classes and for the Northern sand district

## Appendix 8 Time patterns of flux averaged concentrations

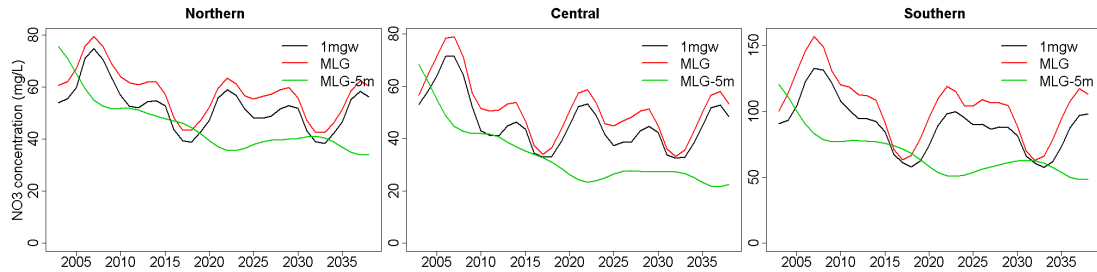


Fig. A8.1 Five-year advancing averaged nitrate concentration in the 1<sup>st</sup> meter below a fluctuating groundwater level, at the mean lowest groundwater level (MLG) and at 5 meter below the mean lowest groundwater level (MLG-5m) in the Northern, Central and Southern sand district.



Fig. A8.2 Five-year advancing averaged nitrate concentration in the 1<sup>st</sup> meter below a fluctuating groundwater level (1mgw), at the mean lowest groundwater level (MLG) and at 5 meter below the mean lowest groundwater level (MLG-5m) in dry, moderate and wet soils of the Northern, Central and Southern sand district

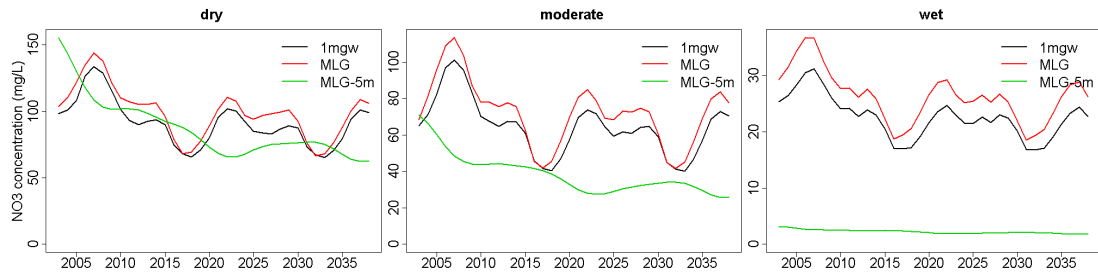


Fig. A8.3 Five-year advancing averaged nitrate concentration in the 1<sup>st</sup> meter below a fluctuating groundwater level (1mgw), at the mean lowest groundwater level (MLG) and at 5 meter below the mean lowest groundwater level (MLG-5m) in dry, moderate and wet sandy soils.

## Appendix 9 Total-N and nitrate -transport to surface waters per sand district

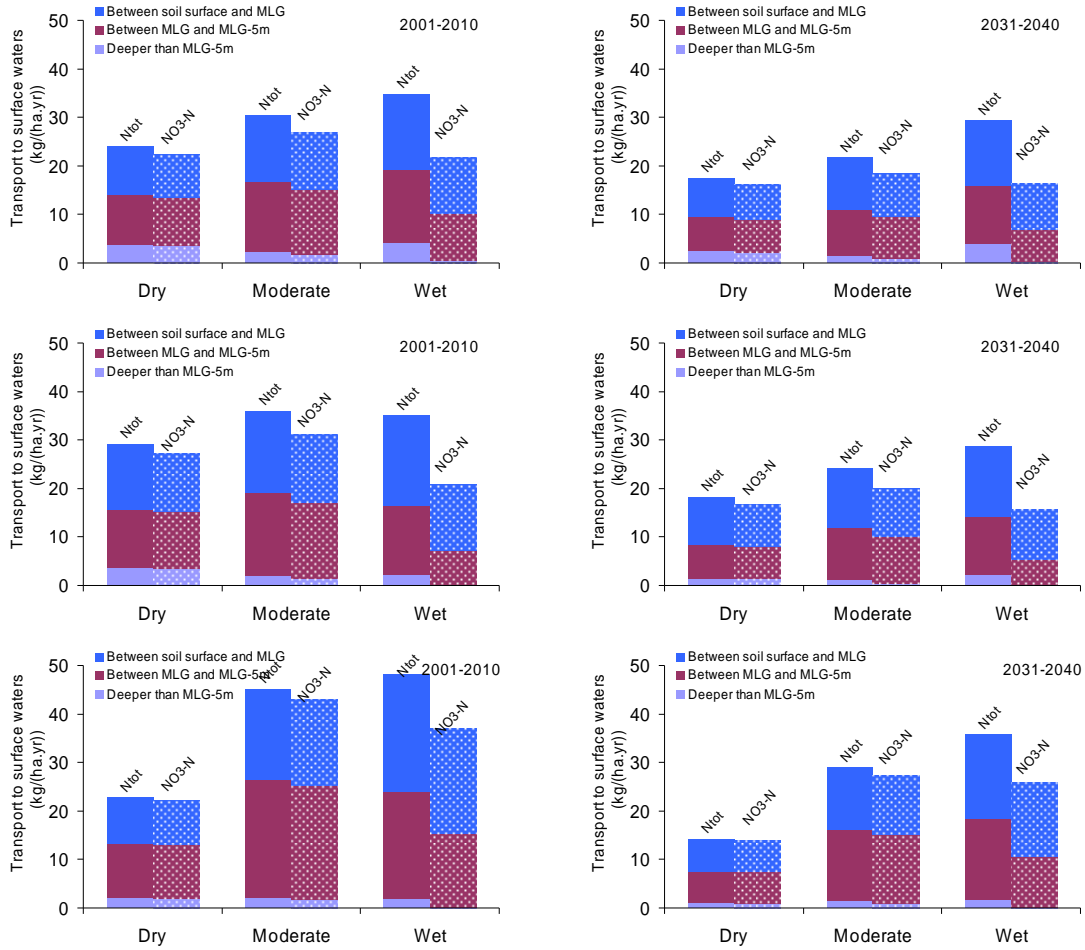


Fig. A9.1 Total-N and nitrate-N transport to surface water from three soil layers in the Northern (top), Central (middle) and Southern (bottom) sand district for three groundwater classes and for two periods

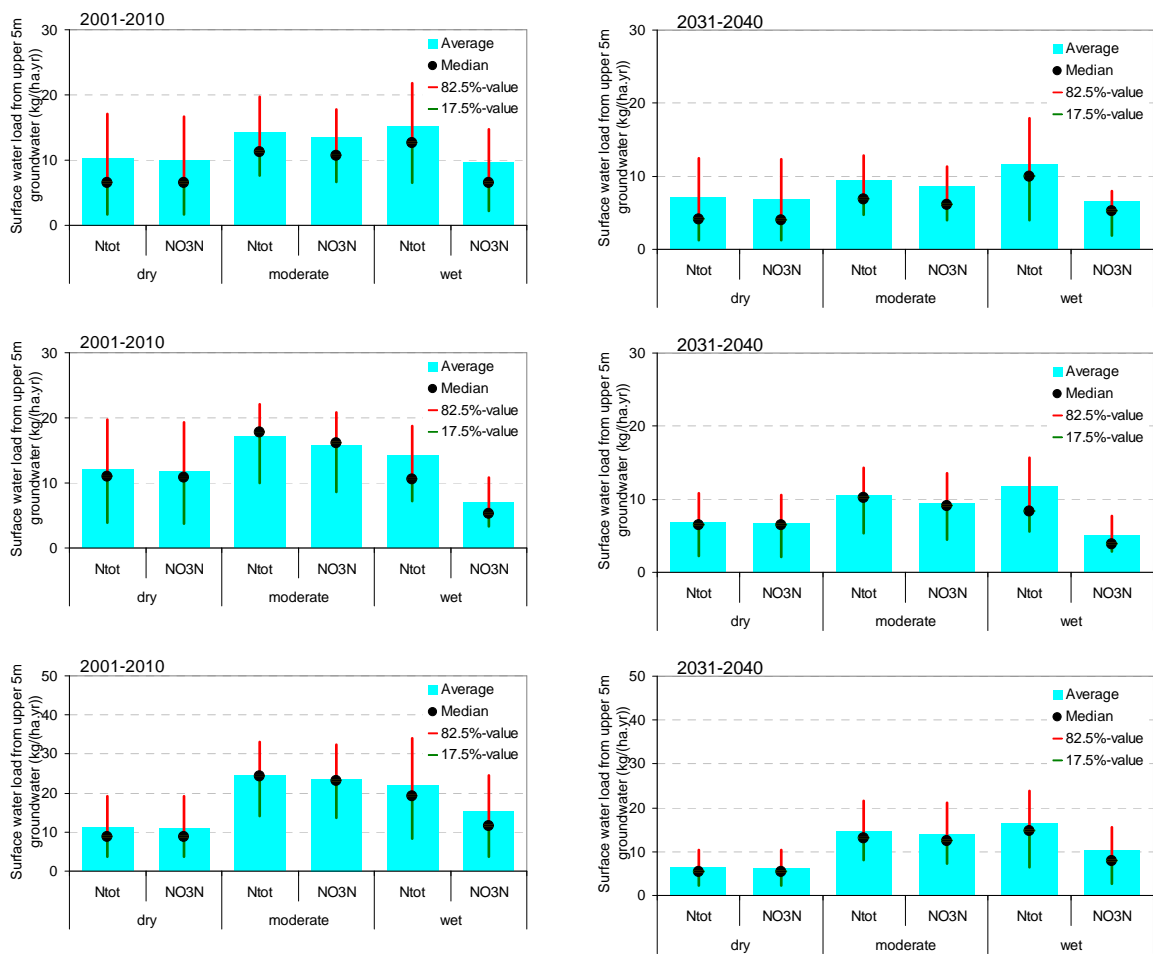


Fig. A9.2 Statistical properties of the total-N and nitrate-N transport to surface waters from the layer between MLG depth and 5m below MLG depth for two periods, three groundwater classes and for the Northern (top), Central (middle) and Southern (bottom) sand district

## Appendix 10 Actual and potential denitrification in groundwater

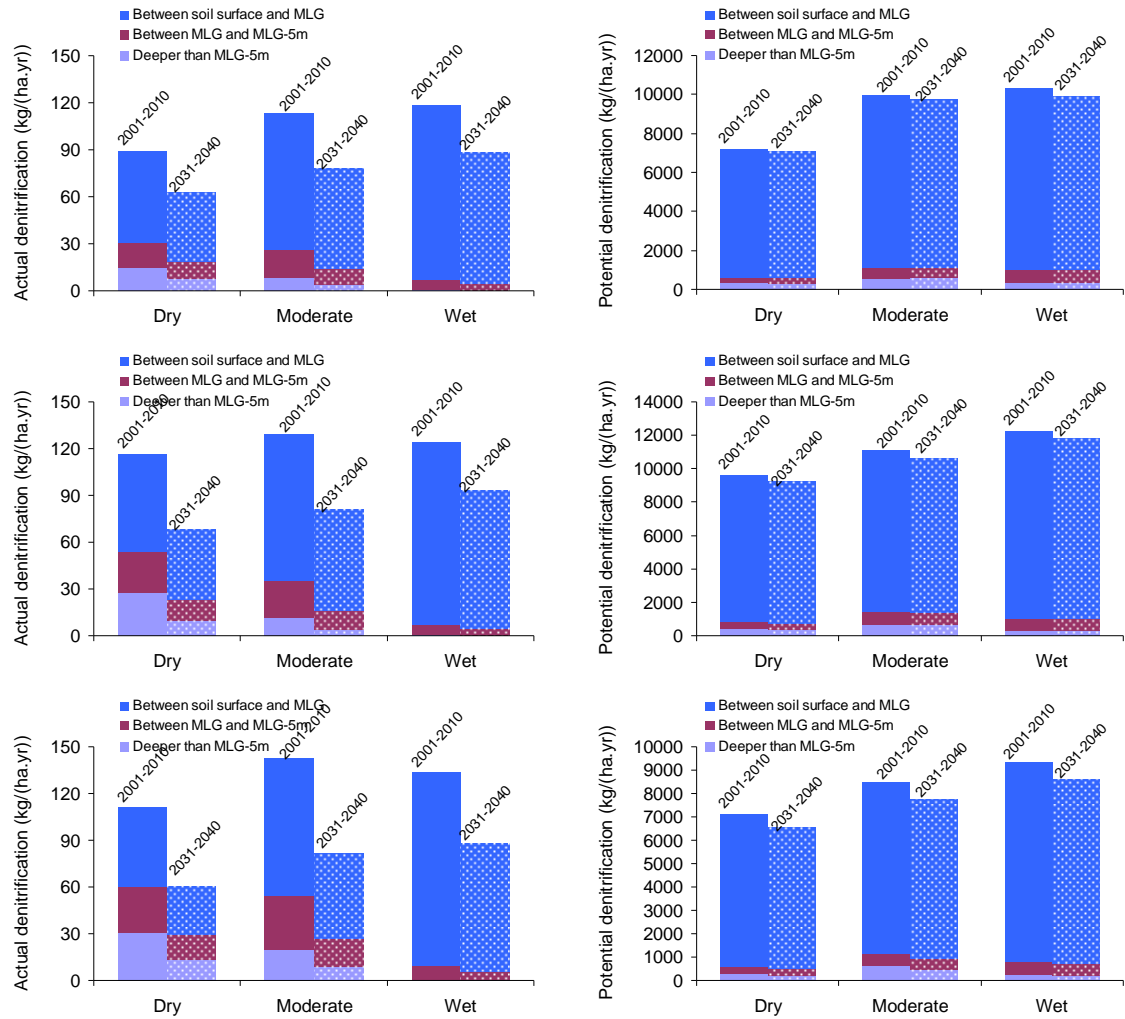


Fig. A10.1 Actual denitrification (left) and potential denitrification (right) in the distinguished soil layers for two periods and for three groundwater classes in the Northern (top), Central (middle) and Southern (bottom) sand district

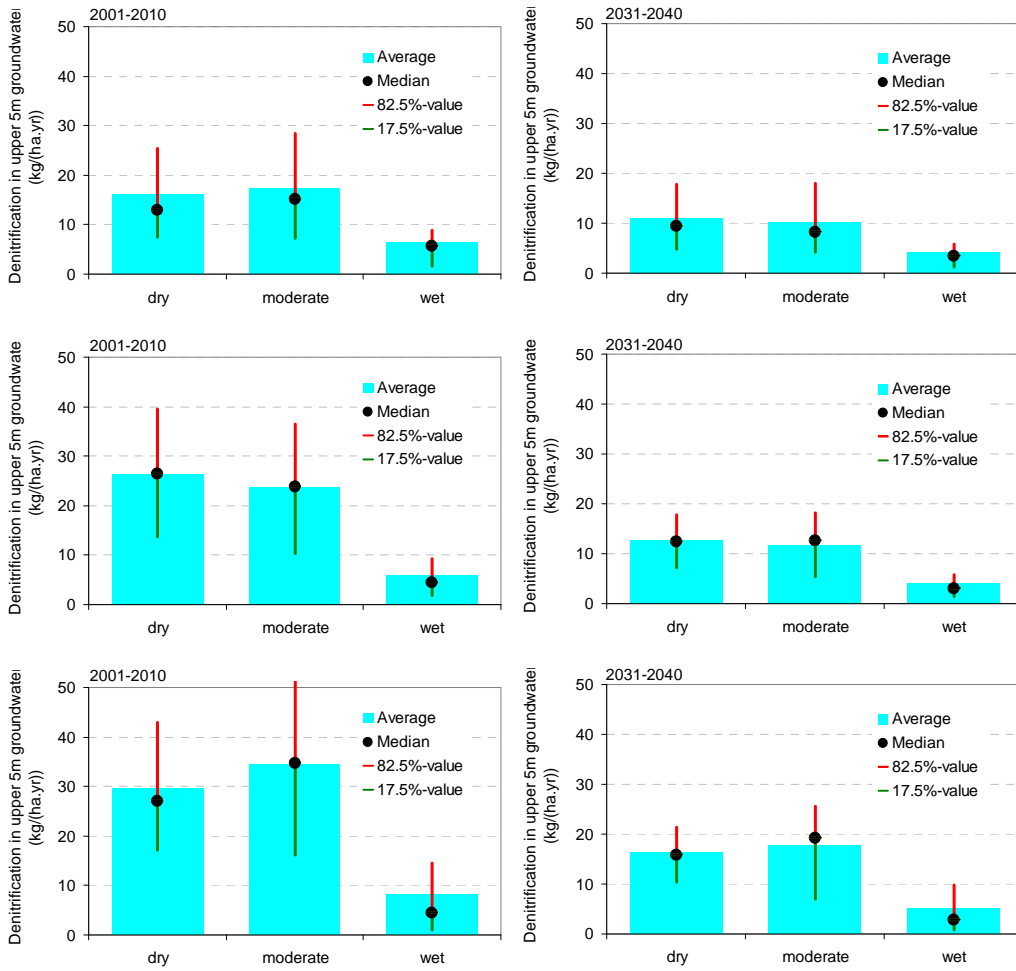


Fig. A10.2 Statistical properties of the denitrification in the layer between MLG depth and 5m below MLG depth for two periods, three groundwater classes and for the Northern (top), Central (middle) and Southern (bottom) sand district

# Appendix 11 Schematic representation of total N and nitrate balances per region and/or per groundwater class

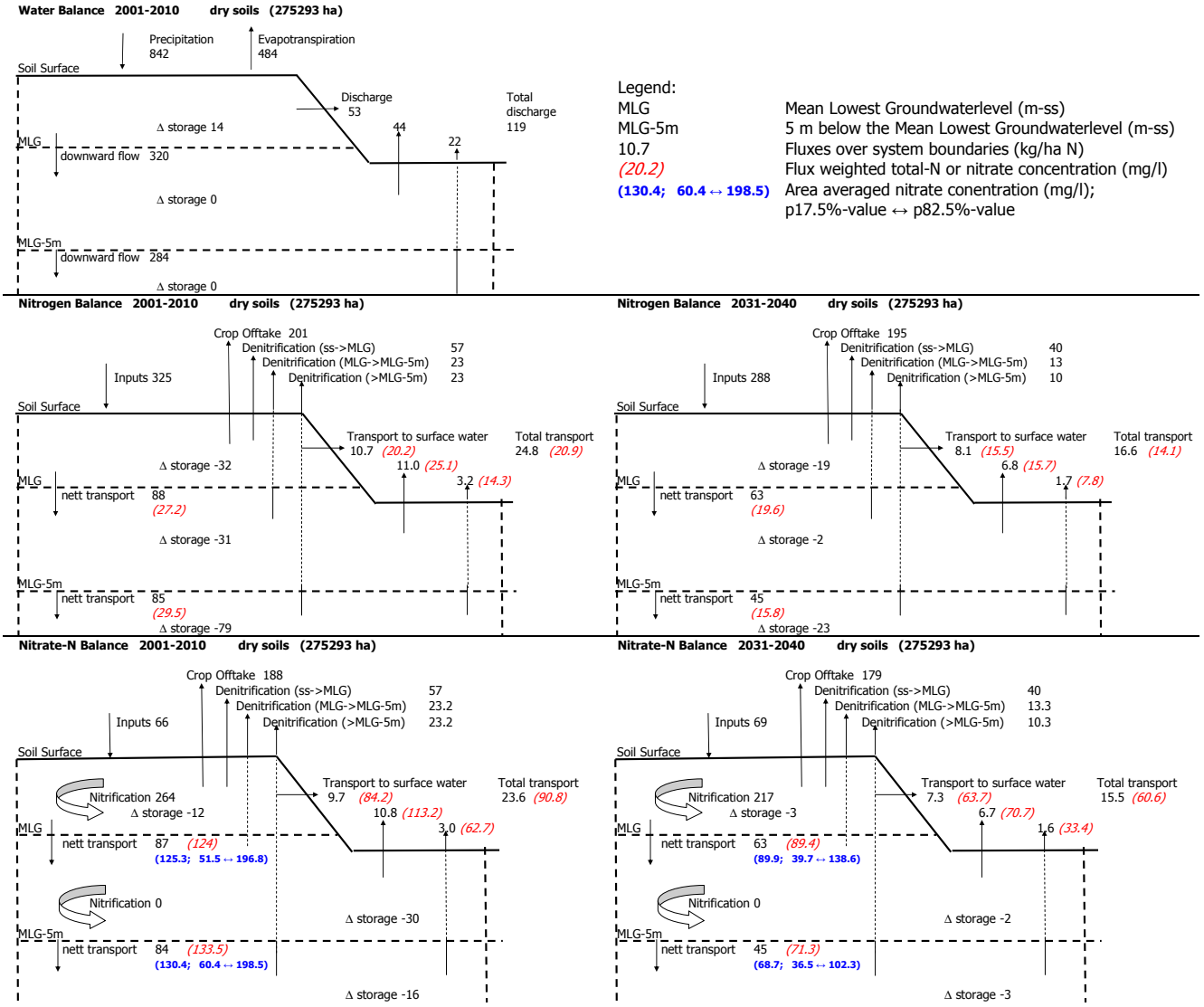


Fig. A11.1 Balances of water, total-N and nitrate for dry sandy soils

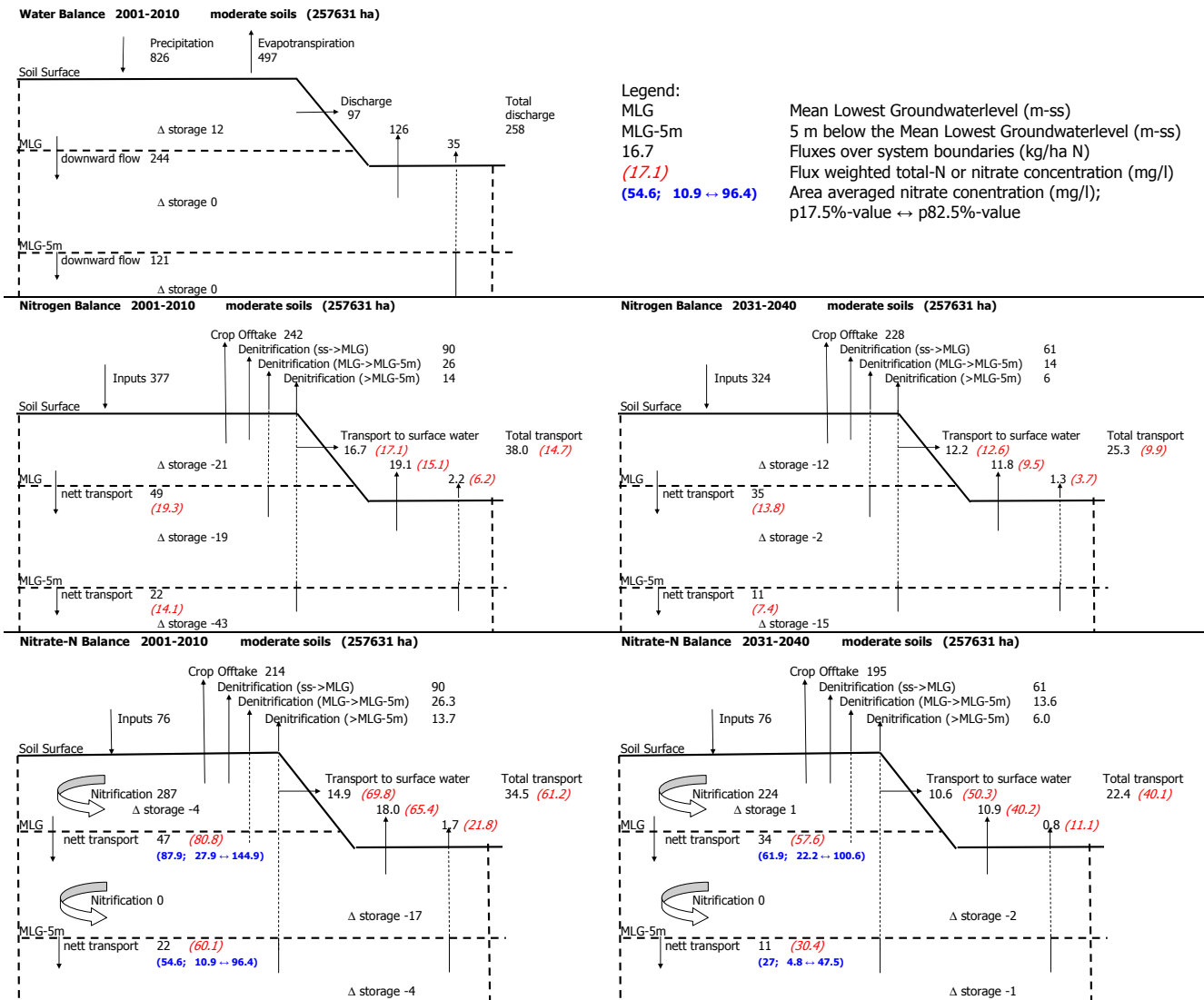


Fig. A11.2 Balances of water, total-N and nitrate for moderate sandy soils

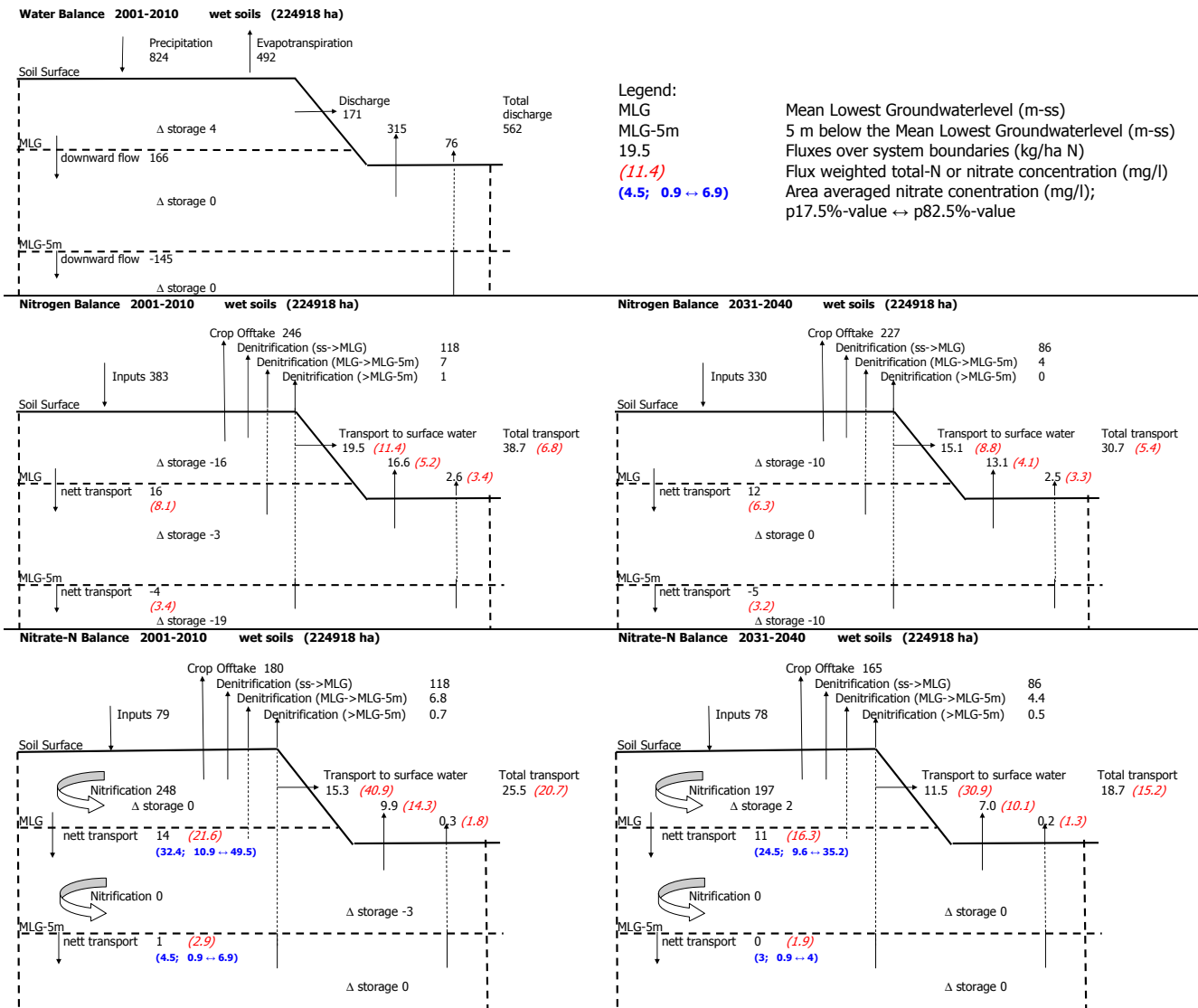


Fig. A11.3 Balances of water, total-N and nitrate for wet sandy soils

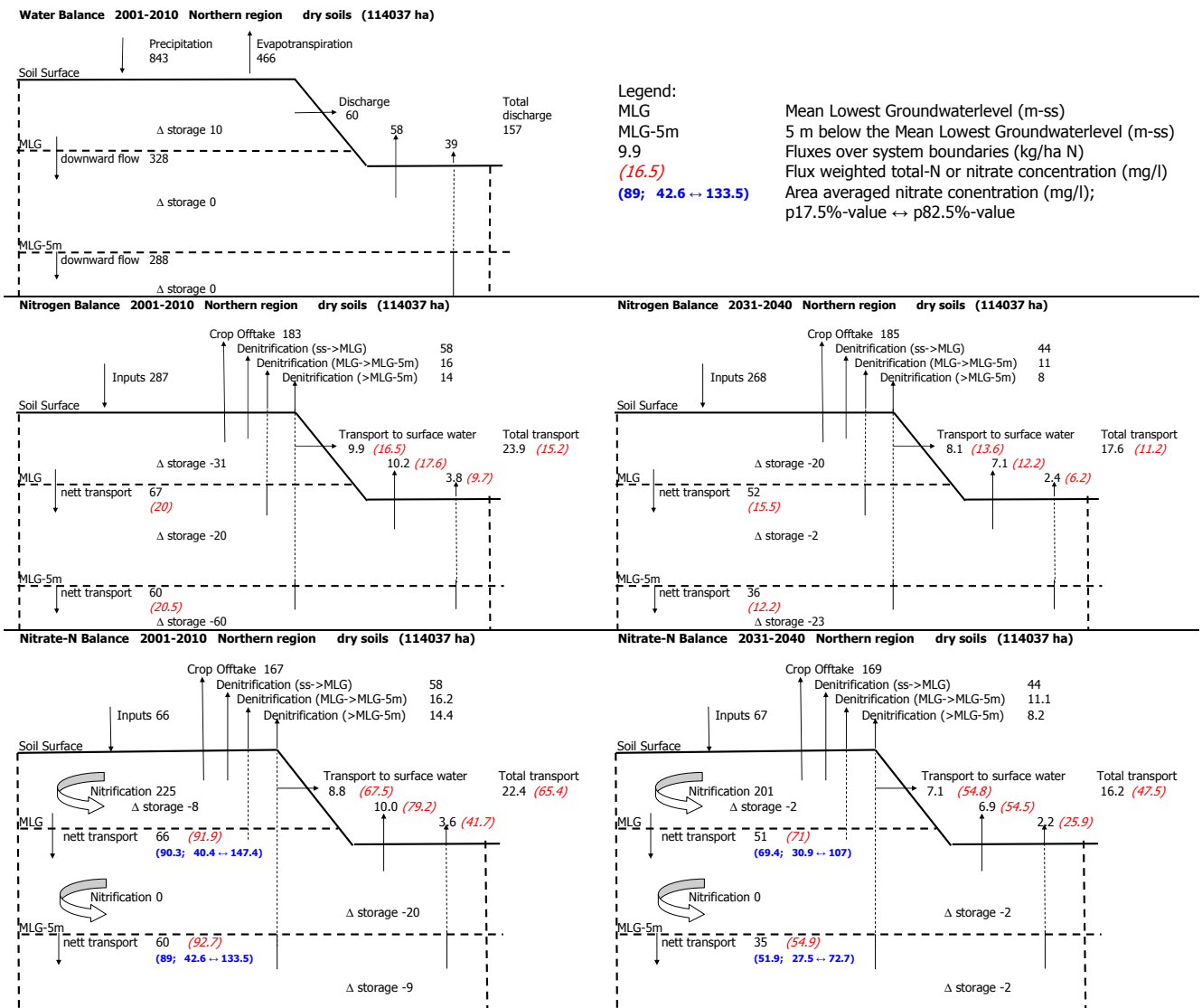


Fig. A11.4 Water, total-N and nitrate balances of dry soils in the Northern sand district for two periods

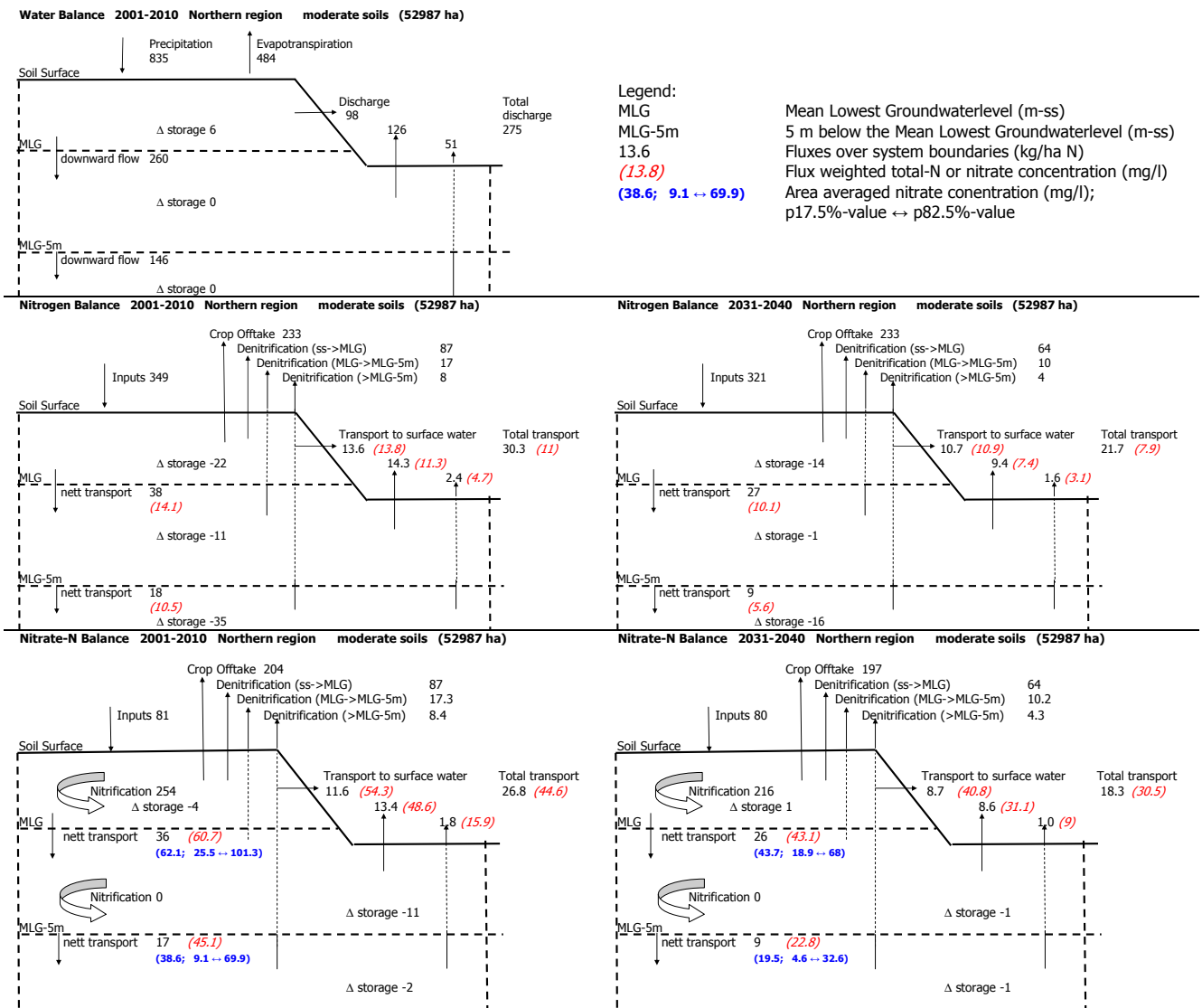


Fig. A11.5 Water, total-N and nitrate balances of moderate soils in the Northern sand district for two periods

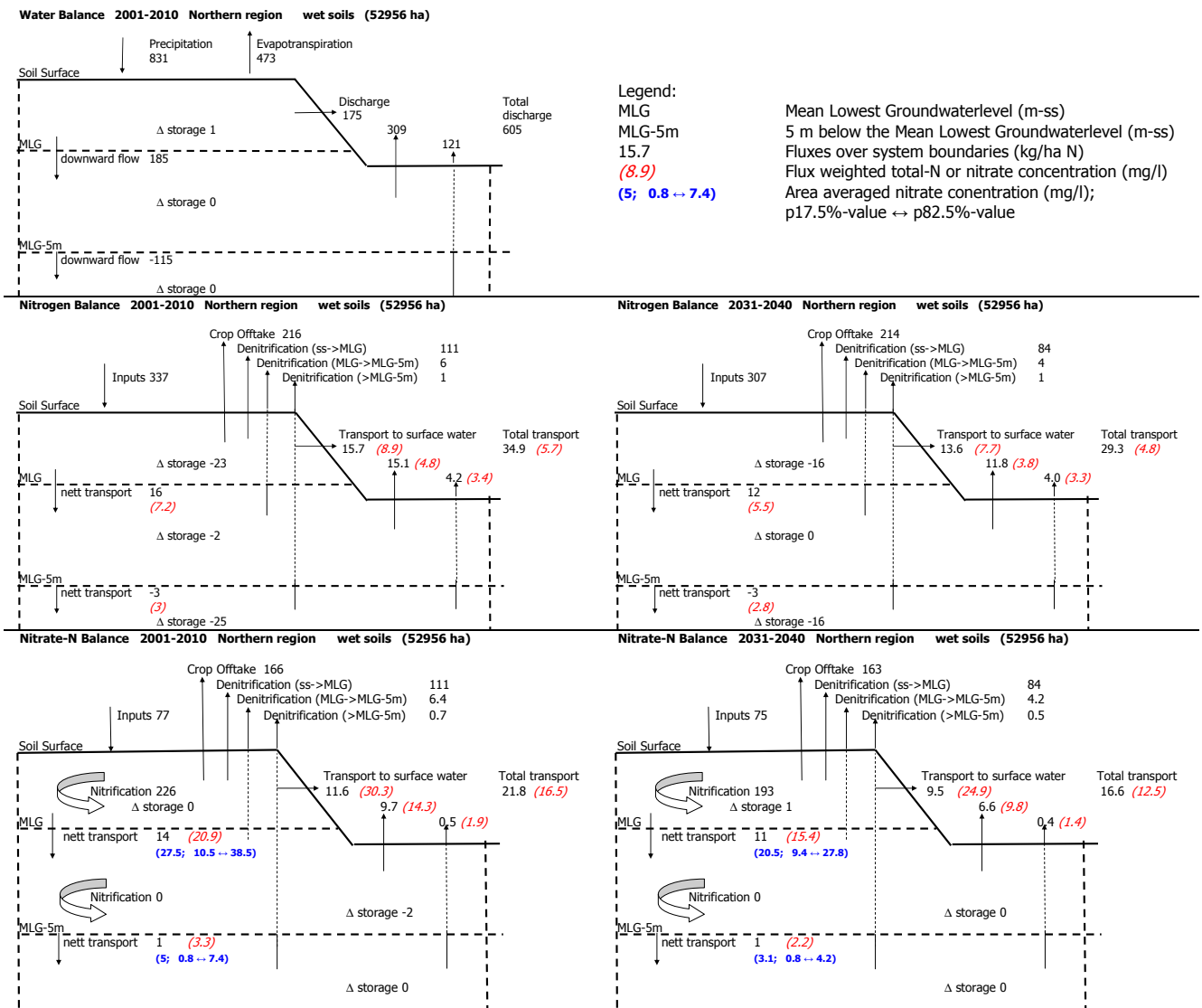


Fig. A11.6 Water, total-N and nitrate balances of wet soils in the Northern sand district for two periods

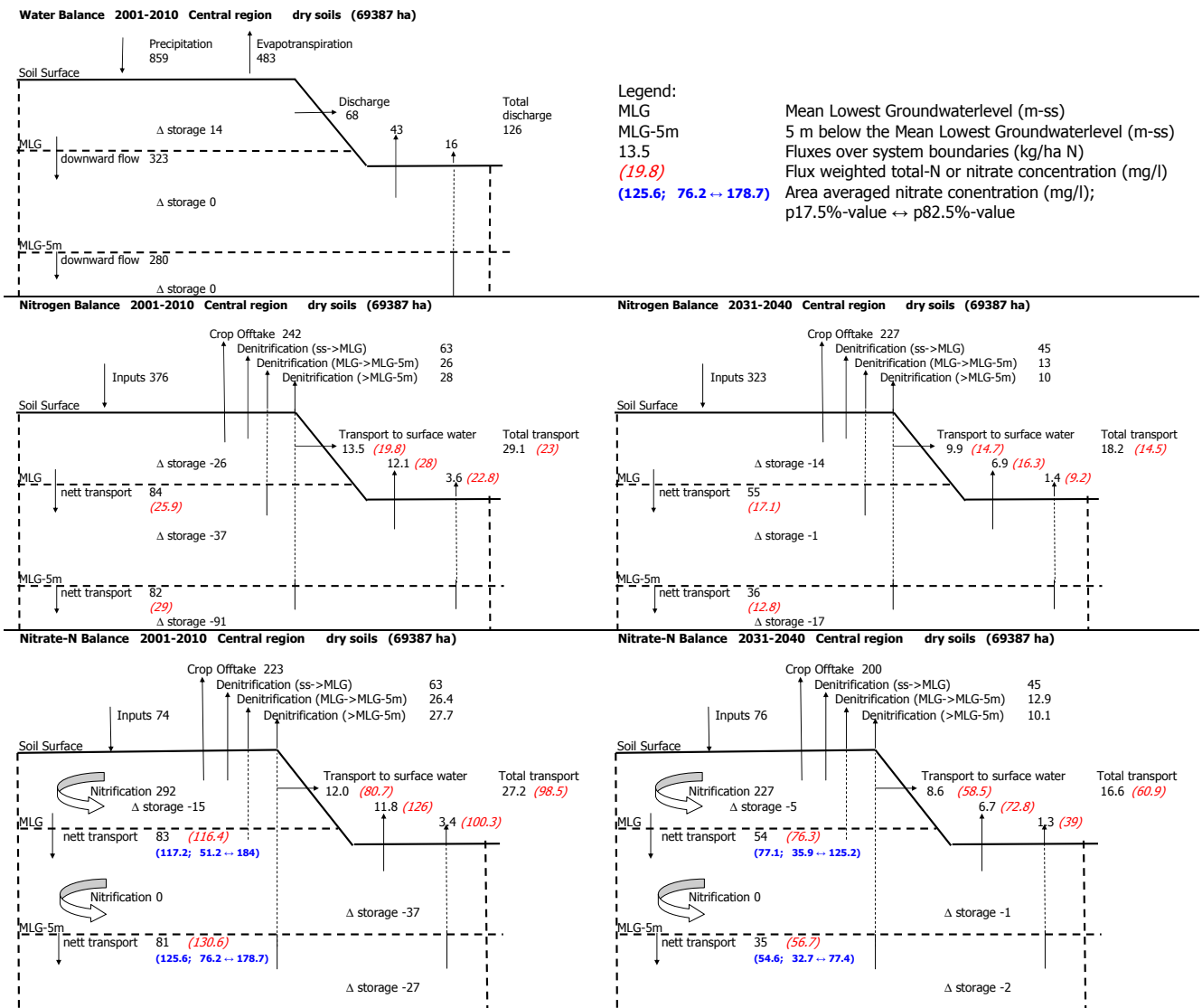


Fig. A11.7 Water, total-N and nitrate balances of dry soils in the Central sand district for two periods

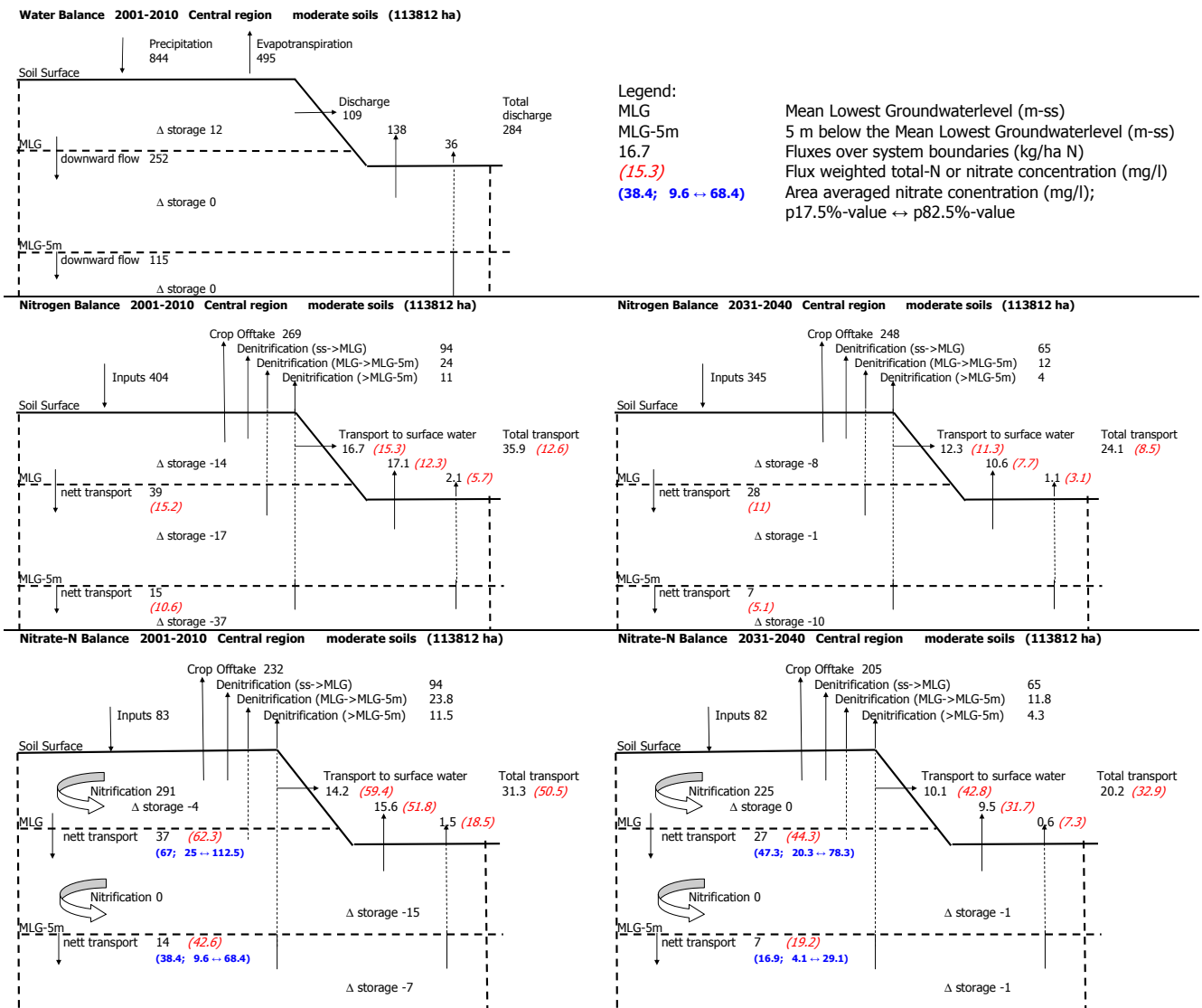


Fig. A11.8 Water, total-N and nitrate balances of moderate soils in the Central sand district for two periods

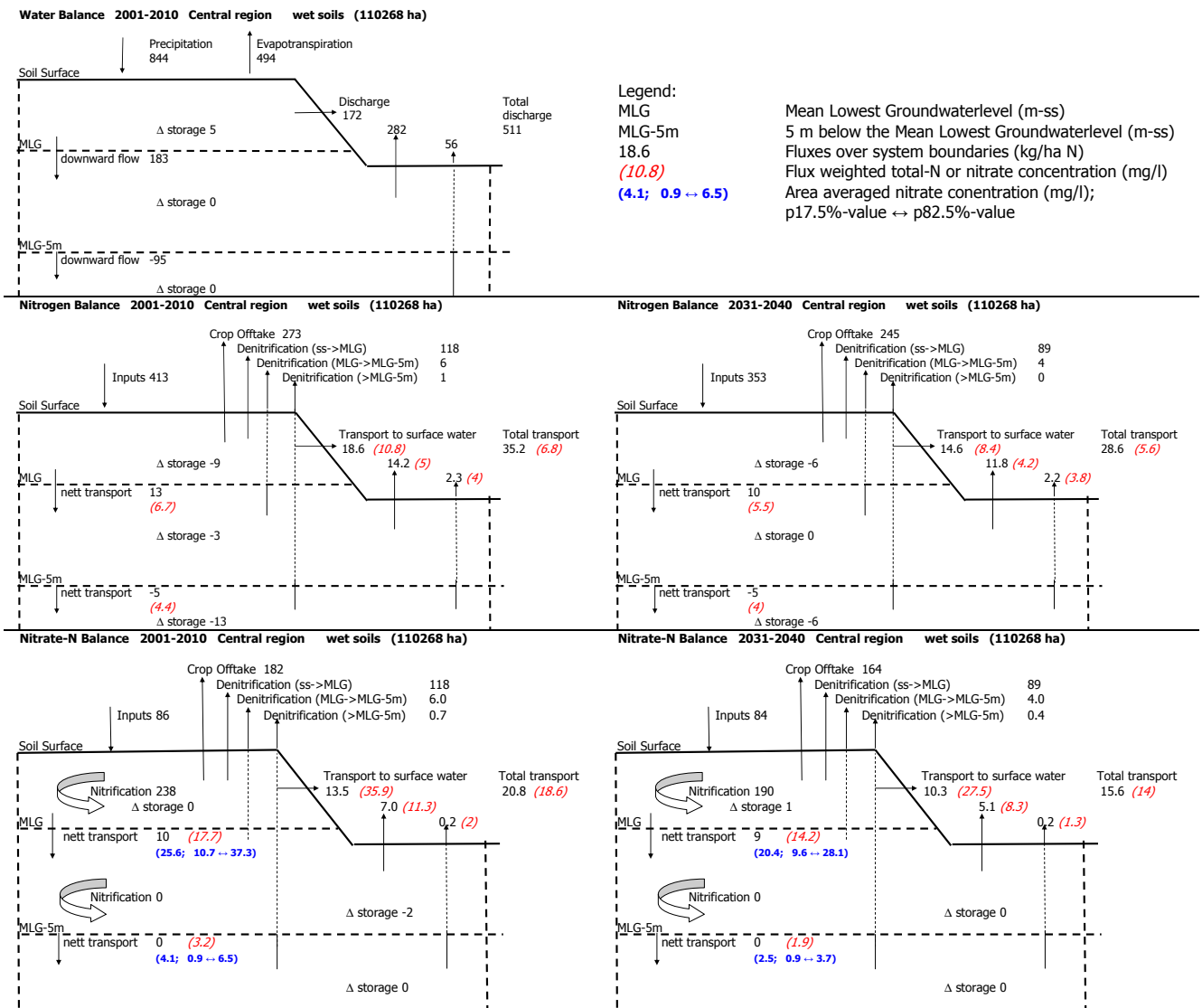


Fig. A11.9 Water, total-N and nitrate balances of wet soils in the Central sand district for two periods

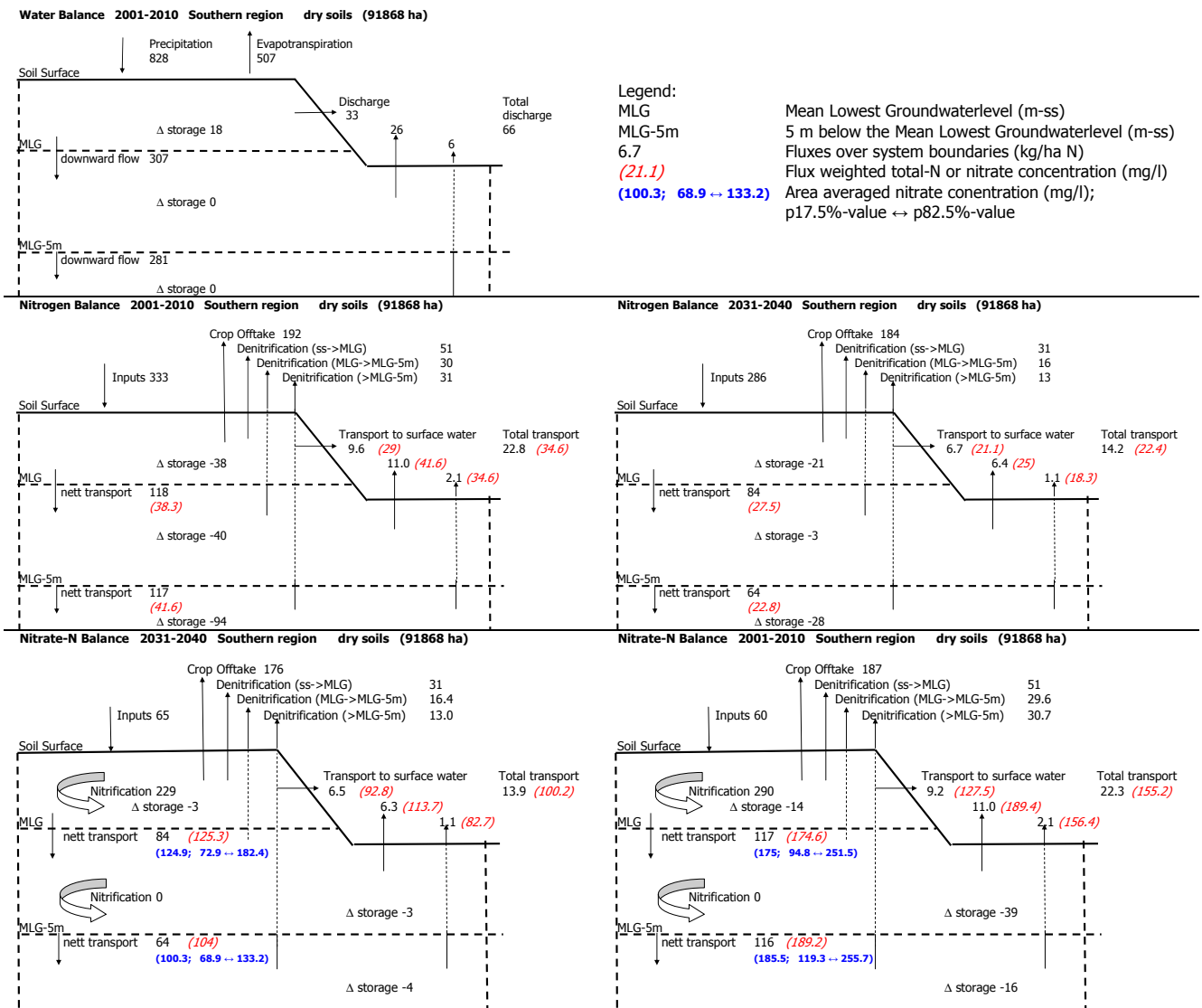


Fig. A11.10 Water, total-N and nitrate balances of dry soils in the Southern sand district for two periods

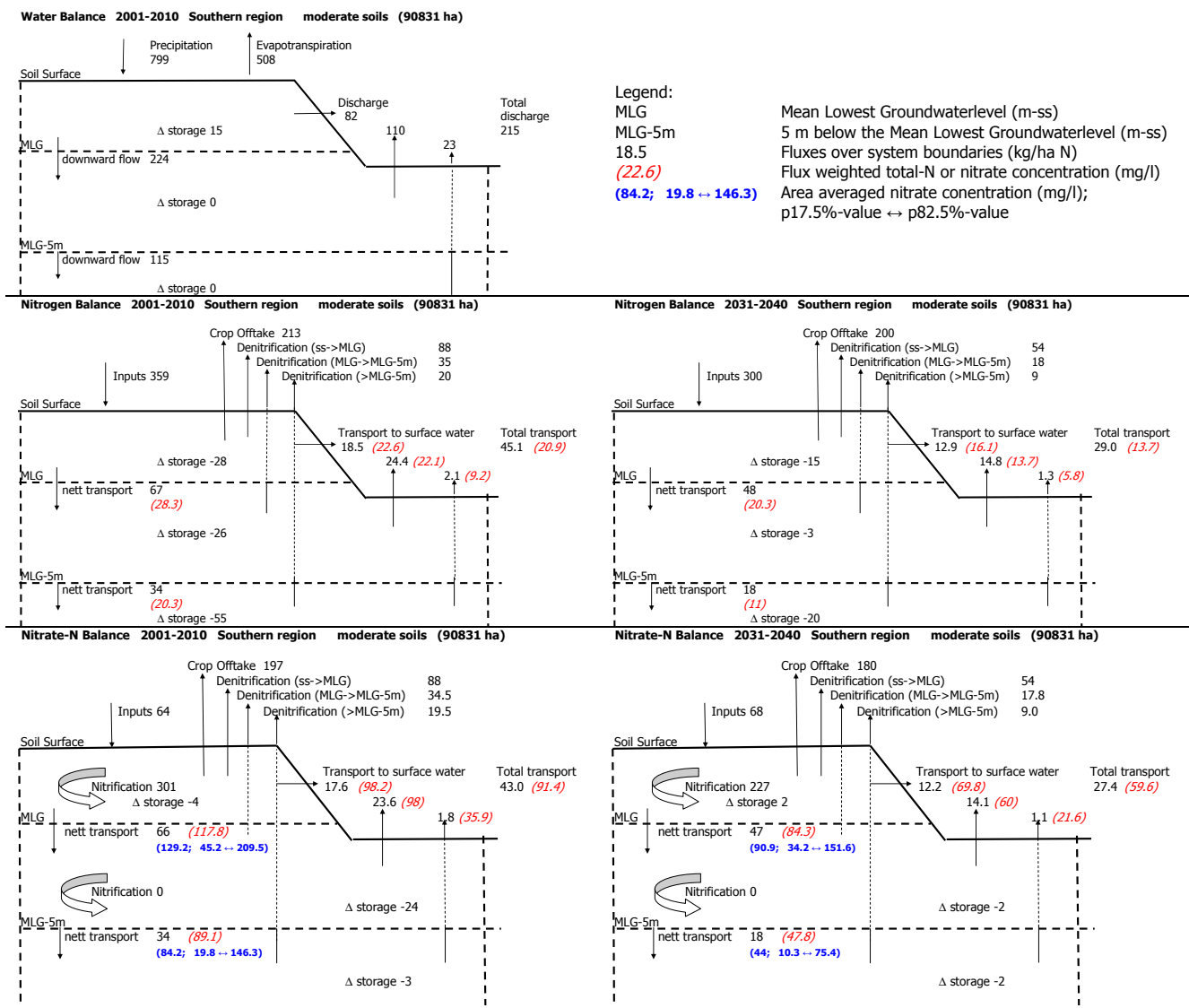


Fig. A11.11 Water, total-N and nitrate balances of moderate soils in the Southern sand district for two periods

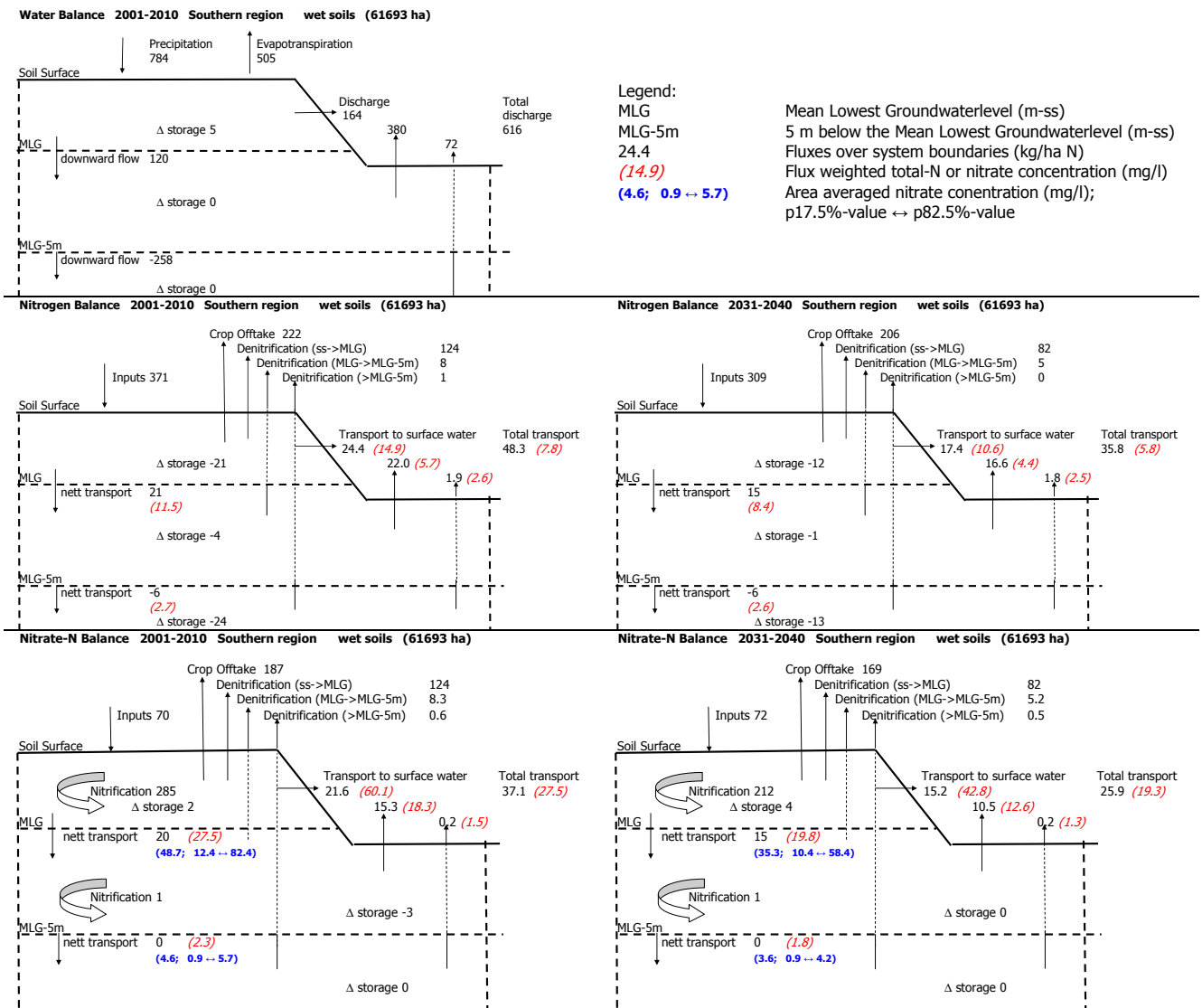


Fig. A11.12 Water, total-N and nitrate balances of wet soils in the Southern sand district for two periods

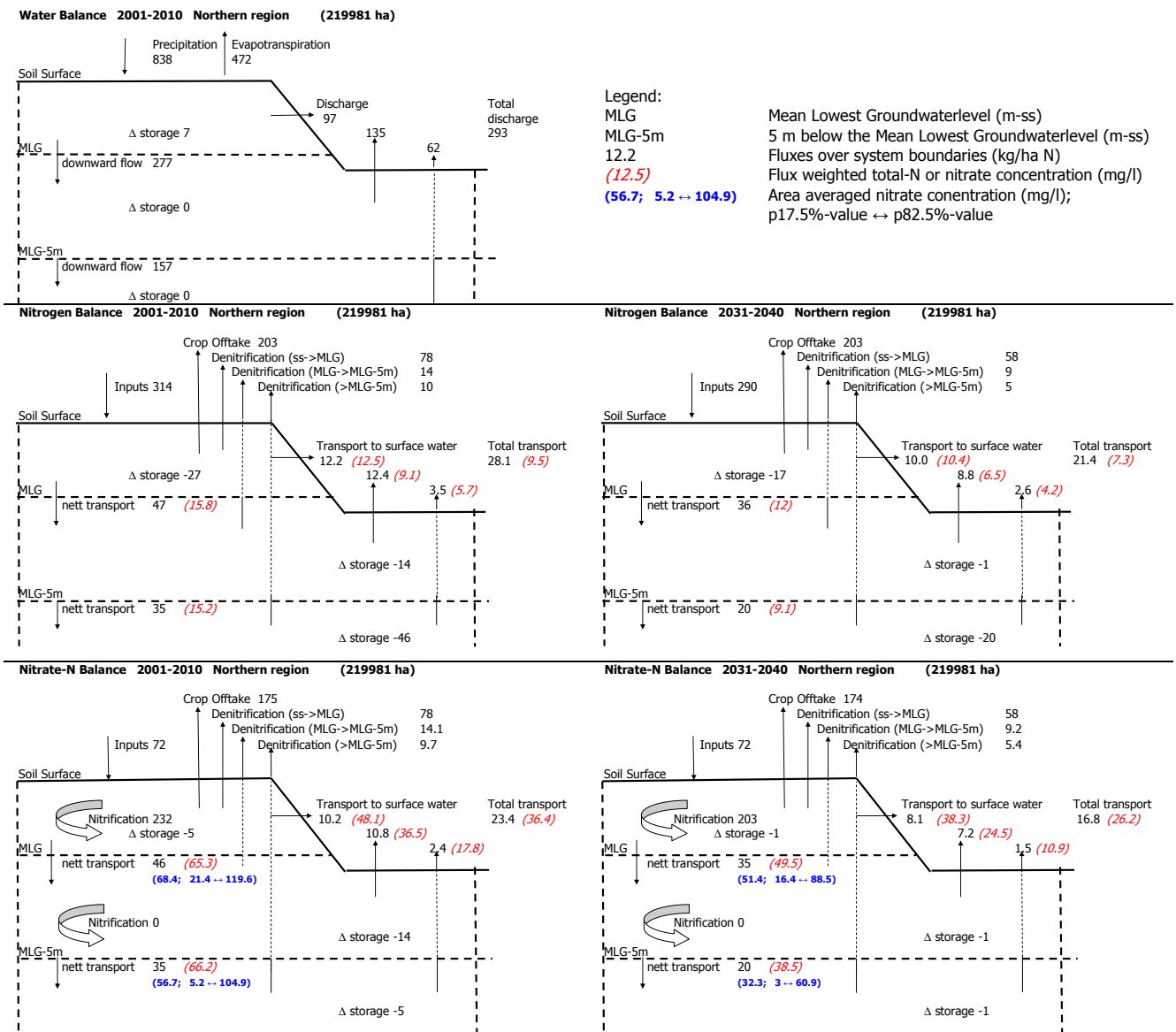


Fig. A11.13 Water, total-N and nitrate balances of all sandy soils in the Northern district for two periods

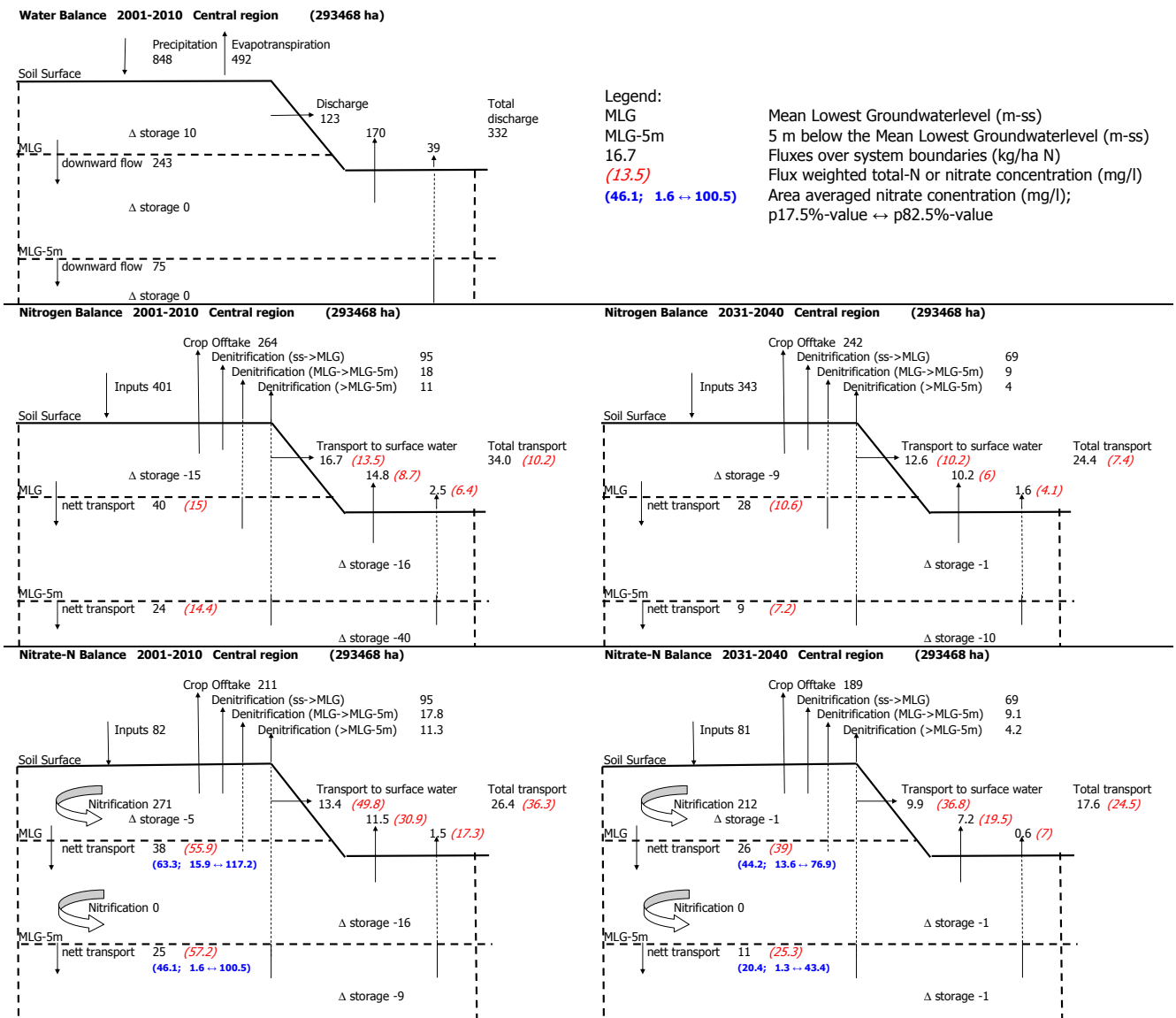


Fig. A11.14 Water, total-N and nitrate balances of all sandy soils in the Central district for two periods

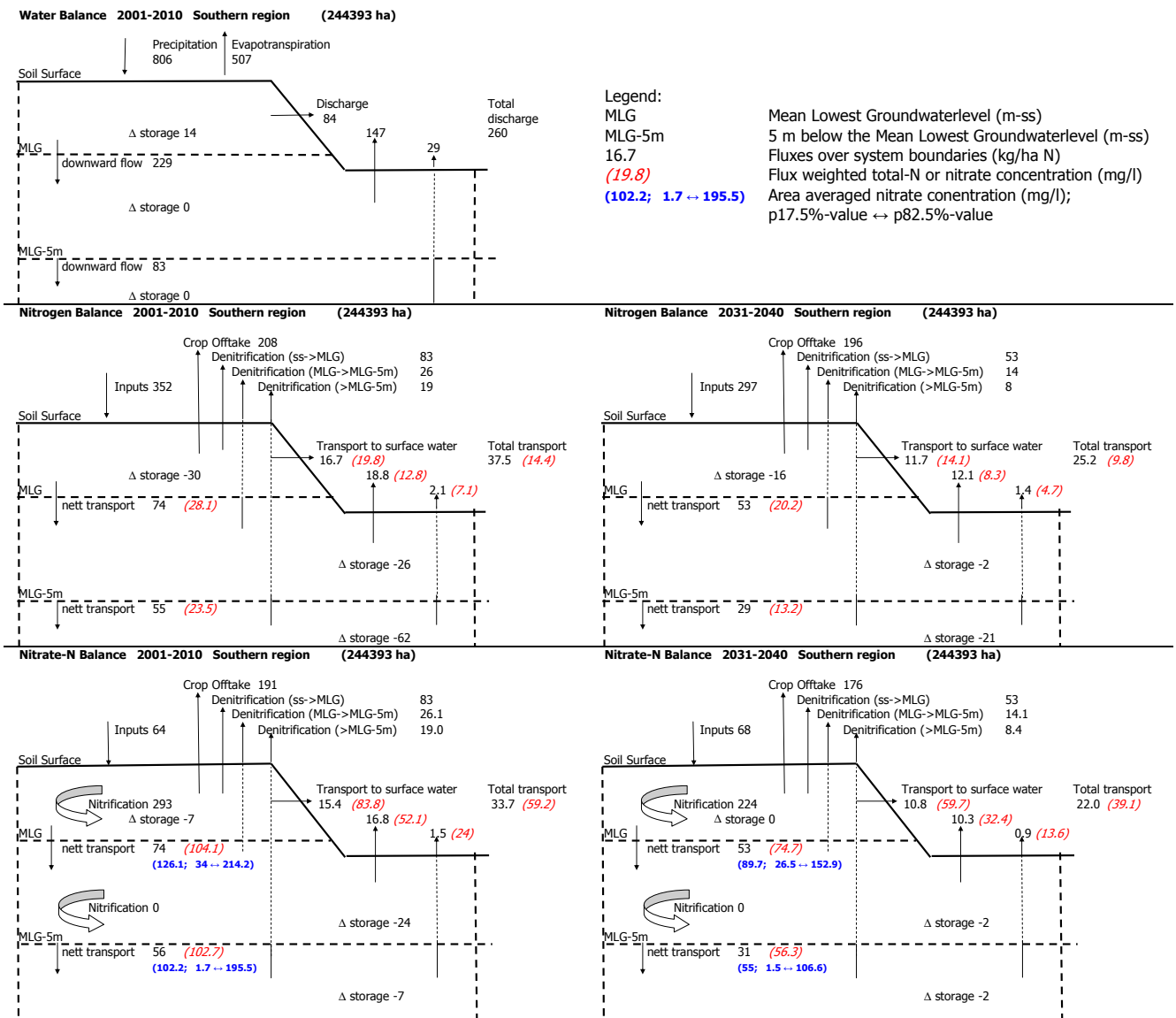


Fig. A11.15 Water, total-N and nitrate balances of all sandy soils in the Southern district for two periods

## Appendix 12 Nitrate balances of the upper 5m groundwater zone

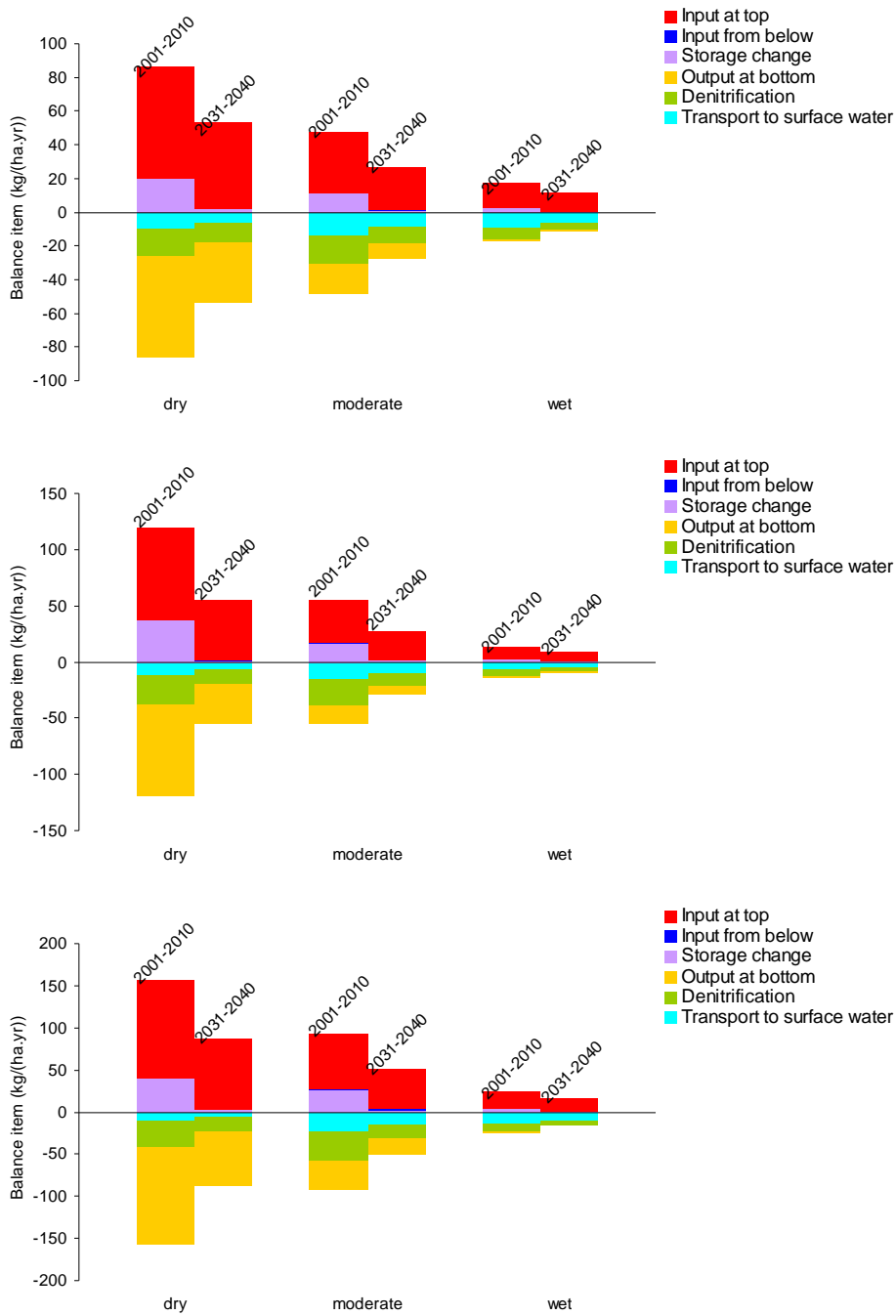


Fig. A12 Nitrate balance of the soil layer between MLG and MLG-5m for the Northern (top), Central (middle) and Southern (bottom) sand district for two periods and for three groundwater classes

## Appendix 13 Tentative sensitivity analysis at farm level of subsoil organic matter attribution to pools

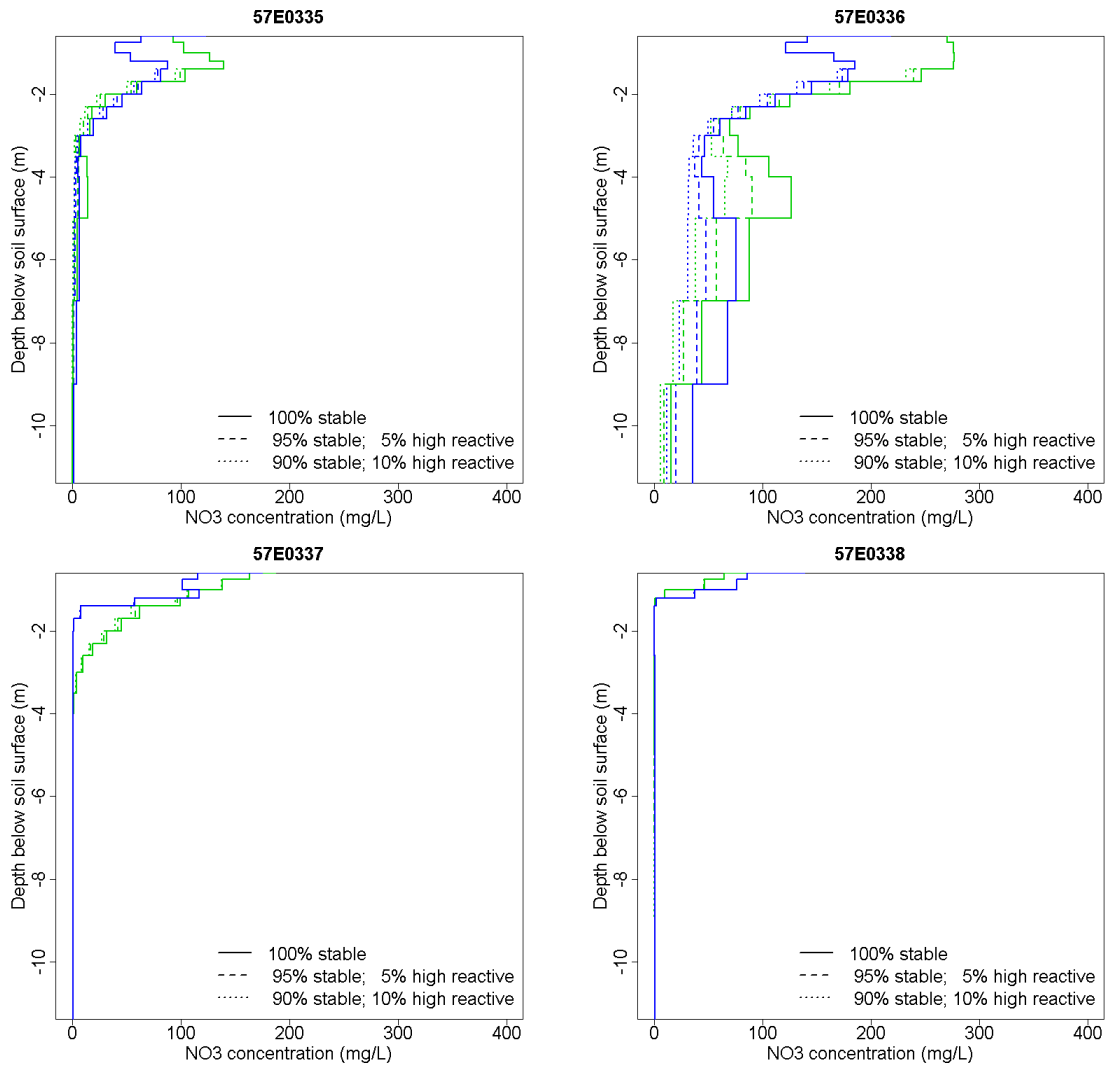


Fig. A13.1 Simulated nitrate concentrations for grassland (green) and silage maize (blue) as a function of depth for four fields of the Maarbeeze farm. Results for the 100% solid organic matter attributed to a stable pool with a low reaction rate are given by solid lines, the results where 5% of the material is attributed to a relatively highly reactive pool and 95% to the stable organic matter pool are given by the dashed lines and the results where 10% of the material is attributed to a relatively highly reactive pool and 90% to the stable organic matter pool are given by the dotted lines.

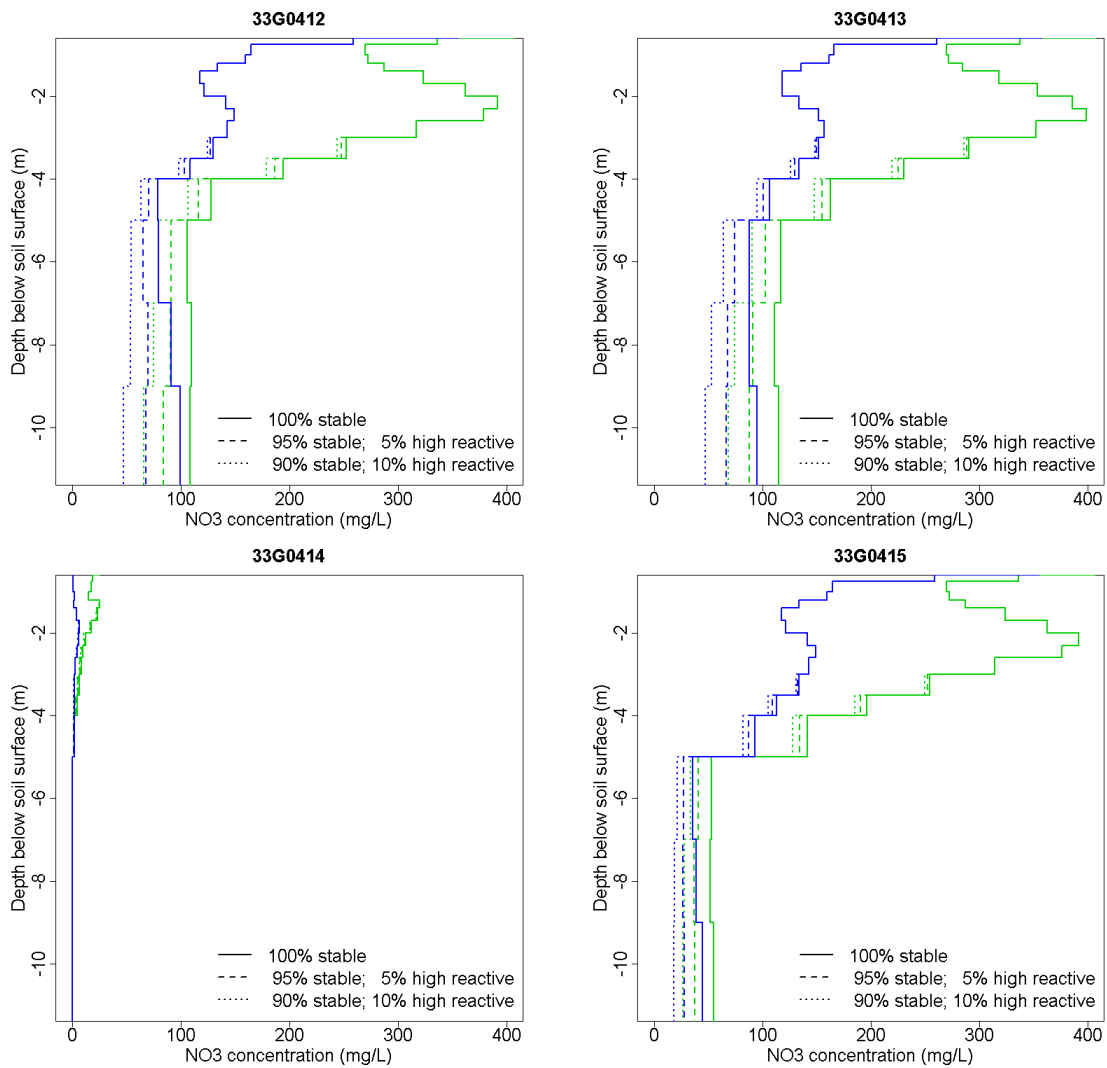


Fig. A13.1 Simulated nitrate concentrations for grassland (green) and silage maize (blue) as a function of depth for four fields of the Spankeren farm. Results for the 100% solid organic matter attributed to a stable pool with a low reaction rate are given by solid lines, the results where 5% of the material is attributed to a relatively highly reactive pool and 95% to the stable organic matter pool are given by the dashed lines and the results where 10% of the material is attributed to a relatively highly reactive pool and 90% to the stable organic matter pool are given by the dotted lines.

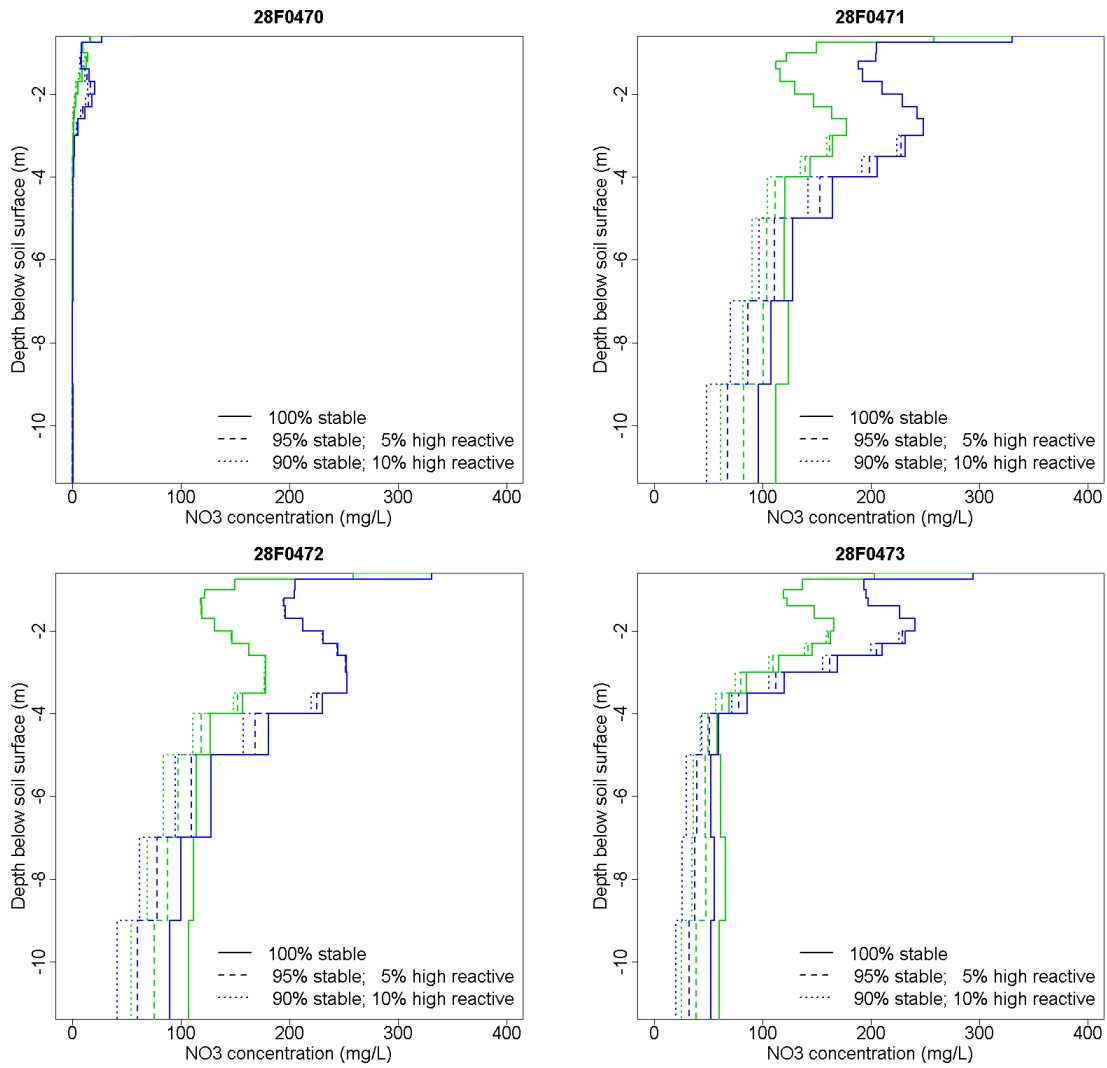


Fig. A13.1 Simulated nitrate concentrations for grassland (green) and silage maize (blue) as a function of depth for four fields of the Nutter farm. Results for the 100% solid organic matter attributed to a stable pool with a low reaction rate are given by solid lines, the results where 5% of the material is attributed to a relatively highly reactive pool and 95% to the stable organic matter pool are given by the dashed lines and the results where 10% of the material is attributed to a relatively highly reactive pool and 90% to the stable organic matter pool are given by the dotted lines.

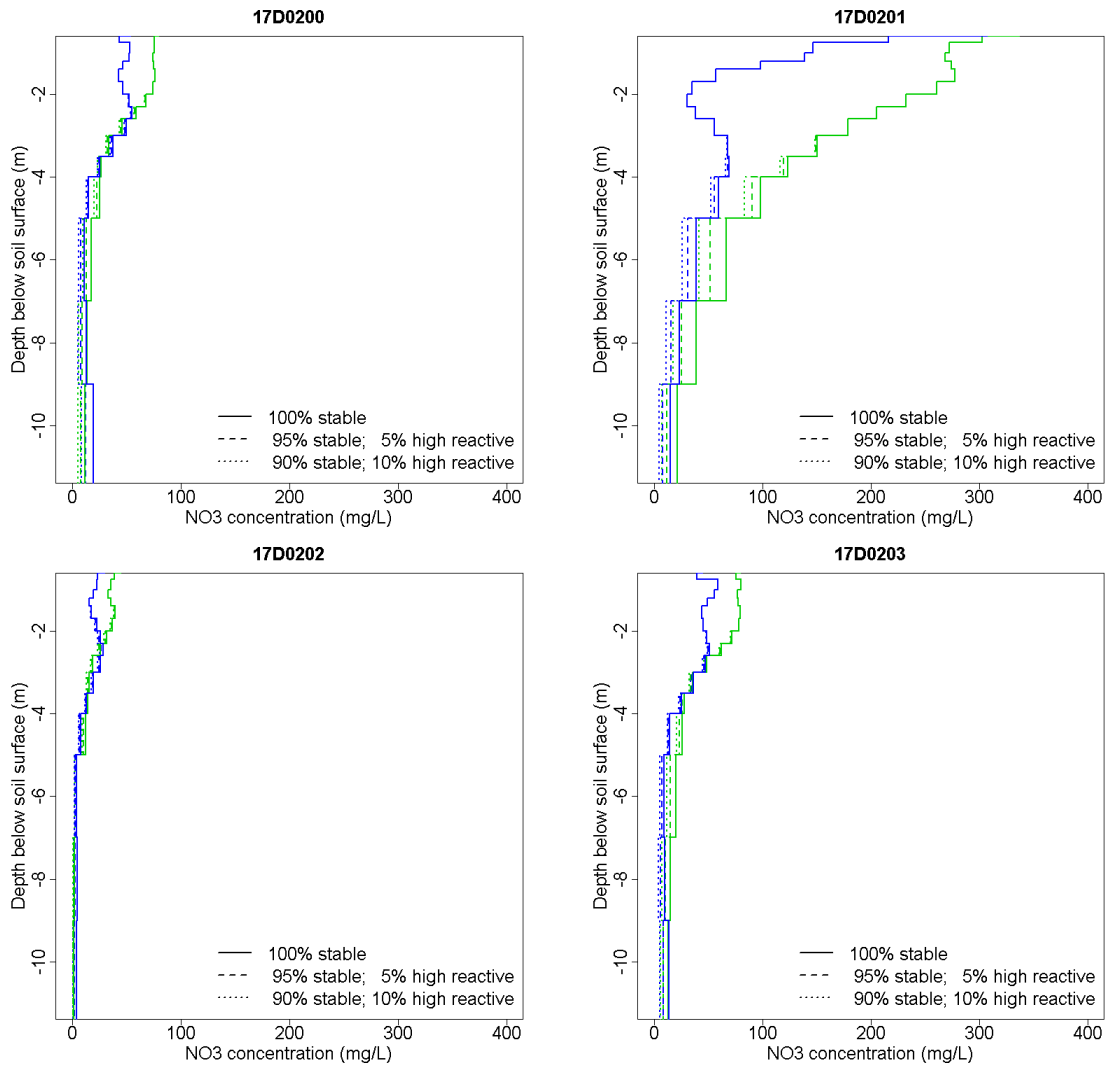


Fig. A13.1 Simulated nitrate concentrations for grassland (green) and silage maize (blue) as a function of depth for four fields of the Nieuweoord farm. Results for the 100% solid organic matter attributed to a stable pool with a low reaction rate are given by solid lines, the results where 5% of the material is attributed to a relatively highly reactive pool and 95% to the stable organic matter pool are given by the dashed lines and the results where 10% of the material is attributed to a relatively highly reactive pool and 90% to the stable organic matter pool are given by the dotted lines.

## Appendix 14 Modelling side effects of denitrification in groundwater

### A14.1 Introduction

#### *A14.1.1 General*

Denitrification may happen in aquifers in association with oxidation of pyrite or sedimentary organic matter (SOM). It is well recognised that the first process may cause, however, increased hardness and sulphate and trace element concentrations in groundwater as side effects. Whether or not side effects happen for denitrification with SOM oxidation is not well considered. In this study we quantify the side effects in a generic manner for Dutch Pleistocene sandy aquifers.

Geochemical characteristics of the sediment important to assess the negative effects - e.g. organic matter content, decay rate of organic matter, pyrite content, trace element content in pyrite, CEC - were varied in a range that is representative for Pleistocene sandy aquifer sediments in The Netherlands. We need, therefore, to set up different scenarios in which we take into account these ranges.

#### *A14.1.2 Trace Elements in Pyrite*

Trace elements incorporated in pyrite may become mobilized when nitrate oxidizes pyrite. Huerta-Diaz & Morse (1992) have reported trace element concentrations in pyrites from various marine and freshwater sediments. Larsen & Postma (1997) determined the nickel concentration in pyrites from a Pleistocene aquifer in Denmark. Broers & Buijs (1997) determined arsenic, cobalt, nickel and zinc concentrations in pyrites from a Dutch Pleistocene aquifer. Table A14.1 summarizes these studies. The data indicate that broad ranges are found for all trace elements.

Three phases can be distinguished in sediments with respect to the availability of trace elements. Trace elements can be incorporated in silicates, these trace elements are immobile. Trace elements can also be sorbed to organic matter, clay or (hydr)oxides, this is often defined as the reactive phase. Trace elements can also be incorporated in pyrite (Alvarez-Iglesias, 2008). Several studies have focused on degree of trace element pyritization (DTMP; Huerta-Diaz & Morse, 1990,1992; Billon *et al.*, 2001; Otero & Marcias, 2003, Otera *et al.*, 2005; Scholz & Neumann, 2007). DTMP is defined as:

$$\text{DTMP} = \text{Pyrite-TM} / (\text{Pyrite-TM} + \text{Reactive-TM})$$

where Pyrite-TM is the trace metal content ( $\mu\text{g/g}$ ) incorporated in pyrite and Reactive-TM is de trace metal content ( $\mu\text{g/g}$ ) sorbed to organic matter, clay or (hydr)oxides. DTMP can be explained as the affinity of a certain trace element for the pyrite phase relative to the reactive phase. Huerta-Diaz & Morse (1992) classified three groups of trace elements with respect to their affinities for pyrite in various sediments. The first group, composed of Ag,

Hg, and Mo, show a high affinity for pyrite. These elements are enriched in pyrite relative to the reactive phase. The second group, consists of transition elements Co, Cu, Mn, and Ni. These elements are about equally partitioned between the pyrite and the reactive phase. The final group consists of Cr, Cd, Pb, and Zn. These elements are relative depleted in the pyrite relative to the reactive phase. The other studies (Billon *et al.*, 2001; Otero & Marcias, 2003, Otera *et al.*, 2005; Scholz & Neumann, 2007) find similar values for DTMP. Elements with a high DTMP may favour their release by oxidation of pyrite, making them a threat to water quality.

In above mentioned studies various sediments were investigated which may often differ from Dutch Pleistocene aquifer sediments, with respect to geochemistry. Broers & Buijs (1997) investigated trace element concentrations in pyrites from Dutch Pleistocene aquifer sediments. Broers & Buijs(1997) only determined As, Ni, Co and Zn concentrations in pyrite, since for these trace elements (too) high concentrations were found in groundwater in these aquifers. The concentrations found by Broers & Buijs (1997) are within the range given by Huerta-Diaz & Morse(1992) and Larsen & Postma (1997).

Table A14.1 Trace element contents in pyrite (%) taken from literature.

	Broers & Buijs (1997)	Huerta-Diaz & Morse (1992, table 3)	Larsen & Postma (1997)	Huerta-Diaz & Morse (1992, table 2)
As	290	<1.6 - 850	-	< 4 - 925
Cd	-	-	-	< 0.06 - 121
Co	70	< 2.0 - 260	-	< 3 - 3837
Cr	-	-	-	3 - 946
Cu	-	< 1.6 - 1000	-	55 - 16970
Fe	-	-	-	-
Hg	-	-	-	< 0.0006 - 89
Mn	-	< 4.4 - 2200	-	Jun-70
Mo	-	6.3 - 83	-	< 0.4 - 328
Ni	50	2.0 - 8200	40 -140	< 5.9 - 8920
Pb	-	< 0.58 - 52	-	< 0.47 - 4700
Zn	90	< 5.5 - 550	-	17 - 9500

## A14.2 Modelling

### A14.2.1 PHREEQC

We used the PHREEQC code (Parkhurst & Apello, 1999), a computer program for simulating chemical reactions and transport processes in natural or polluted water. The program is based on equilibrium chemistry of aqueous solutions interacting with minerals, gases, solid solutions, exchangers, and sorption surfaces, but also includes the capability to model kinetic reaction with rate equations that are completely user-specified. We model 1D- transport in PHREEQC. Our profile is 5 meters long and divided in 10 cells of 0.5 meter. The top of cell 1 represents the redox cline below which pyrite or SOM are present as reactive reductants. Dispersivity is assumed to be low, near zero. Diffusion is also set to zero. All cells do have the same geochemical characteristics.

### A14.2.2 Future concentrations at phreatic level and actual groundwater composition

Four different water compositions are used in the simulation: infiltration pore water (referred to as ‘phreatic’) and actual groundwater both having either a slightly acid or a neutral pH. These reflect in a general way the compositions of the infiltration pore water and shallow groundwater in agricultural areas in the Pleistocene part of the Netherlands. Future concentrations of phreatic groundwater and the two actual groundwater compositions (table A14.2) are based on data of (Van der Grift, 2003; Van der Grift *et al*, 2004) and on expert judgement (Van der Grift, 2008, pers. commun.). The assumed pH of 5 and 6.5 are based on Vermooten *et al.* (2006).

Table A14.2 Phreatic and shallow groundwater composition used as model input.

pH	Phreatic groundwater composition				Shallow groundwater composition			
	5.5		6.5		5.5		6.5	
Main elem.	mg l <sup>-1</sup>	mmol l <sup>-1</sup>	mg l <sup>-1</sup>	mmol l <sup>-1</sup>	mg l <sup>-1</sup>	mmol l <sup>-1</sup>	mg l <sup>-1</sup>	mmol l <sup>-1</sup>
Alkalinity	10	0.164	80	1.31	10	0.164	80	1.31
Cl	33	0.927	33	0.927	33	0.927	33	0.927
NO <sub>3</sub>	50	0.806	50	0.806	50	0.806	50	0.806
SO <sub>4</sub>	33	0.348	33	0.348	33	0.348	33	0.348
Na	8	0.333	8	0.333	8	0.333	8	0.333
K	48	1.22	48	1.22	48	1.22	48	1.22
Mg	4	0.165	9	0.357	4	0.165	9	0.357
Ca	20	0.499	41	1.02	20	0.499	41	1.02
Al	—	—	—	—	1	0.0372	1	0.0372
Fe	—	—	—	—	35	0.63	35	0.63
Trace elem.	μ l <sup>-1</sup>	mmol l <sup>-1</sup>	μ l <sup>-1</sup>	mmol l <sup>-1</sup>	μ l <sup>-1</sup>	mmol l <sup>-1</sup>	μ l <sup>-1</sup>	mmol l <sup>-1</sup>
Cd	—	—	—	—	2	1.8x10 <sup>-5</sup>	2	1.8x10 <sup>-5</sup>
Ni	—	—	—	—	2	3.4x10 <sup>-5</sup>	2	3.4x10 <sup>-5</sup>
Zn	667	1.02x10 <sup>-2</sup>	667	1.02x10 <sup>-2</sup>	1000	1.5x10 <sup>-2</sup>	1000	1.5x10 <sup>-2</sup>
Cu	3	5.05x10 <sup>-5</sup>	3	5.05x10 <sup>-5</sup>	2	3.1x10 <sup>-5</sup>	2	3.1x10 <sup>-5</sup>
Br	Charge				Charge			

### A14.2.3 Minerals in sediments

Calcite, siderite, goethite and pyrite are abundant non-silicate minerals in Dutch Pleistocene sediments (Vermooten *et al*, 2006). These minerals, therefore, are in the model. Siderite and calcite are only found in specific regions of the Netherlands. Initial calcite and siderite concentrations are, therefore, set to zero. They may precipitate, however, when calcium or iron and carbonate concentrations are high. Initial amount of pyrite is calculated from the data sets mentioned in table A14.3. The initial amount of goethite is set to zero in the pyrite scenarios (described below), since only anoxic conditions occur and no goethite will be present when pyrite is present under equilibrium conditions as assumed in this modelling. In the organic-matter scenarios (described below) initially (at t=0) oxic or suboxic conditions occur, so goethite is calculated from initial iron concentrations.

*Table A14.3 Datasets used to calculate organic matter content, pyrite and CEC in Pleistocene sandy aquifer sediments.*

Dataset	Region	Number of analyses	Date of analyses	Reference
Noord-Nederland / NNL	The Netherlands North	1864	2006-2007	Heerdink, 2008
Midden-Nederland / MNL	The Netherlands Central	340	2007-2008	-
Zuid-Nederland / ZNL	The Netherlands South	286	2007-2008	Klein, 2008

### A14.2.4 Trace element concentrations in pyrite

As described before, a broad range of trace element concentrations in pyrite is found. We have defined a pyrite with relatively low trace element concentrations and a pyrite with relatively high concentrations. The pyrite with relatively low trace element concentrations has concentrations that are half times the concentrations found by Broers & Buijs (1997), except for Co. Cobalt is not taken into account in this modelling exercise, since PHREEQC has no Co in its databases. The pyrite with relatively high trace element concentrations has concentrations that are two times the concentrations found by Broers & Buijs (1997), except for Co. To the pyrite with relatively high trace element concentrations also copper and manganese are added. Concentrations of copper and manganese in pyrite are based on Huerta-Diaz & Morse (1992). The formulas used for pyrite are:

**Fe0.99930 Ni0.00025 Zn0.00045 S2 As0.00145;**  
**Fe0.9912 Ni0.001 Zn0.0018 Cu0.0016 Mn0.0044 S2 As0.0058.**

### A14.2.5 Cation Exchange Capacity

The total cation exchange capacity (CEC) is defined as the sum of three cation exchanger types. The first cation exchanger represents clay minerals. In this model every cation may be sorbed to clay, except H<sup>+</sup>. The second and third cation exchangers represent SOM. For these, every cation may be sorbed to organic matter, also H<sup>+</sup>. These two exchangers differ with respect to their affinity for H<sup>+</sup>: they will buffer the pH within a pH-range of 4–6 or 6–

8. Clay and organic matter content of the sediment are calculated from the databases mentioned in table A14.3. For each region/dataset (The North-, Central-, South-Netherlands) the mean clay and organic matter content is calculated. The means differ from region to region. Two mean clay contents and two mean organic matter contents are taken. The highest means are used in scenario's representing Pleistocene Dutch sediments having high CEC and lowest means are used in scenario's representing Pleistocene Dutch sediments having low CEC.

#### *A14.2.6 Decay of Organic Matter*

First-order decay of SOM is assumed in this model. Values for the first-order decay rate constant  $k$  ( $\text{yr}^{-1}$ ) are taken from Appelo & Postma (2005). Decay rates ( $\text{mol l}^{-1} \text{yr}^{-1}$  SOM) are calculated by multiplying the first-order decay constant with SOM content calculated from datasets. These decay rates are within the range found in literature (see Appendix 2, this report)

### **A14.3 Scenarios**

Since characteristics of the sediment like organic matter content, decay rate of organic matter, pyrite content, trace element content in pyrite and CEC vary in a broad range, we defined several scenarios that cover this range. Definition of the scenarios is shown in table A14.4 and table A14.5. Table A14.4 shows eight scenarios in which pyrite ( $0.1 \text{ mol l}^{-1}$ ) is assumed to be initially present in the sediment. Characteristics of the sediment that are set either to a minimum or a maximum value is: 1. CEC: clay (X-exchanger) and organic matter (Y,Z-exchangers), 2. pH of infiltration pore water and shallow groundwater, and 3. trace element concentrations in pyrite.

*Table A14.4 Parameterization in eight pyrite scenarios (X,Y and Z in  $\text{mol l}^{-1}$  CEC)*

Scenario	X	Y	Z	Pyrite Composition (%)					pH
				As	Cu	Mn	Ni	Zn	
XYZminPYRlowpH5	0.03	0.095	0.095	0.145	0	0	0.025	0.04	5
XYZmaxPYRlowpH5	0.12	0.95	0.95	0.145	0	0	0.025	0.04	5
XYZminPYRhighpH5	0.03	0.095	0.095	0.58	0.16	0.44	0.1	0.18	5
XYZmaxPYRhighpH5	0.12	0.95	0.95	0.58	0.16	0.44	0.1	0.18	5
XYZminPYRlowpH65	0.03	0.095	0.095	0.145	0	0	0.025	0.04	6.5
XYZmaxPYRlowpH65	0.12	0.95	0.95	0.145	0	0	0.025	0.04	6.5
XYZminPYRhighpH65	0.03	0.095	0.095	0.58	0.16	0.44	0.1	0.18	6.5
XYZmaxPYRhighpH65	0.12	0.95	0.95	0.58	0.16	0.44	0.1	0.18	6.5

Table A14.5 shows eight scenarios in which no initial amount of pyrite is assumed, but in which decay of organic matter is assumed. Again minimum and maximum values are taken for: 1. CEC: clay (X) and organic matter (Y,Z), 2. pH of infiltration pore water and shallow groundwater. Additionally, the first-order decay constant of organic matter is varied.

*Table A14.5 Parameterization in eight organic matter scenarios (X, Y and Z in mol l<sup>-1</sup> CEC).*

Scenario	X	Initial Y	Initial Z	pH	First order decay constant (yr <sup>-1</sup> )
XYZminkOMlowpH5	0.03	0.095	0.095	5	4.2E-06
XYZmaxkOMlowpH5	0.12	0.08	0.08	5	4.2E-06
XYZminkOMhighpH5	0.03	0.095	0.095	5	8.3E-04
XYZmaxkOMhighpH5	0.12	0.08	0.08	5	8.3E-04
XYZminkOMlowpH65	0.03	0.095	0.095	6.5	4.2E-06
XYZmaxkOMlowpH65	0.12	0.08	0.08	6.5	4.2E-06
XYZminkOMhighpH65	0.03	0.095	0.095	6.5	8.3E-04
XYZmaxkOMhighpH65	0.12	0.08	0.08	6.5	8.3E-04

Since our model has 10 cells of 0.5 meter, and we assume a vertical pore water flow rate of groundwater of 1 meter per year, the water is shifted from one cell to the next each half a year (transport time step in PHREEQC). For interpretation of results we need the moles of organic matter that will be oxidized each transport time step (half year). These depend on the first-order decay constant  $k$  (yr<sup>-1</sup>) and the organic matter content of the sediment. The moles of organic matter that will be oxidized are given in table A14.6.

*Table A14.6 First-order decay constants of organic matter (0.5yr<sup>-1</sup>, yr<sup>-1</sup>), organic matter content (moles/litre) and decay rate of organic matter (moles/0.5year/litre and moles/year/litre) in organic matter scenarios*

Scenario	First order decay constant (k)		OM content	Decay rate	
	k (half yr <sup>-1</sup> )	k (yr <sup>-1</sup> )	moles/l	moles/l/half year	moles/l/year
XYZmaxOMhigh	4.2E-04	8.3E-04	1.9	7.9E-04	1.6E-03
XYZmaxOMlow	2.1E-06	4.2E-06	1.9	4.0E-06	7.9E-06
XYZminOMhigh	4.2E-04	8.3E-04	0.19	7.9E-05	1.6E-04
XYZminOMlow	2.1E-06	4.2E-06	0.19	4.0E-07	7.9E-07

## A14.4 Results and Discussion

### A14.4.1 Main processes

In this study we are most interested in hardness, sulphate and trace elements since these species are recognised side effects. pH and main elements control the behaviour of trace elements in groundwater. To explain trace element concentrations, we, therefore, need to understand pH and main element concentrations. As consequence, this chapter first presents the major hydrochemistry and subsequently the behaviour of individual trace elements.

### A14.4.2 pH, nitrate and sulphate

There are some main processes determining the pH. Generally, acid is produced or consumed in redox reactions and pH is thus affected in this way. The pH is a master

variable in sorption of trace elements on humic or fulvic acids as well as oxides of Al, Fe (and Mn). The main processes are:

- Oxidation of organic matter by oxygen – acid production;
- Oxidation of organic matter by nitrate – acid production or consumption, depending on pH; this process causes pH change to neutral pH (pH 7);
- Reductive dissolution of goethite, iron (III) – acid consumption; this process may cause precipitation of iron(II) minerals like pyrite – slight acid consumption or siderite - slight acid production;
- Oxidation of organic matter by sulphate – acid consumption; this process may cause, in presence of iron(III) minerals, precipitation of iron sulfides – acid consumption.
- Formation of methane from organic matter oxidation – acid production;

Oxidation of organic matter directly below the redox-cline is the driving force for processes. As oxidation rate of organic matter is high then first oxygen is depleted, followed by nitrate reduction, reactive Fe(III) minerals become reduced, sulphate reduction happens and finally methanogenesis. In this study goethite represents reactive iron(III) minerals. The reductive dissolution of goethite entails a large acid consumption.

As oxidation rate of organic matter is low oxygen concentrations might not reach zero. Oxygen will then be transported along the profile. After a certain time period, so at a certain depth, oxygen will be depleted, and from this depth downwards nitrate reduction will take place. As long as nitrate is not depleted no reductive dissolution of goethite will occur and little acid will be consumed.

For the scenarios in which pyrite is oxidized, the only redox process affecting pH is the oxidative dissolution of pyrite. In this process, in this model, only the sulfides of the pyrite are oxidized, since pyrite is in excess to the oxygen and nitrate and the oxidation of the sulfides is energetic favourable compared to the oxidation of iron(II). This process produces acid.

The acid production or consumption in the redox reactions will be buffered by H<sup>+</sup>-sorption to humic and fulvic acids as part of SOM. When this buffering occurs other cations, incl. trace metals will adsorb or desorb from SOM as sorbent.

pH as a function of depth at different time intervals is shown in figure A14.1. In scenarios in which the decay rate of organic matter is high, e.g. XYZmaxOMhighpH5 (table A14.5), pH increases in time in the groundwater directly below the redox-cline (0–2m; fig. A14.1-*left*). In these scenarios 0.79 mmol/l organic matter is oxidized each time step. The oxidation of organic matter at this rate may reduce almost all nitrate at once since nitrate has a concentration of 0.8 mmol/l. In cell 1 (0–0.5m), oxygen concentrations are depleted and part of nitrate is reduced (fig. A14.2-*top left*). In cell 2 (0.5–1m) nitrate is depleted (fig. A14.2-*top right*) and reductive dissolution of goethite will occur. Due to this reductive dissolution pH increases. After goethite is fully reduced, sulphate reduction will

occur in cell 2 and 3 (0.5–1.5m, fig. A14.3-*top left*). Since sulphate reduction also consumes acid, pH further increases. After sulphate is depleted at depth of 2 meters, methanogenesis will occur. Methanogenesis will produce acid. At pH of 5 this acid-increase is buffered and pH will not decrease therefore at depths below 2 meters (2–5 m).

These high organic matter decay scenarios are, however, not representative for Pleistocene sandy aquifer sediments. The high organic matter decay causes, next to oxygen and nitrate reduction, sulphate reduction within the first meter below the redox cline. Sulphate reduction in shallow groundwater is only found in 7 of 45 shallow observation wells in brook valleys in Northern Brabant, The Netherlands (Van der Grift *et al.*, 2004; Foppen & Van der Grift; 2009). These Holocene brook valley sediments are organic rich compared to Pleistocene sandy aquifer sediments. Sulphate reduction is, therefore, not expected in Pleistocene sandy aquifer sediments and we will therefore not further discuss these scenarios in this report.

In scenarios with a moderate organic matter decay rate, e.g. XYZminOMhighpH65 (table A14.5), 0.079 mmoles/l organic matter are oxidized each time step. At this decay rate oxic conditions will last in the upper part of the profile. Nitrate concentrations only change from 1 meter depth (1–5 m, fig. A14.2-*top right*). At this depth oxygen is depleted and in each time step part of nitrate is reduced. So the nitrate concentration decreases and water with lower nitrate concentrations is transported downward. At next depth again part of nitrate is reduced. Therefore in fig. A14.2-*top right* nitrate concentrations are decreasing with depth. Nitrate concentrations are not depleted in the upper 5 meters of the groundwater system. At depth of 5 meter the nitrate concentration is still 20 mg l<sup>-1</sup>. In scenarios in which a low first-order decay constant ( $k = 4.2 \times 10^{-6} \text{ yr}^{-1}$ , table A14.6) is assumed no nitrate and sulphate are reduced. Only oxygen is reduced by organic matter. No reductive dissolution of goethite will occur either in these scenarios as a consequence of organic matter decay. With respect to pH only relative small amounts of acid are either produced (oxidation of organic matter by oxygen), or consumed (oxidation of organic matter by nitrate at a pH of 6.5). pH will therefore not change (fig. A14.1-*right*).

In scenarios with a low organic matter decay rate, e.g. XYZmaxOMlowpH5 (table A14.5), only oxygen will be reduced. Nitrate concentrations do not change with depth. By the oxidation of organic matter by oxygen in these scenarios only relative small amounts of acid is produced. pH does not change either therefore.

In scenarios in which pyrite is oxidized acid is produced, but this acid production is buffered by proton-buffering of organic matter. pH does not change in these scenarios therefore. In pyrite scenarios all nitrate is reduced by pyrite directly below the redox cline (fig. A14.2-*bottom right*). Since sulfide from pyrite is oxidized sulphate concentrations will increase. Sulphate concentrations will increase from 33 mg l<sup>-1</sup> (concentration in infiltrating pore water, table A14.2) to 105 mg l<sup>-1</sup> (fig. A14.3-*bottom left*).

Decay of organic matter will not affect sulphate concentrations in shallow groundwater since the decay rate of organic matter in Pleistocene sandy aquifer sediments is only moderate or low.

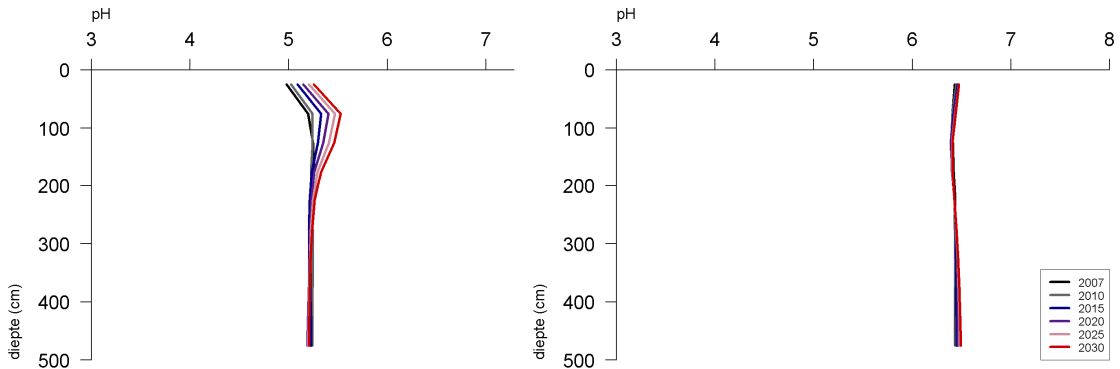


Fig. A14.1 pH concentration-depth profiles in 2007, 2010, 2015, 2020, 2025 and 2030 in scenarios XYZmaxOMboogpH5 (left) and XYZminOMboogpH65 (right)

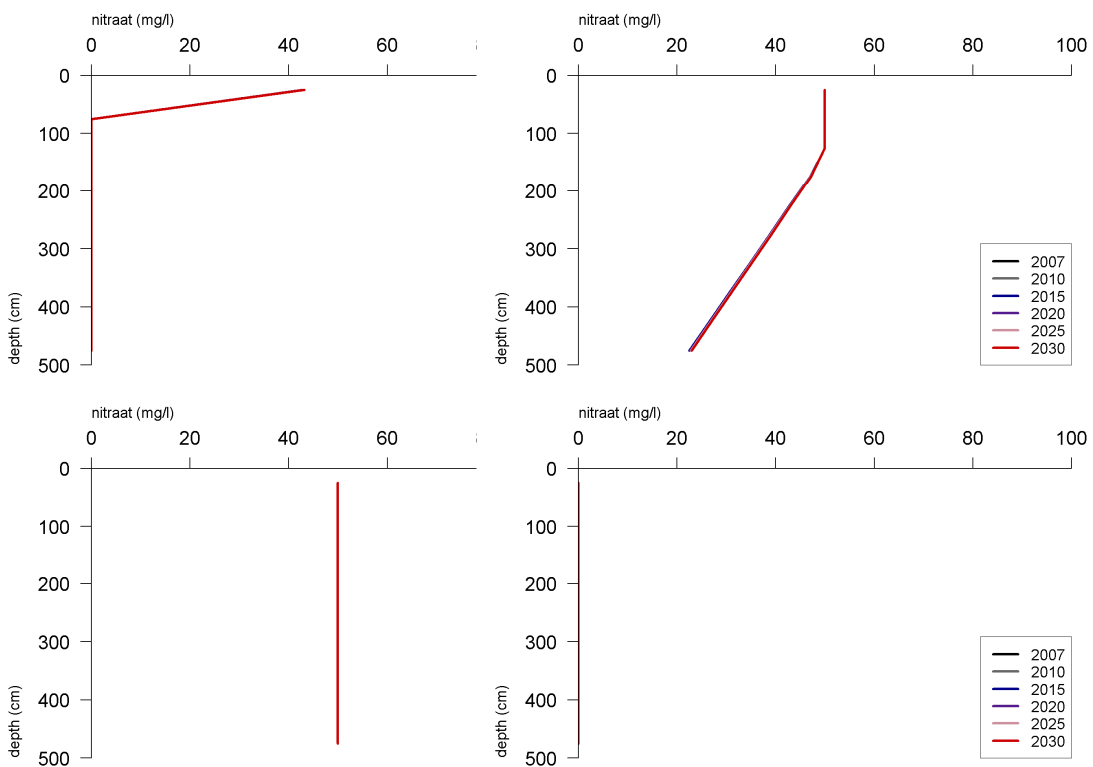


Fig. A14.2 Nitrate concentration-depth profiles in 2007, 2010, 2015, 2020, 2025 and 2030 in scenarios XYZmaxOMhighpH5 (top, left), XYZminOMhighpH65 (top, right), XYZmaxOMlowpH5 (bottom, left) and XYZmaxPYRlowpH5 (bottom, right)

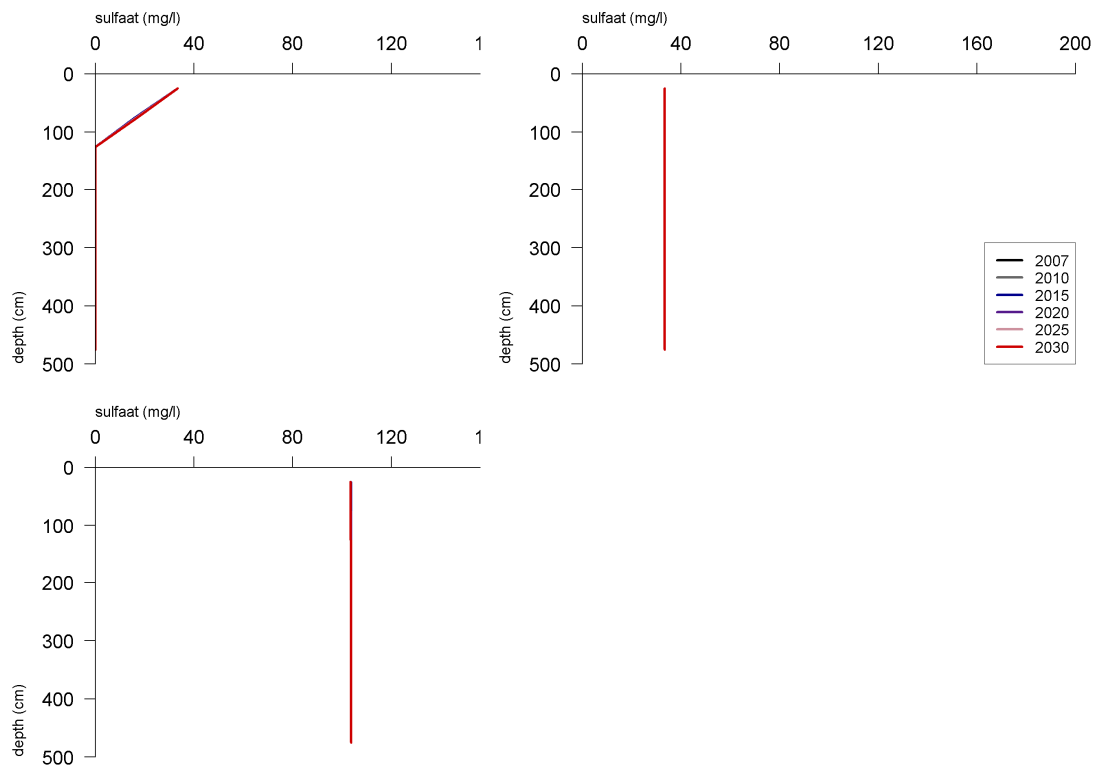


Fig. A14.3 Sulphate concentration-depth profiles in 2007, 2010, 2015, 2020, 2025 and 2030 in scenarios XYZmaxOMhighpH5 (top, left), XYZmaxOMlowpH5 (top, right) and XYZmaxPYRlowpH5 (bottom, left)

#### A14.4.3 Hardness: calcium and magnesium

Three main processes determine the hardness of water. First, dissolution or precipitation of calcium or magnesium bearing minerals, like calcite ( $\text{CaCO}_3$ ). Second, acid production or consumption in redox processes, mentioned above, may cause sorption or desorption of  $\text{H}^+$  to SOM and may affect in that way the sorption or desorption of calcite and magnesium to SOM. Third, changes in infiltration pore water composition may cause sorption and desorption of cations, including calcium and magnesium. E.g. increased potassium loads may cause desorption of calcium and magnesium and therefore may cause increased hardness.

In organic matter scenarios with moderate or low organic matter decay rates no significant changes occur to hardness. In the pyrite scenarios hardness will increase in time (fig. A14.4-top left). This increase is caused by the oxidation of pyrite, since acid is produced then. The presence of acid causes desorption of calcium and magnesium.

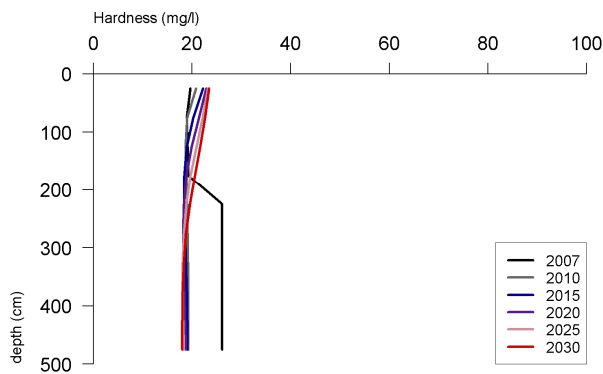


Fig. A14.4 Hardness-depth profiles in 2007, 2010, 2015, 2020, 2025 and 2030 in scenario XYZMinPYRbighpH5

#### A14.4.4 Trace elements

##### Arsenic

Arsenic can be released from pyrite when pyrite is oxidized. Arsenic concentrations depend on trace element composition in pyrite. Two different trace element compositions in pyrite are modelled (table A14.4). When high trace element concentrations in pyrite are assumed, arsenic concentrations in groundwater may increase to  $160 \mu\text{g l}^{-1}$  (fig. A14.5-top right). When low trace element concentrations in pyrite are assumed, arsenic concentrations in groundwater may increase to  $40 \mu\text{g l}^{-1}$  (fig. A14.5-top left). It is assumed that no arsenic is added to the system at phreatic level, therefore pyrite is the only source of arsenic. Scenarios without pyrite oxidation do have arsenic concentrations of zero  $\mu\text{g l}^{-1}$ .

Besides the release of arsenic from pyrite the arsenic transport in this model is conservative, this means no sorption or desorption will occur. Normally arsenic may sorb to surfaces, this process is called ‘surface-complexation’. The ‘surface-complexation’ is not taken in account in this model, however. The surface-complexation is neglected since it is generally assumed that surface-complexation is far less important than cation-exchange (sorption of cations to clay (X), and organic matter (Y,Z)).

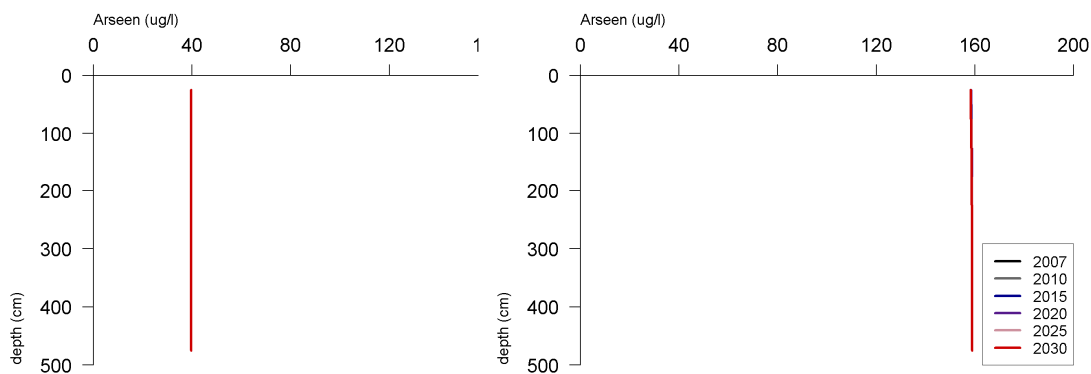


Fig. A14.5 Arsenic concentration-depth profiles in 2007, 2010, 2015, 2020, 2025 and 2030 in scenarios XYZmaxPYRlaagpH5 (left) and XYZmaxPYRhoogpH5 (right)

### Manganese

In this study the only source of manganese is pyrite, and only when high trace element concentrations are assumed (table A14.4). The oxidation of pyrite directly below phreatic level will occur as long as pyrite is available, since the supply of oxidisers - oxygen, nitrate and oxygen and iron(III) - is a continuous process. Release of manganese is therefore also a continuous process. When manganese is released from pyrite directly below the redox cline it will partly be sorbed to clay minerals and organic matter; and will not be transported down with the groundwater. Therefore, concentrations of manganese will increase in time (fig. A14.6-*left* and A14.6-*right*). The amount of manganese that can be sorbed is mainly determined by the amount of sorption sites. If many sorption sites are available, e.g. in scenario XYZmaxPYRhighpH5 (table A14.4), therefore, manganese will be relatively heavily sorbed and high manganese concentrations only occur in the upper meters (fig. A14.6-*left*). If less sorption sites are available, e.g. in scenario XYZminPYRhighpH5 (table A14.4), manganese concentrations will reach greater depths (A14.6-*right*).

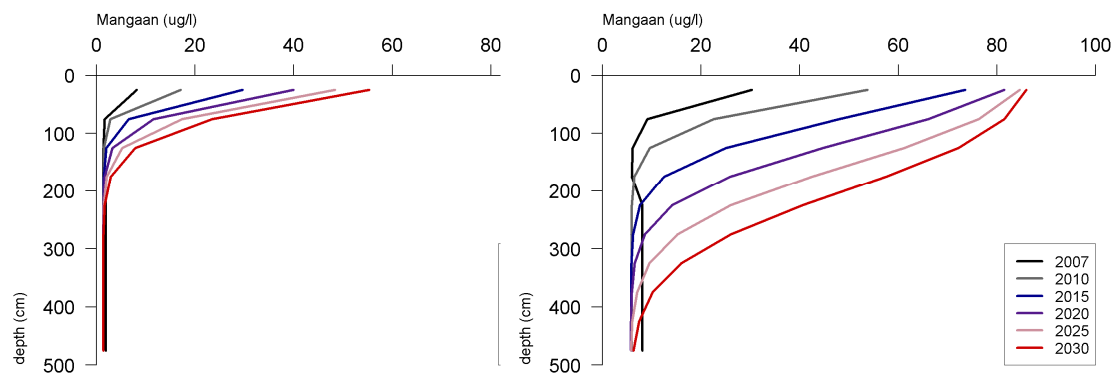


Fig. A14.6 Manganese concentration-depth profiles in 2007, 2010, 2015, 2020, 2025 and 2030 in scenarios XYZmaxPYRhighpH5 (left) and XYZminPYRhighpH5 (right)

### Nickel

It is assumed that no nickel is added from phreatic level to the system from 2005 onwards. The nickel initially present in the groundwater system is partly sorbed to clay minerals and organic matter. Infiltrating of pore water without nickel, causes desorption of nickel within the porous medium. In scenarios without pyrite oxidation desorption is the only source of nickel. Since nickel concentrations at the sorption sites are not high, nickel will not reach problematic concentrations.

When pyrite oxidation occurs nickel is released from pyrite. This leads to increased nickel concentrations (fig. A14.7-*left* and A14.7-*right*). Nickel released from pyrite directly below the redox cline will be sorbed to clay minerals and organic matter. As for manganese the amount of nickel that will be sorbed is mainly determined by the amount of sorption sites available. When many sorption sites are available, e.g. in scenario XYZmaxPYRhighpH5, nickel will be relatively heavily sorbed and high nickel concentrations only occur in the upper meters (fig. A14.7-*left*). When less sorption sites are available, e.g. in scenario XYZminPYRhighpH5, the nickel front will reach greater depths (fig. A14.7-*right*).

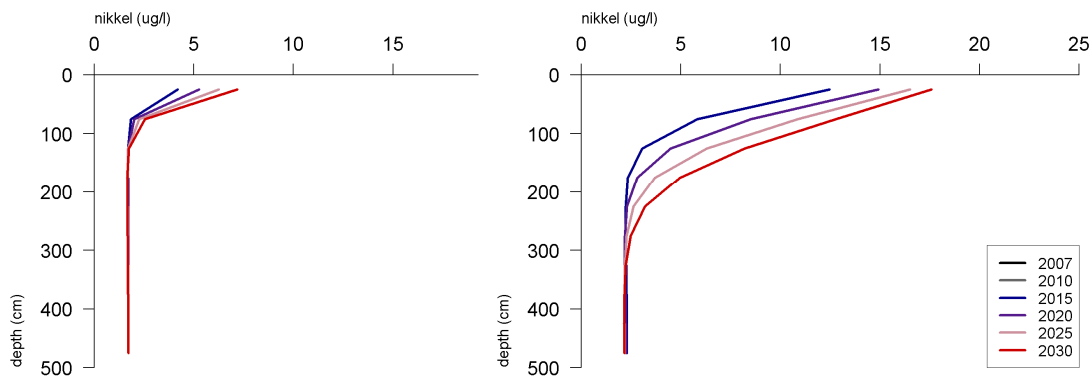


Fig. A14.7 Nickel concentration-depth profiles in 2007, 2010, 2015, 2020, 2025 and 2030 in scenarios XYZmax:PYRhighpH5(left) and XYZmin:PYRhighpH5 (right)

### Zinc

Zinc concentrations in shallow groundwater are high due to high field loads (1 mg l<sup>-1</sup> table A14.2), and are problematic already (table A14.7). Zinc concentrations will not significantly increase by pyrite oxidation. Even in the scenarios with high trace element concentrations in pyrite, pyrite oxidation does not cause increased zinc concentrations. When organic matter decay is assumed zinc concentrations will not change in Pleistocene sandy aquifer sediments, neither.

### Copper

Copper does strongly sorp to humic and fulvic acids, i.e. SOM. When expressed per volume of pore water, concentrations at sorption sites are about 1000 times higher than in solutions. A large reservoir of sorbed Cu may thus be present, that may get mobilised major cation concentrations (calcium, magnesium) or H<sup>+</sup> concentrations increase, as these compete with copper for the sorption sites.

Very high copper concentrations are found in all pyrite scenarios. Initially 2 µg l<sup>-1</sup> copper is in the shallow groundwater. When pyrite is oxidized a large amount of acid is produced. The presence of acid causes desorption of a part of the copper sorbed on SOM (fig. A14.8-bottom row). In acid conditions (pH 5) the desorption rate of copper is less than in more alkaline conditions (pH 6.5). In more alkaline conditions, therefore, copper concentrations in the water will reach the most extreme levels and reach greatest depths (fig. A14.8-top left)

These results indicate that pyrite oxidations may cause high copper concentrations. The concentrations modelled in this scenario, however, are probably too dramatic. During the initialisation of the model, the model calculates too high concentrations at sorption sites. Therefore the model calculates too high desorption of copper when acid is produced during pyrite oxidations. Under field conditions less copper is removed from the sorption sites than calculated by the model and copper concentrations will therefore be less dramatic.

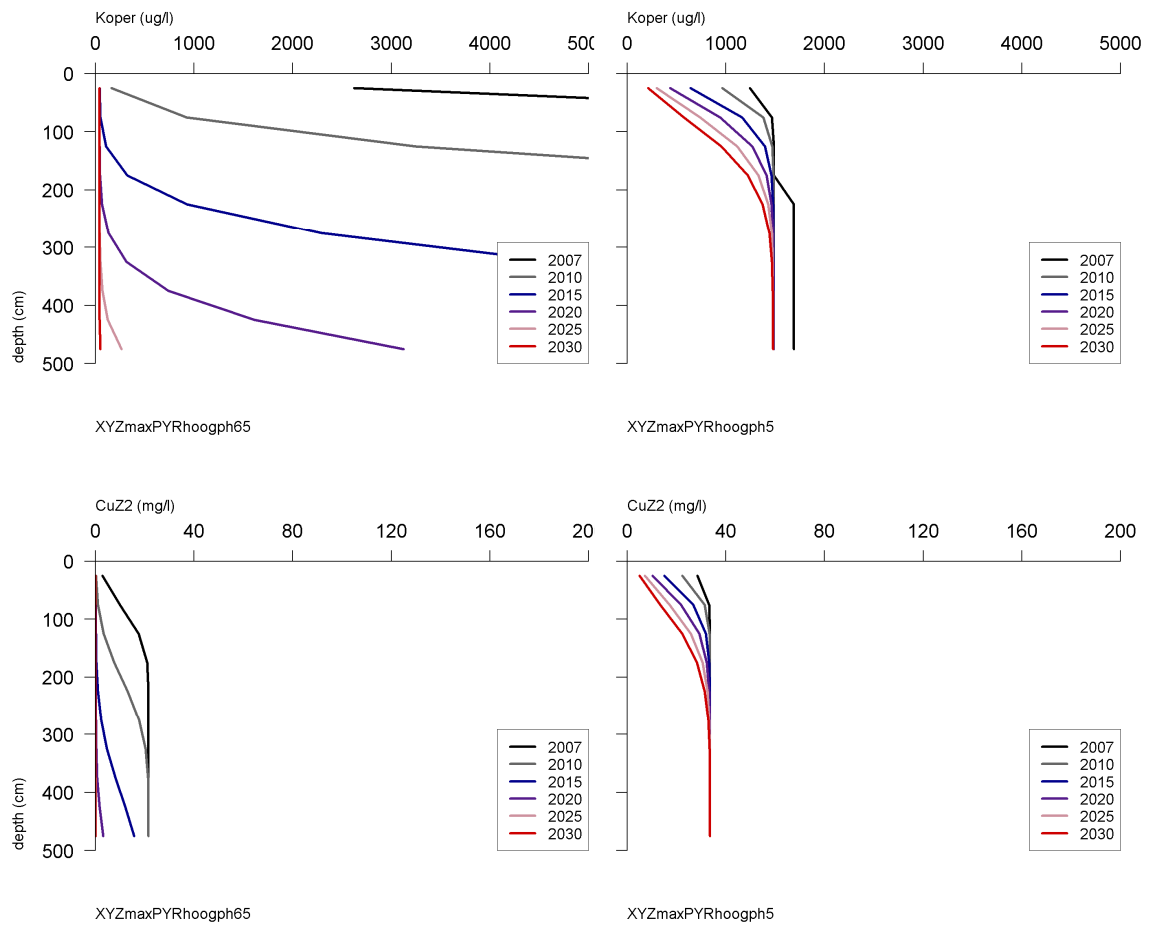


Fig. A14.8 Copper (top row) and copper sorbed to SOM (bottom row) concentration-depth profiles in 2007, 2010, 2015, 2020, 2025 and 2030 in scenarios XYZmaxPYRhoogph65 (left) and XYZmaxPYRhoogph5 (right)

### **Cadmium**

The only sources of cadmium are the sorption sites. Cadmium does neither infiltrate with the inflowing pore water nor is it released from pyrite. In all scenarios cadmium concentrations are low and stay low.

## **A14.5 Conclusions**

### *A14.5.1 General*

In this study side effects of denitrification are modelled. Possible side effects are increased hardness, sulphate and/or trace element concentrations. Geochemical characteristics of the sediment like organic matter content, decay rate of organic matter, pyrite content, trace element composition of pyrite and CEC vary among several Pleistocene sandy aquifer sediments in The Netherlands. In this study side effects are determined for different Pleistocene sandy aquifer sediments.

#### *A14.5.2 Side effects for denitrification with oxidation of sedimentary organic matter*

Side effects that may be expected from organic matter decay are increased trace metal concentrations. Trace metals are sorbed to organic matter and can be released from the sediment when acid ( $H^+$ ) replaces trace metals at the sorption complex. This replacement of trace metals by  $H^+$  may occur when acid-producing reactions occur like oxidation of organic matter by oxygen. Increased sulphate concentrations cannot be expected during decay of SOM.

In sediments with a relatively high rate of SOM oxidation, trace metal concentrations – cadmium, copper and zinc – reach high concentrations. Cadmium, copper and zinc concentrations increase to levels much higher than intervention levels (table A14.7). The high organic matter decay scenario is, however, not representative for Pleistocene sandy aquifer sediments.

In sediments with moderate organic matter decay, nitrate concentrations are gradually decreasing with depth. The oxidation of organic matter by nitrate does not cause side effects. Sediments with low organic matter decay are very common in Pleistocene sandy aquifers. In these sediments nitrate concentrations do not decrease in the first 5 meters below the redox cline and no side effects occur. So, side effects due to denitrification with SOM oxidation are minimal in Pleistocene sandy aquifer sediments. In sediments with high organic matter decay, however, many geochemical processes happen and trace metals become mobilised when present. The concentrations of these trace metals may reach high levels. It might be interesting for further research to investigate side effects in organic rich sediments.

*Table A14.7 Target levels and intervention levels for Dutch groundwater (according Staatscourant, 2000)*

	Target level		Intervention level
	Shallow	Deep	
Main elements	mg/l		
Sulphate	150	150	150
Trace elements	µg/l		
Arsenic	10	7.2	60
Cadmium	0.4	0.06	6
Copper	15	1.3	75
Nickel	15	2.1	75
Zinc	65	24	800

#### *A14.5.3 Side effects in sediments containing pyrite*

In pyrite containing sediments increased sulphate and trace metal concentrations are expected side effects as well as increased hardness. This research shows that indeed high

sulphate concentrations may occur due to oxidation of pyrite by oxygen and nitrate. These concentrations do, however, not reach intervention levels.

Trace metals may become problematic when pyrites have high trace element concentrations. Arsenic, manganese and nickel concentrations increase significantly as a consequence of pyrite oxidation. Arsenic concentrations become higher than intervention level when trace element concentrations in pyrite are high. Nickel concentrations stay below intervention level but become much higher than target level.

Effects of pyrite oxidation on zinc concentrations are not clear, since zinc concentrations are already much higher than intervention level due to high concentrations in infiltration pore water.

Copper concentrations become much higher than intervention level as a consequence of pyrite oxidation. Copper concentrations increase immediately due to pyrite oxidation when pyrite contains copper, but more important is the desorption of copper as a consequence of the sorption of  $H^+$ .  $H^+$  concentrations significantly increase during pyrite oxidation.

Pyrite does not contain cadmium, so pyrite oxidation does not affect cadmium concentrations.

#### *A14.5.4 Effect of acidity of groundwater system on side effects*

The initial pH of the shallow groundwater and the pH of the infiltration pore water does not significantly affect the side effects.

#### *A14.5.5 Effect of CEC on side effects*

CEC determines whether increased trace elements below the redox cline will be sorbed and stay for years in the upper meters of the shallow groundwater system or will be transported by the groundwater and reach greater depth. This difference has important consequences for transport of trace elements to the surface water system. Aquifer sediments containing high CEC may keep trace elements in the sediments and therefore trace element concentrations will only reach surface water after many years. Aquifer sediments containing low CEC may release trace elements to the surface water.